

Mechanistic studies of the explosive degrading enzyme, pentaerythritol tetranitrate (PETN) reductase

Huma Khan

**Thesis submitted for the degree of Doctor of Philosophy (PhD)
at the University of Leicester, U.K.**



Huma Khan (BSc Biochemistry)

Department of Biochemistry

University of Leicester

October 2004

UMI Number: U195828

All rights reserved

INFORMATION TO ALL USERS

The quality of this reproduction is dependent upon the quality of the copy submitted.

In the unlikely event that the author did not send a complete manuscript and there are missing pages, these will be noted. Also, if material had to be removed, a note will indicate the deletion.



UMI U195828

Published by ProQuest LLC 2013. Copyright in the Dissertation held by the Author.
Microform Edition © ProQuest LLC.

All rights reserved. This work is protected against
unauthorized copying under Title 17, United States Code.



ProQuest LLC
789 East Eisenhower Parkway
P.O. Box 1346
Ann Arbor, MI 48106-1346

ABSTRACT

Mechanistic studies of the explosive degrading enzyme, pentaerythritol tetranitrate (PETN) reductase

Huma Khan

PETN reductase is a member of the old yellow enzyme (OYE) family of flavoproteins. The enzyme is able to utilise diverse substrates such as α/β -unsaturated compounds, nitrate esters and nitroaromatic explosives, which makes it of potential interest for phytoremediation purposes. This thesis describes the characterisation of PETN reductase and investigates the role of four active site residues. Trp 102 is shown to influence the binding and transformation of TNT/picric acid. PETN reductase transforms TNT via two competing pathways; (i) nitro group reduction and (ii) direct ring reduction leading to hydride-Meisenheimer complex formation. Mutation of Trp 102 significantly affects the stability of the hydride-Meisenheimer complex, which is sufficient to affect the concentration distribution and/or nature of final TNT degradation products. The ability to produce the TNT hydride-Meisenheimer complex is abolished in the H181A and H184A mutant enzymes indicating that His 181 and His 184 determine the initial route of TNT transformation. These residues are also crucial in ligand binding. Hydride transfer to 2-cyclohexenone and nitrocyclohexene is compromised in the H181A and H184A PETN reductases, owing to the altered mode of substrate binding. Tyr 186 was initially proposed to act as a proton donor in the reduction of α/β -unsaturated compounds, however, studies presented herein reveal that this is not the case. Trp 102 and Tyr 186 are also shown to play a key role in GTN reduction. Studies on the reductive half-reaction reveal that the rate of NADPH-enzyme complex formation occurs too fast to be measured with Y186F enzyme. Conversely, no complex formation between NADPH and the H181A and H184A mutant enzymes is observed, attributed to the perturbation in NADPH binding, which favours hydride transfer. Collectively, the research described proposes interesting implications into the underlying mechanism of TNT and 2-cyclohexenone reduction by the OYE family of enzymes.

PREFACE

Mechanistic studies of the explosive degrading enzyme, pentaerythritol tetranitrate (PETN) reductase

Huma Khan

The research described in this thesis was conducted during September 2000 to September 2003 by the author, unless otherwise stated. No part of this thesis has been submitted for a degree or a diploma or other qualification at any other university.

October 2004
University of Leicester
Leicester

Huma Khan

ACKNOWLEDGEMENTS

I am grateful to Prof. Nigel Scrutton for providing me with the opportunity to undertake the present research and for his supervision and advice in writing this thesis.

Special thanks to Dr Terez Barna who trained me on the skills required to undertake the research presented. In particular, I would like to thank her for her invaluable advice and support throughout the course of the research and her enthusiasm for the project.

I wish to thank Dr Richard Harris for his support and in particular his help with the stopped-flow studies. In addition, I am grateful to Dr Terez Barna, Dr Peter Moody and Dr David Leys for providing images of the solved enzyme structures and their time in making them. Thank you also to Dr Igor Barsukov, for his help with the NMR studies.

The work of Dr Daniel Craig, provided a useful foundation to the studies described here.

Many thanks go to all the members of Lab 124, past and present, who have helped me in differing ways and have been there for support and advice. I would like to thank Dr Jaswir Basran for her help in the mutagenesis studies and her advice to all the questions that were asked. I am particularly grateful to Selena Burgess, Parvinder Hothi and Hanan Messiha for their support and advice and foremost for making this experience an enjoyable one!

To my family, for loads of love and support over the years thanks and "big-up!".

ABBREVIATIONS

2 H-TNT	dihydride-Meisenheimer complex of TNT
2,4-DNP	2,4-dinitrophenol
2H-PA	dihydride-Meisenheimer complex of picric acid
ADNT	aminodinitrotoluene
APS	ammonium persulphate
AZT	tetranitroazoxytoluene
CDNB	1-chloro-2,4-dinitrobenzene
Cyt P450	cytochrome P450
DANT	diaminonitrotoluene
DCNB	1,2-dichloro-4-nitrobenzene
DHANT	dihydroxyaminonitrotoluene
DNT	dinitrotoluene
EBP	estrogen binding protein
EDTA	diaminoethanetetra-acetic acid
FAD	flavin adenine dinucleotide
FMN	flavin mononucleotide
GDN	glycerol dinitrate
GMN	glycerol mononitrate
GTN	glycerol trinitrate
HADNT	hydroxylaminodinitrotoluene
HMX	high melting explosive
H-PA	hydride-Meisenheimer complex of picric acid
H-TNT	hydride-Meisenheimer complex of TNT
IPTG	isopropyl- β -D-thiogalactopyranoside
K_d	dissociation constant
k_{lim}	limiting rate constant
LB	Luria-Bertani (medium)
MNT	mononitrotoluene
MR	morphinone reductase
NADH	nicotinamide adenine dinucleotide (reduced form)

NADPH	nicotinamide adenine dinucleotide phosphate (reduced form)
NO	nitric oxide
OYE	old yellow enzyme
PAGE	polyacrylamide gel electrophoresis
PDA	photodiode array
PEG	polyethyleneglycol
PETN	pentaerythritol tetranitrate
RDX	royal demolition explosive
SDS	sodium dodecyl sulphate
TAT	triaminotoluene
TEMED	<i>N,N,N',N'</i> -tetramethylethylenediamine
Tetryl	2,4,6-trinitrophenyl- <i>n</i> -methylnitramine
TNT	trinitrotoluene

CONTENTS

<i>Abstract</i>	i
<i>Preface</i>	ii
<i>Acknowledgements</i>	iii
<i>Abbreviations</i>	iv

CHAPTER ONE

Introduction	1
1.1 Introduction	2
1.2 Application of research: Nitro-substituted compounds - their use, contamination and remediation strategies	3
1.2.1 Nitro-compounds and their environmental concern	3
1.2.2 Bioremediation	5
1.2.3 Phytoremediation and transgenic plants	12
1.3 Transformation pathways for nitro-substituted compounds	14
1.3.1 Chemistry of TNT	15
1.3.2 Reduction of TNT nitro-groups by nitroreductases	17
1.3.3 Hydrogenation of the aromatic ring system in nitroaromatic compounds	20
1.3.4 Reduction of nitrate esters	25
1.4 Flavoproteins	27
1.4.1 Chemical properties of flavins	30
1.4.2 Catalytic cycles and stereospecificity of flavins	34
1.4.3 Methods of study	35
1.4.4 β,α -barrel proteins	36
1.4.5 Classification of flavoproteins	37
1.5 Enzymes related to PETN reductase: Old yellow enzyme	38
1.5.1 Structure and general properties	39
1.5.2 Reductive half-reaction of OYE	41
1.5.3 Oxidative half-reaction	43

1.5.4	Summary	46
1.6	<i>Enzymes related to PETN reductase: Morphinone reductase</i>	48
1.6.1	Physical and structural properties	48
1.6.2	Reductive half-reaction	52
1.6.3	Oxidative half-reaction	53
1.7	<i>PETN reductase</i>	54
1.7.1	Physical and structural properties of PETN reductase	55
1.7.2	Catalytic mechanism of PETN reductase	59
1.8	<i>Aims of thesis</i>	60

CHAPTER TWO

Materials and Methods **63**

2.1	<i>Materials</i>	64
2.1.1	Chemicals and reagents	64
2.1.2	Bacterial strains and enzymes	64
2.1.3	Chromatographic media and membranes	65
2.2	<i>Recombinant DNA techniques</i>	65
2.2.1	Preparation and digestion of plasmid DNA	65
2.2.2	Submarine agarose gel electrophoresis	65
2.2.3	Mutagenesis of pONR1 plasmid	66
2.2.4	Transformation of Y186F mutated pONR1 plasmid into <i>E.coli</i> JM109 cells	67
2.2.5	Sequencing of Y186F PETN reductase	67
2.3	<i>Preparation and purification of wild-type and mutant forms of PETN reductase</i>	67
2.3.1	Bacterial strains and media	67
2.3.2	Preparation of PETN reductase	69
2.3.3	Purification of wild-type PETN reductase	70
2.3.4	Purification of mutant PETN reductase enzymes	70
2.4	<i>SDS Polyacrylamide Gel Electrophoresis</i>	71
2.5	<i>Ligand binding studies</i>	72

2.6	<i>Single wavelength stopped-flow studies of the reductive half-reaction</i>	73
2.7	<i>Anaerobic conditions</i>	74
2.8	<i>Anaerobic single and multiple turnover studies</i>	75
2.8.1	Spectral single turnover studies	75
2.8.2	Spectral multiple turnover studies with TNT and picric acid	75
2.8.3	NMR analysis of the multiple turnover of TNT	76
2.8.4	Spectral multiple turnover studies with nitrocyclohexene	76
2.9	<i>Anaerobic stopped-flow studies</i>	77
2.9.1	Single wavelength studies on the oxidative half-reaction	77
2.9.2	Multiple wavelength stopped-flow studies	78
2.10	<i>Anaerobic redox potentiometry</i>	79
2.11	<i>X-ray crystallography</i>	80

CHAPTER THREE

	Mechanism of explosive degradation: role of Trp 102	81
3.1	<i>Introduction</i>	82
3.1.1	Transformation of nitroaromatic compounds by PETN reductase	82
3.1.2	Crystal structure of PETN reductase in complex with nitroaromatic compounds	85
3.2	<i>Purification and characterisation of wild-type and Trp 102 mutant PETN reductases</i>	90
3.2.1	Purification of wild-type, W102F and W102Y PETN reductases	90
3.2.2	Ligand binding studies	90
3.2.3	Reductive half-reaction	96
3.2.4	TNT single turnover studies	101
3.2.5	Multiple turnover studies with TNT	104
3.2.6	NMR analysis of multiple turnover reactions with TNT	109
3.2.7	Single turnover studies with picric acid	112
3.2.8	Multiple turnover studies with picric acid	116
3.2.9	Multiple wavelength stopped-flow studies of the oxidative half-reaction with TNT	118

3.2.10	Single wavelength stopped-flow studies of the oxidative half-reaction with TNT	122
3.2.11	Single wavelength stopped-flow studies of the oxidative half-reaction with 2-cyclohexenone and GTN	125
3.2.12	Redox potentiometry	130
3.3	<i>Discussion</i>	132
3.3.1	Mechanism of nitroaromatic transformation	132
3.3.2	Role of Trp 102 in nitroaromatic binding	134
3.3.3	Oxidative half-reaction with GTN and 2-cyclohexenone	136
3.3.4	Kinetics of the reductive half-reaction	137
3.3.5	Summary	138

CHAPTER FOUR

Role of Tyr 186 in the oxidative half-reaction of PETN reductase: a potential proton donor **140**

4.1	<i>Introduction</i>	141
4.1.1	Mode of steroid binding	141
4.1.2	Mechanism of reduction of α,β -unsaturated compounds: a search for the active site acid	147
4.2	<i>Construction and purification of the Y186F mutant of PETN reductase</i>	149
4.2.1	Mutation of Tyr 186 to Phe 186 in PETN reductase	149
4.2.2	Purification of the Y186F PETN reductase	151
4.3	<i>Characterisation of Y186F PETN reductase and comparisons to wild-type enzyme</i>	151
4.3.1	Ligand binding studies	151
4.3.2	Single wavelength stopped-flow studies of the reductive half-reaction	156
4.3.3	Multiple wavelength stopped-flow studies of the oxidative half-reaction with TNT	160
4.3.4	Single wavelength stopped-flow studies of the oxidative half-reaction with 2-cyclohexenone	162

4.3.5	Single wavelength stopped-flow studies of the oxidative half-reaction with TNT and GTN	165
4.3.6	Anaerobic redox potentiometry	168
4.3.7	X-ray crystallography	168
4.4	<i>Discussion</i>	170
4.4.1	Crystal structure of Y186F PETN reductase	174
4.4.2	Oxidative half-reaction with α,β -unsaturated compounds	174
4.4.3	Oxidative half-reaction with nitro compounds	175
4.4.4	Kinetics of the reductive half-reaction	176
4.4.5	Implications into the mechanism of α,β -unsaturated compound reduction by the OYE family of enzymes	177

CHAPTER FIVE

	Establishing the roles of His 181 and His 184 in PETN reductase	182
5.1	<i>Introduction</i>	183
5.1.1	Active site structure of PETN reductase	183
5.1.2	Search for the active site acid of PETN reductase	188
5.2	<i>Purification of the H181A and H184A mutant forms of PETN reductase</i>	190
5.3	<i>Characterisation of the H181A and H184A PETN reductases</i>	192
5.3.1	Ligand binding	192
5.3.2	Anaerobic single wavelength stopped-flow studies on the reductive half-reaction	196
5.3.3	Anaerobic multiple wavelength stopped-flow analysis of the reductive half-reaction	197
5.3.4	Single wavelength stopped-flow studies of the oxidative-half reaction with 2-cyclohexenone	202
5.3.5	Anaerobic studies following the multiple turnover of nitrocyclohexene	205
5.3.6	Single wavelength stopped-flow studies of the oxidative-half reaction with TNT	210
5.3.7	Anaerobic multiple wavelength stopped-flow studies with TNT	212

5.3.8	Anaerobic redox potentiometry	212
5.3.9	Crystallography	215
5.4	<i>Discussion</i>	215
5.4.1	Function of His 181 and His 184 in ligand/substrate binding	217
5.4.2	Implications of His 181 and His 184 in TNT binding and transformation	218
5.4.3	Mechanism of 2-cyclohexenone and nitrocyclohexene reduction	220
5.4.4	Function of His 181 and His 184 in the reductive half-reaction of PETN reductase	223

CHAPTER SIX

	Discussion	225
5.1	<i>General properties of PETN reductase and residues involved in ligand binding</i>	226
5.2	<i>Reductive half-reaction</i>	228
5.3	<i>Oxidative half-reaction</i>	230
5.3.1	Oxidative half-reaction with TNT	230
5.3.2	Oxidative half-reaction with 2-cyclohexenone	233
5.3.3	Oxidative half-reaction with GTN	236
5.4	<i>Conclusion</i>	237
5.5	<i>Future areas of research</i>	238
	<i>References</i>	240

Chapter One

Introduction

CHAPTER ONE

Introduction

1.1 Introduction

The research described in this thesis concerns the enzyme pentaerythritol tetranitrate (PETN) reductase from *Enterobacter cloacae* PB2, isolated on the basis of its ability to degrade high explosives (i.e. nitro-compounds). The introductory chapter begins by discussing the potential application of this enzyme and the purpose behind its characterisation. Accordingly, an overview on the use of nitro-substituted compounds and the growing concern over their environmental contamination is given, followed by a brief review on the possible methods used to remedy this problem. Furthermore, an account on the transformation pathways of explosive compounds is presented in addition to outlining enzymes known to be involved in this process. Since PETN reductase is a flavin-dependent β/α -barrel protein, an overview of the properties and chemistry of the flavin co-actor and the classification system used for such proteins is presented. PETN reductase shows high similarity to old yellow enzyme (OYE) and morphinone reductase, and the introductory chapter will also briefly review the physical and structural properties of these enzymes, followed by an up to date account of our understanding of PETN reductase. Chapter 2 outlines the methods used to conduct the research described, with Chapters 3 to 5 presenting the results obtained. Each of the results chapters begin by providing a brief background to the work undertaken. Chapter 3 aims to elucidate the nature of TNT transformation in PETN reductase and the possible involvement of an active site Trp 102 residue. Chapter 4 probes the role of Tyr 186 in the enzyme, proposed to act as an active site acid in the reduction of α,β -unsaturated compounds, an important group of substrates for PETN reductase. Chapter 5 aims to establish the role of two active site histidine residues as the primary determinants of ligand binding, in addition to investigating their role as the potential active site acid. Chapter 6 gives an overview of the results obtained, followed by suggestions for future research.

1.2 Application of research: Nitro-substituted compounds - their use, contamination and remediation strategies

1.2.1 Nitro-compounds and their environmental concern

Natural organic compounds are readily biodegradable and can serve as efficient carbon and energy sources for micro-organisms. In contrast, xenobiotic compounds exhibit structural elements or substituents that are rarely found in natural products and are therefore generally recalcitrant to biodegradation (Spain, 1995a; Esteve-Nunez *et al*, 2001). Naturally occurring nitro-substituted compounds are extremely rare in nature and are released into the environment from anthropogenic sources. Such compounds are extensively used in the synthesis of synthetic intermediates, dyes, pesticides and explosives (Spain, 1995a)

Nitro-substituted compounds used as high explosives include the nitroaromatics, 2,4,6-trinitrotoluene (TNT) and 2,4,6-trinitrophenol (Picric acid), the nitroamines, hexahydro-1,3,5-trinitro-1,3,5-triazine (RDX; Royal Demolition Explosive) and octahydro-1,3,5,7-tetranitro-1,3,5,7-tetrazocine (HMX; High Melting Explosive) and the nitrate esters, pentaerythritol tetranitrate (PETN) and glycerol trinitrate ([GTN; nitroglycerin] see Figure 1.1; Boyd and Bruce, 2002). The manufacture, use and disposal of such explosives over the last hundred years has resulted in a large number of Army Ammunition Plant (AAP) sites becoming heavily contaminated (Hannink *et al*, 2001; Tamalge *et al*, 1999). In addition to soil contamination, groundwater pollution is also prevalent. For example, during shell loading operations, hot water saturated with residual explosive is discharged into lagoons allowing TNT to gradually pass into local streams (Higson, 1992). TNT concentrations of up to 200g/kg of solid have been found in some soils (Hooker and Skeen, 1999). Major international concern is growing over this wide-scale contamination and many AAPs have been placed on the National Priorities List for Superfund Cleanup (Tamalge *et al*, 1999). Many of these sites are based on large areas of undisturbed land which provide diverse habitats to a variety of aquatic and terrestrial species. This presents significant concern as explosives are toxic and mutagenic to biological systems and consequently pose a potential hazard to human health (Binks *et al*, 1996; Hooker and Skeen, 1999). TNT is toxic to freshwater unicellular algae, oyster alarvae, and is a frameshift mutagen to *Salmonella typhimurium*. During the world wars, death from toxic hepatitis and aplastic anaemia due to TNT exposure were significant. TNT is also known to affect liver function, the lens of the eye and the survival of erythrocytes, among many other effects (Higson, 1992).

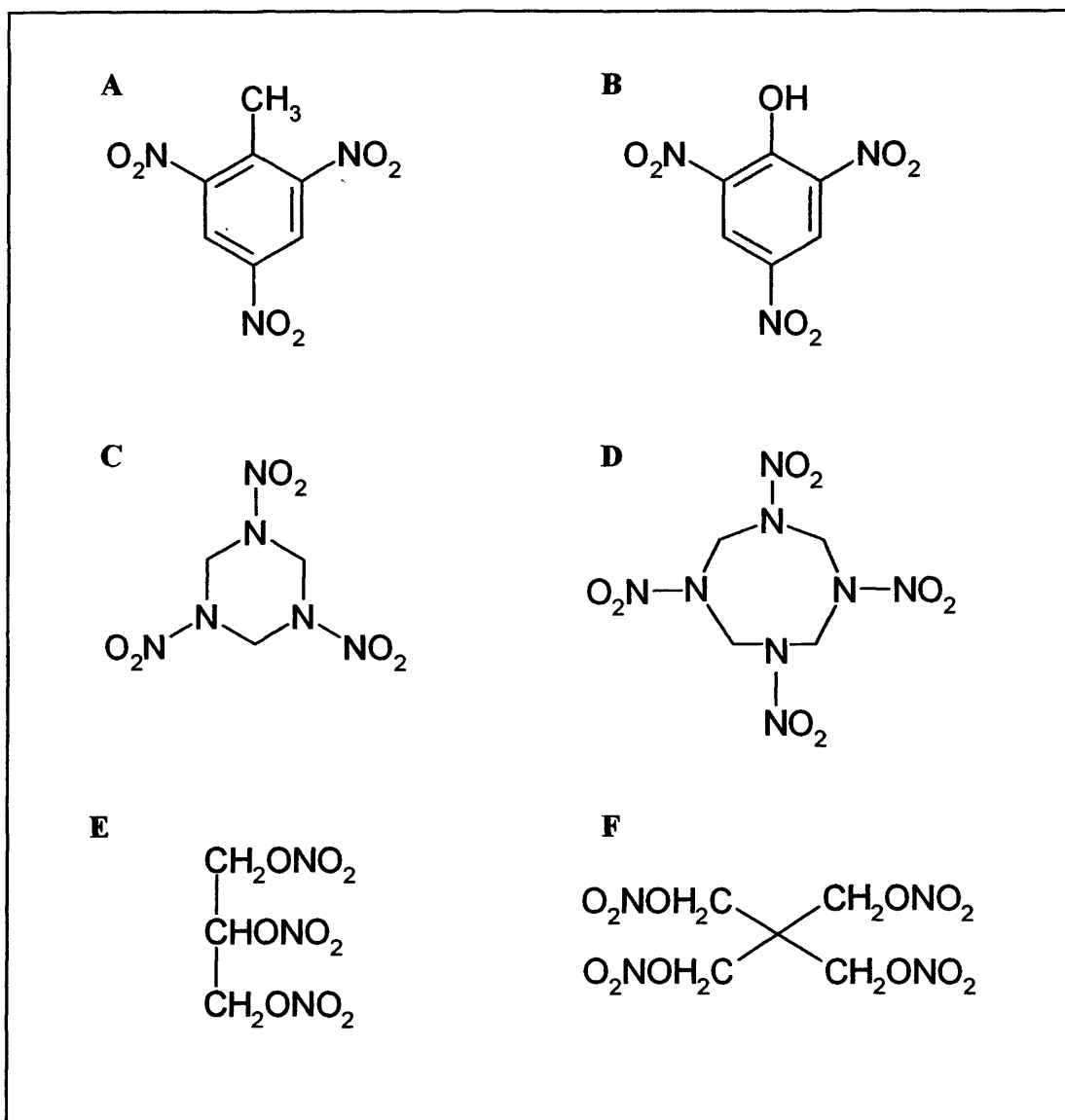


Figure 1.1. Structures of nitro-substituted explosive compounds. (A) 2,4,6-trinitrotoluene (TNT); (B) 2,4,6-trinitrophenol (picric acid); (C) hexahydro-1,3,5-trinitro-1,3,5-triazine (RDX; Royal Demolition Explosive); (D) octahydro-1,3,5,7-tetranitro-1,3,5,7-tetrazocine (HMX; High Melting Explosive); (E) glycerol trinitrate (GTN; nitroglycerin) and; (F) pentaerythritol tetranitrate (PETN). (Figure adapted from Boyd and Bruce, 2002).

Given their potential hazard, the accumulation of explosives and their environmental fate is becoming a matter of increasing concern. Accordingly, this has initiated a vast amount of research focused on prospective methods for the remediation of contaminated soil and water. Currently, the only effective treatment used for the treatment of explosive contaminated land is incineration (Hannink *et al*, 2001). However, this method generates toxic by-products and unusable ash which must be treated as hazardous waste and disposed of in hazardous chemical landfills. Also, incomplete combustion results in the release of greenhouse effect gases such as CO₂ and NO_x, which raises additional concerns of air pollution (Kalafut *et al*, 1998; Snellinx *et al*, 2002). In addition to the high cost of incineration, these problems emphasise the need for alternative technologies to be developed, such as bioremediation and phytoremediation.

1.2.2 Bioremediation

Bioremediation involves the application of micro-organisms to clean-up contaminated soil. Given their anthropogenic nature, nitroaromatic compounds are expected to be unrecognisable by micro-organisms, which leads to their accumulation in the environment. However, micro-organisms are capable of adapting and continuously evolving biodegradative pathways necessary for their survival. As a result, micro-organisms exposed to xenobiotic compounds for a considerable length of time have evolved biodegradative pathways that permit the degradation of man-made compounds, previously considered to be recalcitrant (Perec and Agathos, 2000; Parales *et al*, 2002). Consequently, more and more micro-organisms are being identified that are capable of utilising/degrading high explosive contaminants in soil. Most of these organisms have been isolated from explosive contaminated soil samples near ammunition plants.

Microbial degradation of explosives and nitroaromatic compounds has been demonstrated extensively (Table 1.1) and the enzymes responsible for these processes are continuously being identified. Traditionally, most research into the bioremediation of explosives has focused on anaerobic bacteria and fungi. Studies focusing on the capabilities of aerobic bacteria are relatively recent (Kalafut *et al*, 1998). Generally, most aerobic bacteria transform nitroaromatic compounds such as TNT by reducing one or two of the nitro groups to hydroxylamino or amino groups, yielding hydroxylaminodinitrotoluene (HADNT) and aminodinitrotoluene (ADNT) isomers. These partially reduced compounds are usually not metabolised further by the micro-organism and therefore accumulate in the culture medium

Organism	Enzyme	Reaction	Reference
<i>P. putida</i> II-B	Xenobiotic reductase A	Reduces terminal or central NO ₂ group of GTN. Reduces the NO ₂ groups of TNT to yield hydroxylamine derivatives of parent compound.	Blehert <i>et al.</i> , (1999); Pak <i>et al.</i> , (2000)
<i>P. fluorescens</i> I-C	Xenobiotic reductase B	Reduces central NO ₂ group of GTN. Transforms TNT → H-TNT → 2H-TNT (i.e via ring reduction) and also reduces the NO ₂ groups of TNT.	Blehert <i>et al.</i> , (1999); Pak <i>et al.</i> , (2000)
<i>P. pseudoalcaligenes</i> JS45	Nitrobenzene nitroreductase	Nitrobenzene → hydroxylaminobenzene	Sommerville <i>et al.</i> , (1995)
<i>Mycobacterium sp.</i> Pyr I	Lipoamide dehydrogenase	Catalyses the reduction of nitro-substituted compounds (e.g. 4-benzoic acid and 1-nitropyrene) → corresponding amines.	Rafii <i>et al.</i> , (2001) and (1994)
<i>Enterobacter cloacae</i>	NAD(P)H nitroreductase	Reduces a wide range of nitro compounds e.g. TNT, 2,4,6-trinitrophenyl- <i>n</i> -methylnitramine (tetryl), pentryl, TNC, RDX, HMX, di-nitrobenzene.	Nivinskas <i>et al.</i> , (2000)
<i>Anabaena</i> PCC 7119	Ferredoxin NADP oxidoreductase (Type II)	1e ⁻ reduction of tetryl leading to nitrite release via the formation of a nitroanion radical of the parent compound.	Shah and Spain (1996); Anusevicius <i>et al.</i> , (1999)
	NADPH:cytP450 reductase	1e ⁻ reduction of tetryl → nitroanion radical	Anusevicius <i>et al.</i> , (1998)
<i>P. aeruginosa</i> strain MX		Nitro group reduction of TNT → HADNTs (accumulate transiently) → ADNTs and AZTs accumulate in culture medium.	Oh <i>et al.</i> , (2000)
	NAD(P)H:quinone reductase	2e ⁻ reduction of nitroaromatics leading to the formation of nitroso compounds.	Cenas <i>et al.</i> , (2001)

Table 1.1. Summary of the wide range of micro-organisms and their purified enzymes that are capable of transforming a variety of nitro-substituted compounds. The types of reactions catalysed by each organism/enzyme and the identified intermediates/products are also listed.

Organism	Enzyme	Reaction	Reference
<i>Sacchromyces</i> sp. ZS <i>Candida</i> sp. AN-L14 <i>Candida</i> sp. L-13		TNT → 2-HADNT and 4-HADNT (nitro group reduction) TNT → 2-HADNT and 4-HADNT, TNT → H-TNT (i.e. NO ₂ group and ring reduction) TNT → H-TNT (ring reduction)	Zaripov <i>et al</i> , (2002)
<i>Nematoloma frowardii</i> (white rot fungus)	Manganese peroxidase	Degrades wide spectrum of aromatic and aliphatic substrates including TNT, PCP, 2,4-DCP, and 2-ADNT → CO ₂ and polar fission product (2-amino-4,6-dinitrotoluene)	Hofrichter <i>et al</i> , (1998); Scheibner <i>et al</i> , (1997)
	NAD(P)H:FMN oxidoreductase	TNT → 2-HADNT and 4-HADNT → →	Riefler and Smetts (2002)
<i>Phlebia radiate</i> (white rot basidiomycete)	Manganese dependent peroxidase	Transforms TNT via nitroreductase activity.	Aken <i>et al</i> , (1999)
<i>Clostridium thermoaceticum</i>	CO dehydrogenase	TNT → 4-HADNT (80 %) + 2-HADNT (20 %) → 2,4-DHANT → Bamberger re-arrangement product	Huang <i>et al</i> , (2000)
<i>Actinomyces</i> strains		TNT → 4-ADNT + 2,4-DANT	Pasti-Grigsby <i>et al</i> , (1996)
<i>Clostridium bifermentans</i> LJP-1		TNT → → → triaminotoluene (TAT; end product) + phenolic products of TAT hydrolysis	Lewis <i>et al</i> , (1996)

Table 1.1. (continued) Summary of the wide range of micro-organisms and their purified enzymes that are capable of transforming a variety of nitro-substituted compounds. The types of reactions catalysed by each organism/enzyme and the identified intermediates/products are also listed.

Organism	Enzyme	Reaction	Reference
<i>Pseudomonas</i> sp. JLR11		Uses nitrite, nitrate and TNT as N ₂ source under anoxic conditions. Is able to use TNT as a final electron acceptor in the respiratory chain under anoxic conditions.	Esteve-Nunez <i>et al</i> , (2000)
<i>Clostridium acetobutylicum</i>	Fe-only hydrogenase	TNT → 2-HADNT + 4-HADNT → 2,4-DHANT + polar species resulting from Bamberger rearrangement of 2,4-DHANT.	Watrous <i>et al</i> , (2003)
<i>Mycobacterium</i> sp. HL 4-NT-1		Reduces nitroaromatics via NO ₂ group reduction to corresponding amino derivatives and also via hydride addition to the aromatic ring. With TNT as substrate, 5 % is reduced to 4-ADNT and 40 % is accumulated transiently as H ⁻ -TNT (indicating importance of hydride addition mechanism for TNT metabolism). Uses 4-nitrotoluene as N ₂ source.	Zaripov <i>et al</i> , (2002)
<i>P. pseudoalcaligenes</i> JS52 (derived from strain JS45)	Nitrobenzene nitroreductase and another unidentified enzyme	During TNT transformation, DHANT and 2-hydroxylamino-4-aminonitrotoluene are detected in the culture medium. Nitrobenzene reductase transforms TNT to DHANT but is unable to reduce the NO ₂ to the corresponding amines; therefore the bacterium must contain another enzyme to reduce the NO ₂ groups to the corresponding amine derivative.	Fiorella and Spain (1997)
Bovine Lens	ζ-crystallin	1e ⁻ reduction of TNT → superoxide anions (leading to oxidative stress, which causes cataract).	Kumagai <i>et al</i> , (2000)
<i>Pseudomonas</i> sp. Strain CISI and <i>Pseudomonas</i> sp. Clone A		Uses TNT as a sole N ₂ source. TNT → 2,4- and 2,6-dinitrotoluene → 2-nitrotoluene and toluene. Both organisms reduce the nitro groups to hydroxylamino and amino groups.	Duque <i>et al</i> , (1993)
Gram- TNT8, Gram+ TNT32, <i>Pseudomonas</i> sp. clone A		Uses TNT as a sole N ₂ source. Reduces TNT via nitro group reduction.	Vorbeck <i>et al</i> , (1998)

Table 1.1. (continued) Summary of the wide range of micro-organisms and their purified enzymes that are capable of transforming a variety of nitro-substituted compounds. The types of reactions catalysed by each organism/enzyme and the identified intermediates/products are also listed.

Organism	Enzyme	Reaction	Reference
<i>R. erythropolis</i> HL PM-1 <i>Mycobacterium</i> <i>sp. strain</i> HL 4NT-1		Reduces TNT via nitro group and ring reduction: TNT → 2- and 4- HADNT + 2- and 4-ADNT TNT → Hydride-Meisenheimer → Dihydride-Meisenheimer (and protonated form).	Vorbeck <i>et al</i> , (1998)
<i>Cenocephalum</i> <i>conicum</i> , <i>Sphagnum</i> <i>caplifotium</i> , <i>Ascophylum nodosum</i> . Glycine max cultures, <i>Laminaria digitata</i> , <i>Enteromorpha bulbosa</i>	Glutathione S- transferase activity	Nitrobenzene derivative e.g. CDNB, DCNB, activity found in soluble and microsomal enzyme fractions.	Pfulgmacher <i>et al</i> , (2000)
<i>Rhodococcus</i> <i>rhodochrous</i> strain 11Y		RDX used as sole N ₂ source. Products of RDX degradation in resting cell incubations include nitrite, formaldehyde and formate.	Seth-smith <i>et al</i> , (2002)
<i>Rhodococcus</i> strain DN22	Possibly cytP450	RDX is used as N ₂ source. Observed nitrite, nitrous oxide, ammonia, formaldehyde, carbon dioxide and another dead-end metabolite (C ₂ H ₅ N ₃ O ₃) production. (See Hawari and Spain (2003) for review)	Coleman <i>et al</i> , (1998, 2002); Fournier <i>et al</i> , (2002).
	cytP450 2B4 (from rabbit liver)	Reduces RDX via 2 single e ⁻ transfers causing double denitration, which leads to spontaneous hydrolytic ring cleavage decomposition to produce 4-nitro-2,4-diazabutanal.	Bhushban <i>et al</i> , (2003)
<i>Ralstonia eutropha</i> JMP134	FADH ₂ -utilising monooxygenase	Able to grow on aromatic pollutants including 2,4,6-TCP, 2,4-dichlorophenoxyacetate, 2-chloro-5-nitrophenol. Transforms 2,4,6-TCP → 2-chloromaleylacetate.	Louie <i>et al</i> , (2002); Schenzle <i>et al</i> , (1999)

Table 1.1. (continued) Summary of the wide range of micro-organisms and their purified enzymes that are capable of transforming a variety of nitro-substituted compounds. The types of reactions catalysed by each organism/enzyme and the identified intermediates/products are also listed.

Organism	Enzyme	Reaction	Reference
<i>P. putida</i> 2NP8		A wide range of mono- or di-nitroaromatic substrates are transformed to ammonia via 3-nitrophenol induced enzyme pathway. Nitrobenzene is reduced to aminophenol, with subsequent hydrolysis to ammonia and benzoquinone.	Zhao and Ward (2001)
<i>R. erythropolis</i> HL PM-1		Uses picric acid as sole N ₂ , C and energy source. Picric acid → Hydride-Meisenheimer (and protonated form) → 2,4-DNP. Rearomatisation to DNP leads to nitrite elimination.	Rieger <i>et al.</i> , (1999)
<i>Nocardioides simplex</i> FJ2-IA	F ₄₂₀ -dependent hydride transferase	Part of a three component system of coenzyme F ₄₂₀ . Able to use picric acid and 2,4-DNP as sole carbon and energy source	Ebert <i>et al.</i> , (1999)
<i>Nocardioides sp.</i> strain CB22-2		Mineralises picric acid and uses it as a carbon and energy source. Picric acid → Hydride-Meisenheimer → DNP → 3-hydride-Meisenheimer of DNP	Behrend and Heesche-Wagner (1999)
<i>R. erythropolis</i> HL 24-I		Reduces ortho-substituted (-Cl, -CH ₃ , -NH ₃) 2,4-DNPs. 2-amino-4,6-DNP → Hydride-Meisenheimer → 2-amino-6-DNP + nitrite. 2-chloro-4,6-DNP → 4,6-dinitrohexanoate + 2,4-DNP (2-chloro-4,6-DNP → Hydride-Meisenheimer → 2,4-DNP + Cl + nitrite ?)	Lenke and Knackmuss (1996)
<i>Rhodobacter capsulatus</i>	Nitrophenol reductase	Under anaerobic and light conditions: 2,4-DNP → 2-amino-4-nitrophenol	Saez <i>et al.</i> , (2001)
<i>R. erythropolis</i> HL PM-1	npd I (hydride transferase II), C (hydride transferase I), G (NADPH-dependent F ₄₂₀ reductase)	Picric acid → Hydride-Meisenheimer → Dihydride-Meisenheimer complex of picric acid. 2,4-DNP → Hydride-Meisenheimer complex	Heiss <i>et al.</i> , (2002)

Table 1.1. (continued) Summary of the wide range of micro-organisms and their purified enzymes that are capable of transforming a variety of nitro-substituted compounds. The types of reactions catalysed by each organism/enzyme and the identified intermediates/products are also listed.

(Esteve-Nunez *et al*, 2001). In addition, the transformed products are sometimes more toxic and mutagenic than the parent compound (Honeycutt *et al*, 1996; Banerjee *et al*, 1999). Furthermore, in the presence of oxygen, HADNT and ADNT isomers have been found to react with each other resulting in the formation of azoxytetranitrotoluene (AZT; Haidour and Ramos, 1996; McCormick *et al*, 1976; Wang *et al*, 2000), which itself causes a higher rate of mutation than TNT (George *et al*, 2001). A few strains of aerobic bacteria and fungi have been reported to use TNT as a nitrogen or carbon source (see Table 1.1) by removing nitrogen under aerobic conditions. Strains of *Pseudomonas* (Duque *et al*, 1993; Haidour and Ramos, 1996; Ramos *et al*, 1995), *Rhodococcus erythropolis* (Lenke and Knackmuss, 1992; Rieger *et al*, 1999) and *Enterobacter cloacae* (French *et al*, 1998), are reported to utilise TNT and picric acid as sole sources of nitrogen by removing the nitro groups from the aromatic ring of these substrates. This process is reported to occur via direct reduction of the aromatic ring, leading to the formation of a hydride-Meisenheimer complex and eventual nitrite release (see Section 1.3.3 for further details).

Anaerobic micro-organisms such as *Clostridium* (Lewis *et al*, 1996; Esteve-Nunez *et al*, 2001) and *Desulfovibrio* (Preuss *et al*, 1993; Esteve-Nunez *et al*, 2001) primarily reduce the nitro groups of TNT to the corresponding amines, eventually forming triaminotoluene (TAT) and other phenolic compounds. In addition, some strains are reported to reduce TNT to the corresponding HADNTs (Huang *et al*, 2000; Hughes *et al*, 1998). Hawari and co-workers (Hawari *et al*, 1998) have suggested that TAT is a dead-end product from microbial TNT transformation reactions, which prevents the mineralization of the parent nitroaromatic compound.

Fungal metabolism of nitroaromatic compounds initially involves reduction of the nitro groups, yielding HADNTs and ADNTs. Research into the fungal metabolism of nitroaromatic compounds has mostly involved the white rot fungus *Phanerochaete chrysosporium* (Stahl and Aust, 1993; 1995; Michels and Gottschalk, 1995; Esteve-Nunez *et al*, 2001). However, other fungi such as white rot fungus from basidiomycete *Nematoloma frowardii* (Scheibner *et al*, 1997) and *Phelibia radiata* (Van Aken *et al*, 1999; 1997) are also able to transform TNT. Further reduction and eventual mineralisation of the reduced products of TNT by these fungal strains is believed to involve the enzyme lignin peroxidase (Scheibner *et al*, 1997; Van Aken *et al*, 1999; 1997; Esteve-Nunez *et al*, 2001).

Generally, the primary intermediates of TNT transformation by micro-organisms are HADNTs, ADNTs, diaminonitrotoluenes (DANTs) and azoxytetranitrotoluene (AZTs). The reactions by which these micro-organisms transform TNT are believed to involve

nitroreductase enzymes (see Section 1.3.2; Oh *et al*, 2000). The application of microbes for bioremediation purposes, although cost-effective, has important limitations that need to be considered. For instance, micro-organisms added to contaminated soil samples are often unable to compete with indigenous soil bacteria. Also, the addition of other substances may be required to induce the expression of enzymes necessary for their biodegradative pathways. These additional substrates can sometimes be toxic and expensive (Hooker and Skeen, 1999). The toxicity to the micro-organism, of the nitroaromatic compound to be degraded and the by-products (such as HADNTs, ADNTs), often poses problems for effective bioremediation methods. Often, the rates of degradation are limited by the accumulation of toxic metabolites produced during transformation of the parent compound. The toxicity of such metabolites causes additional concerns to human health, during the handling of contaminated/treated soil. The low bioavailability of the nitroaromatic compound to micro-organisms, due to their insolubility and/or adsorption to soil particles, also causes additional problems (Spain, 1995a). However, recent studies have shown that the addition of compounds such as the food-grade surfactant, Tween 80 (monooleate), accelerates biodegradation rates by enhancing the removal of TNT from soil matrix, in turn increasing the bioavailability of the explosive for microbial degradation (Boopathy *et al*, 2002). However, the addition of other substances can again increase expenditure and long-term operating costs. Ongoing research is focussing on addressing the problems associated with bioremediation methods, which has the potential of being an effective strategy for decontaminating explosive polluted soil. A vast amount of research is being conducted on identifying microbial metabolic pathways and the enzymes involved in the degradation of nitroaromatic compounds for the means of manipulating the production of less toxic products. Equally, a large amount of research is focussing on alternative remediation strategies such as the more recent method of phytoremediation.

1.2.3 Phytoremediation and transgenic plants

Phytoremediation involves the use of plants and the associated rhizosphere micro-organisms to remove, transform or store toxic chemicals located in soil, water and the atmosphere (Susarla *et al*, 2002). Plants possess the ability to extract compounds from their surrounding environments. In addition, their extensive root systems and ability to release exudates (sugars, phenolics, organic acids, alcohols and proteins), dramatically promotes increased microbial numbers and activity in their rhizosphere (Schnoor *et al*, 1995; Anderson *et al*, 1993). This interaction between plants and micro-organisms stimulates the biochemical

transformation of organic chemicals in the root-soil interface (Snellinx *et al*, 2002). A number of researchers have reported the ability of plants to take up and transform explosive chemicals such as TNT, from soil and groundwater (Schnoor *et al*, 1995; Medina and McCutcheon, 1996; Best *et al*, 1997). Although plants stimulate the degradation of explosives via microbial contribution, they themselves have been reported to possess the innate ability to transform TNT (Vanderford *et al*, 1997; Hughes *et al*, 1997). The uptake and reduction of TNT has been demonstrated in plant cell and organ cultures (Giri *et al*, 2001). Increasing evidence has shown that plants possess and release a number of degradative enzymes, mainly nitroreductases, which reduce the nitro groups of nitroaromatic compounds (Susarla *et al*, 2002). For example, hybrid poplar trees (*Populus* spp.), Eurasian watermilfoil (*Myriophyllum spicatum*), Stonewort (*Nitella* spp.) and parrot feather (*Myriophyllum aquaticum*), have all shown to reduce the nitro groups of nitroaromatic explosives, mainly owing to nitroreductase activity (Burken and Schnoor, 1997; Hughes *et al*, 1997; Susarla *et al*, 2002; Best *et al*, 1997). In most studies, the transformation of TNT by plants usually leads to the formation of 2- and 4-ADNT (Hughes *et al*, 1997; Thompson *et al*, 1998; Esteve-Nunez *et al*, 2001). Product profiles following the formation of these intermediates are still unknown. The toxicity of these unknown products to the plant and other biological systems causes some concern.

Most research into explosive phytoremediation has focussed on TNT. Less work has been done on the treatment of other munitions such as RDX, HMX and GTN. Preliminary studies have shown that the treatment of these compounds by plants is not as successful as the phytoremediation of TNT. Although RDX and HMX uptake has been demonstrated in hydroponic bush bean plants (Harvey *et al*, 1991) and axenic roots of *Catharanthus roseus* (Bhadra *et al*, 2001), they tend to be recalcitrant to transformation or slow to disappear. However, the findings of one study have suggested that the phytodegradation of GTN can be accomplished (Goel *et al*, 1997).

Overall, phytoremediation of TNT shows signs of being an effective technique, due to rapid removal and transformation, rather than phytoaccumulation. However, there are certain limitations with phytoremediation that prevent its wide-scale use. Importantly, much research needs to be done in assessing the toxicity of by-products produced during the transformation of TNT and on the treatment of other munitions such as RDX, HMX and GTN. Another concern comes from the fact that many of the plant species studied for phytoremediation purposes are aggressive non-native species. The use of non-native plant species can cause considerable economic burden and environmental degradation by displacing valuable native plant and animal species (Susarla *et al*, 2002). However, the use of genetic engineering can

overcome many of the potential constraints associated with phytoremediation. For example, the introduction and expression of microbial genes into plant systems for the remediation of explosive compounds has recently come under investigation. Despite the innate ability of plants to transform TNT, plants commonly exhibit a range of adverse effects upon exposure to low TNT concentrations: Such effects include, stunted or inhibited root growth and bleaching. French *et al.*, (French *et al.*, 1999) demonstrated that the introduction and expression of the bacterial enzyme PETN reductase into tobacco plants resulted in the transgenic plants being able to tolerate and detoxify TNT concentrations that are commonly found in contaminated sites and which normally inhibit the growth of wild-type seedlings. Hence, given the appreciable amount of research conducted on isolating microbial enzymes that mediate explosive degradation pathways, the approach of engineering transgenic plants to remove toxic compounds has the potential of being an efficient strategy for remediating explosive contaminated soil and water. Further investigations into the efficacy and any limitations that may be associated with this technique are being undertaken. In addition, ongoing research is being undertaken to explore the differential routes of TNT/nitroaromatic degradation and the toxicity of products/intermediates produced. Understanding of the mechanism of nitroaromatic breakdown pathways and the associated toxicity of by-products in combination with genetic manipulation, promises to be an additional improvement for remediation purposes. For example, engineering key enzymes to catalyse specific reactions for the production of less toxic products in combination with the use of transgenic plants may prove to be an efficient and desirable strategy for explosive remediation.

1.3 Transformation pathways for nitro-substituted compounds

The most widely used nitroaromatic compound is TNT, which has been extensively used in explosives since 1902 (Higson, 1992). TNT is known to be more recalcitrant than mono- and dinitrotoluenes due to the presence of three nitro groups and their symmetric location on the aromatic ring. Therefore, the chemical structure of nitroaromatic compounds influences their biodegradation (Esteve-Nunez *et al.*, 2001).

1.3.1 Chemistry of TNT

The use of X-ray excited Auger electron spectroscopy has enabled detailed investigation into the arrangement of electrons in explosive molecules. Unlike electron beams, this technique uses soft X-rays which are gentle enough to excite the electrons within the atoms of the nitroaromatic compound without causing the explosive to detonate (Science News, 1987). The nitro groups on TNT consist of the highly electronegative atoms, N and O, with the oxygen atom being more electronegative than the nitrogen atom. Consequently, the N-O bond becomes polarised and the nitrogen atom retains a net positive charge (Riefler and Smets, 2002; Preub and Rieger, 1995). The nitro groups are therefore highly susceptible to reduction, thus nitroaromatic compounds are subject to initial reductive transformation reactions (Heiss and Knackmuss, 2002). In addition, the strong electron withdrawing nature of the nitro groups on TNT leads to the withdrawal of π -electrons from the aromatic ring, making the nucleus electrophilic. This further renders nitroaromatic compounds less susceptible to oxidative transformation reactions by oxygenases, adding to their recalcitrant nature. Reduction of the nitro groups on aromatic rings is widely distributed among living organisms. The rate of nitro group reduction is determined by the chemical properties of the whole molecule and is therefore influenced by the electrochemical nature of other substituents present on the ring. Typically, the rate of nitro group reduction increases with the increasing electronegativity of functional groups located at the *para* position to the nitro group. Hence, the order of the following substituents $\text{NH}_2 < \text{OH} < \text{H} < \text{CH}_3 < \text{COOH} < \text{NO}_2$ corresponds to their enhancing effect on the rate of nitro group reduction in nitroaromatic compounds. Consequently, reduction of one nitro group to the corresponding amino group will increase the electron density of the aromatic ring, which leaves the molecule and any remaining nitro groups less susceptible to reduction (McCormick *et al.*, 1976; Preub and Rieger, 1995).

The structure of TNT can be pictured as the resonance hybrid of several canonical forms, owing to the symmetrical location of the electronegative nitro groups (Rieger and Knackmuss, 1995; Figure 1.2). The resonance stabilisation of TNT enhances the electrophilicity of the C3 and C5 atoms, which allows the addition of hydride equivalents to the aromatic ring facilitating reduction of the compound. Hence, reduction of nitroaromatic compounds can proceed via two distinct mechanisms; (i) reduction of the nitro groups by classical nitroreductases (Section 1.3.2) and (ii) reduction of the aromatic ring (Section 1.3.3).

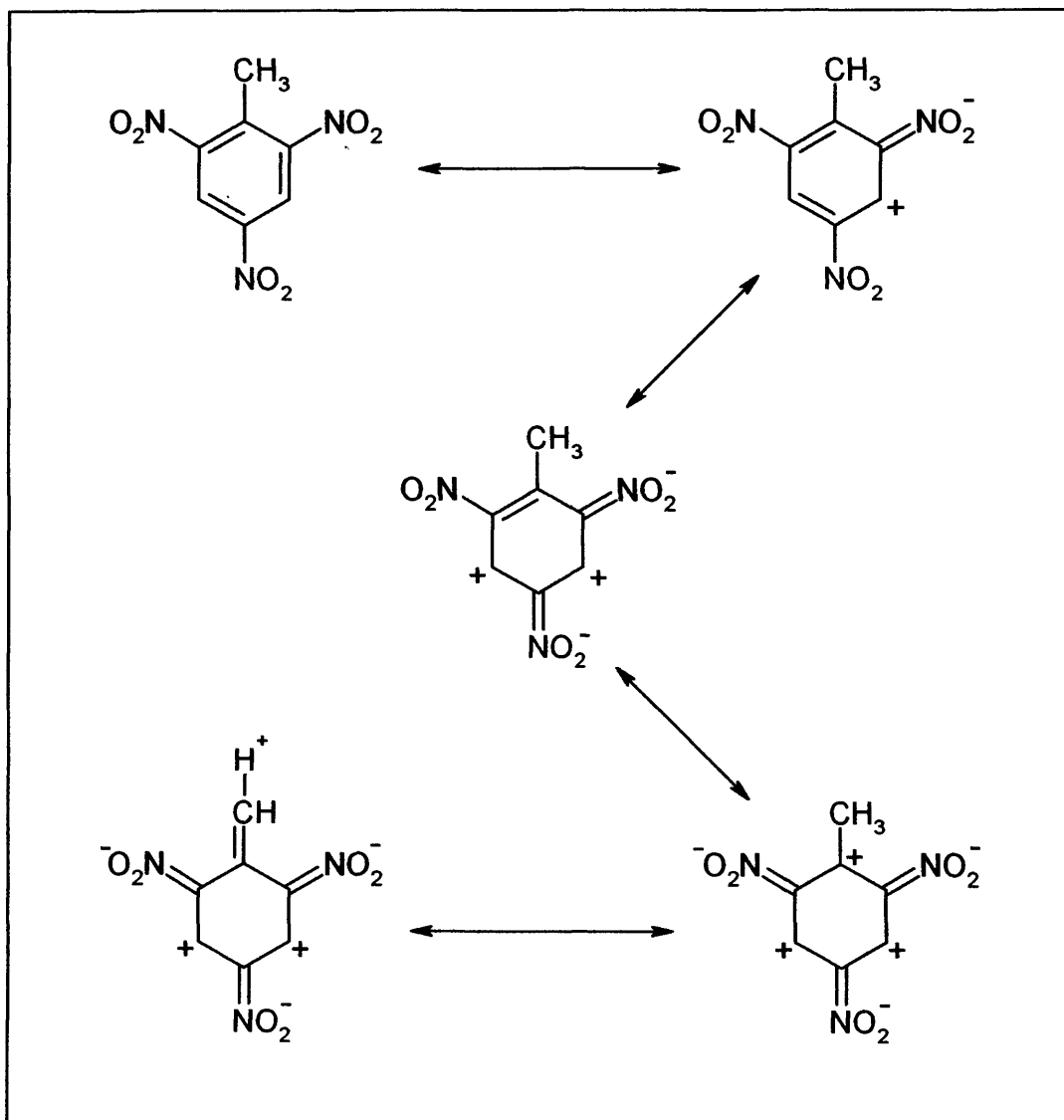


Figure 1.2. The different resonance hybrid stabilised forms of TNT. The symmetrical location of the electronegative nitro groups allows TNT to adopt several resonance stabilised forms. Consequently, the electrophilicity of the C3 and C5 atoms of TNT is enhanced allowing nucleophilic attack to take place at these positions.

1.3.2 Reduction of TNT nitro-groups by nitroreductases

For manifestation of their therapeutic and/or toxic properties, most nitroaromatic compounds are activated by either one-electron or two-electron enzymatic reduction (Cenas *et al*, 2001). Enzymes which catalyse the reduction of nitroaromatic compounds using reduced pyridine nucleotides are termed nitroreductases and are distinguished by their sensitivity of activity to oxygen (Kobori *et al*, 2001). Oxygen-sensitive (Type II) nitroreductases catalyse one-electron transfer reactions to nitro groups to form a nitroanion radical intermediate. In the presence of oxygen the radical is re-oxidised back to the parent compound while molecular oxygen is reduced to a superoxide anion radical (Figure 1.3). Therefore, a futile cycle is established where reducing equivalents are consumed without the progress of nitro group reduction and the nitroaromatic rather serves as a free radical mediator (Shah and Spain, 1996). This futile cycle can cause oxidative stress by producing large amounts of superoxide (Koder *et al*, 2002). Oxygen-sensitive nitroreductases can therefore only mediate reduction of nitroaromatic compounds under anaerobic conditions (Watanabe *et al*, 1998). Enzymes which catalyse the single-electron reduction of nitroaromatics include; NADPH-cytochrome P450 oxidoreductase, NAD(P)H cytochrome b₅ oxidoreductase and ferredoxin NADP⁺ oxidoreductase from spinach and *Anabaena* PCC7119 (Nivinskas *et al*, 2000; Shah and Spain, 1996; Anusevicius *et al*, 1999).

The most widespread and investigated mechanism of nitro-group reduction is the two-electron reduction of nitroaromatics. Enzymes that catalyse the obligatory two-electron reduction of nitroaromatic compounds are classed as oxygen-insensitive (Type I) nitroreductases. Reduction of the nitro groups via a series of two-electron transfer steps, yields nitroso, hydroxylamino, and finally amino derivatives of the parent compound (Kobori *et al*, 2001). The nitroso and hydroxylamine intermediates are extremely reactive and account for much of the toxicity and carcinogenicity associated with nitroaromatic compounds (Banerjee *et al*, 1999; Honeycutt *et al*, 1996; Rafii *et al*, 1994; Zaripov *et al*, 2002). Enzymes with oxygen-insensitive nitroreductase activity include nitroreductase from *Enterobacter cloacae* (Byrant *et al*, 1991; Haynes *et al*, 2002), nitroreductases from *E. coli* (Nfs A, B, C; Kobori *et al*, 2001), the *Salmonella enterica serovar typhimurium* TA1535 nitroreductase, SnRA (Nokhbeh *et al*, 2002) and NAD(P)H:quinone oxidoreductase (formerly known as DT-diaphorase; Cenas *et al*, 2001), among many others (see Table 1.1).

Reduction of TNT is hypothesised to occur via a radical anion reduction mechanism. In the first step of this mechanism, TNT accepts an electron which is delocalised over the nitro groups leading to the formation of a transient nitroanion radical (Figure 1.3). The second

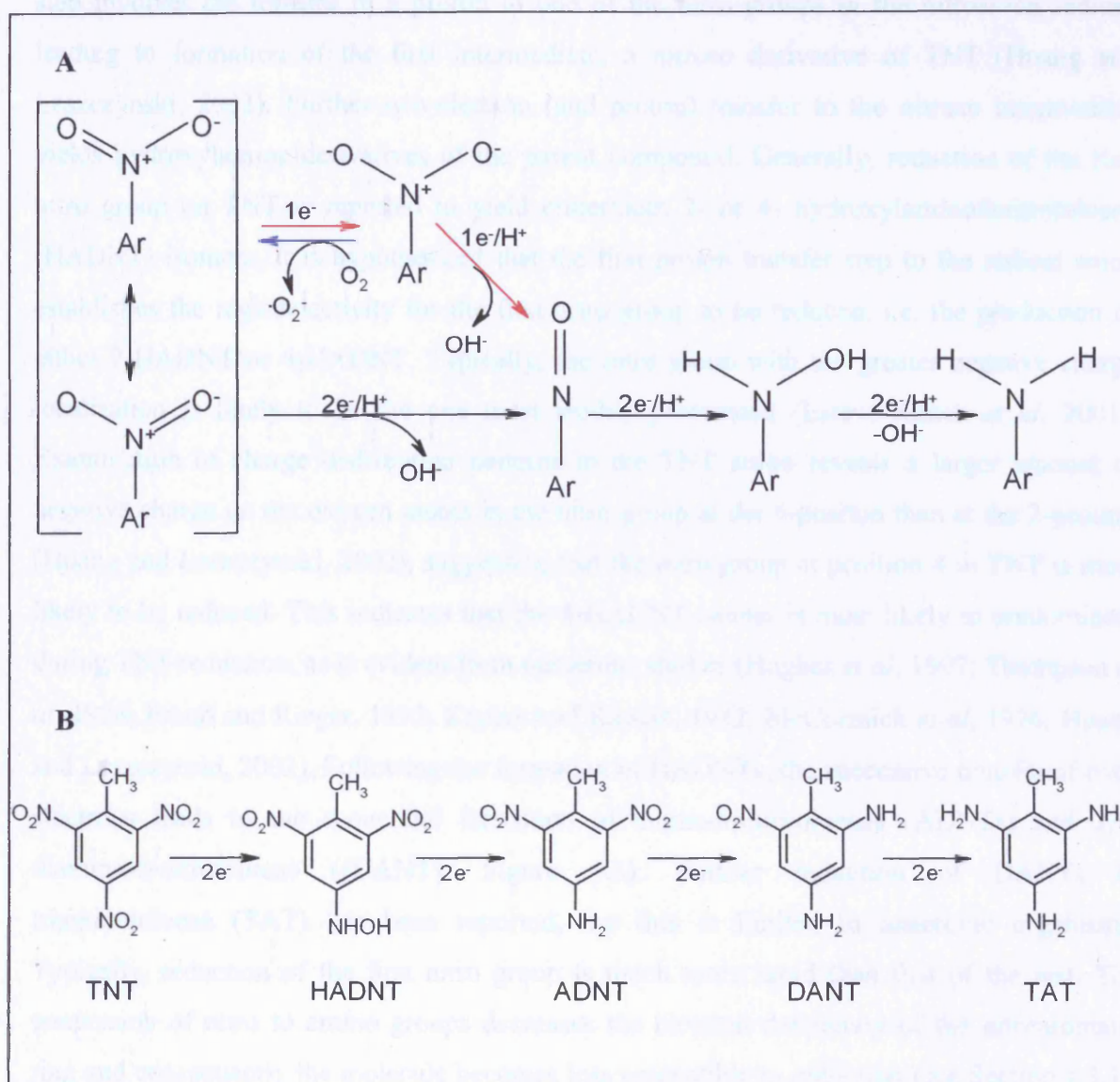


Figure 1.3. Mechanism for the reduction of nitro groups in nitroaromatic compounds. Panel A, the first step in the reduction of nitro groups can be achieved through one-electron transfer (red arrows) or two-electron transfer (black arrows). The first mechanism produces a nitroanion radical that can react with oxygen to form a superoxide radical and the parent nitro-compound through a futile cycle (blue arrows). Reduction via two-electron transfers leads to the formation of a nitroso derivative. Further two-electron transfers leads to the consecutive formation of a hydroxylamine and amine group. Panel B, reduction of TNT nitro groups via two-electron transfers leads to the successive formation of hydroxylaminodinitrotoluene (HADNT) via the formation of a nitroso derivative (not shown), aminodinitrotoluene (ADNT), diaminonitrotoluene (DANT) and under anaerobic conditions, complete reduction to triaminotoluene (TAT). (Figure adapted from Esteve-Nunez *et al*, 2001 and Spain, 1995).

step involves the transfer of a proton to one of the nitro groups in the nitroanion radical, leading to formation of the first intermediate, a nitroso derivative of TNT (Huang and Leszczynski, 2002). Further two-electron (and proton) transfer to the nitroso intermediate yields hydroxylamine derivatives of the parent compound. Generally, reduction of the first nitro group on TNT is reported to yield either/both 2- or 4- hydroxylaminodinitrotoluene (HADNT) isomers. It is hypothesised that the first proton transfer step to the radical anion establishes the regioselectivity for the first nitro group to be reduced, i.e. the production of either 2-HADNT or 4-HADNT. Typically, the nitro group with the greater negative charge localisation is likely to be the one most readily protonated (Esteve-Nunez *et al*, 2001). Examination of charge distribution patterns in the TNT anion reveals a larger amount of negative charge on the oxygen atoms in the nitro group at the 4-position than at the 2-position (Huang and Leszczynski, 2002), suggesting that the nitro group at position 4 in TNT is most likely to be reduced. This indicates that the 4-HADNT isomer is most likely to predominate during TNT reduction, as is evident from numerous studies (Hughes *et al*, 1997; Thompson *et al*, 1998; Preuß and Rieger, 1995; Kaplan and Kaplan, 1982, McCormick *et al*, 1976; Huang and Leszczynski, 2002). Following the formation of HADNTs, the successive transfer of two-electrons leads to the sequential formation of aminodinitrotoluenes (ADNTs) and 2,4-diamino-6-nitrotoluene ([DANT]; Figure 1.3). Further reduction of DANTs to triaminotoluene (TAT) has been reported, but this is limited to anaerobic organisms. Typically, reduction of the first nitro group is much more rapid than that of the rest. The conversion of nitro to amino groups decreases the electron deficiency of the nitroaromatic ring and consequently the molecule becomes less susceptible to reduction (see Section 1.3.1). As a result, the formation of the fully reduced product, TAT, requires reduction potential values below -200 mV, which are only found in anoxic environments (Spain 1995a; Esteve-Nunez *et al*, 2001). Therefore, ADNTs have generally been reported to be the end-point of aerobic TNT transformation (Duque *et al*, 1993; Fiorella and Spain, 1997; see Table 1.1).

As outlined above, many bacterial species are capable of nitro-group reduction. The enzymes involved in this process are typically soluble flavoproteins that use NADPH/NADH as electron donors. For these enzymes, TNT reduction is believed to be a gratuitous reaction, which does not appear to benefit the organism from which the enzymes are purified from. This is in contrast to an uncharacterised reductase in *Pseudomonas sp.* strain JLR11, which, in the absence of other terminal electron acceptors is able to use TNT as a final electron acceptor in its respiratory chain (Esteve-Nunez *et al*, 2000).

1.3.3 Hydrogenation of the aromatic ring system in nitroaromatic compounds

The strong electron withdrawing character of the nitro groups renders the π -system of nitroaromatics increasingly electron deficient with increasing number of nitro substituents. Consequently, this makes the aromatic nucleus of TNT highly amenable to nucleophilic attack, providing an alternative mechanism for the reduction of nitroaromatic compounds (Vorbeck *et al*, 1998; Esteve-Nunez *et al*, 2001). Reduction of the aromatic ring system via hydride addition seems to be a rare initial reaction observed mostly in gram-positive bacteria (Heiss and Knackmuss, 2002). Hydrogenation of the aromatic ring generates hydride-Meisenheimer complexes. As mentioned previously (Section 1.3.1), the different resonance stabilisation forms of TNT enhances the electrophilic nature of the C3 and C5 atoms in particular. Consequently, these atoms on the aromatic ring are most likely to accept a hydride ion, generating the hydride-Meisenheimer complex of TNT ([H-TNT]; Figure 1.4). Subsequent to H-TNT complex formation, the successive transfer of another hydride ion to the C5 atom of the H-TNT complex (where the C3 atom is hydrogenated) generates the dihydride-Meisenheimer complex of TNT (2H-TNT; Figure 1.4). Formation of these Meisenheimer complexes has been proposed to facilitate the removal of a nitro group from nitroaromatic compounds, leading to eventual nitrite release (Esteve-Nunez *et al*, 2001). Duque and co-workers (Duque *et al*, 1993) isolated a *Pseudomonas* strain from soil around an explosive factory and found that it was able to grow with TNT as its sole nitrogen source. The identification of dinitrotoluenes (DNTs), mononitrotoluenes (MNTs), toluene and the accumulation of nitrite in the culture supernatant indicated the sequential removal of all three nitro groups. It was subsequently proposed that the release of nitrite from TNT by this *Pseudomonas* strain occurs via the production of a Meisenheimer complex (Haidour and Ramos, 1996; Ramos *et al*, 1995). Subsequently, rigorous evidence for the conversion of TNT to the corresponding H-TNT complex was provided by Vorbeck and co-workers (Vorbeck *et al*, 1994). Resting cells of *Mycobacterium* sp. strain HL 4-NT-1 pre-grown with 4-nitrotoluene, converted TNT by hydride addition at the C3 atom to the respective Meisenheimer complex. The major metabolite produced was the hydride-Meisenheimer complex (40 %), in addition to a small amount of 4-ADNT (5 %) and another unidentified metabolite, indicating the importance of hydride addition in TNT degradation. Although a small amount of nitrite was released, no DNTs were detected (Vorbeck *et al*, 1994).

The formation of Meisenheimer complexes as a metabolite has also been reported to occur during the transformation of other polynitroaromatic compounds; in particular for 2,4,6-

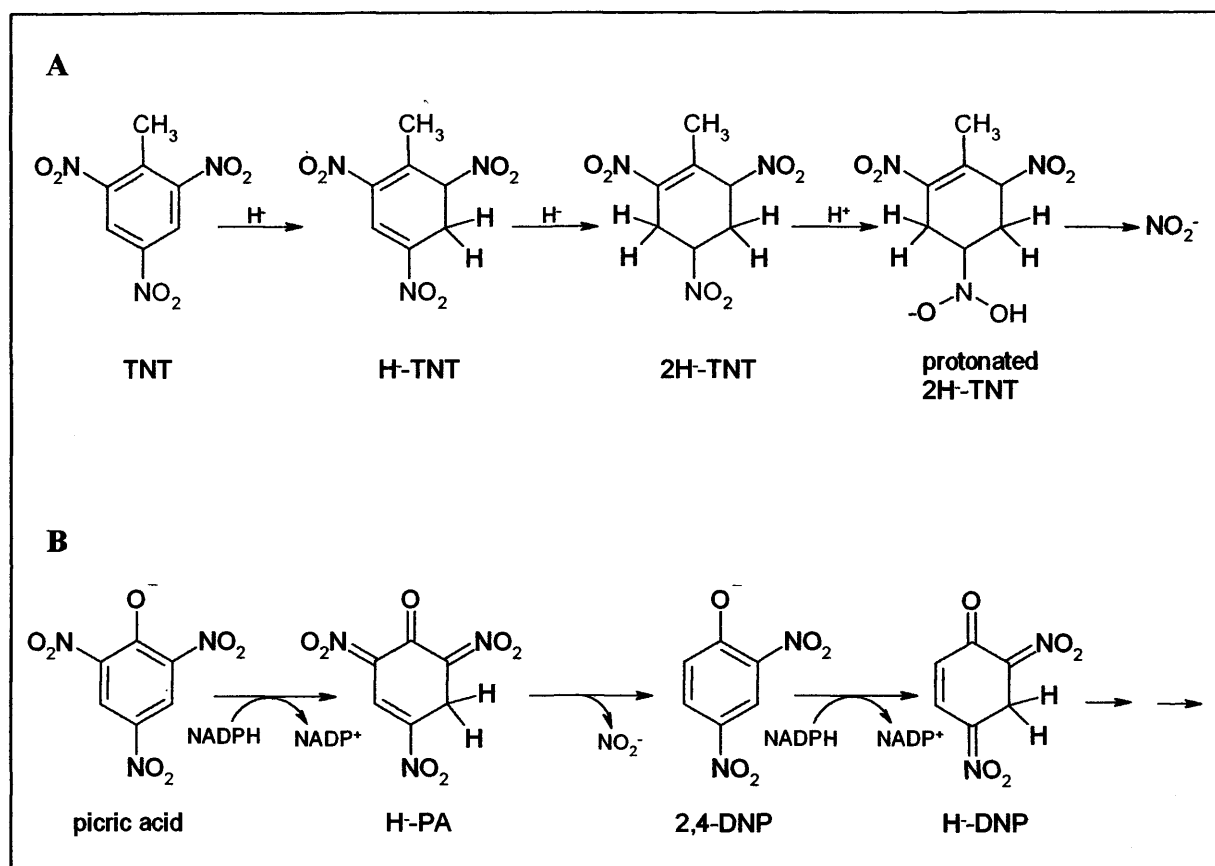


Figure 1.4. Hydrogenation reactions of TNT and picric acid. Panel A, hydride addition to the aromatic ring of TNT yields the hydride-Meisenheimer complex of TNT (H-TNT). Further hydride addition leads to the formation of a dihydride-Meisenheimer complex (2H-TNT). The protonated form of the 2H-TNT complex has also been identified during the reduction of TNT. Subsequent reactions leading to nitrite release have not yet been identified. Panel B, reductive denitration mechanism for picric acid transformation. The first step leads to the formation of the hydride-Meisenheimer complex of picric acid (H-PA). Subsequently, re-aromatisation of the ring and nitrite release leads to the formation of 2,4-DNP. The formation of a hydride-Meisenheimer complex of 2,4-DNP (H-DNP) has also been identified during the transformation of picric acid. (Figure adapted from Vorbeck *et al*, 1998 and Behrend and Heesche-Wagner, 1999).

trinitrophenol (picric acid) and 2,4-dinitrophenol (2,4-DNP). These compounds are structurally similar to TNT except a hydroxyl group replaces the methyl group of TNT. Lenke *et al*, (Lenke *et al*, 1992; Lenke and Knackmuss, 1992) isolated a *Rhodococcus erythropolis* strain able to use 2,4-DNP as a sole nitrogen source. Accumulation of 4,6-dinitrohexanoate in the culture medium indicated that the degradation of 2,4-DNP might occur via hydrogenation of the aromatic ring (Lenke *et al*, 1992). Additional support for this mechanism came from observations of *R. erythropolis* being able to utilise picric acid as a substrate and nitrogen source. During the growth of the strain, a temporary orange-red colour of the culture medium was observed, which was attributed to the formation of the hydride-Meisenheimer complex of picric acid (H⁻PA). Recently, Rieger and co-workers (Rieger *et al*, 1991) confirmed the formation of this H⁻PA complex by comparing the spectral properties of the orange metabolite to that of the synthesised authentic standard form of the H⁻PA complex. Furthermore, based on the identification of metabolites like 2,4-DNP and 4,6-dinitrohexanoate, which also form during the degradation of picric acid, the production of the Meisenheimer complex was confirmed to be a central intermediate in the degradation of picric acid. Consequently, Rieger *et al*, (Rieger *et al*, 1999) proposed a reductive denitration mechanism for the transformation of picric acid (Figure 1.4). In the first step of picric catabolism by *R. erythropolis* HL PM-1, the addition of a hydride ion to the aromatic ring system generates the hydride-Meisenheimer complex of picric acid. Following on, the production of the protonated form of the H⁻PA complex is proposed to provide a reactive intermediate for nitrite elimination. Subsequent to H⁻PA complex protonation, re-aromatisation of the ring occurs leading to the elimination of nitrite and formation of 2,4-DNP. A similar mechanism for picric acid metabolism has been identified in *Nocardioides* sp. strain CB 22-2 (Behrend and Heesche-Wagner, 1999). Consequently, this reductive denitration mechanism seems to be a common route for the degradation of picric acid. However, because of the difficulty in lysing cells, the enzymes involved in picric acid metabolism have until now remained unknown.

Recently, Heiss *et al* (Heiss *et al*, 2002) identified a gene cluster involved in picric acid degradation, in *R. erythropolis* HL PM-1. The functional assignment of these genes named *npd* (for nitrophenol degradation) and characterisation of their proteins was reported (Figure 1.5). Npd I, a hydride transferase (hydride transferase II), catalyses the hydride transfer from reduced F₄₂₀ to the aromatic ring of picric acid, generating the H⁻PA complex. Npd C, a second hydride transferase (hydride transferase I), catalyses the hydride transfer from F₄₂₀ to H⁻PA, giving rise to a dihydride-Meisenheimer complex of picric acid (2H⁻PA).

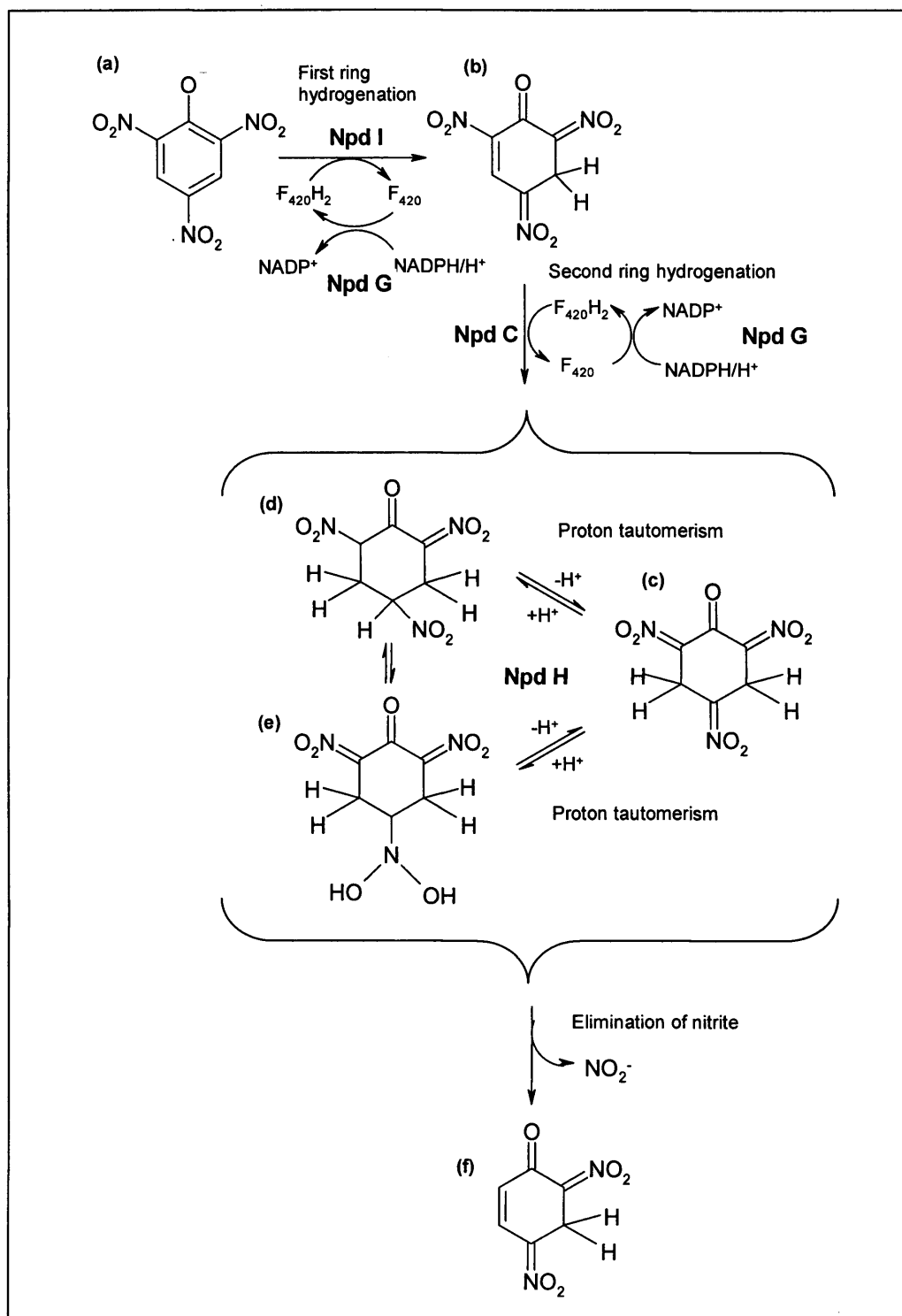


Figure 1.5. Proposed picric acid degradation pathway in *R. (opacus) erythropolis* HL PM-1. (a) picric acid; (b) H-PA; (c) 2H-PA; (d) and (e) tautomeric forms of the protonated 2H-PA; (f) H-DNP. Npd C, hydride transferase I; Npd G, NADPH-dependent F_{420} reductase; Npd H, converts 2H-PA to a tautomer of the protonated 2H-PA; Npd I, hydride transferase II. (Figure taken from Heiss and Knackmuss, 2002).

All reactions required the activity of Npd G, an NADPH-dependent F_{420} reductase, for shuttling hydride ions from NADPH to F_{420} . Npd H converted $2H^-$ -PA to an unknown product, suggested to be a tautomeric form of the protonated $2H^-$ -PA, which may be required to facilitate the subsequent release of nitrite, generating 2,4-DNP (Figure 1.5). A similar hydride transferring system has been reported for *Nocardioides simplex* FJ2-1A (Ebert *et al*, 1999). From this strain, a purified hydride transferase (and an NADPH-dependent F_{420} reductase) converted picric acid to the H^- -PA complex. In addition, the same transferase catalysed a second hydride transfer, converting H^- -PA to the $2H^-$ -PA complex (Ebert *et al*, 2001). Hence, the hydride transferase from *N. simplex* FJ2-1A appears to possess broader substrate specificity than the Npd I from *R. erythropolis* HL PM-1 (Ebert *et al*, 2001; Heiss and Knackmuss, 2002). In addition to the transformation of picric acid, the hydride transferases of *N. simplex* FJ2-1A and *R. erythropolis* HL PM-1 were also observed to convert 2,4-DNP to the respective hydride-Meisenheimer complex form (H^- -DNP). Formation of H^- -DNP as a metabolite of picric acid catabolism has been identified by Behrend and Heesche-Wagner (Behrend and Heesche-Wagner, 1999). Following the successive conversion of H^- -PA to 2,4-DNP by *Nocardioides* sp. strain CB 22-2, the formation of the hydride-Meisenheimer complex of 2,4-DNP was reported. However, the authors proposed that the enzyme which catalyses the hydride transfer to 2,4-DNP differs to that responsible for formation of the H^- -PA complex (Behrend and Heesche-Wagner, 1999). Consequently, the H^- -DNP complex has been proposed to be the product of nitrite release from $2H^-$ -PA in *N. simplex* FJ2-1A (Ebert *et al*, 2002) and also in *R. erythropolis* HL PM-1, given that cell extracts of *R. erythropolis* convert $2H^-$ -PA to H^- -DNP (Heiss and Knackmuss, 2002). Hence, H^- -DNP is suggested to be a true metabolite of picric acid degradation.

Since re-aromatisation and nitrite release was well established for picric acid metabolism, Duque *et al* (Duque *et al*, 1993) suggested that a corresponding reductive denitration mechanism may operate with TNT in *Pseudomonas* sp. clone A. Initially, Haidour and Ramos (Haidour and Ramos, 1996) reported the formation of 2,4-dinitrotoluene as a result of the *in vitro* metabolism of the H^- -TNT complex by this strain. However, Vorbeck and co-workers (Vorbeck *et al*, 1998) demonstrated that *Pseudomonas* sp. clone A does not produce or convert the H^- -TNT complex. Instead, only nitro-reduced products were identified as dead-end metabolites. Vorbeck *et al* (Vorbeck *et al*, 1998) further investigated whether the reductive denitration of TNT occurs with *R. erythropolis* HL PM-1 and *Mycobacterium* sp. Hl 4-NT-1. These organisms were unable to utilise TNT as a nitrogen source, but were able to produce the H^- -TNT and $2H^-$ -TNT complexes. These complexes were analogous to the

complexes of picric acid, but further denitrated products such as 2,4- or 2,6- dinitrotoluene, were not observed. However, further conversion of the 2H-TNT complex to a yellow metabolite by *R. erythropolis* was reported. This metabolite was identified as the protonated form of 2H-TNT (Vorbeck *et al*, 1998). This protonated complex is comparable to the proposed tautomeric protonated 2H-PA complex catalysed by Npd H of the same strain (Heiss *et al*, 2002). Other groups have also detected several protonated forms of 2H-TNT (Pak *et al*, 2000; French *et al*, 1998). On the whole, the reductive denitration mechanism proposed for picric acid catabolism has not yet been identified for the degradation of TNT.

The first report on the reduction of the aromatic ring system and concomitant nitrite release from TNT by a purified enzyme was by French *et al* (French *et al*, 1998). They purified the enzyme PETN reductase from *Enterobacter cloacae* PB2, which was able to reduce TNT to the H-TNT complex, with concomitant NADPH oxidation and release of nitrite. The enzyme also catalysed the conversion of the H-TNT complex to the 2H-TNT complex. In addition, based on the identification of HADNTs and ADNTs, it was suggested that the enzyme also had nitroreductase activity (French *et al*, 1998). Recently, Pak and co-workers (Pak *et al*, 2000) reported on the characterisation of another purified enzyme, Xenobiotic reductase B from *Pseudomonas fluorescens* I-C, able to convert TNT to the H-TNT and 2H-TNT complex, in addition to reducing the nitro groups. Furthermore, the authors proposed that the non-enzymatic dimerisation of the 2H-TNT complex with a 4-HADNT isomer, leading to formation of amino-dimethyltetranitrobiphenyl, causes the eventual liberation of nitrite (Pak *et al*, 2000). Hence, they put forward the idea of cross-talk between the nitroreductase and hydrogenation pathway in a single enzyme system. However, recently the results of Williams *et al* (Williams *et al*, 2004) have contradicted this idea (see Chapter Three).

Given the extensive research conducted on hydrogenation of the aromatic ring system in nitroaromatic compounds, identification of the Meisenheimer complexes has been made simple. Formation of each complex during picric acid and TNT turnover can typically be characterised by their colour and more precisely by their spectral properties.

1.3.4 Reduction of nitrate esters

Nitrate esters such as glycerol trinitrate (GTN) and pentaerythritol tetranitrate (PETN) are widely manufactured as explosives and as pharmaceutical vasodilators in the treatment of angina (Accashian *et al*, 1998). Consequently, their exploitation in these applications has led

to significant contamination of land sites and water, causing environmental concern. Given the rarity of these compounds in nature, the discovery of micro-organisms able to transform such compounds is of particular interest. In addition, an investigation into the metabolic pathways and the mechanism by which nitrate esters are transformed may provide an insight into their pharmaceutical mode of action. Although there is widespread agreement that nitrate esters are reduced to nitric oxide (NO), which eventually leads to smooth muscle relaxation, the exact mechanism by which NO is generated is still unknown (Wong and Futuko, 1999; Doel *et al*, 2001).

Blehert *et al* (1997) isolated from GTN contaminated land two species of *Pseudomonas* capable of utilising GTN as a sole nitrogen source. The two species identified as *P. putida* II-B and *P. fluorescens* I-C, produced different mixtures of the isomer of glycerol dinitrate (1,2- and 2,3- GDN) and glycerol mononitrates (GMNs). The sequential reduction of GTN to GDNs and GMNs by these strains was found to be mediated by NADPH-dependent GTN reductases. The purified reductase from *P. putida* II-B was observed to selectively denitrate the C3 nitro group from GTN and the C1 nitro group of 1,2-GDN, suggesting a preference for the removal of terminal nitro groups. In contrast, the purified reductase from *P. fluorescens* I-C had a higher selectivity for the C2 position of GTN. Neither enzyme could denitrate GMNs to yield glycerol (Blehert *et al*, 1997). White and Snape (White and Snape, 1993) also reported on the ability of an *Agrobacterium radiobacter* strain capable of utilising GTN as a sole nitrogen source. Pure cultures of *A. radiobacter* reduced GTN to mainly 1,3-GDN and small amounts of the corresponding 1,2-GDN isomer, with concomitant formation of nitrite. Cells were able to denitrate both isomers to 1- and 2- GMNs, but not beyond. In addition, the denitration of PETN to tri- and di-nitrates was also observed with this strain (White and Snape, 1993). An NADH-dependent GTN reductase was subsequently purified from *A. radiobacter* (Snape *et al*, 1997) and was observed to mediate the reduction of GTN to GDN (yielding mainly the 1,3-GDN isomer) only. Binks *et al* (Binks *et al*, 1996) also observed a similar activity in cell extracts of *Enterobacter cloacae* PB2. The purified recombinant protein originally isolated from *E. cloacae* was shown to produce nitrite during the NADPH-dependent denitration of GTN. No analysis on the regioselectivity of nitro group removal was reported. The first report for the complete denitration of GTN was reported for cell extracts of *Bacillus thuringiensis/cereus* and *Enterobacter agglomerans* (Meng *et al*, 1995). These strains were effective in transforming GTN to GDN isomers, GMN isomers and glycerol. In addition, Accashian *et al*, (Accashian *et al*, 1998) also reported on the ability of a mixed microbial culture to grow on GTN as the sole carbon, nitrogen and energy source. The

biotransformation of GTN by this mixed culture resulted in the accumulation and subsequent removal of GDN and GMN esters. The complete denitration of GTN is desirable for detoxification purposes, as GDNs and GMNs retain some toxic properties (Accashian *et al*, 1998).

Previous studies investigating the transformation of GTN by bacterial cultures have generally shown that nitrate ester reduction is mediated by a flavoprotein (Blehert *et al*, 1997; Snape *et al*, 1997; White *et al*, 1996). Subsequently, it has been suggested that a flavoprotein may be involved in the bioactivation of organic nitrate esters to NO in mammalian muscle cells. Wong and Fukuto (Wong and Fukuto, 1999) demonstrated that FMN is capable of catalysing the reduction of organic nitrate esters by NAD(P)H to reduced nitrogen species (nitrite esters), which may be a precursor to NO formation. The mammalian flavoprotein, xanthine oxidoreductase, has also recently been reported to catalyse the reduction of GTN to inorganic nitrite/NO (Doel *et al*, 2001). More recently, however, a mammalian nitrate reductase purified from mammalian mitochondrial cells has been shown to specifically catalyse the conversion of GTN to 1,2-GDN and nitrite. These compounds have been suggested to be the predominant metabolites in vascular smooth muscle cells. The purified protein has been identified as mitochondrial aldehyde dehydrogenase (mtALDH) and has been demonstrated to catalyse the biotransformation of GTN predominantly in mitochondrial cells. Production of nitrite from the denitration of GTN is suggested to be an obligate intermediate in the generation of NO bioactivity i.e. vascular smooth muscle relaxation (Chen *et al*, 2002).

The transformation of nitro-substituted compounds via the diverse pathways outlined above has generally been reported to be mediated by flavin-dependent enzymes. PETN reductase, the focus of the research outlined in this thesis, is also a flavoprotein. It would therefore seem appropriate that the next section should focus on the typical properties associated with flavins and the classification of proteins containing such co-factors.

1.4 Flavoproteins

Enzymes catalyse a large variety of reactions in cellular systems. The participation of certain active site residues in forming transient covalent bonds and charge-charge interactions underlies their ability to stabilise transition states necessary for catalysis. However, these

active site residues alone are insufficient in catalysing redox reactions as they are unable to store electrons. Hence, redox enzymes usually require the assistance of a coenzyme, co-factor, or prosthetic group to function. A coenzyme is a co-substrate that transiently associates with the enzyme during a reaction and is regenerated by another enzyme. Nicotinamides such as NADPH and NADH are typical examples of co-enzymes. A co-factor can be defined as a compound that participates in a reaction but remains bound to the enzyme in a catalytic cycle (Duine, 2001). When a co-factor is covalently bound to the apoprotein so that it is difficult to remove without damaging the enzyme, it is sometimes known as a prosthetic group. The most common co-factors employed by enzyme systems are flavins. Proteins that possess one or more flavin molecules as their co-factor are known as flavoproteins (or flavoenzymes).

Flavin is a generic term for a group of compounds that have a tricyclic isoalloxazine moiety in common. The name flavin is derived from the yellow colour exhibited by the isoalloxazine chromophore when in its fully oxidised state; *flavius* is Latin for yellow. Flavins are derivatives of riboflavin (vitamin B₂), where the N10 atom of the basic isoalloxazine moiety is connected to a ribityl side-chain (Figure 1.6). The two most common flavins found in flavoproteins are flavin mononucleotide (FMN) and flavin adenine dinucleotide (FAD; Muller, 1983). FMN consists of riboflavin phosphorylated at the ribityl 5-OH group, while FAD consists of FMN plus an additional adenine and phosphate moiety (Figure 1.6). In most cases, the flavin co-factors are tightly, but non-covalently, bound to the apoprotein (with dissociation constant often in the nanomolar range). However, there are a number of flavoproteins (25 or more) which covalently attach the flavin to an amino acid in the polypeptide chain. Flavoproteins that bind their flavin co-factors covalently fall into two categories; (i) those which bind the flavin at the 8 α -methyl group and (ii) those where the linkage is to the C6 atom of the isoalloxazine ring (Mewies *et al*, 1998; Decker, 1991).

Several hundred flavin-containing enzymes have been uncovered to date (Massey, 2000). Over two hundred entries have been made in the protein data bank (PDB) for FMN and FAD-dependent proteins (Fraaije and Mattevi, 2000). These flavoenzymes have been isolated and characterised from sources ranging from microbes to mammals, including humans (Miura, 2000). Hence, flavoenzymes are capable of catalysing a variety of biochemical reactions, ranging from dehydrogenation, electron transfer, activation of molecular oxygen and repair of damaged DNA (Yano, 2001; Massey, 2000). This unique feature of flavoenzymes is primarily attributed to the chemical versatility of the isoalloxazine

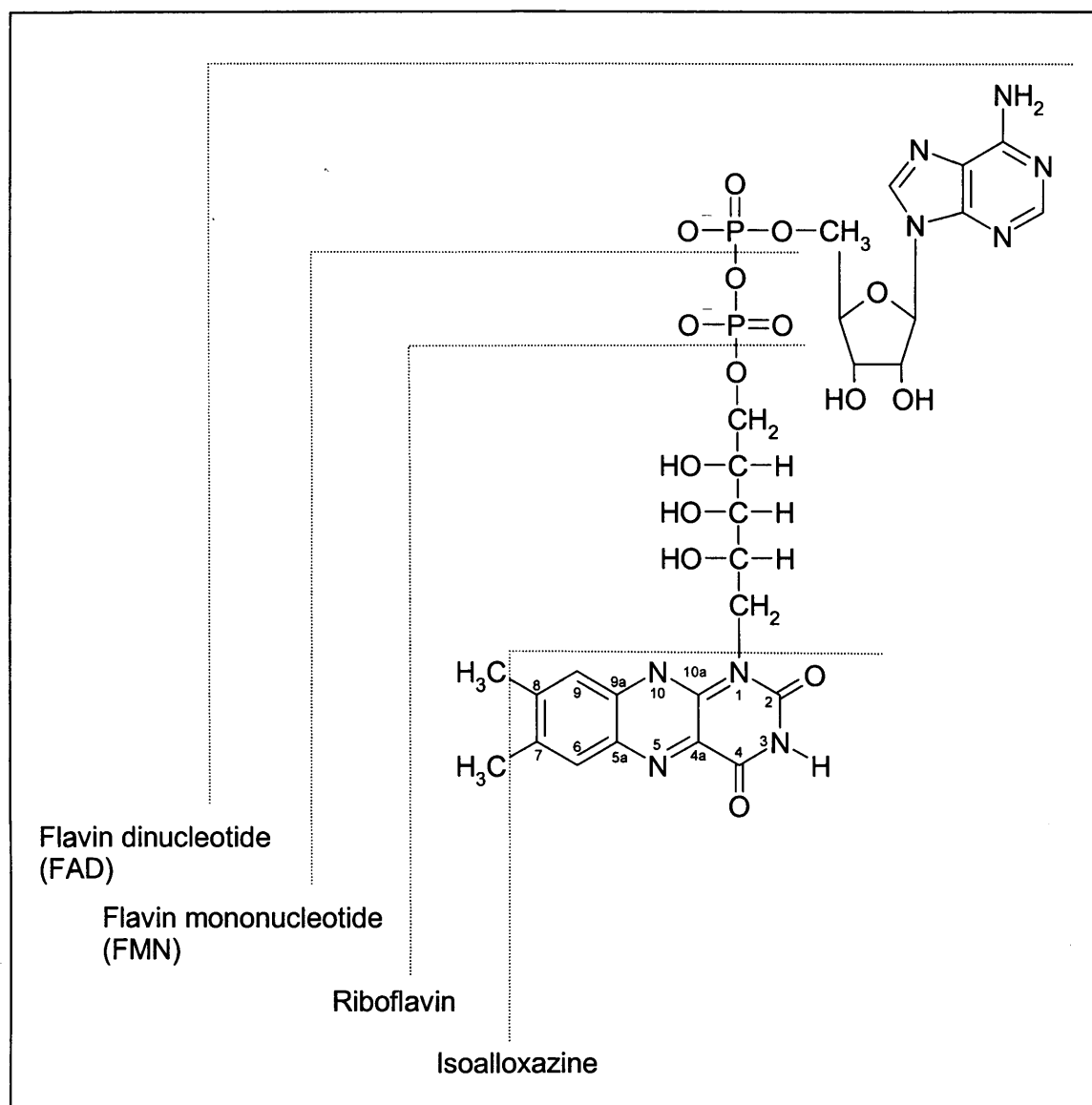


Figure 1.6. The structure of flavins and the numbering system for the isoalloxazine ring. Flavins are typically derivatives of riboflavin (vitamin B₂), where the N1 atom of the basic isoalloxazine moiety is connected to a ribityl side-chain. The two most common flavins found in flavoproteins are flavin mononucleotide (FMN) and flavin adenine dinucleotide (FAD). FMN consists of riboflavin phosphorylated at the ribityl 5-OH group, while FAD consists of FMN plus an additional adenine and phosphate moiety. (Figure adapted from Miura *et al.*, 2001).

ring, the basic unit which functions in catalysis (Fitzpatrick, 2001). Modulation of enzyme function is usually acquired by the protein component, where specific interactions (typically hydrogen bonds) between the protein and isoalloxazine ring serve to control the reactivity of the flavin nucleus (Palfey and Massey, 1998; Yano, 2001; Breinlinger *et al*, 1998).

1.4.1 Chemical properties of flavins

The chemically active portion of flavins is the isoalloxazine nucleus. The side-chain functions, such as the ribityl side chain and adenine moiety, simply serve to anchor the co-factor into the active site. The most prominent feature of flavins is their redox properties, hence flavoenzymes most commonly catalyse reactions involving the redox transformation of substrates (Muller, 1991). However, there are a few cases where the flavin molecule simply serves to generate a reactive enzyme-bound intermediate, via their redox chemistry. This is typically followed by the reversal of the activation reaction; hence no net redox transformation of the substrate occurs (Palfey and Massey, 1998). The importance of flavins in most redox reactions is largely attributed to their ability to undertake both one-electron and two-electron transfer reactions. This feature provides flavoproteins with the potential to transfer single electrons, hydrogen atoms or hydride ions (Dreyer 1984; Fitzpatrick, 2001). This vital property of flavins accounts for their broad involvement in biological reactions. In particular, flavoenzymes act as key mediators in respiratory chains, where they oxidise organic substrates or reduced pyridine nucleotides by two-electron transfers and subsequently pass one electron at a time to obligate one electron acceptors such as cytochromes and metal ion centres (Palfey and Massey, 1998; Massey, 2000). In addition, they are frequently found in enzymes containing multi-redox centres, such as succinate dehydrogenase, NADH dehydrogenase, xanthine oxidase and cytochrome P₄₅₀ systems (Massey, 2000).

The ability of flavins to undergo one- and two-electron transfer reactions implies that they must exist in different redox states. Evidently, flavin can exist in a reduced, semiquinone, and oxidised state. In addition, flavin is an amphoteric molecule, hence in all three states it can take the form of three species; neutral, cationic and anionic (Figure 1.7A; Muller, 1983; 1991). Fortunately, the different flavin redox/ionic states can be easily distinguished by their spectral properties (Figure 1.7B). Oxidised flavin (flavoquinone) is stable in solution and typically in its neutral form at pH values between 1 and 9. Oxidised flavin exhibits a strong absorbance band between 400 to 500 nm. The transfer of electrons to the flavin, typically affects the N1, C4a and N5 positions. Addition of a single electron (e.g. from dithionite) to

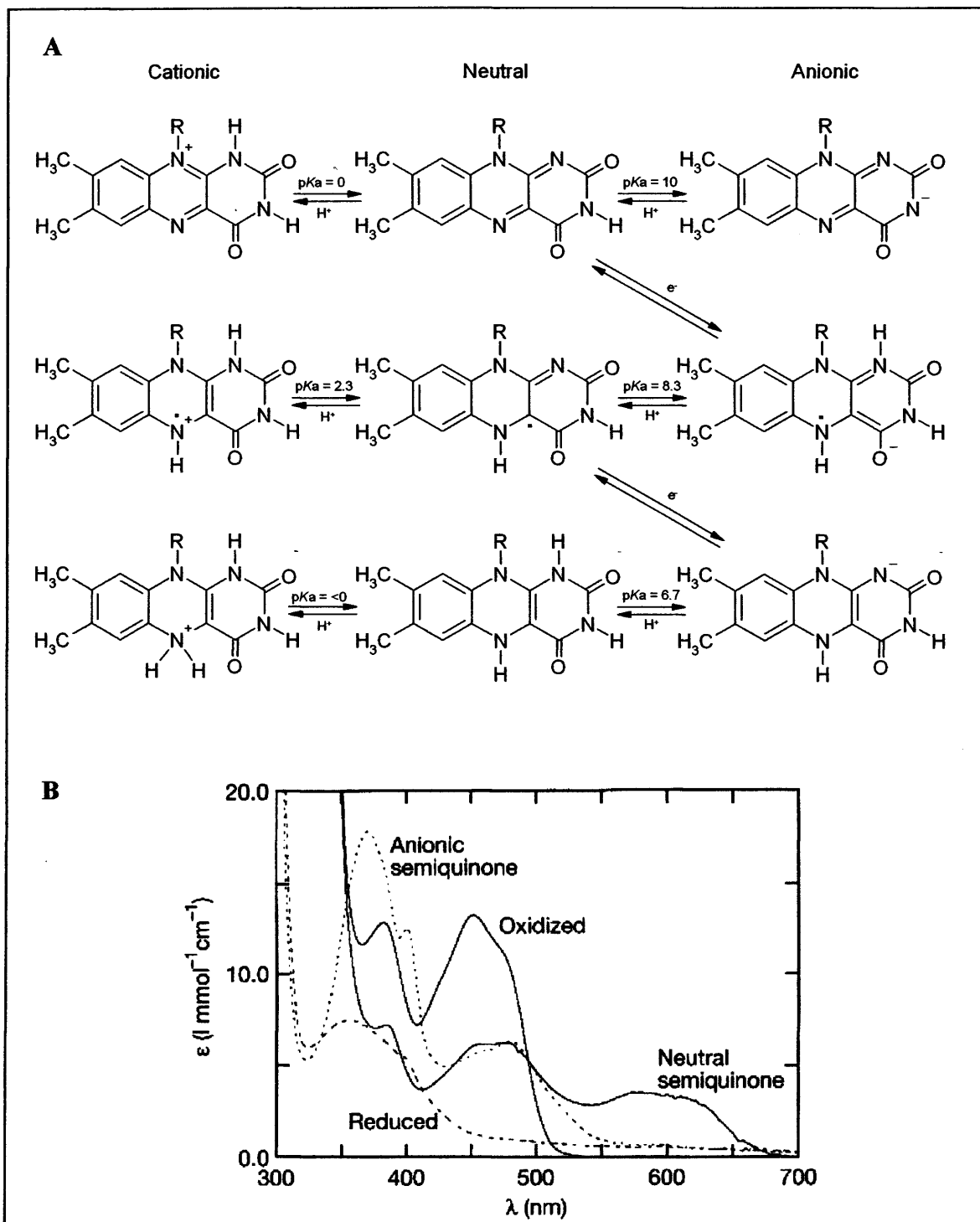


Figure 1.7. Redox and ionic states of flavin and the spectra for the physiologically possible semiquinones. Panel A, redox and ionic states of flavin. (Figure adapted from Miura *et al*, 2001); Panel B, absorption spectra for the different redox states of flavin. (Spectra are from the enzyme 2-methyl-3-hydroxypyridine-5-carboxylic acid oxygenase; Figure taken from Palfey and Massey, 1998).

the stable oxidised flavin ring yields a semiquinone radical flavin which is resonance stabilised. When bound to a protein, the stability of the flavin radical is enhanced and physiologically either the neutral or anion form is stabilised (Massey and Hemmerich, 1980). For the flavin to effectively mediate between one-electron and two-electron transfer, stability of the semiquinone state is important. The two physiological semiquinone forms of the flavin differ in their spectral characteristics (Figure 1.7B) and are therefore named after their characteristic colour. The neutral/protonated semiquinone has a broad absorbance band between 580 to 620 nm, and is therefore identified as the blue semiquinone. The anionic semiquinone displays a strong absorbance peak at 380 nm and is consequently known as the red semiquinone (Miura, 2000; Muller, 1983; 1991). Addition of another electron to the flavin produces the fully reduced form, 1,5-dihydroquinone. Reduction of oxidised flavin occurs reversibly by either (i) two direct one-electron transfer reactions between the flavin and other redox centres such as heme or iron-sulphur centres, or (ii) one two-electron transfer reaction, where hydride transfer to the flavin occurs via attack at the flavin N5 atom (Palfey and Massey, 1998). The flavin N5 position is highly electrophilic in many flavoenzymes and is therefore commonly the site of nucleophilic attack. Reduction of the flavin causes the bleaching of the broad absorbance band between 400 to 500 nm, typical of oxidised flavin. Fully reduced flavin is an effective reductant and consequently readily reacts with molecular oxygen. The potential for free flavin reduction is -207 mV at pH 7 but can be markedly lowered or increased in an approximate range of 600 mV by protein interactions (Ghisla and Massey, 1989). Hence, the reactivity of free flavin differs significantly from that of the apoprotein-bound flavin (Muller, 1983). Typical factors governing flavin reactivity in proteins include the control of solvent accessibility to the flavin nucleus, hydrogen-bond interactions made to the isoalloxazine moiety and the nature of residues located in close proximity to the flavin. The protein environment surrounding the isoalloxazine moiety therefore plays a critical role in controlling the broad reactivity potential of the flavin so that the true function of the flavoenzyme is enhanced and other potential reactions are suppressed.

In many flavoenzymes the flavin molecule is buried within the apoprotein in a hydrophobic active site. This location of the flavin controls solvent accessibility and modulates the redox potential of flavoproteins via specific interactions between amino acid residues and the isoalloxazine sub-function (Muller, 1983). The pyrimidine nucleus of the isoalloxazine moiety can be viewed as an “electron sink” due to its highly electron deficient nature (and therefore is easily reduced). Consequently, any interaction which lowers its electron/negative charge density will tend to increase its redox potential (i.e. ease of which it

accepts electrons). Therefore, the presence of a positive charge in the protein around the pyrimidine ring will increase the flavins redox potential and hence facilitates its reduction (Ghisla and Massey, 1989). In addition, it is generally observed that the presence of a positive charge near the flavin helps to stabilise the anionic semiquinone (Fraaije and Mattevi, 2000). In contrast, the presence of a negative charge near the isoalloxazine moiety will decrease the redox potential of the flavin (Ghisla and Massey, 1989).

Each flavoenzyme is characterised with a unique hydrogen-bonding network associated with the flavin. The flavin ring when oxidised and reduced has both hydrogen-bond donating and accepting sites. The N1, C2=O, C4=O and N5 of oxidised flavin and the C2=O and C4=O of reduced flavin are hydrogen-bond accepting sites, while the N3 of oxidised and reduced and N1 and N5 of reduced flavin can be either hydrogen-bond accepting or donating sites. Generally a hydrogen-bond made to oxidised flavin at a hydrogen-bond accepting site (N1, N5, C2=O, C4=O) reduces the electron density of the flavin and therefore enhances the ease of electron acceptance for oxidised flavin (i.e. facilitates flavin reduction). However, the same hydrogen bond to reduced flavin will decrease the electron density of reduced flavin and therefore reduce the electron donating property of reduced flavin as well (i.e. is therefore less favourable for substrate reduction). Therefore, this type of hydrogen bond will be favourable for the reductive half-reaction but unfavourable for the oxidative half-reaction of the flavoenzyme (Miura, 2000).

The N5 atom of the flavin is an important position and is generally believed to be the entry and exit point of electrons (Muller, 1983), therefore, any interaction involving this atom is likely to affect catalysis. Generally, a hydrogen-bond made to the (oxidised) N5 atom is expected to increase the electron acceptability of the flavin. However, following flavin reduction the N5 atom becomes protonated and so the same bond is likely to be energetically less favourable for the reduced form of the flavin (Fraaije and Mattevi, 2000). Hydrogen-bonding to the N5 atom is also thought to stabilise the neutral semiquinone form of the flavin. The reactivity of the N5 atom is also influenced by hydrogen-bonds made to other sites of the flavin. The occurrence of a hydrogen-bond at N1 position enhances the electrophilicity of the N5 (and N10) position, facilitating the reduction of flavin, but decreasing the reductive power of N5 ([i.e. in substrate reduction] Massey, 1995; Massey and Hemmerich, 1980; Dreyer, 1984; Yano, 2001).

In addition to the redox and ionic states of flavin there are other electronic states that flavin can adopt, known as charge-transfer states. This novel electronic state occurs when a partial charge is transferred to or from one of the three redox states. More precisely, charge-

transfer complexes are formed through the interactions between the highest occupied molecular orbital (HOMO) of an electron donor and the lowest unoccupied molecular orbital (LUMO) of an electron acceptor. This is not to be confused with the electron transfer process of flavoenzymes, which occurs through the transfer of electrons from an electron donor to an electron acceptor, while charge-transfer occurs via electron “sharing” between each molecule, i.e. more precisely, the interaction of π -orbitals between the electron donor and acceptor (Miura, 2000). Formation of charge-transfer interactions are generally characterised by the development of a broad absorbance band in the long wavelength region of the flavoenzymes spectrum.

Overall, each redox/ionic/electronic state of the flavin molecule has different chemical properties and can be modulated in different protein environments. Modulation of each flavin state regulates the redox potential, allowing the diverse range of reactions catalysed by different flavoenzymes.

1.4.2 Catalytic cycles and stereospecificity of flavins

In a typical catalytic cycle for many flavoenzymes, the oxidised co-factor is two-electron reduced by an electron donor such as nicotinamides. NADPH and NADH tend to have more negative redox potentials (-320 mV) than most flavoenzymes and therefore act as effective reducing agents for such enzymes (Walsh, 1980). Following enzyme reduction, the flavin co-factor must be returned to its original state before the enzyme can carry out another catalytic cycle. Given that the flavin co-factor remains tightly bound to the enzyme and is therefore non-dissociable, another substrate must serve to re-oxidise the reduced flavin. It is this reaction (where the second substrate is reduced) that fulfils the true function of the flavoenzyme. For the flavoenzyme to participate in this specific reaction it is an absolute requirement that the substrate molecule be properly positioned over the flavin ring. The substrate molecule can react on either the *si* or *re* face of the isoalloxazine ring, depending on the individual flavoprotein (Pai, 1992; Manstein *et al*, 1988). Furthermore, studies using the modified flavin, 5-deazaflavin indicate that the site of substrate reduction must orientate correctly near the flavin N5 atom of the flavin, as direct hydride transfer to the substrate typically occurs via the N5 atom (the flavin N5 atom is the site of hydride attack when being reduced and the site of hydride transfer during re-oxidation; Massey and Hemmerich, 1980). Given the above reactions, catalysis by flavoenzymes therefore always involves a reductive

half-reaction where enzyme-bound flavin is reduced, coupled to an oxidative half-reaction where reduced flavin is re-oxidised (Walsh, 1980). In most cases it is possible to study these two half-reactions conveniently, allowing the detailed analysis of catalytic events.

1.4.3 Methods of study

The chromophoric nature of the isoalloxazine moiety has permitted the detailed analysis of catalytic cycles and the thermodynamic properties associated with many flavoenzymes. Commonly, absorbance and fluorescence spectroscopy is used to characterise such enzymes. The visible absorbance spectrum for oxidised flavoprotein typically displays absorbance maxima (λ_{max}) at approximately 450 and 380 nm (Figure 1.7B). Frequently, the binding of ligands perturbs the enzymes absorbance spectrum allowing the determination of dissociation constants. Upon two-electron reduction of the flavin/enzyme the absorbance between 450 and 500 nm decreases allowing the determination of redox potentials. Furthermore, the semiquinone states of flavin also differ spectrally from the other redox states of the flavin molecule (Figure 1.7B). Therefore, the number of electrons taken up by the flavin can be easily deduced from the flavins spectral changes, as well as the ionisation state.

Often, studies measuring steady-state initial velocity patterns for flavoproteins indicate a ping-pong mechanism and indeed many flavoenzymes utilise such a mechanism. Furthermore, the use of stopped-flow analysis often provides an effective means for the determination of reaction intermediates and the microscopic rate constants associated with the individual steps of a reaction. In addition, comparison of the absorbance spectrum of synthetic model compounds or intermediates from other well-defined enzyme reactions to the enzyme reaction of interest allows the identification of catalytic intermediates (Palfey and Massey, 1998). Generally, the ease of obtaining absorbance spectra of flavoenzymes has proved to be a frequently used and valuable tool in characterising many flavoprotein-catalysed reactions.

Flavin co-factors are often observed to be bound to proteins with a β/α -barrel topology (Palfey and Massey, 1998). Therefore, given that the properties of the flavin molecule have been reviewed, a brief account of the topology of the most common protein moiety that binds these co-factors is appropriate. This is followed by a short account of the classification system(s) used for grouping the diverse range of flavoenzymes found in biological systems.

1.4.4 β,α -barrel proteins

Roughly 10 % of all proteins with known three-dimensional structures have β/α -barrel domain. Members of this large group of proteins catalyse a versatile range of reactions (Scrutton, 1994). The first protein described to have an eight-stranded β/α -barrel framework was triose phosphate isomerase (Phillips *et al*, 1978). The β/α -barrel fold consists of eight parallel β -strands on the interior of the protein which form a hydrogen-bonding network. β -strand 1 forms backbone hydrogen-bonds with its neighbouring strands β -strand 2 and β -strand 8. Between each neighbouring β -strand there is a single α -helix (total of eight) which constitutes the outer layer of the protein structure (Scrutton, 1994; Hocker *et al*, 2002). The overall sequence of the secondary structure is therefore known as $(\beta/\alpha)_8$ barrel. Although this fold is known as a barrel most of the proteins exhibiting such a framework are elliptical (Reardon and Farber, 1995). The active site residues of $(\beta/\alpha)_8$ barrel proteins are located on the catalytic face of the barrel, comprising of the C-terminal ends of the β -strands and the loops that link the β -strands with the subsequent α -helices. In contrast, the loops on the opposite face of the barrel are important for stabilising the fold (Hocker *et al*, 2001; Gerlt and Raushel, 2003). In addition to the basic $(\beta/\alpha)_8$ structure, many enzymes have additional domains or secondary structures located in the loops that connect the β -strand to the subsequent α -helices (Reardon and Farber, 1995). Sequence analysis of $(\beta/\alpha)_8$ barrel proteins reveals little sequence similarity among members (Scrutton, 1994).

The evolutionary history of the $(\beta/\alpha)_8$ barrel fold has been a matter of much debate. Two distinct evolutionary pathways are proposed to have led to the large family of eight-stranded β/α -barrels. This type of folding motif is particularly stable and therefore many ancestral proteins with different starting sequences could have evolved to this stable shape. The lack of extensive sequence homology among the many members of this family supports such a convergent evolutionary pathway. Alternatively, all $(\beta/\alpha)_8$ barrel proteins could have originated from a common ancestral fold (divergent evolution; Reardon and Farber, 1995).

The large number of flavoproteins with an $(\beta/\alpha)_8$ barrel topology can be divided into two sequence related sub-families. Division of these proteins into type I and type II proteins is based on multiple sequence alignment studies of ten proteins (classified as flavin oxidase/dehydrogenase proteins) possessing this fold. Although members of each sub-family exhibit substantial sequence similarity among themselves, no discernible sequence similarity exists with members of the other class (Scrutton, 1994). Class I $(\beta/\alpha)_8$ barrel flavoproteins

were identified as OYE I from *Saccharomyces carlsbergensis*, NADH oxidase from *Thermoanaerobium brockii*, NADH oxidase and *bai C* from *Eubacterium sp.* V12708, and trimethylamine dehydrogenase (TMADH) from the bacterium W₃A₁. Proteins classified as type II proteins include spinach glycolate oxidase, lactate oxidase from *Mycobacterium smegmatis*, *s*-malate dehydrogenase from *Pseudomonas putida*, rat L- α -hydroxyacid oxidase and flavocytochrome b₂ from *Saccharomyces cerevisiae*. Structural analysis of TMADH, spinach glycolate and flavocytochrome b₂ have revealed alternative modes of residue packing in the core of the β/α -barrel domain which may be responsible for the above sequence related classification (Raine *et al*, 1994). (β/α)₈ barrel proteins have three planes of amino acid side chains in the barrel core; two outer planes and one inner plane, with four amino acids in each plane. This kind of internal packaging gives rise to two types of barrel core structures known as (1:2)₄ and (2:1)₄ structures. In the (1:2)₄ structure strands 1,3,5 and 7 provide residues for the middle plane and strands 2,4,6 and 8 provide residues for the outer plane. In the (2:1)₄ structure the order is reversed, where strands 1,3,5 and 7 make up the outer two planes and strands 2,4,6 and 8 make the middle plane (Lesk *et al*, 1989). Structural analysis of enzymes from both sequence related classes indicate that proteins of the Class I family exhibit (1:2)₄ packing while those from Class II have (2:1)₄ packing. It is therefore most likely that these alternative modes of core packing underlie the division in the sequence related families (Raine *et al*, 1994). PETN reductase, the enzyme of interest in this thesis, is identified as a Class I β/α -barrel flavoprotein (Barna *et al*, 2001).

1.4.5 Classification of flavoproteins

The large family of flavoproteins is diverse both in structure and mechanism, making their classification somewhat difficult. Consequently, a number of schemes attempting to classify these proteins have been put forward. In 1979, Walsh (Walsh, 1979) proposed seven classification groups for flavoproteins based upon the reactions undertaken by each enzyme. This classification system divided flavoproteins into dehydrogenases, oxidases, oxidase-decarboxylases, mono-oxygenases, di-oxygenases, metalloflavoenzymes and flavodoxins. Following on, Massey and Hemmerich (Massey and Hemmerich, 1980) proposed to classify flavoproteins into five major divisions; Class I, the transhydrogenases; Class II, the dehydrogenases/oxidases; Class III, the dehydrogenases/oxygenases; Class IV, the dehydrogenases/electron transferases and; Class V, the pure electron transferases. The Class I

flavoproteins are further sub-divided into the carbon-carbon transhydrogenases, carbon-sulphur transhydrogenases, carbon-nitrogen transhydrogenases and nitrogen-nitrogen transhydrogenases. This classification scheme of Massey and Hemmerich (Massey and Hemmerich, 1980) has been widely accepted, but was proposed over twenty years ago. Recently, Palfey and Massey (Palfey and Massey, 1998) have put forward another classification system where flavoproteins are divided into electron transferases, disulfide oxidoreductases, oxidases and mono-oxygenases. This revised taxonomy attempts to describe simple flavoproteins on the basis of the reactions they catalyse, their reactivity towards a number of reagents and their ability to stabilise the flavin semiquinone. Enzymes in each family therefore share common mechanistic properties; however, some have evolved to catalyse reactions in addition to those by which they are classified (Palfey and Massey, 1998). Simple proteins can be easily assigned to one of the classification groups mentioned above, but this is more difficult for complex flavoproteins. Such enzymes include (i) those where the same enzyme can catalyse reactions characteristic of several of the above families even though the flavin is the only co-factor and (ii) those complex flavoproteins that have other co-factor/prosthetic groups in addition to the flavin. These drawbacks are applicable to each of the classification systems mentioned above.

According to the widely accepted classification system of Massey and Hemmerich (Massey and Hemmerich, 1980), PETN reductase is defined as a Class I carbon-carbon transhydrogenase, as it catalyses the two electron transfer between pyridine nucleotides and carbon atoms of oxidising substrates. Close homologues of PETN reductase, OYE, morphinone reductase and estrogen binding protein are therefore also categorised into the same group. With reference to the classification of Palfey and Massey (Palfey and Massey, 1998), these enzymes are classified as electron transferases.

PETN reductase exhibits a high degree of structural and physical similarity with OYE and morphinone reductase. Therefore, the following sections describes the properties of each enzyme in turn.

1.5 Enzymes related to PETN reductase: Old yellow enzyme

Old yellow enzyme (OYE) was the first discovered flavoprotein isolated from Brewer's bottom yeast by Warburg and Christian in 1933 (Warburg and Christian, 1933). OYE was first purified by Theorell in 1935 and was shown to comprise a yellow FMN co-

factor essential for the enzymes activity (Theorell, 1935). Since then a considerable amount of research has been conducted on this enzyme, with an abundance of information on its chemical and physical properties now being known. In addition, characterisation of OYE has contributed significantly to our understanding of enzymes in general and the role of flavin co-factors in enzymology. Despite this vast amount of research, the physiological role of OYE has yet to be established.

OYE has been shown to consist of several isoforms, each encoded by separate genes (Miura *et al*, 1986; Saito *et al*, 1991; Stott *et al*, 1993). The first gene encoding an isoform of OYE from *Saccharomyces carlsbergensis* (*oye1*) was cloned in 1991 (Saito *et al*, 1991). Since then two further genes encoding OYE (*oye2* and *oye3*) have been cloned from *Saccharomyces cerevisiae*, which show close similarity but not identity to OYE1 (Stott *et al*, 1993; Niino *et al*, 1995). In addition, another yeast OYE clone (*oye4*) has been isolated from *Kluveromyces lactis* (Miranda *et al*, 1995). Each isoform of OYE has slightly different characteristics, which range from differences in their ligand binding properties, catalytic activities towards different electron acceptors, surface charge and their sequence (Miura *et al*, 1986; Saito *et al*, 1991; Stott *et al*, 1993; Niino *et al*, 1995).

A growing number of OYE homologs have been isolated from plants, yeast and bacteria. Related proteins include morphinone reductase from *Pseudomonas putida* (French and Bruce 1995), estrogen binding protein from *Candida albicans* (Madani *et al*, 1994), PETN reductase from *Enterobacter cloacae*, (French *et al*, 1996), 12-oxophytodienoic acid (OPDA) reductases from *Arabidopsis thaliana* and tomato (Schaller and Weiler, 1997; Straßner *et al*, 1999), and more recently, a protein encoded by the *yqjM* gene in *Bacillus subtilis* (Fitzpatrick *et al*, 2003). A number of related proteins have also been identified in the many genome sequences now available in the sequence databases.

1.5.1 Structure and general properties

OYE exists as a dimer of two 49 kDa subunits with one non-covalently bound FMN per subunit (Mathews and Massey, 1969; Abramovitz and Massey, 1976). The crystal structure of OYE 1 in its oxidised and reduced state has been solved at 2 Å resolution (Fox and Karplus 1994; 1999). The enzyme has an $(\beta/\alpha)_8$ framework with the FMN bound to the carboxy terminus end of the barrel (Figure 1.8). The *si* face of the flavin is fully accessible to the solvent and forms the bottom of the active site, while the *re* face is completely buried by

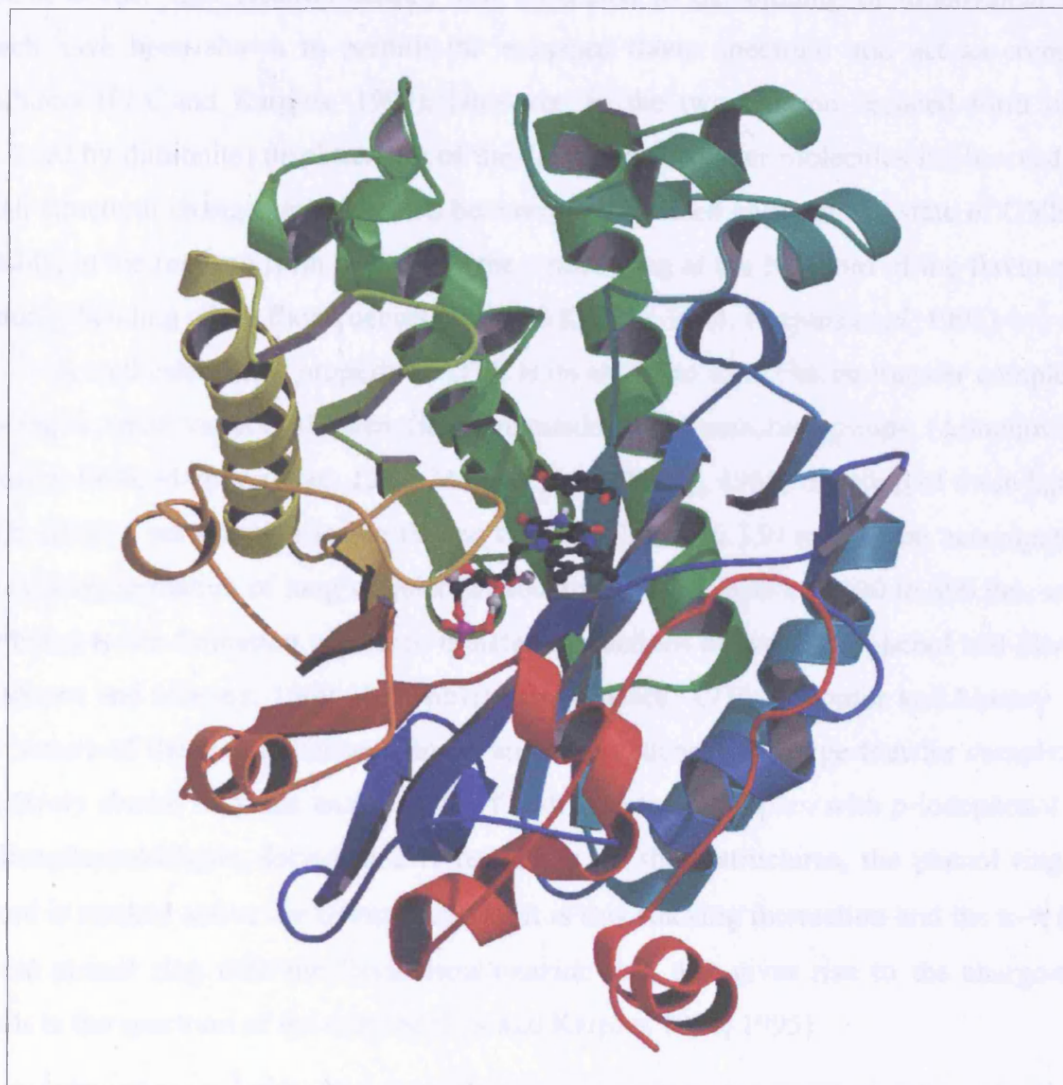


Figure 1.8. Ribbon diagram of the subunit structure of OYE from *Saccharomyces pastorianus*. OYE shows a typical eight-stranded α,β -barrel framework with a non-covalently bound FMN co-factor (shown in ball and stick form) located towards the centre of the barrel axis. The enzyme typically exists in the dimeric form of the pictured subunit. *p*-hydroxybenzaldehyde is shown bound in the active site (shown in ball and stick form). (Figure prepared with MOLSCRIPT (Kraulis, 1991) and Raster 3D (Merritt, 1994), using PDB code 1OYB, by Dr Peter Moody).

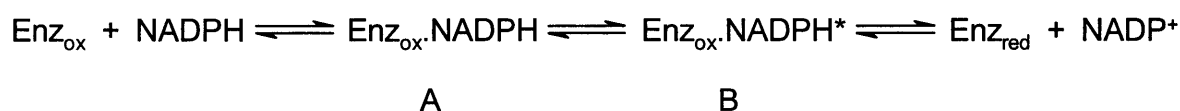
interactions made with the protein main and side chain groups (Fox and Karplus, 1999). In the structure of oxidised OYE, electron density is observed within the active site unattributed to protein atoms. This electron density was attributed to the binding of monovalent anions, which have been shown to perturb the enzymes flavin spectrum and act as competitive inhibitors (Fox and Karplus, 1994). However, in the two-electron reduced form of OYE (reduced by dithionite) displacement of the anion by two water molecules is observed. Other small structural changes are observed between the oxidised and reduced state of OYE. Most notably, in the reduced form of the enzyme a puckering at the N5 atom of the flavin and 15° butterfly bending of the flavin occurs (Fox and Karplus 1994; Karplus *et al*, 1995).

A well established property of OYE is its ability to form charge-transfer complexes on binding a wide variety of phenolic compounds with ionisable groups (Abramovitz and Massey, 1976; Mathews *et al*, 1975; Mathews and Massey, 1969). Binding of these ligands to OYE elicits a perturbation in the flavins spectrum between 350 to 540 nm accompanied by the striking formation of long wavelength absorbance band between 500 to 800 nm, which is attributed to the formation of charge-transfer interactions between the phenol and flavin ring (Mathews and Massey, 1969; Abramovitz and Massey, 1976; Schopfer and Massey, 1990). The nature of these absorbance changes and the existence of charge-transfer complexes are decisively shown from the analysis of OYE structures in complex with *p*-iodophenol and *p*-hydroxybenzaldehyde, solved at 2 Å resolution. In these structures, the phenol ring of the ligand is stacked above the flavin such that it is this stacking interaction and the π - π overlap of the phenol ring with the flavin isoalloxazine ring that gives rise to the charge-transfer bands in the spectrum of the enzyme (Fox and Karplus 1994; 1995).

1.5.2 Reductive half-reaction of OYE

OYE is readily reduced by pyridine nucleotides (NADPH, NADH), dithionite or EDTA/light/deazaflavin (Bright and Porter, 1975; Mathew and Massey, 1971; Massey and Hemmerich, 1978) and is able to stabilise the red semiquinone (Stewart and Massey, 1985). However, the physiological reductant for OYE has been accepted as NADPH (Massey and Schopfer, 1986), therefore, OYE has been described as an NADPH oxidoreductase. Reduction by NADPH does not however produce the semiquinone form of OYE (Nakamura *et al*, 1965; Mathew and Massey, 1971). Both α -NADPH and β -NADPH are capable of reducing OYE and surprisingly the uncommon α -anomer of NADPH is slightly more

effective (Massey and Schopfer, 1986). Reduction of OYE proceeds by hydride transfer from the C4 atom of the nicotinamide ring of NADPH to the flavin N5 atom. Reaction with NADPH under anaerobic conditions results in the rapid equilibrium binding of NADPH to oxidised enzyme (Scheme 1.1, species A), such that a very small change in enzyme absorbance is observed (which typically occurs within dead time of stopped-flow). This initial rapid binding step involves a minor charge-transfer interaction between NADPH and oxidised flavin (explaining the small absorbance changes), but the orientation of NADPH binding is unfavourable for hydride transfer. This step is therefore followed by the rapid re-alignment of NADPH over the flavin ring which elicits a long-wavelength absorbance band (between 500 to 700 nm) and a pronounced perturbation of the flavin spectrum indicating the formation of a “typical” charge-transfer complex (Scheme 1.1, species B). Formation of this charge-transfer complex is presumed to prepare the enzyme for hydride transfer from NADPH to the flavin. This is the next step to occur in the reaction (Scheme 1.1), resulting in the simultaneous disappearance of the long-wavelength charge-transfer band and reduction of flavin (i.e. decrease in 400 to 500 nm absorbance; Massey and Schopfer, 1986; Porter and Bright, 1980). Formation of a charge-transfer band involving the interaction between reduced flavin and oxidised NADPH is not observed because NADP^+ is rapidly expelled from the enzyme (Karplus *et al*, 1995). Although reduction of the enzyme is extensive, it is not complete, indicating that OYE reduction by NADPH is a reversible redox reaction (Massey and Schopfer, 1986). The two-electron midpoint potential for OYE reduction is approximately -235 mV (Stewart and Massey, 1985).



Scheme 1.1

The crystal structure of OYE in complex with the inactive analogue of NADPH, (c-THN)TPN, suggests that the nicotinamide ring of NADPH binds above the *si* face of the flavin, more precisely over the central isoalloxazine ring of FMN (interaction between these molecules leads to the charge-transfer complex). This mode of binding places the C4 position of the nicotinamide ring above the N5 of FMN, suggesting the optimal positioning of NADPH for hydride transfer to the flavin. The orientation of nicotinamide binding is largely determined by the formation of hydrogen bonds between the amide oxygen of NADPH with His 191 and Asn 194 in the active site of OYE (Fox and Karplus, 1994). Interestingly, the co-

crystal structure of OYE with (c-THN)TPN revealed that only the nicotinamide moiety of NADPH is tightly bound and that the adenine phosphate group makes no interaction with the active site. This gives reason to the observation of OYE being reactive with both the α - and β -NADPH anomers (Fox and Karplus, 1994). However, it is difficult to understand why OYE has specificity for NADPH over NADH (Williams and Bruce, 2002).

Recently Thr 37 of OYE has been demonstrated to play a role in influencing the redox potential of OYE and hence, stabilisation of the fully reduced dihydroflavin. Threonine 37 forms a hydrogen bond to the C4 carbonyl oxygen of the flavin isoalloxazine ring. Exchange of this residue for alanine lowers the redox potential of the mutant enzyme in comparison to wild-type enzyme and destabilises the reduced flavin. Consistently, the rate of enzyme reduction in the mutant enzyme is slowed down significantly, whereas the enzymes activity in the oxidative half-reaction is enhanced. Based on these findings it was postulated Thr 37 in wild-type OYE increases the redox potential by stabilising the negative charge of the fully reduced flavin by hydrogen bonding to it (Xu *et al*, 1999).

1.5.3 Oxidative half-reaction

Although the physiological oxidant for OYE has not been identified, many substrates are capable of re-oxidising the enzyme, including methylene blue, ferricyanide, quinones, several α/β -unsaturated carbonyl and nitro compounds (Stott *et al*, 1993; Vaz *et al*, 1995; Meah and Massey, 2000), nitrate esters (Meah *et al*, 2001) and nitroaromatic compounds (Williams *et al*, 2004). OYE is also oxidised by molecular oxygen yielding hydrogen peroxide and superoxide. However, this reaction is assumed to be adventitious due to the substantially slow reactivity of oxygen with reduced enzyme, in comparison to other oxidases (Schopfer and Massey, 1991; Stott *et al*, 1993). These substrates as well as phenolic ligands, anions and substrates for the reductive half-reaction all share a common binding site in OYE, therefore, the kinetic mechanism of OYE is characteristic of a simple Ping Pong reaction (Massey and Schopfer, 1986; 1991; Fox and Karplus, 1994).

α/β -unsaturated carbonyl compounds act as effective electron acceptors for OYE, being more effective than quinones (Stott *et al*, 1993; Vaz *et al*, 1995). In addition, 2-cyclohexenone is found to inhibit the reaction of OYE with molecular oxygen when both substrates are present, indicating the preference of OYE for 2-cyclohexenone as its electron acceptor compared to molecular oxygen (Vaz *et al*, 1995). These observations have led to the

suggestion that the physiological function of OYE might be in the reduction of α/β -unsaturated carbonyl compounds e.g. in sterol metabolism. NADPH-dependent reduction of α/β -unsaturated carbonyl compounds is limited to ketones and aldehyde derivatives. α/β -unsaturated acids, esters, amides and nitriles do not serve as electron acceptors for OYE (and therefore act as inhibitors for the enzyme). Re-oxidation of OYE by α/β -unsaturated carbonyl substrates occurs via the NADPH-dependent reduction of the olefinic bond (Vaz *et al*, 1995). The most widely used α/β -unsaturated carbonyl substrate for OYE is the cyclic enone, 2-cyclohexenone. This substrate is observed to elicit a long-wavelength charge-transfer band upon equilibration with OYE, a feature which contributed significantly to the identification of a novel dismutation reaction in OYE with 2-cyclohexenone. In the absence of reduced pyridine nucleotides, OYE can be reduced by one molecule of 2-cyclohexenone, leading to aromatisation of the substrate and therefore production of the phenol form, cyclohexanol. This reaction is accompanied by a dismutation reaction where the olefinic bond of a second molecule of 2-cyclohexenone is reduced producing the saturated cyclic ketone, cyclohexanone and re-oxidised OYE (Figure 1.9A). The overall dismutation reaction therefore involves the enzyme being reduced by one molecule of the substrate and re-oxidised by another. This leads to the net production of an unsaturated ketone and an aromatic phenol in 1:1 ratio. It is the interaction of the phenol (product from the enzymes reductive half-reaction) with re-oxidised OYE (regenerated from the oxidative half-reaction) that produces the long-wavelength charge-transfer band observed in reaction of OYE with 2-cyclohexenone (Vaz *et al*, 1995). In the presence of NADPH, 2-cyclohexenone serves only to re-oxidise the enzyme leading to the formation of cyclohexanone (Figure 1.9B).

The mechanism of α,β -unsaturated substrate reduction by OYE proceeds via stereospecific hydride transfer from the flavin to the β -carbon (to the carbonyl function) of the compound, followed by proton transfer to the α -carbon, leading to complete reduction of the olefinic bond (Figure 1.9; Vaz *et al*, 1995). The transfer of a hydride ion and proton to 2-cyclohexenone is suggested to occur via a concerted fashion as there is no formation of a carbanion intermediate (Williams and Bruce, 2002).

The structure of OYE with *p*-hydroxybenzaldehyde and phenols in the active site provided a valuable system by which the location of substrates upon binding to the enzyme could be modelled (Fox and Karplus, 1994). The modelling of 2-cyclohexenone into the active site of OYE in an orientation similar to that observed with *p*-hydroxybenzaldehyde, i.e. with the carbonyl oxygen positioned to hydrogen bond to His 191 and Asn 194, and the rest

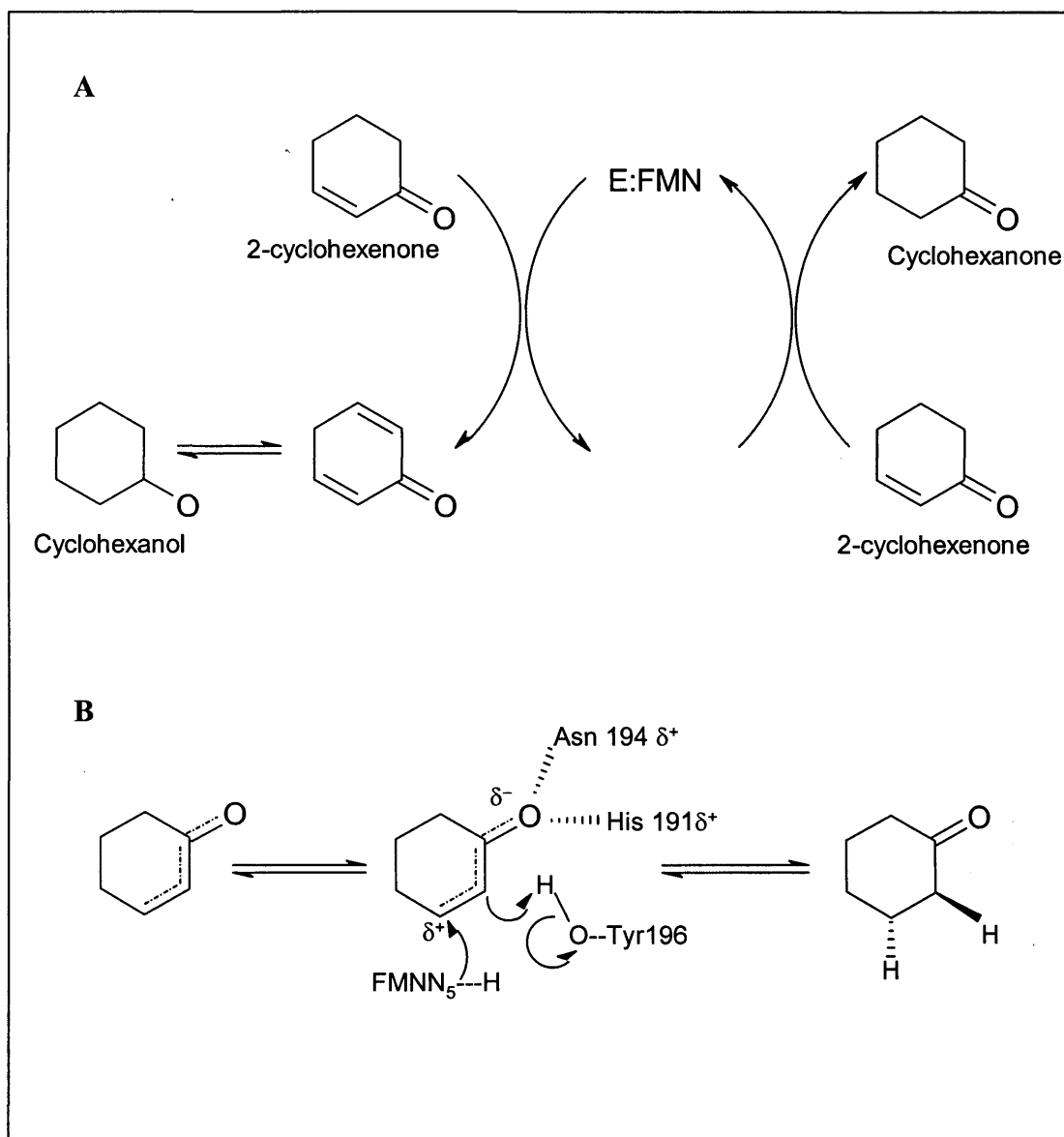


Figure 1.9. Catalysis of 2-cyclohexenone by OYE. Panel A, dismutation reaction of 2-cyclohexenone catalysed by OYE in the absence of NADPH. One molecule of 2-cyclohexenone serves to reduce OYE, yielding the phenol form of the substrate, while another molecule of 2-cyclohexenone serves to re-oxidise OYE, yielding cyclohexanone. Panel B, in the presence of NADPH, OYE reduces 2-cyclohexenone via hydride transfer from the flavin N5 atom and proton transfer from Tyr 196, to the olefinic bond. (Figures adapted from Karplus *et al*, 1995 and Kohli and Massey, 1998).

of the molecule orientated as with phenols, demonstrated that the β -position of the olefinic bond is ideally aligned to receive a hydride ion from flavin N5 atom and the α -carbon positioned close to Tyr 196 in the active site, so as to receive a proton from the residue (Figure 1.10; Karplus *et al.*, 1995; Massey *et al.*, 1999). Based upon this model, mutagenic studies of Tyr 196 in OYE were performed which established this residue as the active site acid in the reduction of α,β -unsaturated substrates (Kohli and Massey, 1998; Meah and Massey, 2000).

The co-crystal structure of OYE with various ligands has also implicated the importance of His 191 and Asn 194 in ligand binding. Indeed, this suggestion has been confirmed by studies involving the mutation of these residues (Brown *et al.*, 1998).

Recently, nitrate esters and nitroaromatic compounds have been shown to serve as electron acceptors for OYE. The NADPH-dependent denitration of nitrates esters such as GTN and propylene dinitrate by OYE leads to the liberation of nitrite. Analyses of products from these reactions reveal that the reduction of the primary nitrate in both compounds is favoured (Meah *et al.*, 2001). Reduction of TNT by OYE is demonstrated to occur via the reduction of the nitro groups, yielding HADNT derivatives; hydrogenation of the aromatic ring is not evident with TNT as the starting substrate. However, OYE is shown to catalyse the reduction of the aromatic ring of the purified hydride-Meisenheimer complex of TNT, yielding the dihydride-Meisenheimer complex, suggesting that the enzyme does possess the partial ability to catalyse reduction of the aromatic ring. The nature of the initial reaction in the transformation of TNT therefore plays a vital role in determining the eventual fate of its transformation products in OYE (Williams *et al.*, 2004).

1.5.4 Summary

As the first flavoenzyme discovered and given the vast amount of research conducted, OYE has provided a significant amount of insight into the mechanism of flavin-dependent catalysed reactions. Despite the detailed characterisation of OYE, its true physiological oxidant has yet to be identified. Elucidation of the crystal structure of OYE in complex with a variety of ligands has proved to be highly valuable in identifying key amino acid residues which influence ligand binding and catalysis, namely His 191, Asn 194 and Tyr 196.

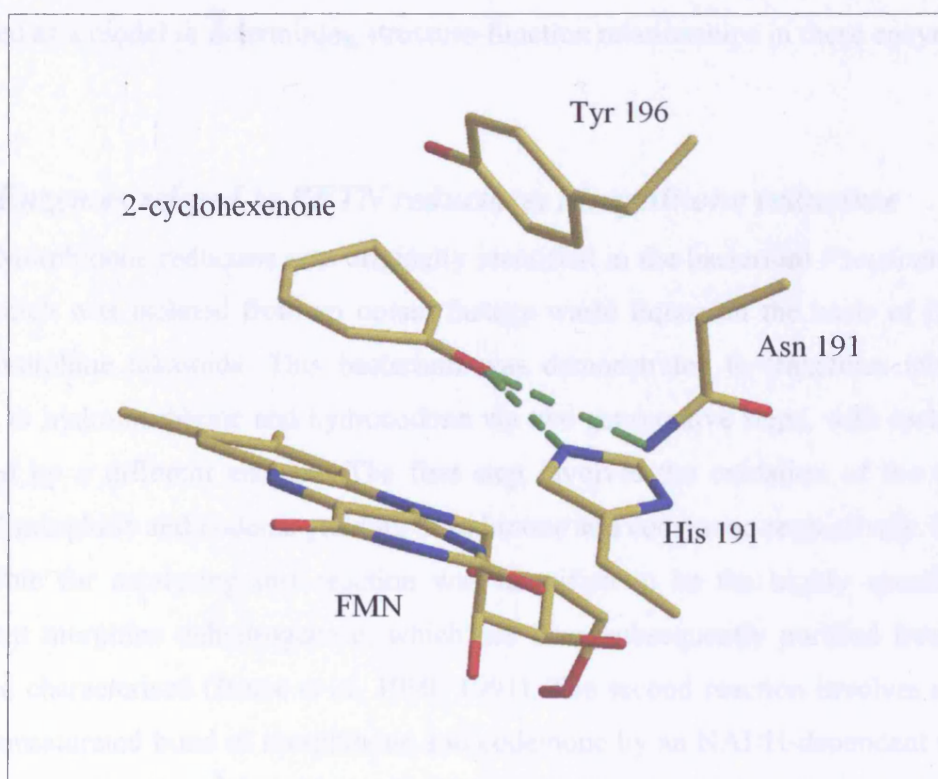


Fig. 1.10. Modelling of 2-cyclohexenone in the active site of OYE from *Saccharomyces pastorianus*., based on the known structure with *p*-hydroxybenzaldehyde. The modelling of 2-cyclohexenone into the active site of OYE in an orientation similar to that observed with *p*-hydroxybenzaldehyde, i.e. with the carbonyl oxygen positioned to hydrogen bond to His 191 and Asn 194, and the rest of the molecule orientated as with phenols, demonstrates that the β -position of the olefinic bond is ideally aligned to receive a hydride ion from flavin N5 atom and the α -carbon positioned close to Tyr 196 in the active site, so as to receive a proton from the residue. (Figure prepared with Xtalview (McRee, 1992) and Raster 3D (Merritt, 1994), using PDB code 1OYB, by Dr Peter Moody).

A growing number of proteins from a variety of sources are, and continuing to be, identified that contain amino acid sequences similar to OYE. OYE shows close sequence, structural and mechanistic similarity to other members of its family, namely, PETN reductase (Barna *et al*, 20001) and morphinone reductase (Barna *et al*, 2002). Consequently, OYE has been used as a model in determining structure-function relationships in these enzymes.

1.6 *Enzymes related to PETN reductase: Morphinone reductase*

Morphinone reductase was originally identified in the bacterium *Pseudomonas putida* M10, which was isolated from an opiate factory waste liquor on the basis of its ability to utilise morphine alkaloids. This bacterium was demonstrated to transform morphine and codeine to hydromorphone and hydrocodone via two consecutive steps, with each step being catalysed by a different enzyme. The first step involves the oxidation of the C6-hydroxy group of morphine and codeine yielding morphinone and codeinone respectively. The enzyme responsible for catalysing this reaction was identified to be the highly specific NADP⁺-dependent morphine dehydrogenase, which has been subsequently purified from *P. putida* M10 and characterised (Bruce *et al*, 1990; 1991). The second reaction involves reduction of the 7,8-unsaturated bond of morphinone and codeinone by an NADH-dependent morphinone reductase, yielding hydromorphone and hydrocodone respectively (Figure 1.11; Hailes and Bruce, 1993). The production of hydromorphone and hydrocodone are of industrial interest owing to their application as analgesics and cough suppressants. Consequently, the potential application of morphinone reductase (MR) in the biosynthesis of powerful analgesics has resulted in its isolation and detailed characterisation (French and Bruce, 1994).

1.6.1 *Physical and structural properties*

The structural gene encoding MR (*mor B*) from *P. putida* M10 has been cloned and overexpressed in *E. coli* cells (French and Bruce, 1995). MR is a homodimeric protein with a molecular weight of 82,200 Da, containing one molecule of non-covalently bound FMN per subunit (French and Bruce, 1995). Sequence analysis has identified MR to belong to the Class I flavin-dependent α/β -barrel oxidoreductases. In particular, MR shows high similarity to OYE (Stott *et al*, 1993), estrogen binding protein (Madani *et al*, 1994) and PETN reductase (French *et al*, 1996), in sequence as well as in its physical and structural properties.

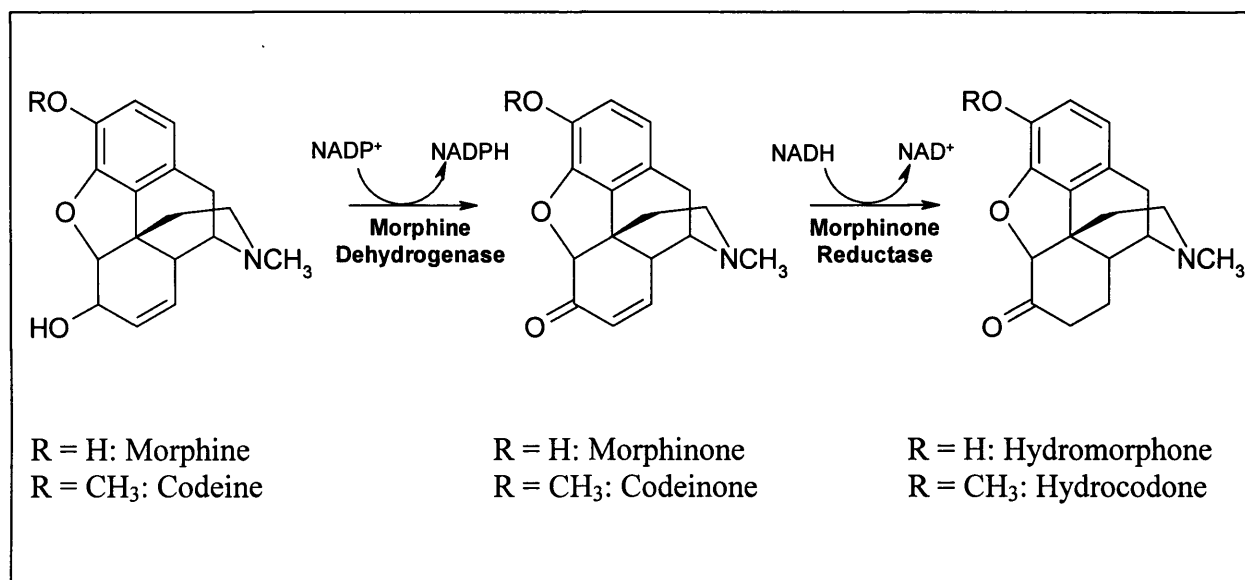


Figure 1.11. Transformation of morphine and codeine by *Pseudomonas putida* M10. *Pseudomonas putida* M10 transforms morphine and codeine to hydromorphone and hydrocodone via two consecutive steps. The first step involves the oxidation of the C6-hydroxy group of morphine and codeine by NADP^+ -dependent morphine dehydrogenase, yielding morphinone and codeinone respectively. The second reaction involves reduction of the 7,8-unsaturated bond of morphinone and codeinone by an NADH -dependent morphinone reductase, yielding hydromorphone and hydrocodone, respectively. (Figure adapted from Craig *et al*, 1998).

The structure of MR has been solved at 2.2 Å resolution (Barna *et al*, 2002). The enzyme has an eight-stranded α,β -barrel topology with the FMN co-factor bound towards the centre and C-terminal end of the barrel domain (Figure 1.12). Structural comparisons of MR reveal that the overall subunit structure is similar to OYE (Fox and Karplus, 1994) and PETN reductase (Barna *et al*, 2001). However, small notable differences in the structure of each enzyme are evident. For example, the subunit interactions of morphinone reductase differ to those reported for OYE. In OYE, the dimer interface involve helices 4,5 and 6 of the α,β -barrel, whereas the interface in MR is less extensive and comprises interactions between the N-terminal β -strand (strands A and B) and helices 2 and 8 of the barrel. In addition, OYE has an α -helix located between β -strands 3 and α -helix 3 of the core barrel domain (Fox and Karplus, 1994), while MR (and PETN reductase) has a β -loop excursion in this region (Barna *et al*, 2002). The structure of MR therefore more closely resembles that of PETN reductase than OYE.

Although the active site structure of MR closely resembles those of OYE (Fox and Karplus, 1994) and PETN reductase (Figure 1.12; Barna *et al*, 2001), important differences can be discerned. The active site of MR is larger than OYE reflecting the ability of MR to bind larger/more bulky substrates such as codeinone and morphinone. The larger active site of MR is attributed to the absence of a hydrophobic insertion lining the entrance to the active site that is found in OYE (Fox and Karplus, 1994; Barna *et al*, 2002). Furthermore, Tyr 196 in OYE, known to function as an active site acid in the reduction α,β -unsaturated enones (Kohli and Massey, 1998), is replaced with Cys 191 in MR (Barna *et al*, 2002). The ligand binding residues of OYE, His 191 and Asn 194 (Brown *et al*, 1998), are conserved in MR as His 186 and Asn 189. Amino acid interactions with the flavin are also conserved among the enzymes. An important residue located close to the flavin N1/C2 region is Arg 238. This region of the flavin is expected to develop a negative charge during enzyme reduction and the presence of a positively charged side chain near this region has been postulated to have a stabilising effect (facilitating reduction). However, studies involving the mutation of Arg 238 have demonstrated that Arg 238 is not required to stabilise the reduced form of the flavin. Although small changes in the reductive half-reaction of the mutant protein were observed, these were attributed to the altered alignment of the reducing co-factor (NADH) with the flavin (Craig *et al*, 2001).

The mechanism of catalysis undertaken by MR consists of two half-reactions; the reductive half-reaction where the reactive dihydroflavin form of the enzyme is generated and

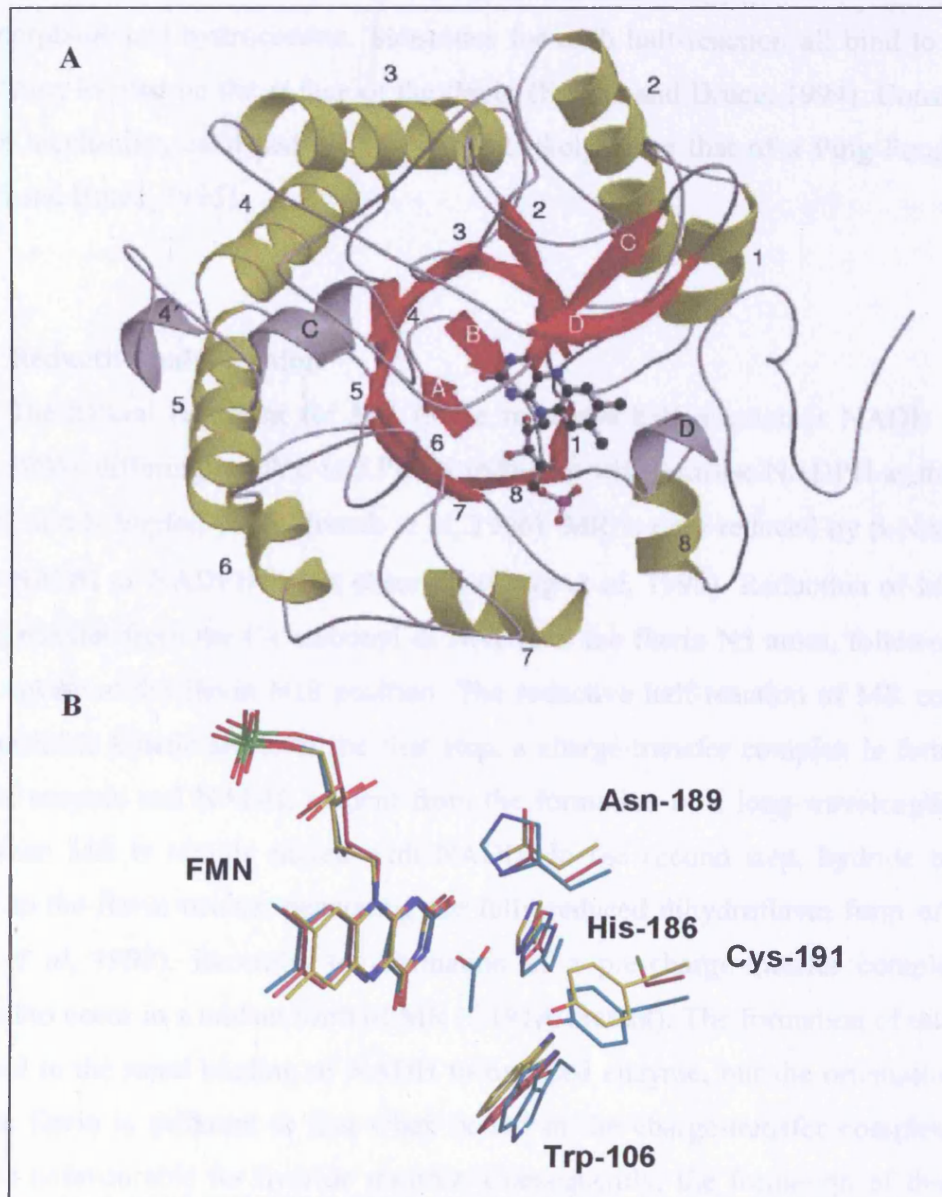


Figure 1.12. Structure of a single subunit of morphinone reductase and its active site in comparison to that of related enzymes. Panel A, morphinone reductase displays a typical eight-stranded α,β -barrel framework with the FMN cofactor located towards the C-terminal end of the barrel domain (shown in ball and stick). Panel B, active site structure of morphinone reductase (shown in magenta), OYE (shown in yellow) and PETN reductase (shown in cyan). Acetate is shown bound in the active site of the enzymes. (Figure taken from Barna *et al*, 2002).

the oxidative half-reaction where morphinone or codeinone (or other oxidising substrates) serve to re-oxidise the enzyme bound flavin, with the simultaneous formation of hydromorphone and hydrocodone. Substrates for each half-reaction all bind to same site of the enzyme, located on the *si* face of the flavin (French and Bruce, 1994). Consequently, the reaction mechanism catalysed by MR is most likely to be that of a Ping Pong mechanism (French and Bruce, 1995).

1.6.2 Reductive half-reaction

The natural reductant for MR in the reductive half-reaction is NADH (French and Bruce, 1994), differing to OYE and PETN reductase which utilise NADPH as their reductant (Massey and Schopfer, 1986; French *et al.*, 1996). MR is only reduced by β -NADH; activity with α -NADH or NADPH is not observed (Craig *et al.*, 1998). Reduction of MR occurs by hydride transfer from the C4 carbonyl of NADH to the flavin N5 atom, followed by solvent proton uptake at the flavin N10 position. The reductive half-reaction of MR comprises two distinguishable kinetic steps. In the first step, a charge-transfer complex is formed between oxidised enzyme and NADH, evident from the formation of a long-wavelength absorbance band when MR is rapidly mixed with NADH. In the second step, hydride transfer from NADH to the flavin occurs, generating the fully reduced dihydroflavin form of the enzyme (Craig *et al.*, 1998). Recently, the formation of a pre-charge-transfer complex has been observed to occur in a mutant form of MR (C191A mutant). The formation of this complex is attributed to the rapid binding of NADH to oxidised enzyme, but the orientation of NADH over the flavin is different to that when bound in the charge-transfer complex and is one which is unfavourable for hydride transfer. Consequently, the formation of this pre-charge transfer complex is followed by the formation of the well-established charge-transfer complex, where NADH re-aligns over the flavin ready for hydride transfer (Barna *et al.*, 2002). This additional discrete binding step has also been identified in the reductive half-reaction of OYE (Massey and Schopfer, 1986). However, direct evidence for the formation of such a complex in wild-type MR has yet to be presented, although, by reason of analogy it is likely that this complex does form in the wild-type enzyme but within the dead-time of the stopped-flow (Barna *et al.*, 2002).

Reduction of MR also proceeds without the formation of a stable semiquinone intermediate (Craig *et al.*, 1998), differing to OYE which has been shown to stabilise the

anionic semiquinone form of the flavin during photoreduction (Stewart and Massey, 1985). These findings indicate that the flavin environment in MR is significantly different to OYE (Craig *et al*, 1998).

Recently, studies investigating the temperature-dependence of the reductive half-reaction in MR have indicated that the hydride transfer step is essentially irreversible and that transfer occurs via a hydrogen tunnelling mechanism assisted by thermally induced vibrations in the protein (Basran *et al*, 2003).

1.6.3 Oxidative half-reaction

Morphinone reductase is able to specifically reduce the olefinic bond of codeinone, morphinone, neopine and 2-cyclohexenone. Codeinone, however, is observed to serve as a more efficient substrate than 2-cyclohexenone suggesting that the alkaloid structure is important for high enzyme activity. In addition, MR shows no activity towards morphine or codeine indicating the importance of the C6 carbonyl group for enzyme activity. Steroids such as progesterone and cortisone have been demonstrated to act as competitive inhibitors of MR and these compounds are bound with higher affinity than the alkaloids. However, none of the steroids tested so far have been shown to act as substrates for the enzyme (French and Bruce, 1994). Despite the enzyme being named MR, most of the work conducted on the enzyme has been done with codeinone as the substrate due to morphinone being unavailable commercially and being difficult to purify (Bruce *et al*, 1990; French and Bruce, 1994). MR also exhibits activity towards molecular oxygen (Craig *et al*, 1998).

The oxidative half-reaction of MR with codeinone as the substrate proceeds in three kinetically identifiable steps. The first step involves the formation of a charge-transfer complex comprised of reduced enzyme bound to codeinone, as characterised by the formation of a long-wavelength absorbance band. The second step involves the hydride transfer from reduced flavin N5 atom to the olefinic bond of the substrate, yielding re-oxidised flavin and hydrocodone. Absorbance changes following this step involve the increased absorbance at 462 nm (representing flavin re-oxidation) with the concomitant decrease in long-wavelength absorbance. The third step was identified by the further slow increase in 462 nm absorbance, attributed to the release of hydrocodone from the enzyme. This step of the reaction is suggested to be the rate limiting step in the overall catalysis of MR (Craig *et al*, 1998), differing to OYE for which enzyme reduction by NADPH is determined to be rate limiting (Massey and Schopfer, 1986).

The oxidative half-reaction of MR with 2-cyclohexenone has been investigated in detail. Reduction of the olefinic bond occurs via hydride transfer from flavin N5 atom and proton transfer to 2-cyclohexenone. Temperature-dependent studies of this reaction indicate that hydride and proton transfer proceeds in a concerted fashion, and that hydride transfer from reduced flavin occurs by hydrogen tunnelling. In contrast to the reductive half-reaction where hydrogen tunnelling is induced by vibrations in the protein, hydrogen tunnelling in the oxidative half-reaction occurs without the assistance of protein motion i.e. ground state tunnelling (Basran *et al*, 2003).

The protonation step in the reduction of 2-cyclohexenone and codeinone has been investigated further, based on studies with OYE which identified Tyr 196 as the proton donor in similar reactions. The equivalent residue in MR is Cys 191 and it was postulated by reason of analogy that this residue may be the active site acid in MR. However, mutation studies of Cys 191 have demonstrated that this is unlikely. Mutation of Cys 191 in MR did not substantially impair the oxidative half reaction with codeinone or 2-cyclohexenone as the substrate (Barna *et al*, 2002), highlighting an important difference in the catalytic mechanism of MR compared to that of OYE. Consequently, the source of the protonation step in 2-cyclohexenone has yet to be identified.

In summary, although MR is closely related to OYE, important mechanistic and structural differences can be discerned. Consequently, MR seems to share a closer structural and possibly mechanistic relationship with PETN reductase from *Enterobacter cloacae*, PB2.

1.7 *PETN reductase*

A strain of *Enterobacter cloacae*, designated PB2, was isolated from explosive contaminated land on the basis of its ability to use nitrate esters such as PETN, ethylene dinitrate (EGDN) and GTN as its sole nitrogen source (Binks *et al*, 1996). *E. cloacae* PB2 was shown to utilise two atoms of nitrogen per molecule of PETN producing pentaerythritol dinitrate, which was subsequently oxidised to the dialdehyde. The ability of the strain to utilise nitrate esters was attributed to the activity of a soluble enzyme designated PETN reductase. This enzyme was observed to reductively liberate nitrite from PETN with the oxidation of NADPH and production of pentaerythritol trinitrate and pentaerythritol dinitrate.

Oxidation of pentaerythritol dinitrate to the dialdehyde was suggested to occur by another enzyme activity in *E. cloacae* PB2 (Binks *et al*, 1996).

E. cloacae PB2 is also capable of growth with TNT as its sole nitrogen source owing to the activity of PETN reductase (French *et al*, 1998). The ability of PETN reductase to transform persistent explosives makes the enzyme attractive in the phytoremediation of explosive contaminated land and water. Consequently, the gene encoding PETN reductase, designated *onr*, has been cloned and overexpressed in *E. coli* cells (French *et al*, 1996). In addition, the *onr* gene has been engineered into tobacco plant seeds. Transgenic plant seedlings expressing PETN reductase have been shown to germinate and grow in the presence of GTN and TNT, at concentrations that normally inhibit the germination and growth of wild-type seedlings. Transgenic plant seeds showed greatly enhanced denitration of GTN and GDN yielding GMN (French *et al*, 1999). This study nicely demonstrated that explosive residues are potentially toxic to plant systems, but the expression of bacterial explosive degrading enzymes provides an effective means for overcoming this toxicity, opening the exciting possibility of generating transgenic plants for phytoremediation purposes. However, further studies on the characterisation of degradation products and their effects on plant life must be explored; hence the mechanism of catalysis undertaken by PETN reductase is being investigated in some detail.

1.7.1 Physical and structural properties of PETN reductase

The gene sequence of PETN reductase reveals that the enzyme is a member of the Class I β/α -barrel family of FMN containing enzymes (French *et al*, 1996; Scrutton, 1994). These include OYE isoforms from *Saccharomyces carlsbergensis* and *Saccharomyces cerevisiae* (Saito *et al*, 1991; Stott *et al*, 1993; Niino *et al*, 1995), bacterial morphinone reductase (MR) from *Pseudomonas putida* M10 (French and Bruce, 1995), estrogen binding protein from *Candida albicans* (Madani *et al*, 1994), 12-oxophytodienoic acid reductase from tomato (Straßner *et al*, 1999) and *Arabidopsis thaliana* (Schaller and Weiler, 1997). The most similar enzyme to PETN reductase is MR which shares 53 % sequence identity (French *et al*, 1996; French and Bruce, 1995), while OYE shares 39 % sequence identity (French *et al*, 1996; Stott *et al*, 1993). Recently, homologs of PETN reductase from strains of *Pseudomonas* (Blehert *et al*, 1999) and *Agrobacterium* (Snape *et al*, 1997) have been isolated and these enzymes also show reactivity with explosive substrates.

PETN reductase has been purified by ion-exchange and affinity chromatography (Binks *et al*, 1996). The enzyme is a monomeric flavoprotein with a M_r of approximately 40,000 Da, containing 1 mol. equivalent of FMN and it is an oxidoreductase using a reduced pyridine nucleotide co-factor as its electron donor (Binks *et al*, 1996).

The structure of PETN reductase has been solved by molecular replacement using OYE as the search model, at 1.5 Å resolution (Moody *et al*, 1998; Barna *et al*, 2001). The enzyme has a typical eight-stranded α/β -barrel framework (Figure 1.13) with a non-covalently bound FMN co-factor located towards the centre and C-terminal end of the barrel domain. The flavin molecule is surrounded by the central β -strand, from which the residues in this strand provides most of the direct contacts with the flavin. Main chain and side chain contacts to the flavin are conserved in PETN reductase, OYE and MR (Barna *et al*, 2001; Fox and Karplus, 1994; Barna *et al*, 2002). As with OYE, an external helix is located between β -strand 8 and helix 8 in PETN reductase, which forms part of the phosphoryl binding site for FMN. Unlike OYE (and MR), PETN reductase is a monomer. The superposition of the subunit structure of OYE with PETN reductase (Figure 1.14) shows the high structural similarity between the two enzymes, with only one significant difference observable. PETN reductase contains a pair of parallel β -strands between β -strand 3 and helix 3 of the barrel that run antiparallel in front of the access channel to the active site (Barna *et al*, 2001). In contrast, OYE contains a β/α -barrel sub-domain between β -strand 3 and helix 3 which is not located adjacent to the active site channel (Fox and Karplus, 1994).

The *si* face of the flavin in PETN reductase is solvent exposed, while the *re* face of the flavin is completely buried within the hydrophobic active site. The active site acid of OYE (Tyr 196) in α/β -unsaturated compound reduction (Kohli and Massey, 1998) is conserved in PETN reductase as Tyr 186, whereas the equivalent residue in MR is replaced with Cys 191 (Barna *et al*, 2002). In PETN reductase, Tyr 186 is placed 3.2 Å from the flavin C4 atom where it forms interactions with Glu 241, Tyr 68 and a water molecule (Barna *et al*, 2001). One of the residues involved in ligand binding in OYE, His 191, is conserved in PETN reductase (His 181) but is rotated 180° about C^β - C^γ , while the other residue, Asn 194 of OYE is replaced with His 184 in PETN reductase (Brown *et al*, 1998; Barna *et al*, 2001). Another difference between the active site of OYE and PETN reductase is that Trp 102 of PETN reductase is inverted with respect to the equivalent (116) in OYE.

The structure of PETN reductase in its two-electron reduced form has also been solved by soaking crystals with sodium borohydride prior to flash freezing (Barna *et al*, 2001). A

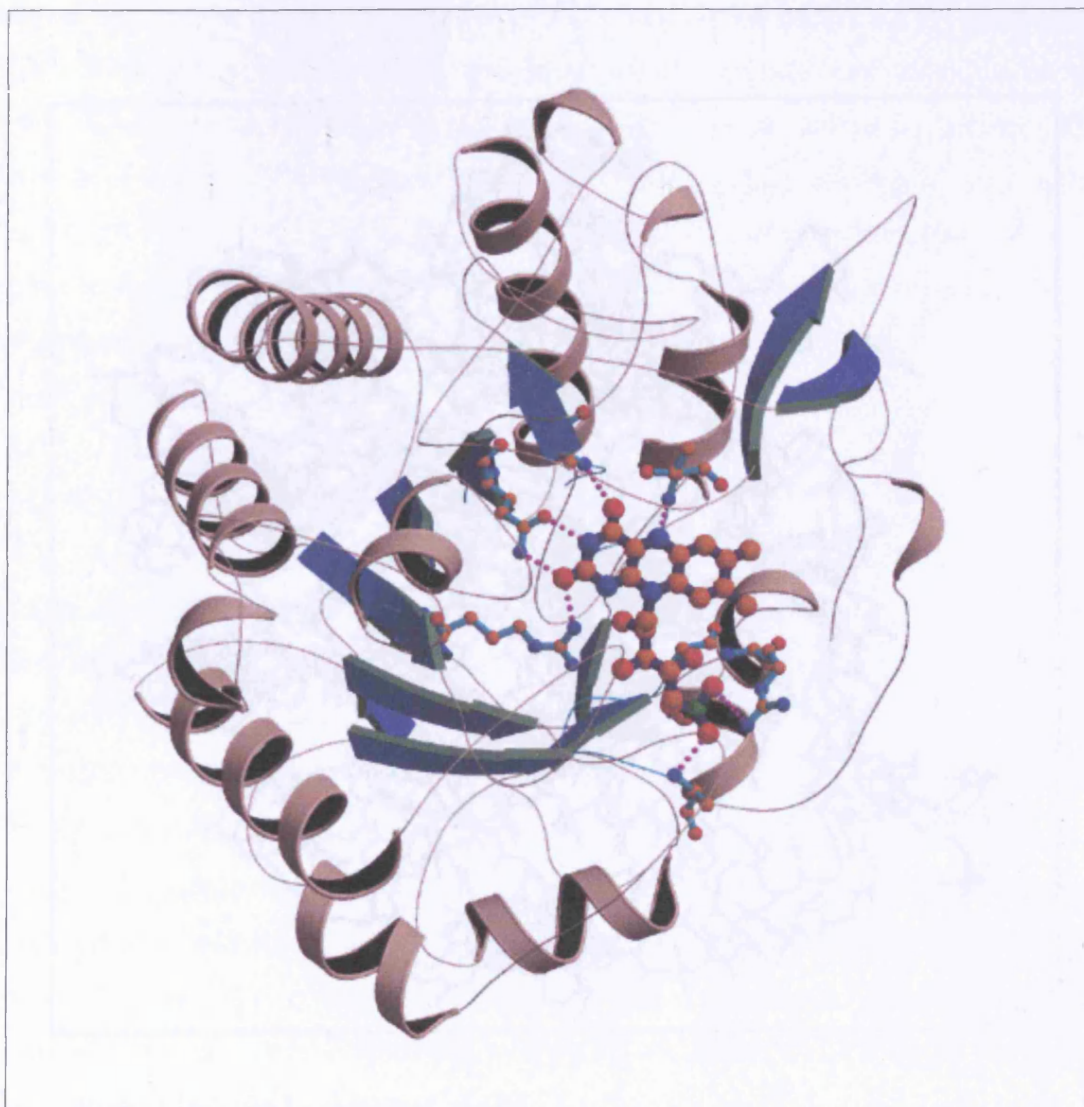


Figure 1.13. Molecular structure of PETN reductase solved to 1.5 Å resolution. The enzyme has a typical eight-stranded α/β -barrel structure and contains a non-covalently bound FMN prosthetic group in its active site. The FMN moiety (shown in ball and stick) is bound towards the C-terminal end of the α/β -barrel domain and positioned towards the centre of the barrel axis. The *si* face of the flavin is open to a well-defined solvent-filled access channel extending from the active site to the surface of the enzyme. (Figure taken from Barna *et al*, 2001. PDB code 1H50).

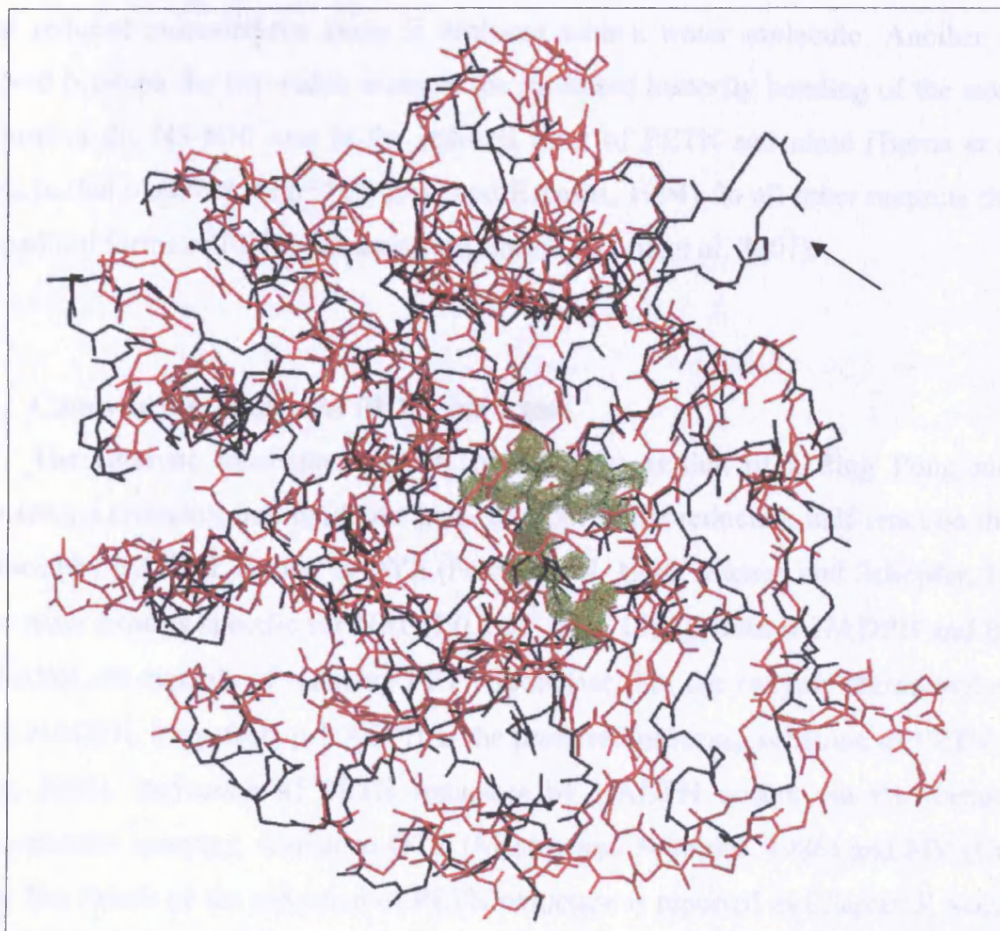


Figure 1.14. Superposition of the subunit structure for OYE with PETN reductase. The structure of PETN reductase is shown in black and that for OYE is shown in red. The electron density for the FMN moiety is also shown. The most notable difference between the structures of both enzymes is the loop comprised of antiparallel β -strands in front of the access channel, indicated by an arrow. (Figure kindly provided by Dr Terez Barna).

notable difference between the reduced and oxidised structure of the enzyme is the absence of an anion in the reduced structure, which is observed to be bound to the active site of oxidised enzyme. The anions bound are reflective of the crystallisation buffer. PETN reductase has an affinity for small negatively charged ions, which act as competitive inhibitors of the enzyme. In the reduced structure the anion is replaced with a water molecule. Another difference observed between the two redox states is the increased butterfly bending of the isoalloxazine ring around the N5-N10 axis in the reduced form of PETN reductase (Barna *et al*, 2001), similar to that observed with OYE (Fox and Karplus, 1994). In all other respects the reduced and oxidised forms of PETN reductase are similar (Barna *et al*, 2001).

1.7.2 Catalytic mechanism of PETN reductase

The catalytic mechanism of PETN reductase is that of a Ping Pong mechanism, comprising a reductive and oxidative half-reaction. In the reductive half-reaction the enzyme is reduced by NADPH, similar to OYE (French *et al*, 1996; Massey and Schopfer, 1986). MR on the other hand is specific for NADH (Craig *et al*, 1998). Both α -NADPH and β -NADPH and NADH are capable of reducing PETN reductase, but the enzyme shows higher activity with β -NADPH. Therefore, β -NADPH is the preferred reducing substrate of PETN reductase (Craig, 2000). Reduction of PETN reductase by NADPH occurs via the formation of a charge-transfer complex, similar to OYE (Massey and Schopfer, 1986) and MR (Craig *et al*, 1998). The details of the reduction of PETN reductase is reported in Chapter 3, Section 3.2.3. Recently, it has been demonstrated that hydride transfer from NADPH to the flavin proceeds by ground state tunnelling (Basran *et al*, 2003).

In the oxidative half-reaction of PETN reductase, the enzyme bound dihydroflavin is oxidised by a variety of substrates which fall into three major classes; (i) nitroaromatic compounds; (ii) nitrate esters and; (iii) α/β -unsaturated compounds. The ability of PETN reductase to denitrate GTN and PETN with the liberation of nitrite was the main basis of its isolation. However, a detailed analysis of the mechanism of this reaction has not yet been made. PETN reductase has also been shown to reduce the nitroaromatic explosives, TNT and picric acid (French *et al*, 1998; Khan *et al*, 2002). Transformation of TNT has been reported to occur via classical nitroreductase activity and through the reduction of the aromatic ring system, leading to nitrite liberation. PETN reductase was the first purified enzyme that was reported to catalyse the hydrogenation of the aromatic ring of TNT (French *et al*, 1998). The

details of nitroaromatic/TNT transformation by PETN reductase is discussed in Chapter 3. The last group of substrates for PETN reductase is the α,β -unsaturated compounds, which are also substrates for OYE (Vaz *et al*, 1995) and MR (French and Bruce, 1994; French *et al*, 1996). In addition, several steroids have also been shown to act as inhibitors of PETN reductase; progesterone, testosterone and cortisone have been shown to inhibit the reduction of GTN by the enzyme (French *et al* 1996). Reduction of α,β -unsaturated compounds typically occurs via the stereospecific transfer of a hydride ion and proton to the olefinic bond, the details of which are discussed in Chapter 4 and 5. PETN reductase and MR are known to bind steroids ligands more tightly than their known substrates, suggesting that they may have descended from a eukaryotic steroid reductase (French *et al*, 1996). The ability of PETN reductase to transform such diverse substrates (especially explosive compounds), and its close relationship to OYE, makes it an enzyme of particular interest. Hence, this thesis will attempt to build on the data already reported for PETN reductase and compare the enzyme's properties with those of its close homologs, namely OYE and MR.

1.8 Aims of thesis

PETN reductase has the remarkable ability to degrade a number of high explosives (French *et al*, 1996; 1998; Williams *et al*, 2001). The potential application of PETN reductase in the remediation of explosive contaminated land and water makes it worthy of investigation. PETN reductase also belongs to the Class I β/α -barrel family of flavoproteins, therefore the detailed characterisation of PETN reductase may add to our body of knowledge on this enzyme family and on the behaviour and catalytic properties of flavoproteins in general. In addition, the ability of OYE family members, including PETN reductase, to utilise a diverse range of substrates and display variable catalytic mechanisms makes a structural and catalytic study of its individual members an attractive proposition.

The intrinsic spectroscopic nature of flavins provides a valuable opportunity for kinetic analysis. In addition, various structures of PETN reductase have been solved and a vast amount of research has been undertaken on the related enzyme, OYE. This provides an excellent opportunity to investigate structure-function relationships in PETN reductase, using OYE as a model. The work described herein investigates the behaviour of wild-type and mutant forms of PETN reductase, using spectroscopy, stopped-flow, redox potentiometry, NMR, crystallography and mutagenesis. The methods used in this research are outlined in

Chapter 2, with Chapters 3, 4 and 5 describing the results obtained. Chapter 6 provides a detailed summary of the results and compares the data to related enzymes.

Chapter 3 of this thesis details the characterisation of wild-type PETN reductase where the pre-steady-state rate constants and catalytic events of the reductive and oxidative half-reaction are investigated. The oxidative half-reaction is characterised with a representative compound from each substrate type utilised by PETN reductase; namely TNT and picric acid (nitroaromatics), GTN (nitrate ester) and 2-cyclohexenone (α,β -unsaturated ketone). Dissociation constants for ligand binding and the redox potential of the enzyme are also established. The characterisation of wild-type enzyme serves as a reference point in comparing data obtained with mutant forms of PETN reductase. Chapter 3 also extends the work into elucidating the role of Trp 102 in nitroaromatic binding and catalysis on the basis of analysed co-crystal structures of the enzyme. Consequently, two Trp 102 mutant forms of PETN reductase (W102F and W102Y) were purified and characterised using the same methods described for wild-type enzyme. NMR and spectral analysis of TNT turnover reactions with wild-type and mutant proteins is discussed in some detail.

Chapter 4 explores the possibility that Tyr 186 of PETN reductase, like Tyr 196 of OYE, functions as the active site acid in the reduction of cyclic enones. Hence, the mutagenesis of Tyr 186 to Phe 186 is reported in addition to the purification and characterisation of the resultant mutant enzyme. The kinetics and sequence of events in the reductive and oxidative half-reaction of Y196F PETN reductase is compared to that of the wild-type enzyme and OYE. The oxidative half-reaction is investigated with GTN, TNT and 2-cyclohexenone with the main focus being on the latter substrate. Crystallisation of the mutant enzyme is also described.

Chapter 5 aims to establish the roles of His 181 and His 184 as being the primary determinants of ligand binding, as inferred from structural studies of PETN reductase. Consequently, the purification of two mutant enzymes, H181A and H184A PETN reductase, is described. Characterisation of the two mutant enzymes is achieved by ligand binding studies, potentiometry and stopped-flow kinetic studies, the results of which are compared to wild-type enzyme. The chapter also investigates the possibility of the histidine residues serving as the active site acid. The turnover of nitrocyclohexene by wild-type PETN reductase and the characterisation of intermediates and products is discussed and compared to OYE. Furthermore, the turnover of this substrate by the histidine mutant enzymes is also reported to

ascertain if either histidine residue plays any significant role in hydride ion or proton transfer to the substrate.

Chapter 6 critically discusses the results obtained from each chapter in the context of data collected for related enzymes. The chapter ends by suggesting areas for future research on PETN reductase.

Overall, the aim of the research conducted in this thesis is to investigate the mechanism of explosive and 2-cyclohexenone reduction in PETN reductase. This will allow for comparisons to be made with the OYE family of enzymes which utilise similar substrates, but potentially transform them via different mechanisms to those undertaken by PETN reductase. This thesis therefore intends to implicate critical active site residues involved in the different mechanisms of substrate reduction and in ligand binding.

Chapter Two

Materials and Methods

CHAPTER TWO

Materials and Methods

2.1 Materials

2.1.1 Chemicals and reagents

All chemicals used were of analytical grade, with the exceptions of methanol and acetic acid, used in polyacrylamide gel electrophoresis (PAGE) gel staining, which were of laboratory grade. *N,N,N',N'*-tetramethylethylenediamine (TEMED), bromophenol blue, Coomassie brilliant blue, β -NADPH, ampicillin, progesterone, 2,4-dinitrophenol (2,4-DNP), tris (hydroxymethyl) amino methane (tris), cacodylic acid, benzyl viologen, methyl viologen, 2-hydroxy-1,4-naphthaquinone and phenazine methosulfate and mineral oil were from Sigma Chemical company. Diaminoethanetetra-acetic acid (EDTA), magnesium sulfate, sodium citrate, sodium acetate, sodium chloride and sodium thiocyanate were from Fisher Scientific UK. Ammonium persulphate (APS), sodium dodecyl sulphate (SDS) and polyethyleneglycol (PEG) 3000 were from BDH Chemicals. Acrylamide/bisacrylamide (30 %) was from National Diagnostics. Tryptone, yeast extract and agar were from Oxoid Limited. Isopropyl- β -D-thiogalactopyranoside (IPTG) was from Melford Research Laboratories Limited. Nitrocyclohexene and 2-cyclohexenone were from Acros Organics. Deuterium oxide (99.9 at %) and deuterated acetone (99.9 at %) were from Goss Scientific Instruments Limited. Trinitrotoluene, glycerol trinitrate, and picric acid were kindly donated by Dr S. Nicklin (Defence Evaluation and Research Agency, Fort Halstead). Oxygen-free nitrogen and pureshield brand argon were from the British Oxygen Company. Water was glass distilled using an Elgastat Option 2 water purifier.

2.1.2 Bacterial strains and enzymes

Dr Neil C. Bruce (Institute of Biotechnology, University of Cambridge) kindly provided the *Escherichia coli* strain JM109 carrying the pONR1 plasmid, encoding for PETN reductase. DNase I was from BDH Biomedical Incorporated. The restriction enzyme *Kpn* I and T4 DNA ligase were from Amersham. *Pfu* turbo DNA polymerase, *Dpn* I and *E. coli*

JM109 competent cells were from Stratagene. Glucose-6-phosphate and glucose-6-phosphate dehydrogenase were from Sigma Chemical Company.

2.1.3 Chromatographic media and membranes

Biomimetic orange resin was obtained from Affinity chromatography Limited. Q-Sepharose resin was from Amersham Pharmacia Biotech. PM 30 Diaflo ultrafiltration membranes (30 kDa cut-off) were from Amicon incorporated. Dialysis tubing was from Medicell International Limited. Nap5 column was from Pharmacia. The 10-DG disposable gel filtration chromatography columns were from Bio-Rad.

2.2 Recombinant DNA techniques

2.2.1 Preparation and digestion of plasmid DNA

Using 5 x 1.5 ml of a late phase culture (see section 2.3.2 for growth of culture), small-scale purification of the pONR1 plasmid was performed using a Hybaid recovery™ plasmid and cosmid prep kit. Purified DNA was collected in 50 µl of sterile water and subsequently stored at -20 °C.

The single restriction digest of purified pONR1 DNA comprised 3 µl plasmid DNA (10 µg DNA), 1 µl *Kpn* I (10 units of activity per µl), 2 µl of 10x *Kpn* I buffer and 14 µl of water, incubated in a water bath at 37 °C, for three hours, before loading onto an agarose gel.

2.2.2 Submarine agarose gel electrophoresis

Agarose gels (100 ml) were comprised of 0.8 % agarose w/v and Tris acetic acid EDTA (TAE) buffer (TAE buffer consists of 4.84 g Tris base, 1.14 ml glacial acetic acid and 2 ml 0.5 M EDTA, pH 8.0 in one litre of water) and 5 µl of 10 mg/ml ethidium bromide solution. The gels were electrophoresed in 1x TAE buffer at 150 V for 60 minutes. Samples were loaded onto the gel after mixing with 6x DNA loading buffer (which comprises 0.25 % bromophenol blue, 0.25 % xylene cyanol and 30 % v/v glycerol in water). A 1 Kb DNA ladder (MBI Fermentas) was also loaded onto the gel as a marker. Gels were analysed using long wavelength ultraviolet (UV) light on a UVP transilluminator.

2.2.3 Mutagenesis of pONR1 plasmid

Mutagenesis of the pONR1 plasmid was performed using the QuikChange Site-directed Mutagenesis Kit from Stratagene. Mutations concerning the substitution of Tyr 186 for Phe 186 involved the use of the following sense and antisense primers (letters in bold denote the bases mutated to code for Phe (WT: these bases were TAC, 5'→3'), and code from base 542 to 576 of the gene):

```

5'   TTCACTCTGCGCACGGTTTTCTGCTGCATCAGTTC   3'
3'   AAGTGAGACGCGTGCCAAAAGACGACGTAGTCAAG   5'

```

The primers were synthesised by the PNAOL department at the University of Leicester. Subsequently, these oligonucleotides were purified by ethanol precipitation as described by Sambrook *et al* (1989).

Mutagenesis was performed on a PHC-3 thermal cycler from Techne Ltd. The polymerase chain reaction (PCR) reaction consisted of 10 µl (50 ng) of pONR1, 4 µl (125 ng) of each primer, 1 µl of dNTP mix (10 mM stock), 1 µl of *Pfu* turbo DNA polymerase, sterile water to a final volume of 50 µl and 30 µl of mineral oil. The mixture was then programmed to cycle 30 times between 94 °C (denaturation step) for 30 sec, 60 °C (annealing step) for 1 min, and 72 °C (extension step) for 6 min. The reaction was then linked to a final step set at 72 °C for 10 minutes. Following temperature cycling the reaction mixture was left on ice for 2 min. Digestion of methylated wild-type DNA was conducted by adding 1 µl of *Dpn* I restriction enzyme (10 units per µl) to the treated DNA samples (after removing them from beneath the mineral oil). The mixture was then mixed and spun down for 1 min in a microcentrifuge and subsequently incubated at 37 °C for one and a half hours. Following digestion of methylated DNA, a ligation step was performed, using 25 µl of *Dpn* I treated PCR DNA, 2.5 µl of 10x DNA ligase reaction buffer, and 1 µl of T4 DNA ligase. The mixture was then incubated at 16 °C for 5 hrs. Following incubation, the ligated DNA was transformed into *E. coli* JM109 cells (Section 2.2.4).

E. coli strains transformed with plasmid pONR1, in which the codon for Trp 102 was replaced for that encoding phenylalanine and tyrosine and where His 181 and 184 were replaced with Ala 181 and 184, were kindly provided by Dr T. Barna. All glycerol stocks were stored at -80 °C.

2.2.4 Transformation of Y186F mutated pONR1 plasmid into *E. coli* JM109 cells

Transformation of the mutated DNA into bacterial cells was performed using 20 µl of treated DNA mixed with 50 µl of *E. coli* JM109 competent cells. The mixture was left on ice for 15-45 min. The reaction was then incubated at 42 °C for exactly 90 s, and then put on ice for 2 minutes. Subsequently, four times the reaction volume of 2YT media (made of 16 g tryptone, 10 g yeast extract and 5 g sodium chloride in 1 litre), i.e. 280 µl, was added to the DNA mixture, which was then incubated at 37 °C in a shaking incubator, for one hour. Following incubation, 100 µl of the transformed cells (i.e. DNA sample in 2YT media) were plated onto LB-agar plates containing 100 µg/ml ampicillin (see Section 2.3.1), and incubated at 37 °C overnight or until visible colonies were identified. The colonies obtained were then inoculated in LB media supplemented with 100 µg/ml ampicillin (one colony per 6.5 ml of media) and incubated at 37 °C in a shaker for 14-15 hrs. The culture was then used for DNA sequencing (Section 2.2.5) and for the preparation of glycerol stocks, for each mutant form of PETN reductase (Section 2.3.1).

2.2.5 Sequencing of Y186F PETN reductase

The entire gene of the Y186F mutant protein was sequenced to ensure that the mutation made was successful and that no other unwanted mutations had been made to the rest of the gene. Transformed cells in LB media (5 ml), grown for at least 14 hrs, were centrifuged at 4000 rpm for 10 min at 25 °C. The sample pellet and four sequencing primers (see Table 2.1), purified by ethanol precipitation, were sent to the PNAACL department at the University of Leicester, for DNA sequencing.

2.3 Preparation and purification of wild-type and mutant forms of PETN reductase

2.3.1 Bacterial strains and media

E. coli JM109 strains carrying the wild-type, W102Y, W102F, H181A and H184A pONR1 plasmids were kindly donated by Dr Terez Barna.

Sequence (5' to 3') and position (bp)		
232	CCGGAACAGATCGCCGCG	249
*300	AACCGCAATACGGCCATC	283
433	GACACCACCACGCCACGC	450
802	TATCTGCACATGTCCGAG	820

Table 2.1. Primers used to sequence the entire gene of the Y186F mutant form of PETN reductase. (*This primer is an antisense primer for the sequence between bases 283 and 300 in wild-type pONR1.)

Glycerol stocks for each enzyme were made by adding 500 μ l of late exponential phase culture (grown in LB media; see below) to 250 μ l of 50% glycerol (sterilised), and stored at -80 °C.

For the initial growth and maintenance of bacterial strains, glycerol stocks of strains were streaked onto solid Luria-Bertani-Millar (LB) media agar plates consisting of: (autoclaved) 10 g bactotryptone, 5 g yeast extract, 10 g NaCl and 15 g bacteriological agar in 1 litre of water supplemented with 100 μ g/ml ampicillin. The plates were left at 25 °C overnight, or until visible colonies of bacterial culture could be seen.

For protein preparation and mini-preparation of plasmid DNA, small-scale bacterial cultures were grown in 10 ml SOB media consisting of: 20 g bactotryptone, 5 g yeast extract, 0.5 g NaCl and 250 mM KCl in 1 litre of water. After autoclaving (and before use), the media was supplemented with 20 ml of sterilised 1M $MgSO_4$ and 100 μ g/ml ampicillin.

2.3.2 Preparation of PETN reductase

For the preparation of the enzymes, a single colony of bacteria was used to inoculate a 10 ml (x6) starter culture of SOB media, supplemented with 10 μ l of sterilised 1M $MgSO_4$ and 100 μ g/ml ampicillin. The starter cultures were grown overnight, in an orbital shaker, at a speed of 220 rpm, at 37 °C. These cultures were then used to further inoculate (x6) 1 litre flasks of SOB media supplemented with 20 ml sterilised 1M $MgSO_4$ and 100 μ g/ml ampicillin. The 1 litre bacterial cultures were grown in the same conditions as the starter cultures until they had reached an optical density of 0.7-1.0 at 600 nm. Subsequently, the cultures were further supplemented with 0.4 mM IPTG to induce the expression of the enzymes and were incubated overnight or for a 20 h period. Cells were harvested in their stationary phase, by centrifugation at 5500 rpm in a Beckman Instruments JA 10 rotor, at 4 °C, for 15 min. Pellets produced from centrifugation were then re-suspended in 50 mM potassium phosphate buffer, pH 7.0. Cells were lysed using a French press (passing the cell suspension twice through the machine, at a pressure between 8000-12000 pounds per square inch). The released DNA was degraded by incubating the cell lysate with deoxyribonuclease I (10 μ g/ml) and 20 mM $MgCl$ for 1-2 h at 4 °C. Solutions of lysed cells were further centrifuged for 60 min at 15000 rpm in a Sorvall Instruments SS-34 rotor, at 4 °C. The pellet was discarded while the yellow supernatant, containing PETN reductase, was dialysed

overnight against 10 litres of 20 mM Tris-HCl buffer, pH 7.0, three times, at 4 °C. Further purification steps were performed at 4 °C.

2.3.3 Purification of wild-type PETN reductase

The dialysed crude protein solution was loaded onto an affinity chromatography column packed with Biomimetic orange 2A6xL, which had been equilibrated with 10 mM Tris-HCl buffer, pH 7.0. The column was then washed with 10 mM Tris-HCl buffer pH 7.0, until the absorbance of the eluent at 280 nm reached approximately 0.01. PETN reductase was eluted from the column with 10 mM Tris-HCl buffer, pH 7.0, containing 15 mM NaCl. Elution of the protein was detected by measuring the absorbance of the eluent at 450 nm, indicating the flavin content. The eluted protein was pooled and dialysed overnight three times, against 10 litres of 20 mM Tris-HCl buffer, pH 7.5.

Dialysed protein was re-chromatographed using an anion exchange column, packed with a high performance Q-Sepharose resin, equilibrated with 20 mM Tris-HCl buffer, pH 7.5. Once the protein sample had been loaded onto the resin, the column was washed thoroughly with 20 mM Tris-HCl buffer, pH 7.5, containing 30 mM NaCl, until the absorbance of the eluent at 280 nm fell relatively low. PETN reductase was eluted using a salt gradient of 20 mM Tris-HCl buffer, pH 7.5, containing 30 mM NaCl and 20 mM Tris-HCl buffer, pH 7.5, containing 150 mM NaCl. The absorbance of the fractions was measured at 450 nm. Fractions showing the highest absorbance were collected and concentrated by ultra-filtration using an Amicon PM 30 membrane. The collected PETN reductase solution was then dialysed overnight three times, against 10 litres of 50 mM potassium phosphate buffer, pH 7.0, and subsequently stored at -80 °C, for long term storage.

2.3.4 Purification of mutant PETN reductase enzymes

The W102F, W102Y and Y186F mutants of PETN reductase were purified using the procedure as described for wild-type enzyme (Section 2.3.3).

The H181A and H184A mutant forms of PETN reductase did not bind to the Biomimetic orange resin, therefore part of the purification procedure was modified. The crude extract (dialysed against 5 mM Tris-HCl buffer, pH 7.5) was loaded directly onto a Q-Sepharose column, pre-equilibrated with 5 mM Tris-HCl buffer, pH 7.5 and washed thoroughly with the same buffer. The enzymes were subsequently eluted using a salt gradient

of 5 mM Tris-HCl buffer, pH 7.5 alone, and with the same buffer including 200 mM NaCl. Following elution, fractions containing the mutant form of the enzyme were pooled and dialysed against 5 mM Tris-HCl buffer, pH 7.5. The enzyme solution was then reloaded onto another clean Q-Sepharose column in an attempt to purify the enzyme further. The column was washed thoroughly with 5 mM Tris-HCl buffer, pH 7.5 containing 15 mM NaCl and eluted with a salt gradient between 15 mM and 150 mM NaCl, in 5 mM Tris-HCl buffer, pH 7.5. The purity of each enzyme sample was analysed by SDS polyacrylamide gel electrophoresis (Section 2.4)

2.4 SDS Polyacrylamide Gel Electrophoresis

SDS polyacrylamide gels (SDS PAGE) were prepared, using the following components (in order of addition):

Resolving gel:

Chemical	Quantity
Distilled water	8 ml
1.5 M Tris-HCl, pH 8.8	7.5 ml
10 % (w/v) SDS	300 μ l
30 % acrylamide/bisacrylamide	10 ml
10 % ammonium persulfate	100 μ l
TEMED	10 μ l

Stacking gel:

Chemical	Quantity
Distilled water	6 ml
1 M Tris-HCl, pH 6.9	1.25 ml
10 % (w/v) SDS	100 μ l
30 % acrylamide/bisacrylamide	1.3 ml
10 % ammonium persulfate	50 μ l
TEMED	5 μ l

(N.B. The quantities stated make two SDS gels)

Protein samples taken before the cells were lysed and were denatured by dissolving them in 6 M urea. Samples were then added to an equal volume of 10 % SDS. All protein samples (10 μ l) were added to sample buffer (consists of 0.4 ml 14.3 M 2-mercaptoethanol solution, 1.6 ml 10 % (w/v) SDS, 1 ml 50 mM Tris-HCl, pH 8.0, 0.8 ml glycerol, 0.4 ml 1 % (w/v) bromophenol blue and 3.8 ml water) by ratio of 1:4 and boiled for five minutes, before being loaded onto the gel. Gels were left to run at a current of 60 mA for 60 min (or until the dye front had reached the base of the gel). Gels were run in running buffer composed of 2.9 g glycine, 6.0 g Tris and 1.0 g SDS in 1 litre of distilled water. Once run, the gels were stained in Coomassie Brilliant Blue R250 for 20 minutes and then destained in a solution of methanol : acetic acid : water in a 5:1:5 v/v ratio.

2.5 Ligand binding studies

Wild-type PETN reductase and the mutant forms of the enzyme, were titrated with stock solutions of picric acid, progesterone (dissolved in methanol), 2,4-dinitrophenol (2,4-DNP) and TNT (dissolved in acetone). Titrations were performed using a 1 ml quartz cuvette containing ~ 10 μ M enzyme in 50 mM potassium phosphate buffer, pH 7.0. Upon each addition of ligand to the enzyme solution, the absorption spectrum of the enzyme plus ligand mixture was measured using a Jasco V-550 UV/Vis spectrophotometer. Increased volumes of ligand were added from a stock concentration to the same enzyme solution until no significant absorption change could be detected in the absorption profile, indicating that the enzyme had been saturated with ligand molecules. From the individual absorption spectra for each ligand concentration, readings were taken at a wavelength (518 nm) where the ligand and enzyme individually had little or no absorption and the initial free enzyme absorbance at 518 nm was subtracted from these data. The absorbance changes at 518 nm were plotted as a function of ligand concentration and analysed for concentration dependence using the Origin 4.0 software package. Data were fitted to either a simple hyperbolic curve or a quadratic fit (Equation 2.1), from which the dissociation constant for enzyme-ligand binding was calculated.

$$A_{\text{obs}} = \frac{\Delta A_M}{2[E]_T} \left[([L] + [E]_T + K_d) - \left(([L] + [E]_T + K_d)^2 - 4[L][E]_T \right)^{0.5} \right]$$

Equation 2.1

ΔA_M is the maximum absorbance change, $[L]$ is the ligand concentration at which the absorbance change is measured (A_{obs}), $[E]_T$ is the total ligand concentration and K_d is the dissociation constant.

2.6 Single wavelength stopped-flow studies of the reductive half-reaction

The reductive half-reaction of the enzymes were investigated using single wavelength stopped-flow analysis. Measurements were made using an Applied Photophysics SX.17MV stopped-flow spectrophotometer. Data were analysed on an Archimedes 410-1 microcomputer. To control the temperature of the reactions, the sampling handling unit of the stopped-flow spectrophotometer was linked to a TE-8A Tempette combined pump, thermostat controlled heater unit and refrigerated water bath from Techne Limited. All reactions were carried out at 5 °C. Measurements were made using ~20 μM of enzyme and varying concentrations of β -NADPH, in 50 mM potassium phosphate buffer, pH 7.0. (twice the concentration of reagents/enzyme had to be placed into the syringes on the machine, as during mixing the concentration of the reagents dilutes two-fold). The lowest β -NADPH concentration used was at least 5-fold greater than that of the enzyme concentration, and the maximum β -NADPH concentration used was a concentration that would give rates less than 600 s^{-1} , to maintain accuracy.

Absorption changes were monitored at two wavelengths: 464 nm and 560 nm, as established by previous studies on PETN reductase by Dr Daniel Craig, (2000). The absorbance change at 464 nm was followed in order to calculate the rate of flavin reduction. The absorbance change at 560 nm was monitored to follow the rate of formation and decay of a charge-transfer intermediate. Averages of three to four individual transients were analysed to give a reaction rate (once fitted to their relevant equation), for each β -NADPH concentration.

Transients were fitted using non-linear least squares regression using Spectrakinetics software (Applied Photophysics). Two equations were used to analyse the transients produced by absorption changes (A) at 464 nm and 560 nm. The first equation, Equation 2.2, describes a single exponential process for the change in absorption:

$$A = Ce^{-k_{\text{obs}}t} + b$$

Equation 2.2

C is a constant related to the initial absorbance and b is an offset value to account for a non-zero baseline. Equation 2.3 describes a double exponential process where the two processes are sequential, but bring about a positive and negative absorbance change (defined as an “up-down” equation).

$$A = k_{\text{obs1}} C \frac{e^{-k_{\text{obs1}}} - e^{-k_{\text{obs2}}}}{k_{\text{obs2}} - k_{\text{obs1}}} + b$$

Equation 2.3

k_{obs1} is the observed rate constant for the increase in absorbance and k_{obs2} is the observed rate constant for the decrease in absorbance. The rates produced by analysis of the stopped-flow data using the above two equations were further analysed for concentration dependence using Grafit 5.0 software package, where the data were fitted to a linear process.

2.7 Anaerobic conditions

Anaerobic conditions were established by the use of a Belle Technology glove box filled with oxygen-free nitrogen. An oxygen-scavenging BASF R3-11 catalyst system fitted within the glove box further minimised oxygen levels. Accordingly, the oxygen level was kept below 7 parts per million (ppm) as measured by a Type O2M-1 oxygen meter (Belle Technology). A nitrogen flushed transfer port was used to transfer objects to and from the anaerobic box. Humidified Pureshield brand argon at 5 psi was bubbled through solutions of buffers and solvents contained within a stirred, sealed container, for one and a half hours. The buffer was then immediately transferred to the anaerobic glove box and was left open overnight, to equilibrate with the anaerobic atmosphere. Substrates were pre-weighed before being transferred to the glove box. Inside the glove box, they were dissolved in anaerobic buffer/solvent and their concentration was checked spectrophotometrically. Enzymes were made anaerobic by passing them through a Bio-Rad 10-DG gel filtration column, which had been pre-equilibrated with anaerobic 50 mM potassium phosphate buffer, pH 7.0. Enzyme solutions were kept in an icebox inside the anaerobic glove box.

2.8 Anaerobic single and multiple turnover studies

To identify intermediates or products, single and multiple turnover studies with TNT, picric acid and nitrocyclohexene were performed using absorption spectroscopy and NMR spectroscopy, under anaerobic conditions, as described in Section 2.7. All optical spectral measurements were made using a 1 ml quartz cuvette and a JascoV-550 UV/Vis spectrophotometer fitted within the glove box.

2.8.1 Spectral single turnover studies

Single turnover studies were performed by initially titrating 15-20 μM of gel-filtered enzyme (in 50 mM potassium phosphate buffer, pH 7.0), with sodium dithionite, to stoichiometrically reduce the enzyme (monitored by the disappearance of the characteristic 450 nm flavin absorbance of the enzymes). The reaction was initiated by the addition of stoichiometric concentrations of TNT (dissolved in HPLC grade acetone) or picric acid. To follow the reaction, absorption spectra of the enzyme plus substrate solution were recorded as soon as the substrate was added. Subsequent spectra were recorded at 2 min intervals, until no significant absorption change could be seen between spectra following the reaction i.e. at least 5-10 of the latest spectra of the reaction were overlaid and no significant difference could be seen between them. Subsequently, the absorption spectra measured over time for each enzyme were overlaid and examined for any evidence of hydride-Meisenheimer complex formation or of any other spectral intermediates.

2.8.2 Spectral multiple turnover studies with TNT and picric acid

The multiple turnover of TNT and picric acid was followed using β -NADPH (100 μM) reduced enzyme (0.2 μM), and an NADPH-regeneration system consisting of 10 mM glucose-6-phosphate, and 1 unit of glucose-6-phosphate dehydrogenase (French *et al.*, 1998), in 50 mM potassium phosphate buffer, pH 7.0. The addition of excess TNT (dissolved in HPLC grade acetone) or picric acid to the enzyme mixture initiated the reaction. Substrate turnover was followed spectrally until no absorption change could be seen between the last 10-15 spectra.

2.8.3 NMR analysis of the multiple turnover of TNT

Due to differences obtained in the spectral analysis of the multiple turnover of TNT with wild-type and W102F and W102Y mutant enzymes, NMR spectroscopy was used to further explore the breakdown of TNT by these enzymes. This was done in an attempt to identify the intermediates and the end product(s) of TNT degradation by wild-type and Trp 102 mutant forms of the enzyme. In turn, this would help in identifying any role that Trp 102 may play in the degradation of TNT in PETN reductase.

All NMR samples were prepared under anaerobic conditions (see Section 2.7) using NMR sample tubes sealed with a rubber septa and nescofilm for transferral to the NMR machine. Individual samples of 1 mM TNT (dissolved in 99.9 % D₂O acetone), 0.2 μM enzyme (passed through a NAP 5 column (pre-packed with sephadex G-25), pre-equilibrated with 50 mM D₂O potassium phosphate buffer, pH 7.0) and 1.5 mM NADPH and 1.5 mM NADP⁺, and a sample of all the above components combined, except enzyme and NADP⁺, was prepared for the assignment of spectral peaks. The reaction mixture was made by the addition of 0.2 μM enzyme to the NMR sample containing NADPH (1.5 mM) and TNT (1mM), inside an anaerobic box. The reaction sample was then immediately analysed using NMR spectroscopy. NMR spectroscopy was performed in collaboration with Dr Igor Barsukov from the NMR department, University of Leicester.

NMR spectra were acquired at 500 and 600 MHz on a Bruker DRX600 and DRX500 spectrometers at 25 °C. Residual water signal was attenuated with low-power presaturation in relaxation delay. The spectra were processed and analysed using XWINNMR 3.5 software (Bruker), and were referenced to the external DSS standard at 0.000 ppm. A sweep width of 12 ppm was used for all 1D spectra. To monitor the reaction course, a continuous set of 1D experiments was recorded at 600 MHz over 3 hr with each 1D spectrum taking 3 min to acquire. 2D COSY-DQF spectra were recorded at 500 MHz using 2048x512 complex data points with a sweep width of 12ppm and processed to 4096x2048 real data points.

2.8.4 Spectral multiple turnover studies with nitrocyclohexene

Studies with nitrocyclohexene were performed using the method outlined by Meah and Massey (2000). A concentrated stock of nitrocyclohexene was introduced into the box in its undiluted form. Subsequent dilutions of nitrocyclohexene were made in anaerobic ethanol. A cuvette consisting of 0.1 μM anaerobic enzyme, 8 μM NADPH, 2 mM glucose-6-

phosphate and 10 units of glucose-6-phosphate dehydrogenase in 50 mM potassium phosphate buffer, pH 7.0, was set as the spectrophotometric blank. The reaction was initiated by the addition of approximately 80 mM nitrocyclohexene to the cuvette and followed spectrally.

2.9 Anaerobic stopped-flow studies

2.9.1 Single wavelength studies on the oxidative half-reaction

Anaerobic stopped-flow studies were performed using an Applied Photophysics SX.17MV stopped-flow spectrophotometer with the sample-handling unit fitted inside an anaerobic Belle Technology glove box. Measurements were made using single wavelength spectroscopy. Maintenance of anaerobic conditions throughout the experiment was conducted using the conditions described under Section 2.7. It should be noted that the concentration of solutions placed into the syringes of the stopped-flow machine must be twice the required concentration as the solutions are diluted two-fold upon mixing.

Enzymes were passed down a Bio-Rad 10-DG size separation column inside the anaerobic box, which had been pre-equilibrated with anaerobic 50 mM potassium phosphate buffer, pH 7.0. The enzymes were collected typically at a concentration of 80 μ M and transferred to a 3 ml quartz cuvette with a self-sealing rubber septa and nescofilm, for the reductive titration of the enzyme with sodium dithionite, outside the anaerobic box. The sodium dithionite solution was made within the anaerobic box, at a high concentration in anaerobic 50 mM potassium phosphate buffer, pH 7.0 and was calibrated with an anaerobic FMN solution, to calculate the volume of sodium dithionite needed to stoichiometrically reduce the enzyme. Reduction of the enzyme proceeded by titration under anaerobic conditions with sodium dithionite using a gas-tight syringe pre-filled with anaerobic dithionite inside the box, and was followed spectrally (on a spectrophotometer outside the glove box), to ensure that the enzyme was reduced with stoichiometric amounts of dithionite (and not excess), thus allowing single turnovers of the enzyme to take place.

The oxidative half-reaction of PETN reductase and the mutant forms of the enzyme were investigated using TNT (at 25 °C), GTN (at 5 °C) and 2-cyclohexenone (at 25 °C) as substrates. TNT was pre-weighed before being introduced into the box. Inside the box, TNT was dissolved in HPLC grade acetone (which had been pre-equilibrated with argon and

anaerobic atmosphere) to give a final concentration of 600 mM. From this stock, dilutions were made in acetone, to give 100x the concentration of TNT required for the reactions. As a result, 1% acetone was maintained in all reactions by mixing 10 μ l of the 100x concentrated TNT stock into 990 μ l of potassium phosphate buffer, pH 7.0, to give the desired TNT concentration. Due to the low solubility of TNT in water, concentrations of up to 1 mM could be used in reactions.

GTN was introduced into the box at a concentration of 450 mM in acetone, in its undiluted form. Further serial dilutions of GTN were made inside the anaerobic box in anaerobic acetone, as described for TNT, to maintain 1% acetone in the reactions at all time.

2-cyclohexenone was introduced in its undiluted form at 10 mM. Dilutions of 2-cyclohexenone were made directly into 50 mM potassium phosphate buffer, pH 7.0.

Pseudo-first order conditions were employed in all studies, which in some cases narrowed the range of substrate concentrations that could be studied. Absorbance changes produced by the rapid mixing of enzyme and substrate were monitored at the maximum flavin absorbance for the particular enzyme (mainly 462 nm). In the case of TNT, absorbance changes were also monitored at 560 nm (the wavelength maxima for the TNT hydride-Meisenheimer complex). Averages of three to four individual transients were analysed to give a reaction rate (once fitted to their relevant equation), for each substrate concentration. Transients were fitted using non-linear least squares regression using Spectrakinetics software (Applied Photophysics). The concentration dependence of rates was analysed using Grafit 5.0 software.

2.9.2 Multiple wavelength stopped-flow studies

Multiple wavelength rapid reaction kinetic studies of the reductive and oxidative half-reactions were performed using an Applied Photophysics SF.17MV stopped-flow spectrophotometer fitted with a photodiode array detector and X-SCAN software. Studies were performed using anaerobic conditions (see Section 2.7), with the sample handling unit of the stopped-flow machine fitted inside an anaerobic glove box. Enzymes were made anaerobic by passing them through a Bio-Rad 10-DG column. For the oxidative half-reaction studies, enzymes were titrated with sodium dithionite until complete reduction of the enzyme was achieved (see Section 2.9.1 for details). Enzymes were mixed with both stoichiometric and ten times excess TNT (made as outlined in Section 2.9.1) or NADPH in 50 mM

potassium phosphate buffer, pH 7.0. Data was analysed for the formation of spectral intermediates by global analysis using PROKIN software (Applied Photophysics).

2.10 Anaerobic redox potentiometry

Redox titrations were performed using anaerobic conditions as described in Section 2.7. The anaerobic box was fitted with a Hanna instruments pH/voltmeter coupled to a Russel platinum/calomel electrode, to measure the electrochemical potential. The electrode had been previously calibrated using the Fe(II)/Fe(III)-EDTA couple (+108 mV) as a standard. Absorbance spectra were measured using a Varian UV-visible spectrophotometer, with the Cary 50 probe fitted within the anaerobic box.

Enzymes were passed through a Bio-Rad 10-DG column and diluted to a final concentration of ~40 μM , in 100 mM potassium phosphate buffer, pH 7.0, collected within a 10 ml beaker. Redox mediators; benzyl viologen, methyl viologen, 2-hydroxy-1,4-naphthaquinone and phenazine methosulfate, were added at a final concentration of 0.5 μM to the enzyme solution. In order to constantly monitor absorbance and potential changes of the enzyme at the same time, the absorbance and electrochemical probes were both positioned to fit within the 10 ml beaker carrying the enzyme solution. The enzyme solution was titrated with sodium dithionite as a reductant. Upon addition of each aliquot of sodium dithionite (typically 30-40 aliquots were made), the enzyme solution was left to equilibrate, monitored by the stabilisation of the observed potential. Upon stabilisation/equilibration of the redox potential, the absorbance of the enzyme solution was measured and the potential noted. The enzyme was titrated with sodium dithionite until complete reduction of the flavin was achieved. Thereafter, the enzyme was titrated with potassium ferricyanide as an oxidant while measuring the absorbance and redox potential of the enzyme solution. This was done to ensure that the potential of the enzyme measured during reduction matched the potential measured during re-oxidation, and to ensure that the enzyme was able to fully re-oxidise.

Data analysis of the observed redox potentials for the reductive and oxidative titrations was performed using Origin software. The observed potentials were corrected to those for the standard hydrogen electrode (+244 mV) and plotted against the corresponding absorbance values at 468 nm (wavelength close to the flavin maximum). Data were fitted to a concerted two electron redox process (Equation 2.4), derived by extension to the Nernst equation and Beer-Lambert Law (Dutton, 1978; Khan *et al.*, 2002).

$$A_{468} = \frac{(a + b10^{(E'-E)/29.5})}{1 + 10^{(E'-E)/29.5}}$$

Equation 2.4

A_{468} is the absorbance value at 468 nm at the electrode potential E , and a and b are the absorbance values at 468 nm, of fully oxidised and reduced enzyme, respectively. E' is the midpoint potential. Throughout the course of the titrations the enzymes remained stable; therefore there was no need to make corrections for turbidity.

2.11 X-ray crystallography

Crystallisation conditions for wild-type PETN reductase have been established (Barna *et al*, 2000). Using the published conditions for wild-type enzyme, crystallisation of Y186F and H181A PETN reductases was attempted. However, in order to produce larger and better quality crystals the conditions were refined, following a number of screens. Mother liquor solutions were made of 30 %, 25 %, 20% and 15 % PEG 3000 (w/v), containing 10 % isopropanol, 0.1 M cacodylic acid combined with either 0.1 M sodium citrate, sodium chloride, sodium acetate or sodium thiocyanate, pH 6.2. Using the sitting drop vapour diffusion method, crystals were grown using 4 μ l of 8-9 mg/ml enzyme mixed with 4 μ l of the mother liquor, at 25 °C. Co-crystallisation of the enzymes with picric acid was also attempted using the condition described above, but with the incorporation 2 mM picric acid into the mother liquor solutions.

Further analysis of the crystals and molecular replacement was done by Dr David Leys at the University of Leicester, who kindly provided the data and images for the solved structures of the mutant forms of PETN reductase.

Chapter Three

Mechanism of Explosive Degradation: Role of Trp 102

CHAPTER THREE

Mechanism of explosive degradation: role of Trp 102

3.1 Introduction

The present chapter covers the purification of PETN reductase and characterisation of its catalytic activity with a representative compound from each substrate group, namely picric acid/TNT (nitroaromatic), GTN (nitrate ester) and 2-cyclohexenone (α,β -unsaturated compound). Based on structural analyses, it was suggested that Trp 102 in the active site of PETN reductase influences the binding and possibly the degradation of nitroaromatic compounds. Therefore, to gain some insight into the mechanism of nitroaromatic degradation by PETN reductase, mutational studies were performed. Accordingly, the purification and characterisation of two Trp 102 mutant forms of PETN reductase is reported herein and comparisons with the wild-type enzyme are made.

Before reporting on the characterization of each enzyme, the chapter begins by describing the rationale behind the work, the mechanism by which PETN reductase is believed to transform nitroaromatic compounds, and the crystal structure of the enzyme complexed with nitroaromatics in the active site.

3.1.1 Transformation of nitroaromatic compounds by PETN reductase

Transformation of nitroaromatic compounds has been shown to proceed via two different mechanisms; (i) the direct two-electron reduction of the aromatic ring via hydride addition (Meisenheimer formation pathway), a mechanism limited to few organisms/enzymes [e.g. *Mycobacterium* sp. strain HL 4NT-1 (Vorbeck *et al*, 1994, 1998), *Rhodococcus erythropolis* strain HL PM-1 (Lenke and Knackmuss, 1992), xenobiotic reductase B from *Pseudomonas fluorescens* I-C (Pak *et al*, 2000)], and (ii) the successive two-electron reduction of the nitro groups (nitroreductase pathway). This latter mechanism is widespread among a number of oxidoreductases [e.g. OYE, xenobiotic reductase A (Pak *et al*, 2000) and bacterial strains TNT8 and TNT32 (Vorbeck *et al*, 1998)] owing to the nitro groups being readily susceptible to enzymatic reduction (see Chapter 1 for a detailed account of nitroaromatic transformation). While some enzymes are capable of catalysing either one of

these reactions, others are able to undertake both methods of nitroaromatic degradation. PETN reductase possesses the ability to catalyse both types of transformation reactions (French *et al*, 1998; Williams *et al*, 2001).

Transformation of TNT via the nitroreductase activity of PETN reductase yields isomers of hydroxylaminodinitrotoluene (HADNT; where either the nitro group at position 4 or 2 is reduced). These compounds are produced rapidly during TNT transformation and subsequently consumed more slowly to yield aminodinitrotoluene (ADNT; French *et al*, 1998; Williams *et al*, 2004). ADNTs have generally been reported to be the end product of TNT transformation by aerobic micro-organisms (Rieger and Knackmuss, 1995). However, Williams and co-workers (Williams *et al*, 2004) recently reported that during the transformation of TNT by PETN reductase, the concentration of ADNT never exceeded 4% of the initial TNT concentration. Moreover, they observed that the ADNT compounds were reduced further to yield a polar metabolite suggested to be 2,4-dihydroxylamino-6-nitrotoluene (Williams *et al*, 2004). Their findings therefore suggest that ADNTs are not the end-point of TNT nitro group reduction, and further reduction steps are likely to occur.

Transformation of TNT by PETN reductase has also been reported to produce an orange/red product, identified as the hydride-Meisenheimer complex of TNT (French *et al*, 1998). This complex is formed by direct reduction of the TNT aromatic ring achieved by the transfer of a hydride ion from the enzymes reduced flavin N5 atom to the electrophilic C3/C5 position of TNT. PETN reductase further reduces the hydride-Meisenheimer complex to form four compounds suggested to be isomers of a dihydride-Meisenheimer complex (Williams *et al*, 2004; French *et al*, 1998). This complex is formed by the addition of a further hydride ion to the aromatic ring of the hydride-Meisenheimer complex. Production of the dihydride-Meisenheimer complex occurs at a faster rate than the formation of the hydride-Meisenheimer complex (French *et al*, 1998). Further reduction of the dihydride-Meisenheimer complex leading to the liberation of nitrite has been reported, but details of these reactions have yet to be identified (French *et al*, 1998; Williams *et al*, 2004). The transformation of TNT via the two competing pathways of PETN reductase (i.e. nitroreductase and ring reduction pathway) is illustrated in Figure 3.1. It has been suggested by Pak and co-workers (Pak *et al*, 2000) that the two pathways of TNT transformation might be interrelated, which eventually leads to the release of nitrite. They suggested that during TNT transformation by xenobiotic reductase B, the dihydride-Meisenheimer complex produced is stable and in the presence of HADNT and oxygen, dimerisation of the complex with HADNT occurs, leading to nitrite release. However, recent studies with PETN reductase indicate that this is unlikely to occur. Williams

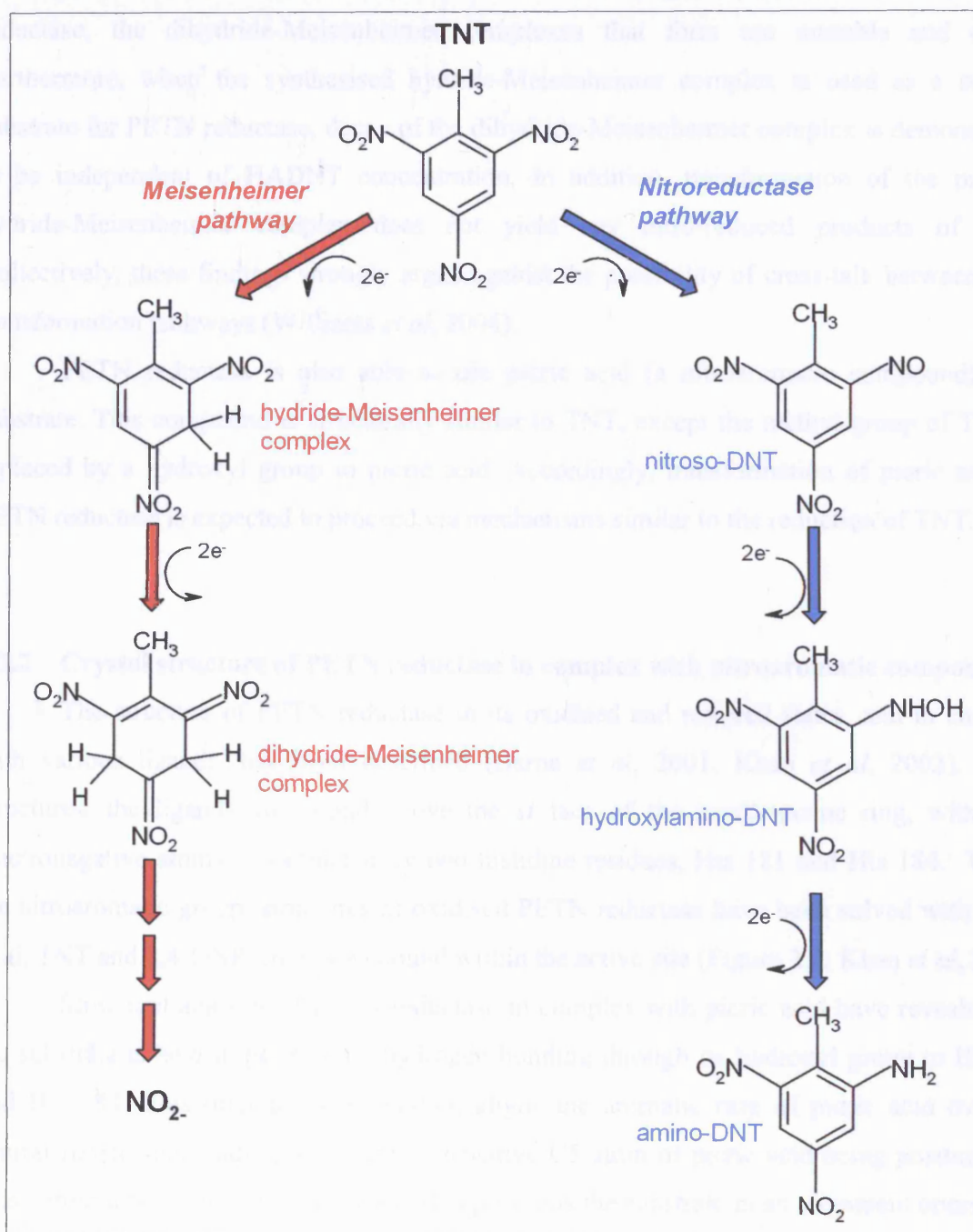


Figure 3.1. Proposed pathway for the degradation of TNT by PETN reductase. PETN reductase possesses the ability to directly reduce the nitro groups of TNT (via nitroreductase pathway; right pathway) and directly reduce the aromatic ring leading to nitrite elimination (Meisenheimer pathway; left pathway). The intermediates formed following the formation of the dihydride-Meisenheimer complex have not yet been identified. (Adapted from Pak *et al*, 2000 and Williams *et al*, 2004).

and co-workers (Williams *et al*, 2004) reported that during TNT transformation by PETN reductase, the dihydride-Meisenheimer complexes that form are unstable and decay. Furthermore, when the synthesised hydride-Meisenheimer complex is used as a starting substrate for PETN reductase, decay of the dihydride-Meisenheimer complex is demonstrated to be independent of HADNT concentration. In addition, transformation of the purified hydride-Meisenheimer complex does not yield any nitro-reduced products of TNT. Collectively, these findings strongly argue against the possibility of cross-talk between TNT transformation pathways (Williams *et al*, 2004).

PETN reductase is also able to use picric acid (a nitroaromatic compound) as a substrate. This compound is structurally similar to TNT, except the methyl group of TNT is replaced by a hydroxyl group in picric acid. Accordingly, transformation of picric acid by PETN reductase is expected to proceed via mechanisms similar to the reduction of TNT.

3.1.2 Crystal structure of PETN reductase in complex with nitroaromatic compounds

The structure of PETN reductase in its oxidised and reduced states, and in complex with various ligands, has been described (Barna *et al*, 2001; Khan *et al*, 2002). In all structures, the ligands are bound above the *si* face of the isoalloxazine ring, with their electronegative atoms co-ordinated by two histidine residues, His 181 and His 184. Within the nitroaromatic group, structures of oxidised PETN reductase have been solved with picric acid, TNT and 2,4-DNP (inhibitor) bound within the active site (Figure 3.2; Khan *et al*, 2002).

Structural analysis of PETN reductase in complex with picric acid have revealed that the substrate is held in position by hydrogen bonding through its hydroxyl group to His 181 and His 184. This orientation of binding aligns the aromatic ring of picric acid over the central flavin ring, leading to the electronegative C5 atom of picric acid being positioned in close proximity to the flavin N5 atom. This positions the substrate in an alignment optimal for hydride transfer, leading to the formation of the hydride-Meisenheimer complex. Although 2,4-DNP binds in a manner similar to picric acid (Figure 3.2), PETN reductase is unable to reduce this nitroaromatic compound. The rationale behind this is due to the different resonance stabilised forms of picric acid and 2,4-DNP. In 2,4-DNP, the positioning of the two nitro groups enhances the electrophilicity of the C3 atom (not C5), whereas it is the C5 atom which is positioned close to the flavin N5 atom. The geometry of 2,4-DNP binding is therefore unfavourable for hydride ion transfer from the flavin N5 atom to the reducible C3 atom in 2,4-DNP. In picric acid and TNT, the electrophilic nature of both the C3 and C5

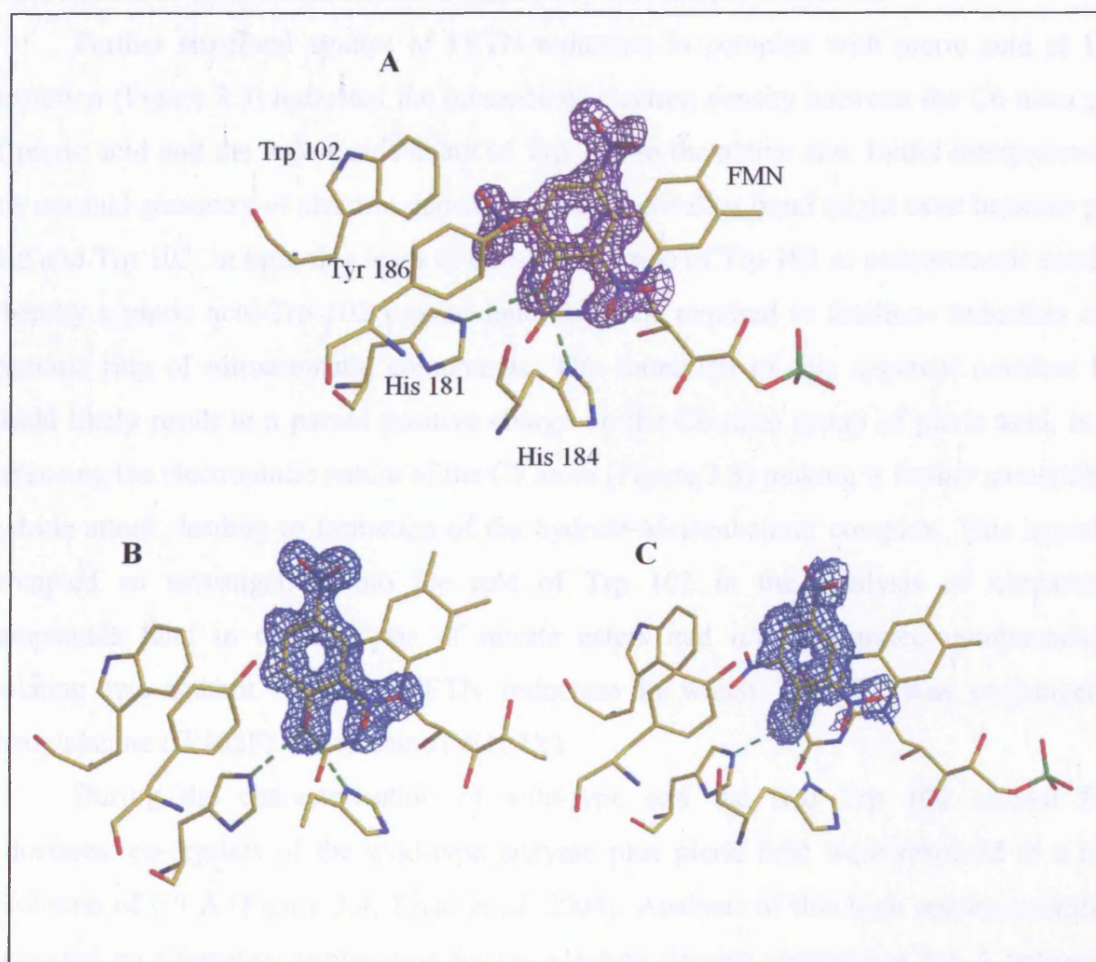


Figure 3.2. Difference electron density for PETN reductase complexed with nitroaromatic compounds. A, the complex of oxidised enzyme and picric acid; B, the complex of oxidised enzyme and 2,4-DNP; C, the complex of oxidised enzyme and TNT . All compounds are held within the active site by hydrogen bonding to His 181 and His 184. This mode of binding places the C5 atom of the nitroaromatics close to the flavin N5 atom so as to receive a hydride ion. In the case of picric acid and TNT, hydride transfer from the flavin to the C5 atom of the substrate leads to the formation of the respective hydride-Meisenheimer complex. However, the C5 atom of 2,4,-DNP does not undergo hydride attack as the positioning of the two nitro groups only enhances the electrophilic nature of the C3 atom and not the C5 atom, hence this ligand acts as a inhibitor for PETN reductase. (Figure abstracted from Khan *et al*, 2002).

atoms is enhanced through resonance stabilisation (Chapter 1; Figure 1.2), which enables hydride ion transfer to the C5 atom of TNT/picric acid to proceed. The electrochemical nature of nitroaromatic compounds therefore plays a key role in their reduction.

Further structural studies of PETN reductase in complex with picric acid at 1.5 Å resolution (Figure 3.3) indicated the presence of electron density between the C6 nitro group of picric acid and the indole side chain of Trp 102 in the active site. Initial interpretation of this unusual geometry of electron density was that a covalent bond might exist between picric acid and Trp 102. In turn, this leads to question the role of Trp 102 in nitroaromatic catalysis, whereby a picric acid-Trp 102 intermediate might be required to facilitate reduction of the aromatic ring of nitroaromatic compounds. The formation of this apparent covalent bond would likely result in a partial positive charge on the C6 nitro group of picric acid, in turn enhancing the electrophilic nature of the C5 atom (Figure 3.3) making it further susceptible to hydride attack, leading to formation of the hydride-Meisenheimer complex. This hypothesis prompted an investigation into the role of Trp 102 in the catalysis of nitroaromatic compounds (and in the catalysis of nitrate esters and α/β -unsaturated compounds), by isolating two mutant forms of PETN reductase in which Trp 102 was exchanged for phenylalanine (W102F) and tyrosine (W102Y).

During the characterisation of wild-type and the two Trp 102 mutant PETN reductases, co-crystals of the wild-type enzyme plus picric acid were resolved at a higher resolution of 0.9 Å (Figure 3.4; Khan *et al*, 2004). Analysis of this high resolution structure suggested an alternative explanation for the electron density observed at 1.5 Å between the picric acid nitro group and Trp 102. Closer inspection of the active site at 0.9 Å revealed that Trp 102 adopts at least two conformations when picric acid is bound in the active site (Figure 3.4). This suggested that a steric clash might exist between the side chain of Trp 102 and the nitro group of picric acid, explaining the anomalous electron density observed in the 1.5 Å structure. However, further solution studies were needed to ascertain any role for Trp 102 in the active site of the enzyme, particularly as regards hydride-Meisenheimer formation. A detailed analysis of the W102Y and W102F PETN reductases is described in this chapter.

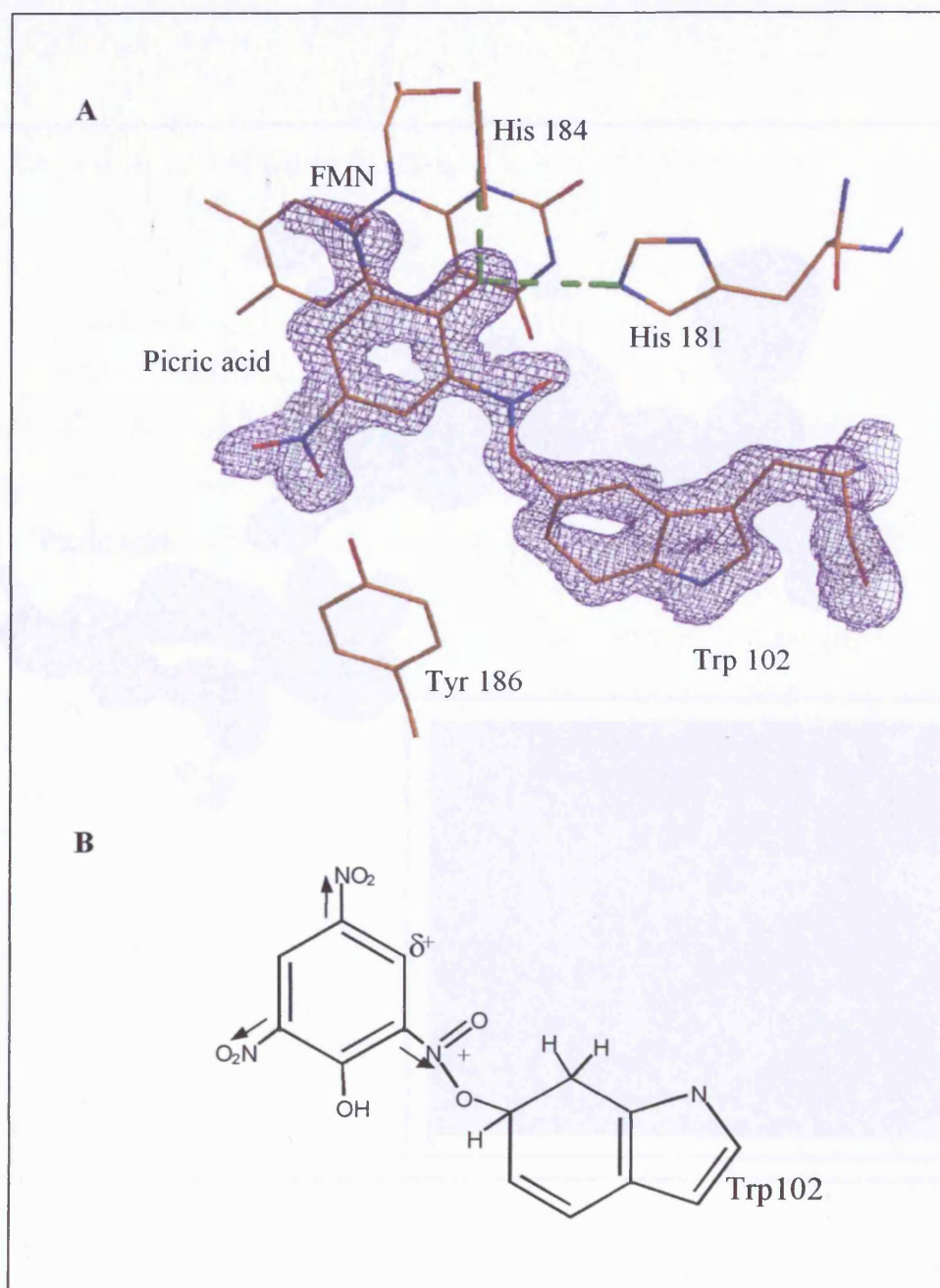


Figure 3.3. Active site structure of PETN reductase in complex with picric acid at 1.5 Å resolution. Panel A, 1.5 Å resolution structure of the active site. The electron density observed between the indole ring of Trp 102 and the nitro group of picric acid suggests that a covalent bond could form between these two groups. Panel B, structure of the potential covalent adduct between Trp 102 and picric acid. Bond formation would produce a partial positive charge on the C6 nitro group of picric acid, which in turn would enhance the electrophilic nature of the picric acid C5 atom (Khan *et al*, 2004).

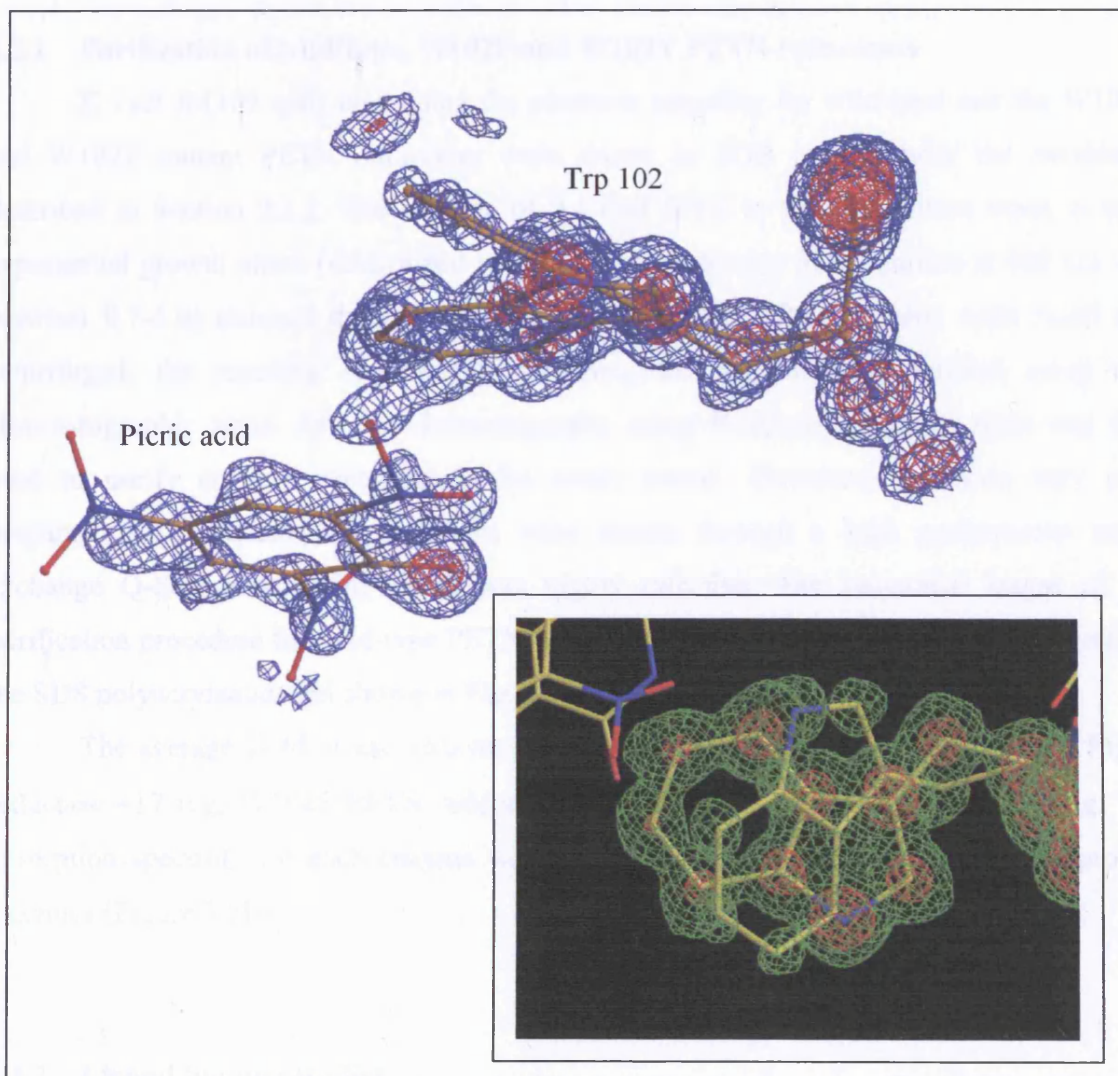


Figure 3.4. Active site structure of PETN reductase in complex with picric acid at 0.9 Å resolution. Trp 102 adopts different conformations with picric acid in the active site, suggesting that steric clashes exist between the side chain of Trp 102 and the C6 nitro group of picric acid. Inset, side view of the different conformations of Trp 102 (Khan *et al*, 2004).

3.2 Purification and characterisation of wild-type and Trp 102 mutant PETN reductases

3.2.1 Purification of wild-type, W102F and W102Y PETN reductases

E. coli JM109 cells containing the plasmids encoding for wild-type and the W102Y and W102F mutant PETN reductases were grown in SOB media under the conditions described in Section 2.3.2. The addition of 0.4 mM IPTG to the cell culture when in mid-exponential growth phase (determined when the optical density of the culture at 600 nm was between 0.7-1.0) induced the expression of the enzymes. After the cells were lysed and centrifuged, the resulting supernatant containing the enzyme was purified using two chromatographic steps. Affinity chromatography using Biomimetic orange resin was first used to purify enzyme contained in the crude extract. However, to obtain very pure preparations of the enzymes, solutions were passed through a high performance anion exchange Q-Sepharose resin, which was highly effective. The sequential stages of the purification procedure for wild-type PETN reductase and the mutant enzymes are depicted in the SDS polyacrylamide gel shown in Figure 3.5A.

The average yield of each enzyme produced, per litre of culture is: wild-type PETN reductase ~17 mg; W102F PETN reductase ~7 mg; W102Y PETN reductase ~4 mg. The absorption spectrum for each enzyme was found to be similar and typical of flavoprotein enzymes (Figure 3.5B).

3.2.2 Ligand binding studies

Equilibrium binding measurements were performed to determine the dissociation constant (K_d) for the oxidised enzyme-ligand complexes. These measurements would ensure that the active site of W102F and W102Y PETN reductases had not been grossly perturbed as a consequence of the mutations made to the enzymes. These studies would also determine whether Trp 102 has any involvement in the binding of various ligands (as suggested in the 0.9 Å structure; Section 3.1.2). Titrations were performed as described in Section 2.5, where wild-type PETN reductase and the W102F and W102Y mutant enzymes were titrated with stock solutions of picric acid, progesterone, 2,4-DNP and TNT. For each titration, absorption spectra were measured as ligand was added and subsequently overlaid (Figure 3.6). Addition of 2,4-DNP, picric acid and progesterone to each enzyme elicited changes in the absorption

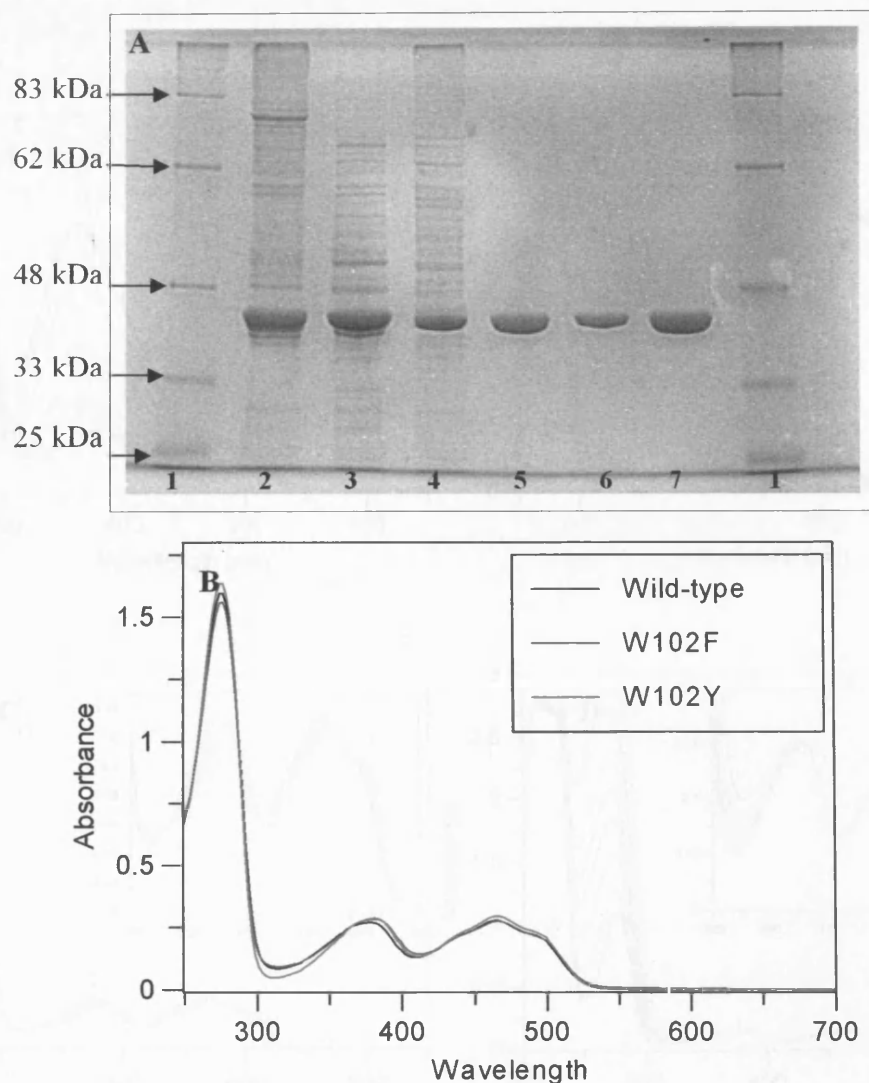


Figure 3.5. SDS PAGE analysis of the purification of wild-type, W102F and W102Y PETN reductases and the absorption spectrum of the purified enzymes. Panel A. Lane 1, molecular weight markers; Lane 2, lysate of grown *E. coli* cells containing the pONR1 plasmid encoding PETN reductase, after being centrifuged and passed through a French press (twice) at a pressure between 8000-12000 pounds per square inch; Lane 3, supernatant of lysed bacterial cells after centrifugation at 15500 rpm; Lane 4, enzyme solution collected once the supernatant had been passed through an affinity chromatography Biomimetic orange resin; Lane 5, purified wild-type enzyme obtained by passing the enzyme solution through a high performance anion exchange Q-Sepharose chromatography column; Lane 6, purified W102F PETN reductase; Lane 7, purified W102Y PETN reductase. Panel B. UV-visible absorption spectra of purified wild-type (black line), W102F (blue line) and W102Y (red line) PETN reductases. (λ_{\max} positions for each enzyme are 280 nm, 380 nm and 464 nm).

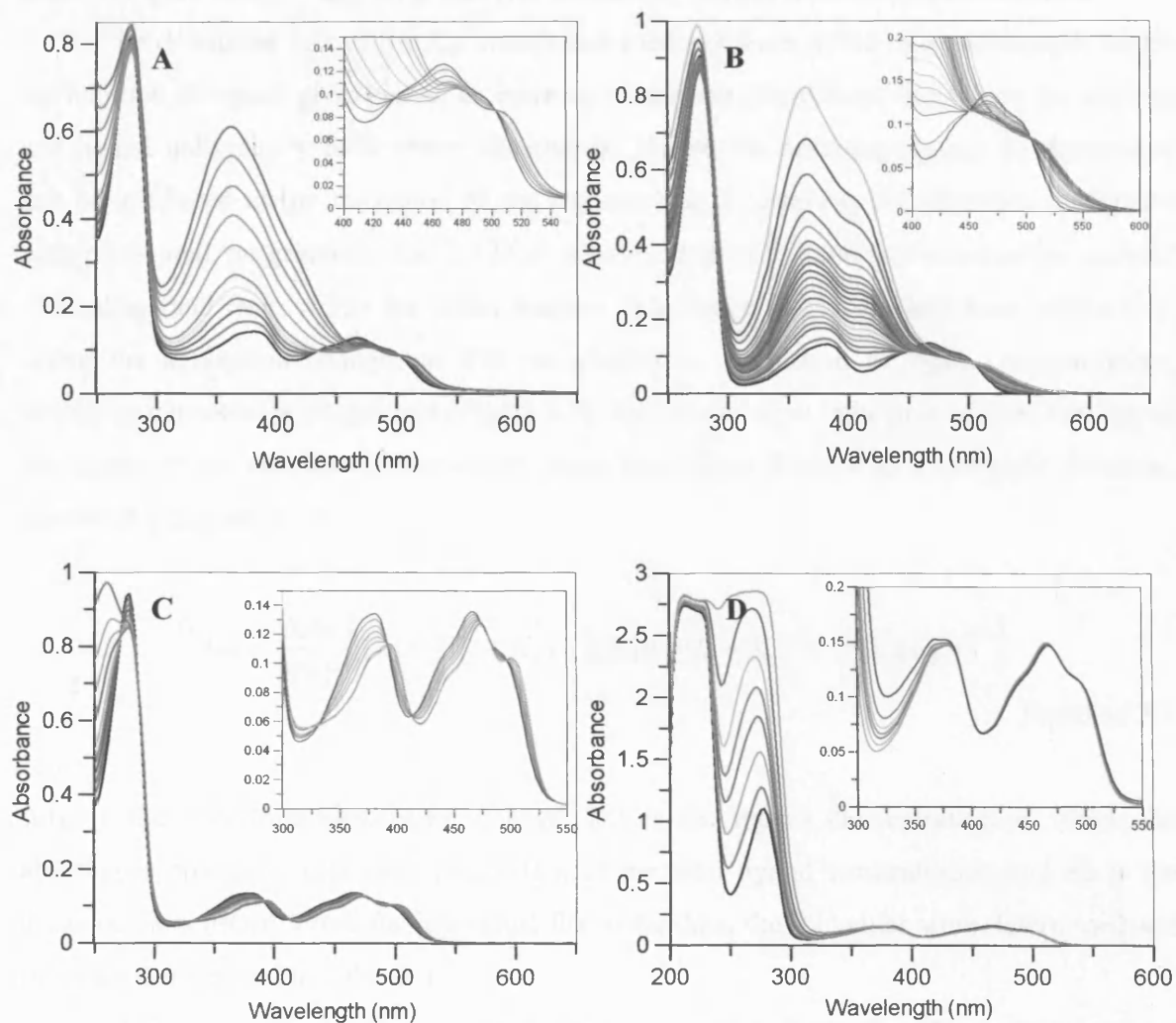


Figure 3.6. Spectra obtained during ligand binding studies of wild-type and Trp 102 mutant PETN reductases. Each panel represents the overlaid spectra monitored during the titration of oxidised enzyme ($\sim 10\mu\text{M}$) with a known stock concentration of ligand. The starting spectrum (free enzyme) is shown in black for each titration. Panel A, titration of W102Y PETN reductase with picric acid; Panel B, titration of W102F PETN reductase with 2,4-DNP; Panel C, titration of wild-type enzyme with progesterone; Panel D, titration of wild-type enzyme with TNT. Insets to panels A-C highlight the isosbestic points for each titration. Isosbestic points are observed at 506 nm for titrations with picric acid and 2,4-DNP, and at 330nm, 392 nm, 413 nm and 497 nm for titrations with progesterone. Similar data sets were also observed for other enzyme-ligand combinations (spectra not shown).

spectra, with well defined isosbestic points, indicating that ligand binding is a simple equilibrium process. Titrations performed with TNT, however, elicited no significant spectral change (Figure 3.6D), suggesting that TNT binds very weakly to the oxidized enzymes.

To determine values for K_d , absorbance readings were noted at a wavelength where the addition of ligand gives rise to an increase in enzyme absorbance, but where the enzyme and ligand individually have minor absorbance. Hence, the resulting change in absorbance can be attributed to the formation of the enzyme-ligand complex. For titrations performed with picric acid, progesterone and 2,4-DNP a wavelength of 518 nm was selected for analysis of binding (and from which the initial enzyme absorbance at 518 nm had been subtracted). Using the absorption changes at 518 nm plotted as a function of ligand concentration, saturation curves were established (Figure 3.7). The curves were indicative of tight binding of the ligand to the enzyme. Consequently, data were fitted directly to a quadratic function, described in Equation 3.1:

$$A_{obs} = \frac{\Delta A_M}{2[E]_T} \left[([L] + [E]_T + K_d) - \left(([L] + [E]_T + K_d)^2 - (4[L][E]_T) \right)^{0.5} \right]$$

Equation 3.1

ΔA_M is the maximum absorbance change, $[L]$ is the ligand concentration at which the absorbance change is measured (A_{obs}), $[E]_T$ is the total ligand concentration and K_d is the dissociation constant. From the individual fits to the data, the K_d values were determined and these are summarised in Table 3.1.

Analyses of the binding constants for picric acid indicate that the mutant enzymes bind this ligand tighter than the wild-type enzyme. This is consistent with the observation of steric clash between the C6 nitro group of picric acid and the indole ring of Trp 102 in the 0.9 Å structure of wild-type enzyme in complex with picric acid (Section 3.1.2). The replacement of Trp 102 with phenylalanine or tyrosine therefore eliminates the steric hindrance associated with picric acid binding to wild-type enzyme. The binding of 2,4-DNP remains largely unaffected by the mutation of Trp 102, suggesting that this ligand binds to the mutant enzymes in the same manner as for wild-type PETN reductase. This is supported by the fact that the C6 nitro group of picric acid observed to clash with Trp 102 in the crystal structure of PETN reductase in complex with picric acid, is not present in 2,4-DNP. Titrations performed with progesterone indicate that this ligand binds with similar affinity to each enzyme, suggesting that Trp 102 has no major involvement in the binding of steroids.

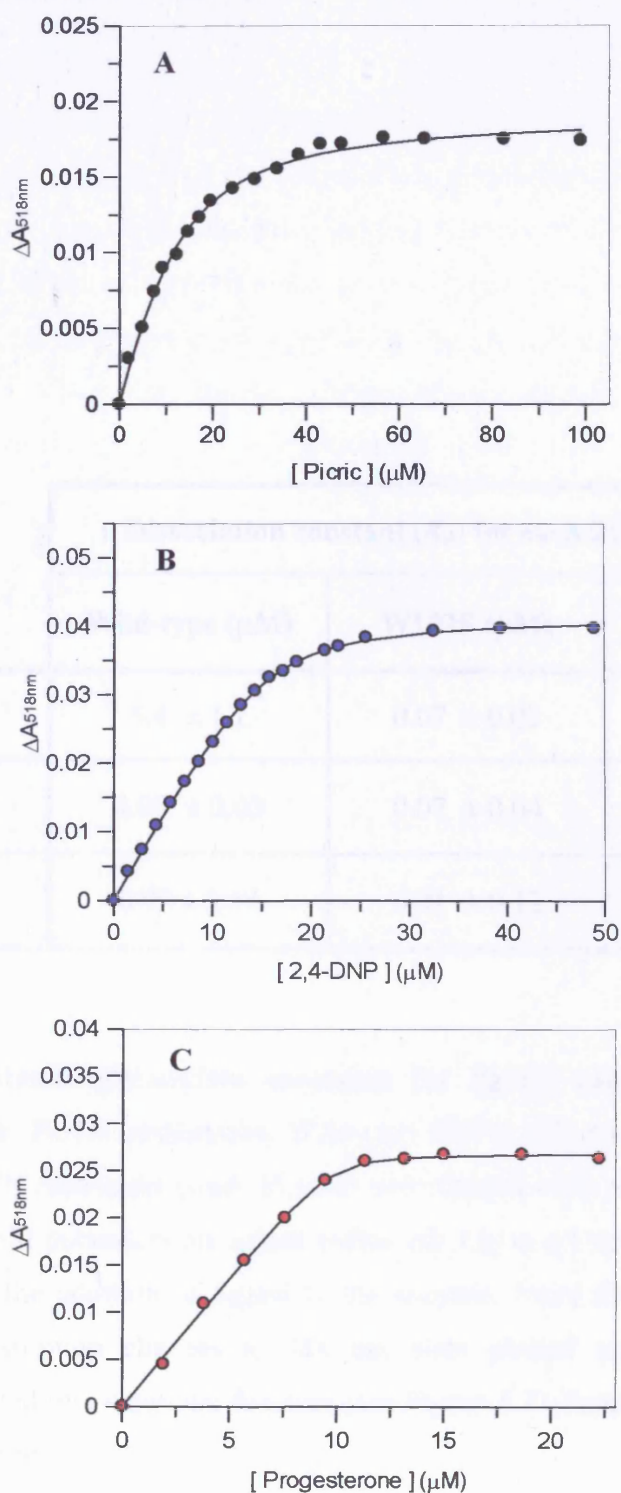


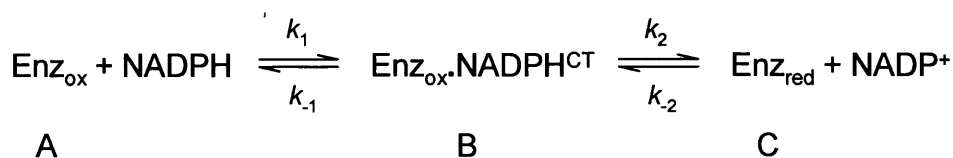
Figure 3.7. Examples of ligand binding titration curves. Each panel shows a representative binding curve for oxidised enzyme ($\sim 10 \mu M$) with ligand. Panel A, titration of wild-type enzyme with picric acid; Panel B, titration of W102F PETN reductase with 2,4-DNP; Panel C, titration of W102Y PETN reductase with progesterone. Similar data sets were collected for other enzyme-ligand combinations (data not shown). The solid line shows the fit of the data to Equation 3.1

	Dissociation constant (K_d) for each PETN reductase		
	Wild-type (μM)	W102F (μM)	W102Y (μM)
Picric acid	5.4 ± 1.1	0.07 ± 0.03	0.24 ± 0.04
Progesterone	0.07 ± 0.03	0.07 ± 0.04	0.03 ± 0.02
2,4-DNP	0.95 ± 0.13	0.21 ± 0.12	1.05 ± 0.09

Table 3.1. Calculated dissociation constants for ligand complexes of wild type, W102F and W102Y PETN reductases. Wild-type PETN reductase and the W102F and W102Y mutant PETN reductases (each 10 μM) were titrated with picric acid, progesterone and 2,4-DNP in 50 mM potassium phosphate buffer, pH 7.0, in a 1 ml quartz cuvette. Spectra were recorded after the addition of ligand to the enzyme. From the resultant spectra (see Figure 3.6), the absorption changes at 518 nm were plotted as a function of ligand concentration and fitted to a quadratic function (see Figure 3.7), from which the dissociation constants were determined.

3.2.3 Reductive half-reaction

To distinguish any involvement of Trp 102 in catalysis and binding of NADPH, single wavelength stopped-flow studies were performed. Previous studies using multiple wavelength photodiode array (PDA) analysis of the reductive-half reaction of wild-type PETN reductase had revealed the existence of three enzyme species (Figure 3.8; Craig, 2000). The first species is oxidised enzyme (Scheme 3.1, species A); the second species is a charge-transfer intermediate (Scheme 3.1, species B); the third is reduced enzyme where hydride transfer from NADPH to the flavin has taken place (Scheme 3.1, species C).



Scheme 3.1

The charge-transfer complex gives rise to an absorbance increase at long wavelengths (540 to 650 nm) and a small decrease in flavin absorbance at 460 nm. The spectral form of the flavin in the charge-transfer state, however, clearly indicates that the enzyme is in its oxidised form (Figure 3.8). Accordingly, in work described in this thesis, the rates of charge-transfer formation and flavin reduction were investigated with wild-type, W102F and W102Y PETN reductases, over a range of NADPH concentration. Measurements were made using 20 μM enzyme in 50 mM potassium phosphate buffer, pH 7.0, at 5 $^\circ\text{C}$. Rates were calculated from an average of three to four transients.

To monitor the rate of flavin reduction, absorbance changes were monitored at 464 nm. These transients showed a rapid decrease in flavin absorbance for each enzyme, indicative of hydride transfer from NADPH to the flavin (Figure 3.9A). Transients following the absorption change at 464 nm were best fitted to a single exponential process (Equation 3.2)

$$A = Ce^{-k_{\text{obs}}t} + b$$

Equation 3.2

A is the absorbance change, C is a constant related to the initial absorbance, k_{obs} is the observed rate constant and b is an offset value to account for non-zero baseline.

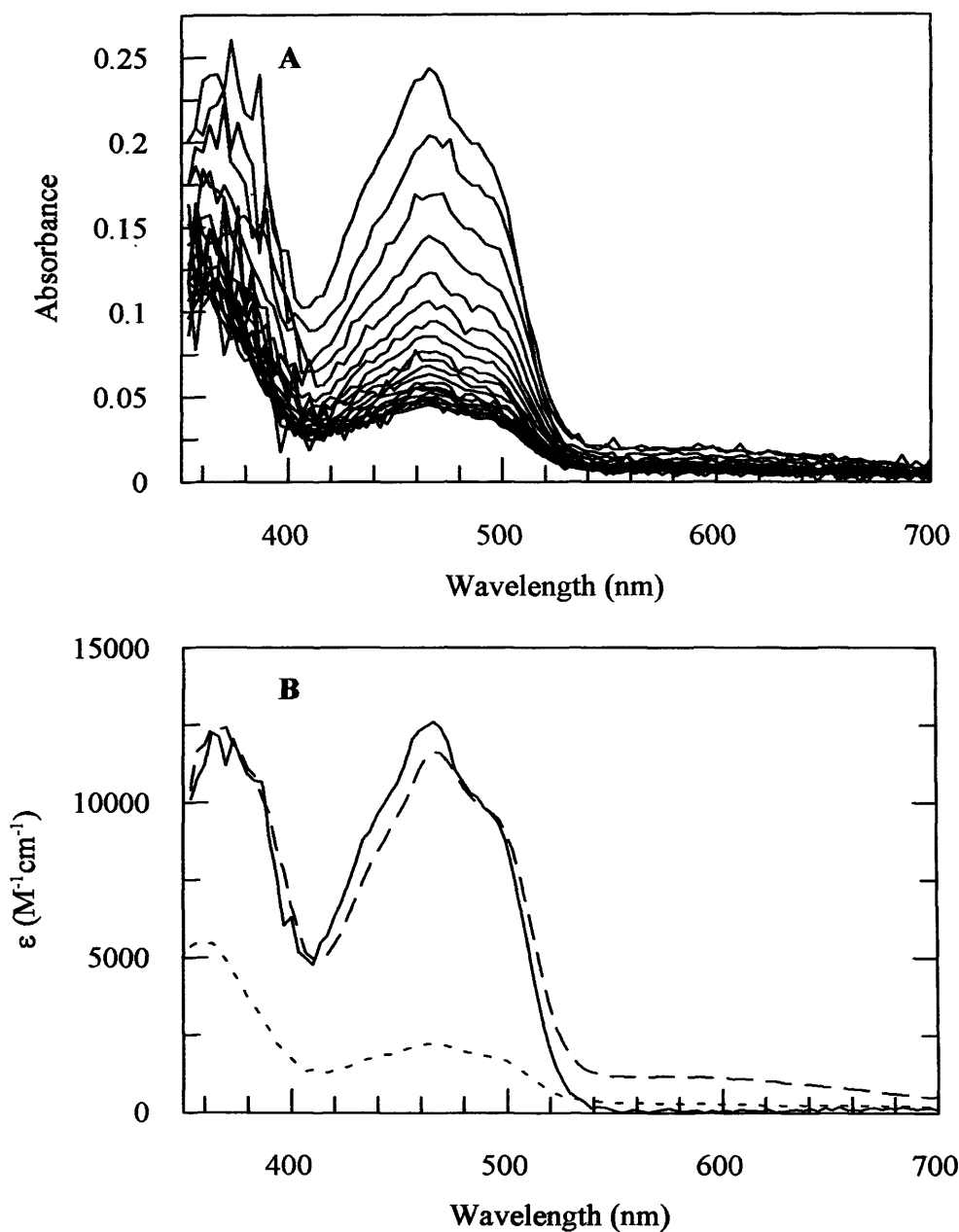


Figure 3.8. Time-dependent photodiode array spectra for the reduction of PETN reductase by β -NADPH. Panel A, PETN reductase (20 μ M) and β -NADPH (20 μ M) were mixed at 5 $^{\circ}$ C, pH 7.0, and four hundred spectra were recorded over a period of one second. One in every twenty of the spectra are displayed above. Panel B, spectra for the three enzyme intermediates observed during the reduction of PETN reductase by β -NADPH. All 400 spectra from the reaction shown in Panel A were analysed by global analysis and numerical integration methods using PROKIN software. The solid line represents oxidised enzyme, the dashed line is a charge-transfer intermediate and the dotted line is two electron-reduced enzyme. (Figures abstracted from Craig, 2000).

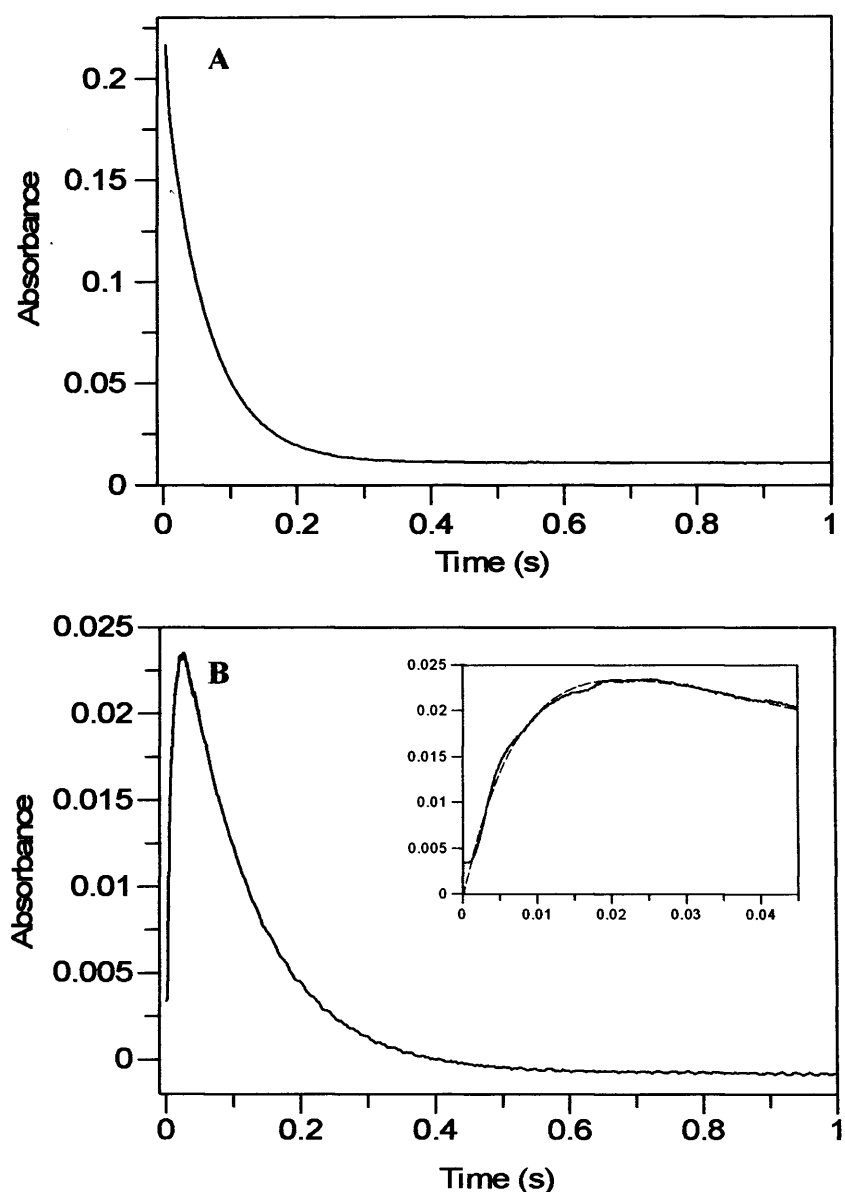


Figure 3.9. Typical stopped-flow transients obtained for the reductive-half reaction. NADPH (200 μM) was mixed with wild-type PETN reductase (20 μM) in potassium phosphate buffer, pH 7.0, at 5 $^{\circ}\text{C}$. Panel A, transient obtained when measuring absorption changes at 464 nm. The absorption changes at 464 nm are associated with flavin reduction. Panel B, transient obtained when measuring absorption changes at 560 nm. Absorption changes at 560 nm are associated with the formation and decay of the charge-transfer complex. The inset shows the fit (dashed red line) of the reaction transient (solid black line), over the first 45 milliseconds, to Equation 3.3. Similar absorption changes were observed with W102Y and W102F PETN reductases.

By measuring absorbance changes at 560 nm the rate of formation and subsequent decay of the charge-transfer intermediate was followed. These transients displayed an initial rapid increase in absorbance, followed by a slower decrease in absorbance, representing the formation and decay of the charge-transfer intermediate, respectively. Transients were typically measured over a 1 s timescale (Figure 3.9B). The 560 nm data fit best to a double exponential equation describing a positive and negative absorbance change (described as an “up-down” equation; Equation 3.3):

$$A = k_{\text{obs1}} C \frac{e^{-k_{\text{obs1}}t} - e^{-k_{\text{obs2}}t}}{k_{\text{obs2}} - k_{\text{obs1}}} + b$$

Equation 3.3

A is the absorbance change, C is a constant related to the initial absorbance, b is an offset, k_{obs1} is the observed rate constant for the increase in absorbance and k_{obs2} is the observed rate constant for the decrease in absorbance.

Analysis of the ‘down phase’ of the 560 nm transients and the 464 nm transients revealed that the changes in absorbance occur with the same observed rate. This suggests that the decay of the charge-transfer complex is a direct consequence of flavin reduction. Consequently, the rates of the down phase at 560 nm were not analysed further, as the larger absorbance changes at 464 nm were more appropriate for the analysis of flavin reduction. Therefore, only the ‘up-phase’ of the 560 nm data was analysed.

The observed rate constants (k_{obs}), produced by the fitting of the 464 nm and 560 nm (up-phase only) transients to the relevant equation were subsequently analysed for their dependence on NADPH concentration using Grafit 5.0 software. Figure 3.10 displays the NADPH concentration-dependence plots for wild type, W102F and W102Y PETN reductases. The plots indicate that the rate of flavin reduction (464 nm data) for all three enzymes is independent of NADPH concentration. The average rates of flavin reduction (k_2 ; Scheme 3.1) for the wild-type, W102Y and W102F enzymes were determined as $11.6 \pm 0.24 \text{ s}^{-1}$, $9.9 \pm 0.21 \text{ s}^{-1}$, and $17.3 \pm 0.5 \text{ s}^{-1}$, respectively. The rate of charge-transfer formation (measured at 560 nm) for all three enzymes is dependent on NADPH concentration and fits of the data to a linear function determined the rate constants outlined in Scheme 3.1.

The gradient of the slope for data collected at 560 nm (Figure 3.10) represents the rate constant for formation of the charge-transfer intermediate (k_1). The intercept of the line gives

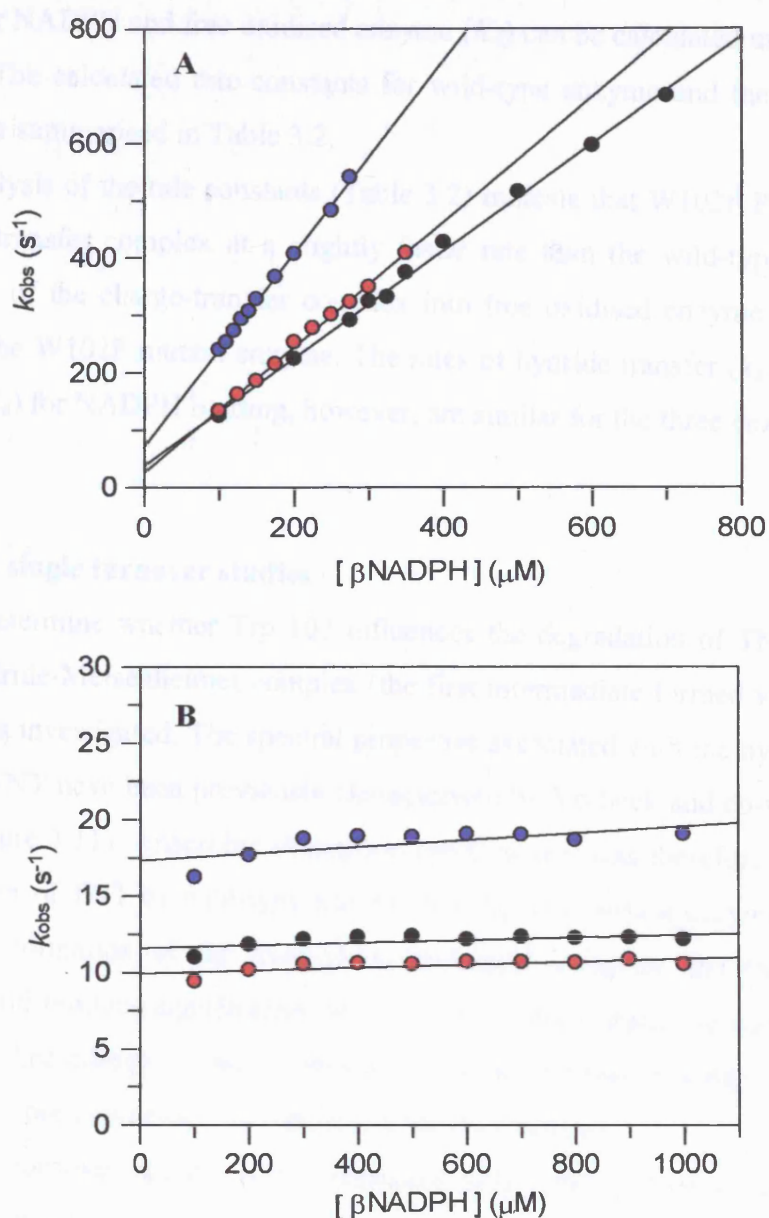


Figure 3.10. The concentration-dependence of the rate of formation of the charge-transfer intermediate and hydride transfer steps in the reductive half-reaction of wild-type, W102F and W102Y PETN reductases. Panel A, rate of formation of the charge-transfer intermediate (560 nm data); Panel B, rate of hydride transfer from NADPH to the flavin (464 nm data). Data were fitted to a linear function, from which the rate constants for the reductive half-reaction with each enzyme were calculated (see Table 3.2). Data shown in black are for wild-type enzyme, data shown in blue are for W102F enzyme and data shown in red are for W102Y enzyme. Measurements were made using $\sim 20 \mu\text{M}$ of each enzyme, in potassium phosphate buffer pH 7.0 at 5°C .

the rate constant for the formation of free enzyme and NADPH (k_{-1}). The dissociation constant for NADPH and free oxidised enzyme (K_d) can be calculated using the expression $K_d = k_{-1} / k_1$. The calculated rate constants for wild-type enzyme and the two Trp 102 mutant enzymes are summarised in Table 3.2.

Analysis of the rate constants (Table 3.2) indicate that W102F PETN reductase forms the charge-transfer complex at a slightly faster rate than the wild-type enzyme. Similarly, dissociation of the charge-transfer complex into free oxidised enzyme and NADPH (k_{-1}) is slower for the W102F mutant enzyme. The rates of hydride transfer (k_2) and the dissociation constants (K_d) for NADPH binding, however, are similar for the three enzymes.

3.2.4 TNT single turnover studies

To determine whether Trp 102 influences the degradation of TNT, the formation of the TNT hydride-Meisenheimer complex (the first intermediate formed via the ring reduction pathway) was investigated. The spectral properties associated with the hydride-Meisenheimer complex of TNT have been previously characterised by Vorbeck and co-workers (Vorbeck *et al.*, 1994; Figure 3.11). Anaerobic absorption spectroscopy was therefore used to monitor the single turnover of TNT by wild-type and the two Trp 102 mutant enzymes. If Trp 102 does facilitate the formation of the hydride-Meisenheimer complex, the two Trp 102 mutant enzymes should produce significantly less or none of the complex in comparison with wild-type enzyme. Accordingly, if this is observed it would indicate that the two mutant enzymes transform TNT predominantly via their nitroreductase activity.

Single turnover studies were performed using the conditions described in Section 2.8.1. Each enzyme was stoichiometrically reduced under anaerobic conditions with sodium dithionite, which had been previously calibrated by titrating against FMN. The addition of stoichiometric concentrations of TNT to the reduced enzyme solution initiated the reaction. Spectral recordings acquired at 2 minute intervals followed the course of TNT transformation by each enzyme. Recordings were taken until no spectral change was observed. Absorption changes accompanying the reaction with wild-type PETN reductase (Figure 3.12) show a rapid increase in flavin absorbance indicative of enzyme re-oxidation by TNT. In addition, an increase in absorbance in the longer wavelength region, with a peak at 580 nm, is observed. Enhanced absorbance is also noted at 460 nm, irrespective of the expected absorbance associated with 20 μ M of re-oxidised enzyme. The spectral changes noted above correspond

	k_1 ($\mu\text{M}^{-1} \text{s}^{-1}$)	k_{-1} (s^{-1})	k_2 (s^{-1})	K_d (μM)
Wild-type PETN reductase	0.95 ± 0.02	31.73 ± 7.45	11.6 ± 0.23	33.4 ± 8.54
W102F PETN reductase	1.68 ± 0.02	70.96 ± 4.45	17.31 ± 0.5	42.23 ± 3.15
W102Y PETN reductase	1.09 ± 0.01	25.71 ± 4.47	9.92 ± 0.21	23.59 ± 4.32

Table 3.2. The pre-steady-state rate constants for the reductive half-reaction of wild-type PETN reductase and the W102Y and W102F mutant enzymes. Rate constants were calculated using 20 μM of each enzyme reduced by varying concentrations of NADPH, in 50 mM potassium phosphate buffer, pH 7.0, at 5 °C. Stopped-flow absorbance spectroscopy was used to monitor the rate of flavin reduction at 464 nm and the rate of formation of the charge transfer complex at 560 nm. Transients were fitted to Equation 3.2 and 3.3, respectively, from which the observed rates were determined. Observed rates were subsequently analysed for their concentration-dependence on NADPH, and fits to the data allowed calculation of the rate constants (according to Scheme 3.1). k_1 is the rate constant for the formation of the charge-transfer complex, while k_{-1} is the dissociation rate constant of this complex. k_2 is the rate constant for flavin reduction and K_d is the dissociation constant for NADPH and enzyme.

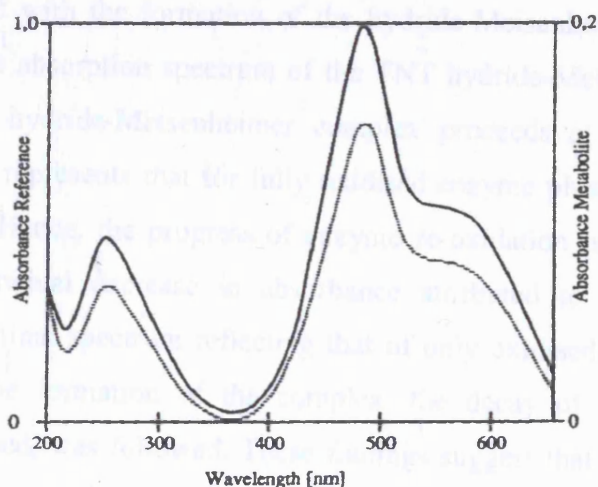


Figure 3.11. The spectrum of the TNT hydride-Meisenheimer complex. Solid line, TNT hydride-Meisenheimer complex obtained by chemical synthesis. Dotted line TNT hydride-Meisenheimer complex obtained by HPLC separation of the culture fluid from the incubation of resting cells of *Mycobacterium* sp. HL 4-NT-1 with TNT (0.5 mM) and $(\text{NH}_4)_2\text{SO}_4$ (1 mM) in phosphate buffer (50 mM) at 30 °C, pH 7.4. (Figure taken from Vorbeck *et al*, 1994).

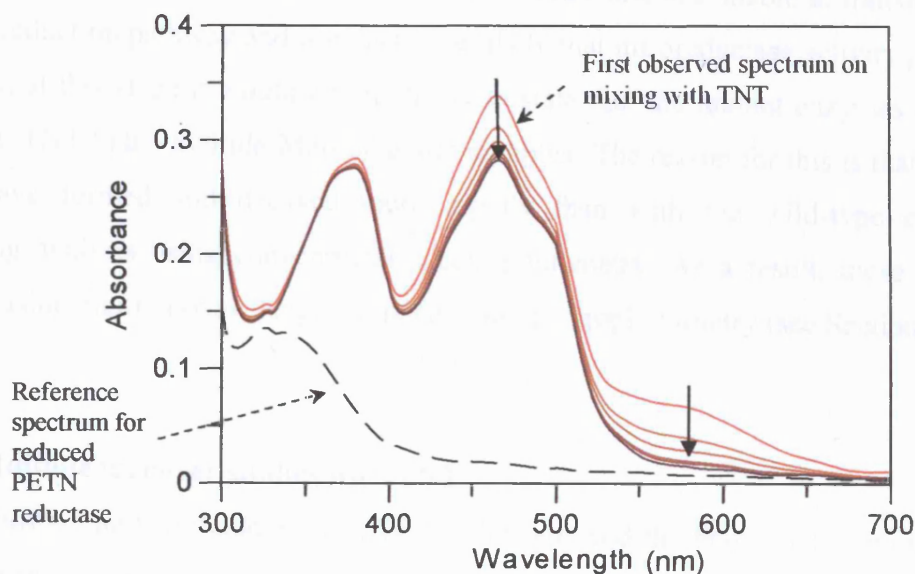


Figure 3.12. Absorption spectra following the single turnover of TNT by wild-type PETN reductase. Spectra recorded at 2 min intervals were used to follow the reaction between 20 μM of sodium dithionite-reduced PETN reductase (dashed line) and 20 μM TNT, in 50 mM potassium phosphate buffer, pH 7.0, under anaerobic conditions. The solid arrows indicate the direction of absorbance change in time.

to those associated with the formation of the hydride-Meisenheimer complex of TNT (see Figure 3.11 for the absorption spectrum of the TNT hydride-Meisenheimer complex alone). Formation of the hydride-Meisenheimer complex proceeds at a rapid rate, as the first spectrum acquired represents that for fully oxidised enzyme plus the hydride-Meisenheimer complex of TNT. Hence, the progress of enzyme re-oxidation is not observed. Subsequent spectra show a gradual decrease in absorbance attributed to the hydride-Meisenheimer complex, with the final spectrum reflecting that of only oxidised enzyme. Therefore, rather than monitoring the formation of the complex, the decay of the hydride-Meisenheimer complex once formed, was followed. These findings suggest that the hydride-Meisenheimer complex is relatively unstable owing to its rapid decay. Given that only a single turnover was possible, it is unlikely that the complex is further reduced to the dihydride-Meisenheimer complex. The decay of the hydride-Meisenheimer complex is likely due to its non-enzymatic conversion to an isomer with differing absorption properties.

Spectral changes accompanying the reaction between TNT and W102F and W102Y PETN reductases (Figure 3.13) indicate that the hydride-Meisenheimer complex does not form. The acquired spectra simply correspond to the profile of re-oxidised enzyme. This suggests that the Trp 102 mutant forms of PETN reductase are unable to transform TNT via the ring reduction pathway and it is therefore likely that nitroreductase activity predominates. However, at this stage it would be unreliable to state that the mutant enzymes are unable to transform TNT to the hydride-Meisenheimer complex. The reason for this is that the complex might have formed and decayed more rapidly than with the wild-type enzyme, thus preventing analysis using conventional spectrophotometry. As a result, these studies were repeated using multiple-wavelength stopped-flow spectrophotometry (see Section 3.2.9).

3.2.5 Multiple turnover studies with TNT

Multiple turnover studies with TNT, wild-type and the two Trp 102 mutant enzymes were performed to assess any role for Trp 102 in the formation of the hydride-Meisenheimer complex and/or subsequent intermediates/products. These studies also provided evidence for the existence of multiple degradation pathways and a preliminary insight into the various intermediates formed during TNT turnover. Multiple turnover studies with TNT were performed using the procedure described in Section 2.8.2.

Under anaerobic conditions, wild-type, W102F and W102Y PETN reductases (each 0.2 μM) were reduced with NADPH (100 μM) in the presence of an NADPH regeneration

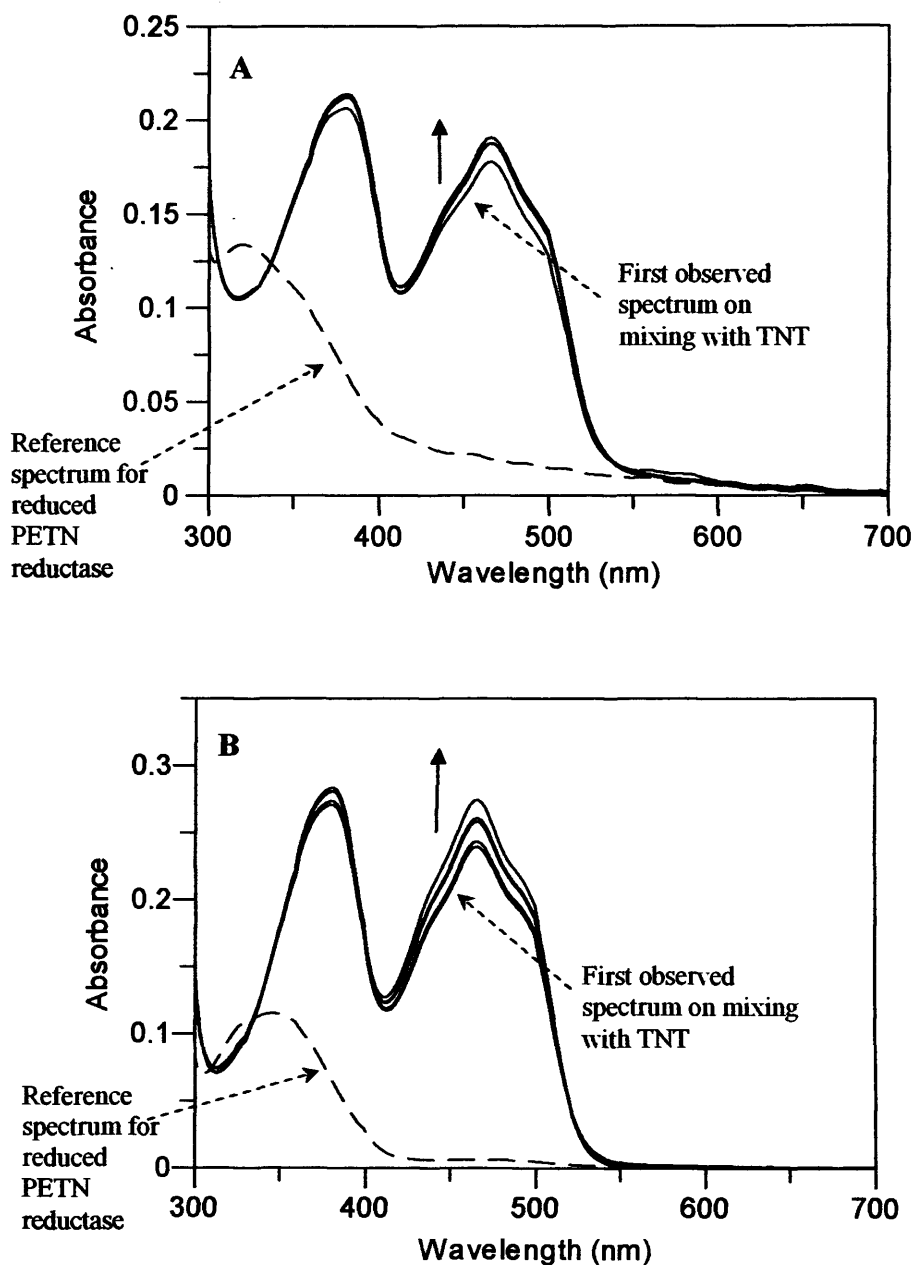


Figure 3.13. Absorption spectra following the single turnover of TNT by W102F (Panel A) and W102Y (Panel B) mutant forms of PETN reductase. The reaction was followed by collecting spectra at 2 min intervals for the reaction of 15.5 μM of sodium dithionite-reduced W102F (Panel A) or W102Y (Panel B) PETN reductase (dashed line) and 20 μM TNT, in 50 mM potassium phosphate buffer, pH 7.0, under anaerobic conditions. The solid arrows indicate the direction of absorbance change in time.

system. The addition of excess TNT (88 μM) to the reduced enzyme solution initiated multiple turnover reactions, which were then followed using absorption spectroscopy. To minimise the interference from enzyme (and NADPH) absorbance, low concentrations of enzyme (and NADPH) were used. Accordingly, any absorption changes identified are primarily attributed to the absorbance of intermediates/products produced during the course of the reaction. Spectra were recorded at two minute intervals until a stable final spectrum was observed.

Spectral changes associated with the multiple turnover of TNT by wild-type enzyme are displayed in Figure 3.14A. Analysis of spectra indicate that the hydride-Meisenheimer complex does not accumulate during the course of the reaction, as increased absorbance beyond 550 nm [the hydride-Meisenheimer has a peak absorbance at 580 nm (Vorbeck *et al*, 1994)] is not observed. However, the development of an absorption band between 350-550 nm, with a peak at 430 nm is observed.

As was found with the wild-type enzyme, evidence for the accumulation of the hydride-Meisenheimer complex of TNT is not reflected in the spectra used to follow the reaction of W102F and W102Y PETN reductases (Figure 3.14B). The gradual development of an absorption band between 350-550 nm is observed during the course of the reaction for both enzymes. Although the absorbance profiles between 350-550 nm for the two Trp 102 mutant enzymes are comparable to each other, they differ from that produced by the wild-type enzyme. The absorption profile produced by the wild-type enzyme has a peak at 430 nm, while the absorption profiles observed with both mutant PETN reductases have peaks at 350 nm and a shoulder at 420 nm. The differences between the acquired spectra for the mutant and wild-type enzymes can be seen more clearly in Figure 3.15, which displays the end spectrum for each enzyme catalysed reaction. The final absorption spectra recorded for each enzyme are likely to reflect the accumulation of a mixture of several products (see Section 3.2.6). These findings clearly indicate that the nature or the accumulation of the reaction products differs for wild-type enzyme and the two Trp 102 mutant PETN reductases. To provide more information on the nature of the compounds produced by each enzyme, NMR analysis of the multiple turnover reactions with TNT were conducted (Section 3.2.6).

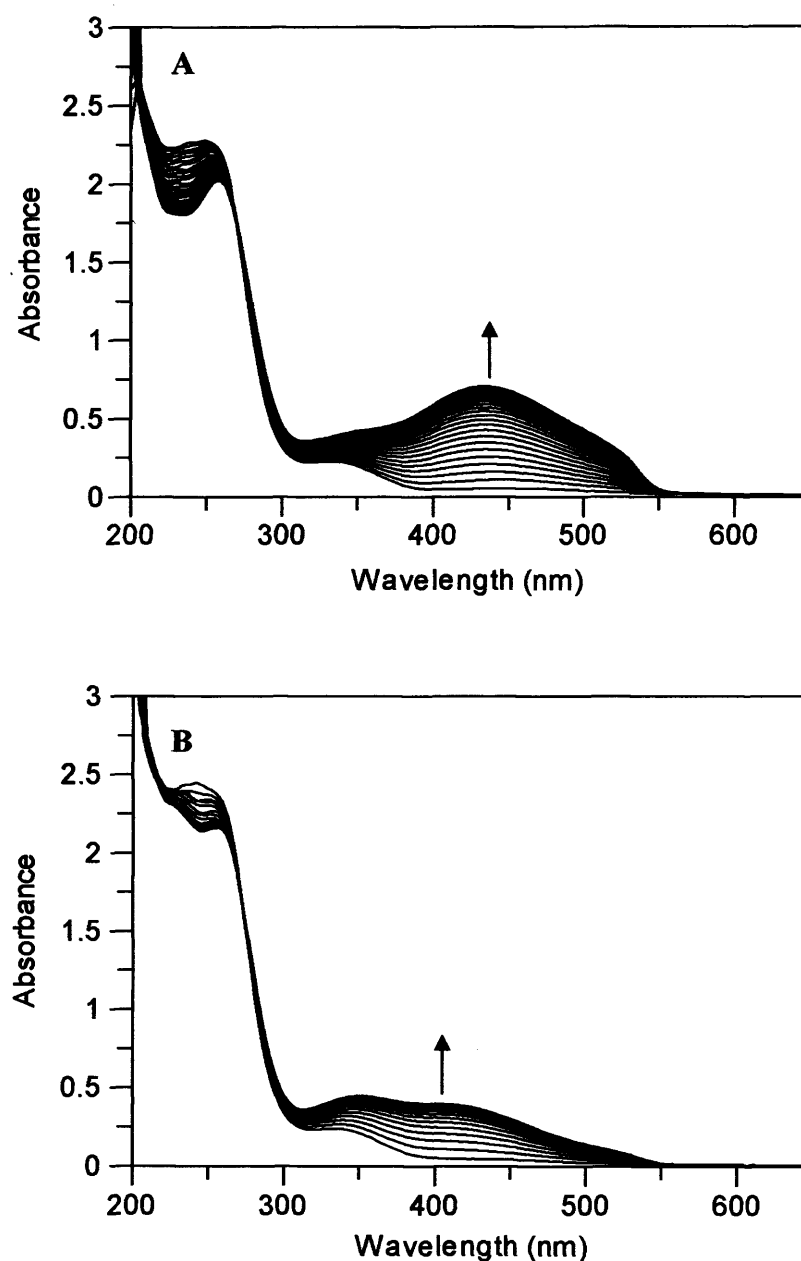


Figure 3.14. Absorption spectra following the multiple turnover of TNT by wild-type (Panel A) and W102F (Panel B) PETN reductase. NADPH-reduced enzyme (0.2 μM) was mixed with 88 μM TNT in the presence of a NADPH regeneration system, in 50 mM potassium phosphate buffer, pH 7.0, under anaerobic conditions. To follow the multiple turnover of TNT, spectra were recorded at 2 min intervals. The arrows indicate the direction of absorbance change in time. Panel A, absorption changes for wild-type enzyme; Panel B, absorption changes for W102F PETN reductase. Absorption changes monitored with the W102Y PETN reductase were similar to those recorded with W102F PETN reductase (Panel B).

3.2.6 NMR analysis of multiple turnover reactions with TNT

To gain insight into the possible intermediates/products produced by PETN reductase during the reduction of TNT, NMR studies were performed. Previous studies investigating the multiple turnover of TNT (Section 3.2.4) indicated that Trp 102 has a significant influence on TNT breakdown. Spectral analysis of the reaction when TNT turnover was assumed to be completed, suggested that the two Trp 102 mutant enzymes produce either a different single

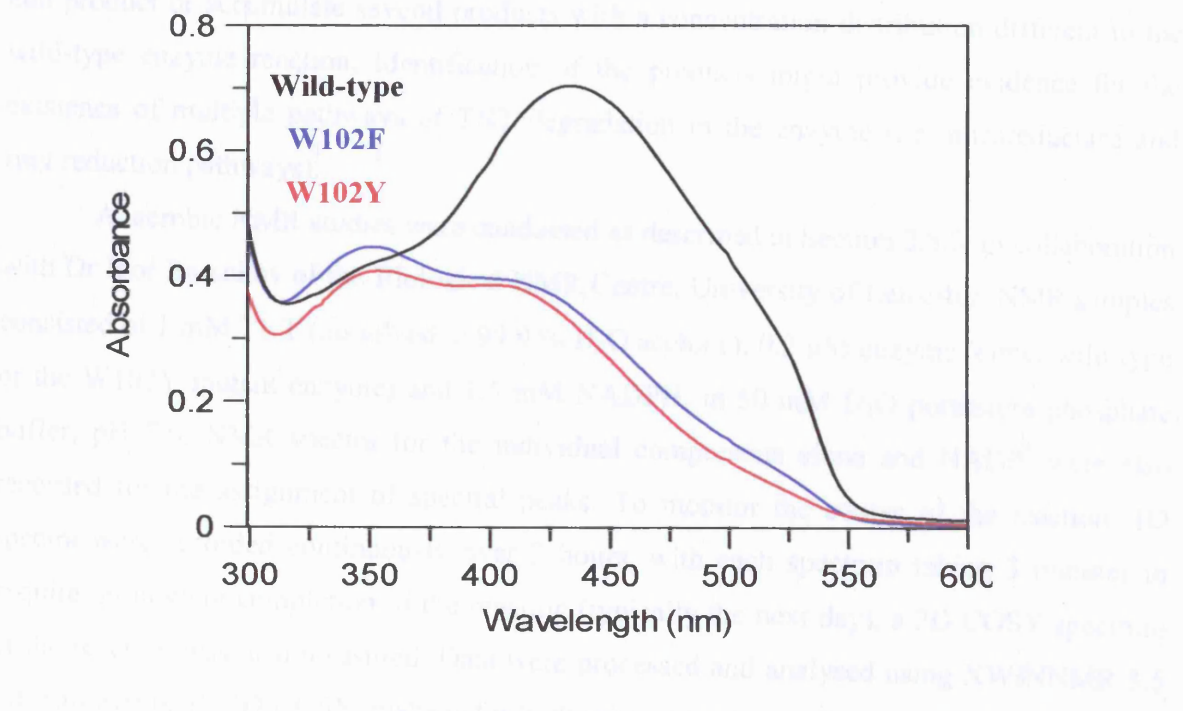


Figure 3.15. End absorption spectra following the multiple turnover of TNT by wild-type (black line), W102F (blue line) and W102Y (red line) PETN reductases. NADPH-reduced enzyme (0.2 μ M) was mixed with 88 μ M TNT in the presence of an NADPH regeneration system, in 50 mM potassium phosphate buffer, pH 7.0, under anaerobic conditions.

3.2.6 NMR analysis of multiple turnover reactions with TNT

To gain insight into the possible intermediates/products produced by PETN reductase during the turnover of TNT, NMR studies were performed. Previous studies investigating the multiple turnover of TNT (Section 3.2.5) indicated that Trp 102 has a significant influence on TNT breakdown. Spectral analysis of the reaction when TNT turnover was assumed to be completed, suggested that the two Trp 102 mutant enzymes produce either a different single end product or accumulate several products with a concentration distribution different to the wild-type enzyme reaction. Identification of the products might provide evidence for the existence of multiple pathways of TNT degradation in the enzyme (i.e. nitroreductase and ring reduction pathways).

Anaerobic NMR studies were conducted as described in Section 2.8.3, in collaboration with Dr Igor Barsukov of the Biological NMR Centre, University of Leicester. NMR samples consisted of 1 mM TNT (dissolved in 99.9 % D₂O acetone), 0.2 μM enzyme (either wild-type or the W102Y mutant enzyme) and 1.5 mM NADPH, in 50 mM D₂O potassium phosphate buffer, pH 7.0. NMR spectra for the individual components alone and NADP⁺ were also recorded for the assignment of spectral peaks. To monitor the course of the reaction, 1D spectra were recorded continuously over 3 hours, with each spectrum taking 3 minutes to acquire. Following completion of the reaction (typically the next day), a 2D COSY spectrum of the reaction was also measured. Data were processed and analysed using XWINNMR 3.5 software (Bruker). 2D COSY analysis for both enzyme reactions allowed the identification of peaks which arise from the same functional groups (e.g. the number of CH₂ groups). Inspection of the 1D (Figure 3.16) and 2D NMR (data not shown) spectra recorded at the end of the 3 hr reaction time identify clear differences between each enzyme; the wild-type enzyme produces a more complex mixture of compounds compared to the W102Y mutant form of PETN reductase. Spectral peaks that arise during the full course of the reaction were then analysed for their pattern of development as a function of time (Figure 3.17). Analyses of the plots reveal that different peaks form and decay at differing times and that the decay of some peaks leads to the concomitant formation of others. Overall, the results of these NMR studies reveal that a number of intermediates are produced during TNT turnover and that these differ either in their nature or in their concentration distribution for wild-type and W102Y PETN reductase. It was not possible to determine the exact nature of the compounds produced during the course of the reaction, as the complexity of the spectra (owing to the presence of many different compounds) prevents the assignment of spectral peaks.

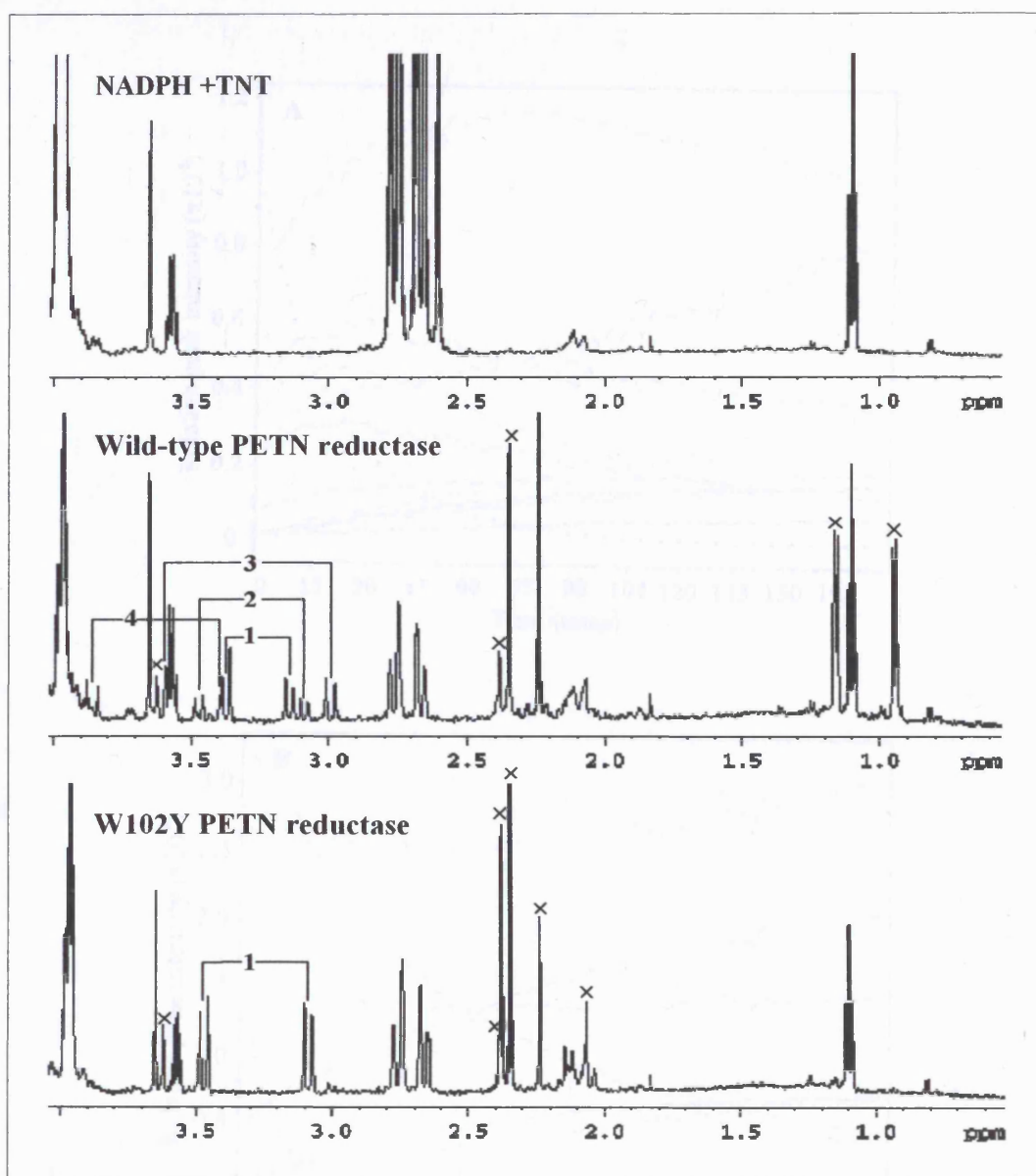


Figure 3.16. NMR spectra following the multiple turnover of TNT by wild-type and W102Y PETN reductase. NMR analysis was used to follow the reaction between 0.2 μM enzyme, 1.5 mM NADPH and 1 mM TNT (in 99.9% D_2O acetone), in 50 mM D_2O potassium phosphate buffer, pH 7.0. The spectrum displayed corresponds to the end spectrum recorded after the reaction was incubated for 3 hrs. The numbers correspond to the formation of peaks, which arise from the same CH_2 groups, identified by the 2D COSY spectrum for each reaction. X highlights the peaks which form during the course of the reaction (which exclude signals from NADPH, NADP^+ (which has a signal at ~ 2.15 ppm) and TNT). The NMR spectrum for NADPH plus TNT is also displayed for comparative purposes.

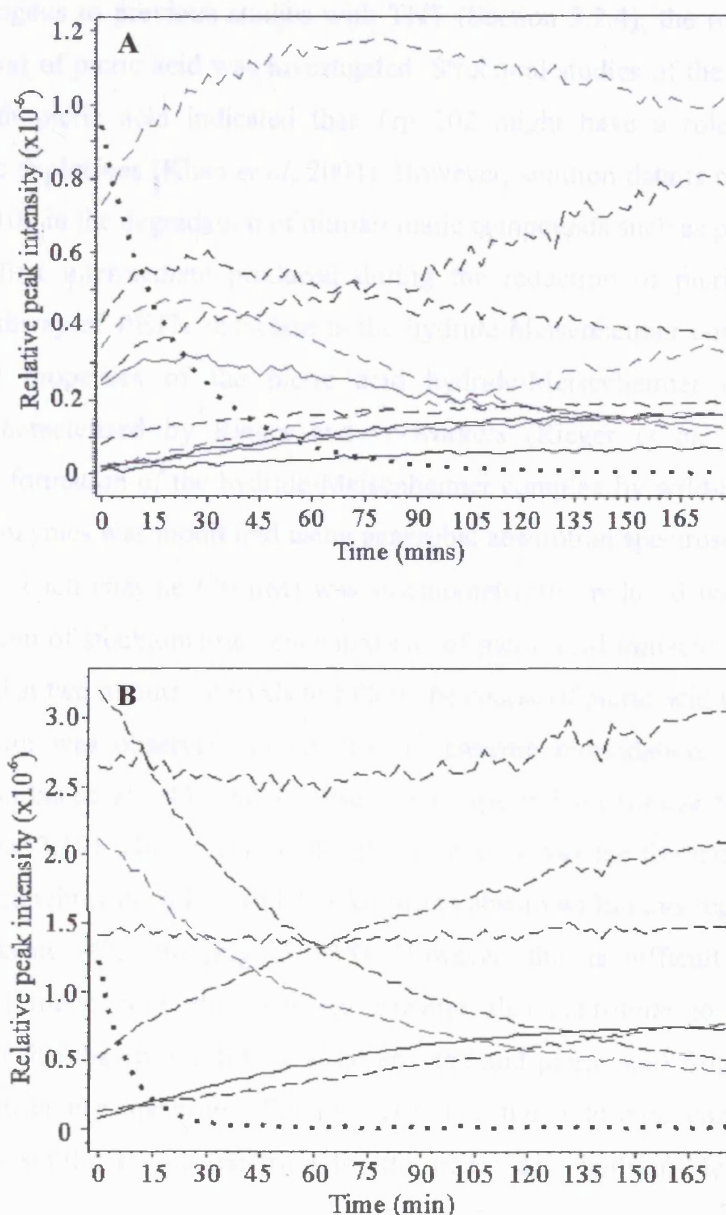


Figure 3.17. Time course profile for the NMR peaks which arise during the course of TNT turnover by wild-type (Panel A) and W102Y (Panel B) PETN reductase. The dotted lines represent the decay of TNT (N.B. in Panel A the intensity of the TNT peak is scaled down by a factor of 4 compared to the intensity of the other peaks), solid lines represent one of the peaks from each CH₂ group, and dashed lines represent all other peaks as identified from the NMR spectra in Figure 3.16 (i.e. ones marked with x in Figure 3.16).

3.2.7 Single turnover studies with picric acid

Analogous to previous studies with TNT (Section 3.2.4), the role of Trp 102 in the single turnover of picric acid was investigated. Structural studies of the wild-type enzyme in complex with picric acid indicated that Trp 102 might have a role in the catalysis of nitroaromatic explosives (Khan *et al*, 2004). However, solution data is required to assess any role for Trp 102 in the degradation of nitroaromatic compounds such as picric acid.

The first intermediate produced during the reduction of picric acid via the ring reduction pathway of PETN reductase is the hydride-Meisenheimer complex of picric acid. The spectral properties of the picric acid hydride-Meisenheimer complex have been previously characterised by Rieger and co-workers (Rieger *et al*, 1999; Figure 3.18). Accordingly, formation of the hydride-Meisenheimer complex by wild-type and the two Trp 102 mutant enzymes was monitored using anaerobic absorption spectroscopy, as described in Section 2.8.2. Each enzyme (20 μM) was stoichiometrically reduced with sodium dithionite and the addition of stoichiometric concentrations of picric acid initiated the reaction. Spectra were acquired at two minute intervals to follow the course of picric acid turnover, until a final stable spectrum was observed. In addition to enzyme re-oxidation, the development of enhanced absorbance at ~ 435 nm is observed in spectral recordings taken with wild-type enzyme (Figure 3.19). This enhanced absorbance may reflect the formation of the picric acid hydride-Meisenheimer complex, which is known to absorb within this region and in particular has a maxima at ~ 435 nm (Figure 3.18). However, this is difficult to ascertain as the absorbance of picric acid plus oxidised enzyme also contribute to the final spectrum. Subtraction of the absorbance for oxidised enzyme and picric acid from the final spectrum produces a difference spectrum (Figure 3.20). For the wild-type enzyme this has some characteristics similar to the spectrum for the picric acid hydride-Meisenheimer complex (Figure 3.20).

Spectra monitoring the single turnover of picric acid by the Trp 102 mutant enzymes (Figure 3.21) differ to that observed with wild-type enzyme. Although enzyme re-oxidation is evident, the enhanced absorbance noted at ~ 435 nm in spectra for wild-type enzyme is not observed with the mutant enzymes. The spectral differences between wild-type and mutant enzyme catalysed reactions can be seen more clearly in Figure 3.20, which displays the difference spectra calculated for each reaction. The difference spectra for the mutant enzymes are similar to each other, but are clearly different to that for the wild-type enzyme. The difference spectrum for wild-type enzyme has properties similar to the spectrum for the picric

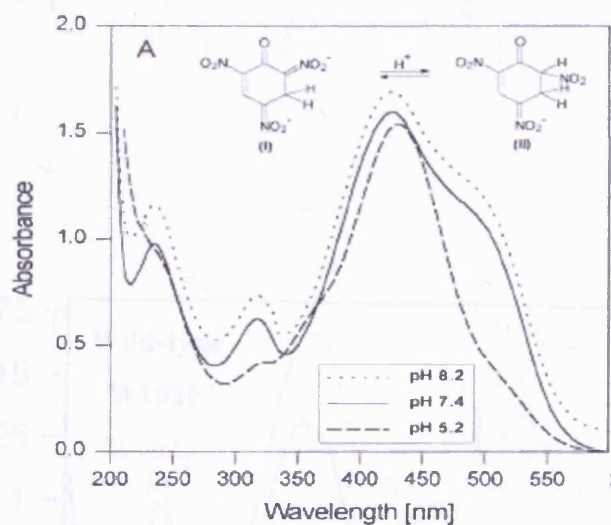


Figure 3.18. UV-visible spectrum of the hydride-Meisenheimer complex of picric acid in water, at different pH values. (Figure abstracted from Rieger *et al*, 1999)

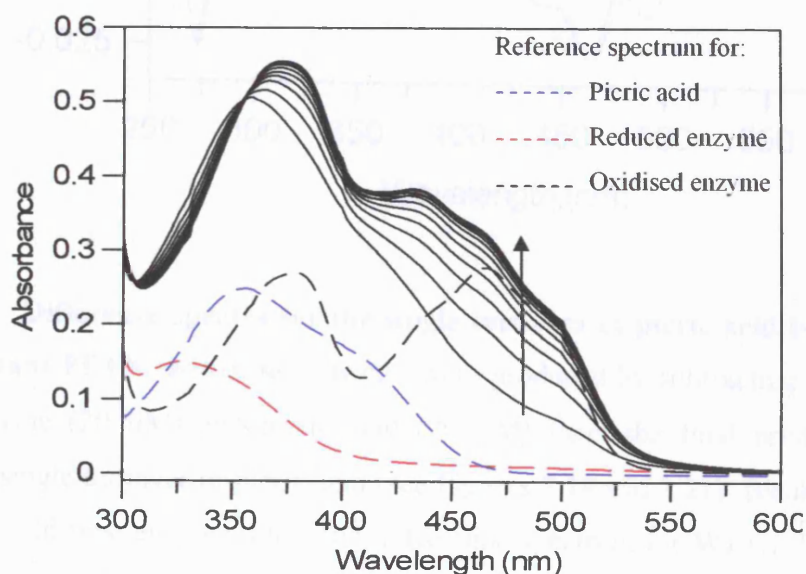


Figure 3.19. Absorption spectra following the single turnover of picric acid by wild-type PETN reductase. Spectra recorded at 2 min intervals were used to follow the reaction between 20 μ M of sodium dithionite-reduced PETN reductase and 20 μ M picric acid, in 50 mM potassium phosphate buffer, pH 7.0, under anaerobic conditions. The solid arrow indicates the direction of absorbance change as a function of time. The spectrum for picric acid (dashed blue line), reduced enzyme (dashed red line) and oxidised enzyme (dashed black line) are also displayed for comparative purposes.

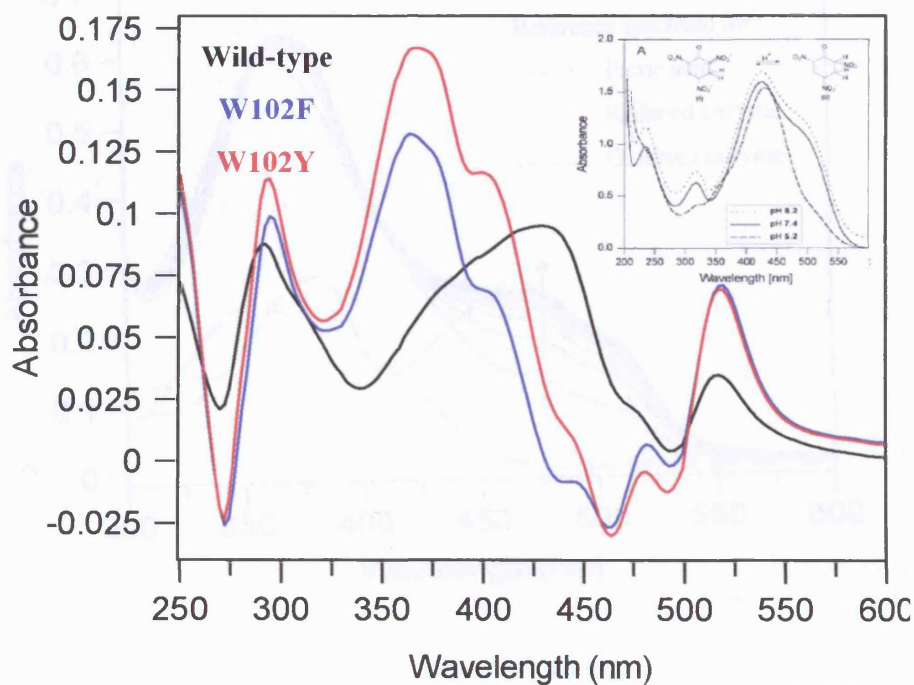


Figure 3.20. Difference spectra for the single turnover of picric acid by wild-type and Trp 102 mutant PETN reductases. Spectra were produced by subtracting the spectrum for oxidised enzyme (20 μM) and picric acid (20 μM) from the final product spectra that followed the single turnover of picric acid (see Figures 3.19 and 3.21). Black line, difference spectrum for wild-type enzyme; blue line, difference spectrum for W102F PETN reductase; red line, difference spectrum for W102Y PETN reductase. Inset: absorption spectra for the picric acid hydride-Meisenheimer complex at different pH values (Rieger *et al*, 1999).

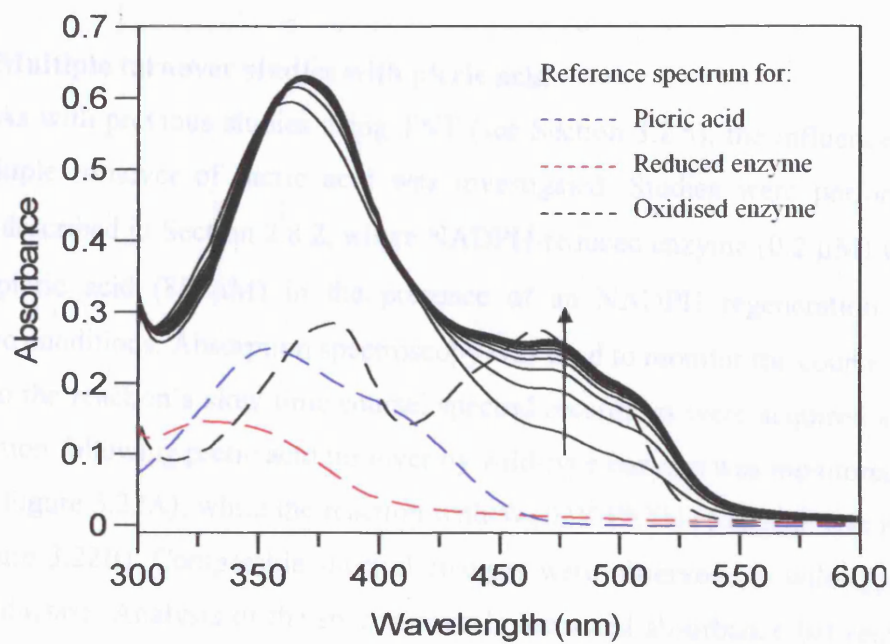


Figure 3.21. Absorption spectra following the single turnover of picric acid by W102F PETN reductase. Spectra recorded at 2 min intervals were used to follow the reaction between 20 μM of sodium dithionite-reduced W102F PETN reductase and 20 μM picric acid, in 50 mM potassium phosphate buffer, pH 7.0, under anaerobic conditions. The solid arrow indicates the direction of absorbance change as a function of time. The spectrum for picric acid (dashed blue line), reduced enzyme (dashed red line) and oxidised enzyme (dashed black line) are also displayed for comparative purposes. Spectra following the course of picric acid turnover by W102Y PETN reductase were similar to that observed with W102F PETN reductase.

acid hydride-Meisenheimer complex. Conversely, the difference spectra for the mutant enzymes do not display any characteristics that resemble the formation of the hydride-Meisenheimer complex. The results of these studies suggest that the Trp 102 mutant enzymes do not stabilise the hydride-Meisenheimer complex of picric acid.

3.2.8 Multiple turnover studies with picric acid

As with previous studies using TNT (see Section 3.2.5), the influence of Trp 102 on the multiple turnover of picric acid was investigated. Studies were performed using the method described in Section 2.8.2, where NADPH-reduced enzyme (0.2 μM) was mixed with excess picric acid (88 μM) in the presence of an NADPH regeneration system, under anaerobic conditions. Absorption spectroscopy was used to monitor the course of the reaction. Owing to the reaction's slow time course, spectral recordings were acquired at 1 h intervals. The reaction following picric acid turnover by wild-type enzyme was monitored over a course of 30 h (Figure 3.22A), while the reaction with W102Y PETN reductase was monitored over 8 h (Figure 3.22B). Comparable spectral changes were observed for wild-type and W102Y PETN reductase. Analysis of the spectra reveals increased absorbance between 425 and 600 nm for both enzyme-catalysed reactions. The development of absorbance between 425-600 nm might indicate the formation of the hydride-Meisenheimer complex, which is known to absorb within this wavelength region (Figure 3.18). However, characteristic peaks associated with the spectrum for the picric acid hydride-Meisenheimer complex, notably at 423 nm and a shoulder at 490 nm, are not evident in the spectral recordings taken for each enzyme. This suggests that the hydride-Meisenheimer complex does not accumulate during the turnover of picric acid by wild-type and W102Y PETN reductases.

Spectra following picric acid turnover by each enzyme also reveal decreased absorbance at 340 nm, where NADPH is known to absorb. Given the slow time course of the reactions, it is likely that this decrease in absorbance at 340 nm is due to the natural decomposition of NADPH at 25 °C. To confirm that the spectral changes observed between 300-400 nm were due to NADPH decomposition and not a feature of picric acid metabolism, a control reaction was performed. The control reaction was set up in the same manner as the enzyme assays, but without enzyme. The reaction was monitored over 21 h and the resultant spectra clearly indicated that the decrease in 340 nm absorbance was due to NADPH decay. Given the long time scale for each enzyme-catalysed reaction and the concomitant

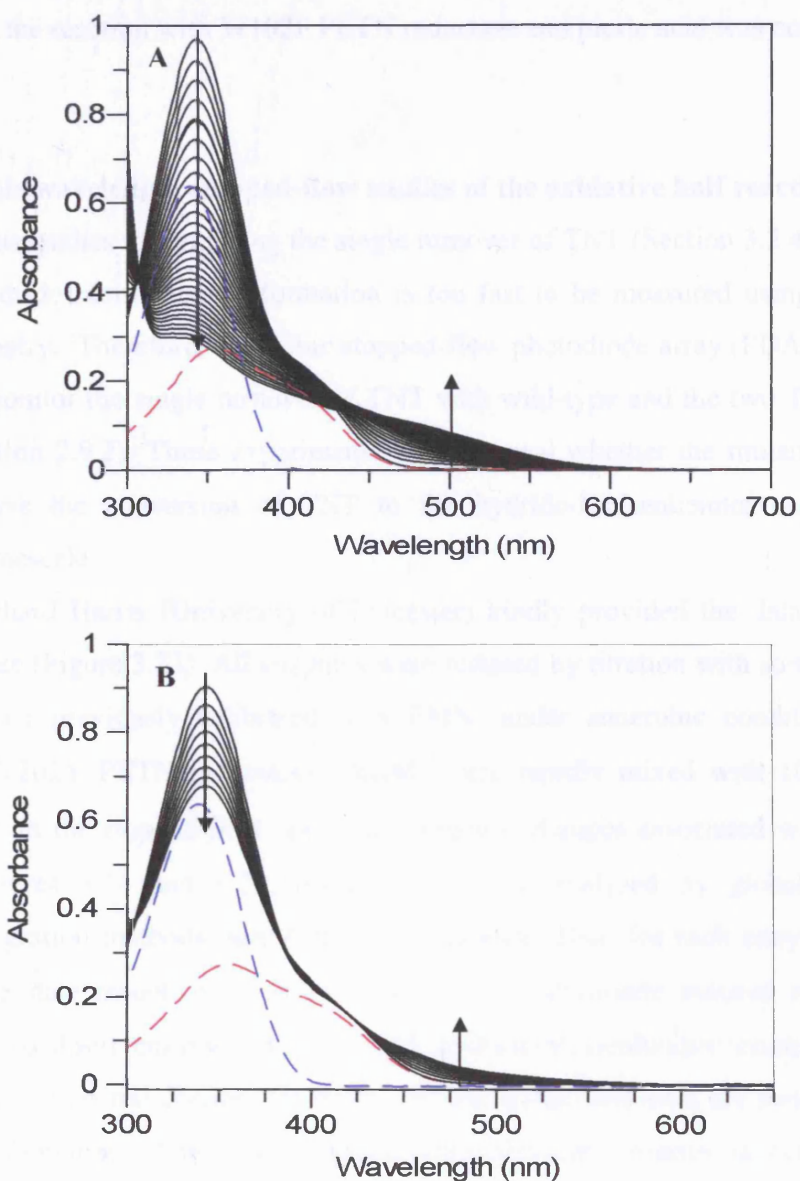


Figure 3.22. Absorption spectra following the multiple turnover of picric acid by wild-type (Panel A) and W102Y (Panel B) PETN reductase. Measurements were made under anaerobic conditions using 0.2 μM enzyme, 100 μM NADPH, 88 μM picric acid, and a NADPH regeneration system, in 50 mM potassium phosphate buffer, pH 7.0. Panel A, reaction with wild-type enzyme; Panel B, reaction with W102Y PETN reductase. To follow the multiple turnover of picric acid, spectra were recorded at 1 h intervals. The arrows indicate the direction of absorbance change as a function of time. The spectrum for picric acid (20 μM ; dashed red line) and NADPH (100 μM ; dashed blue line) are also displayed for comparative purposes.

decomposition of NADPH, reliable conclusions cannot be made from these studies. Consequently, the reaction with W102F PETN reductase and picric acid was not monitored.

3.2.9 Multiple wavelength stopped-flow studies of the oxidative half reaction with TNT

Previous studies investigating the single turnover of TNT (Section 3.2.4) revealed that the rate of hydride-Meisenheimer formation is too fast to be measured using conventional spectrophotometry. Therefore, anaerobic stopped-flow photodiode array (PDA) spectroscopy was used to monitor the single turnover of TNT with wild-type and the two Trp 102 mutant enzymes (Section 2.9.2). These experiments would reveal whether the mutant enzymes are able to catalyse the conversion of TNT to the hydride-Meisenheimer complex over a millisecond timescale.

Dr Richard Harris (University of Leicester) kindly provided the data for wild-type PETN reductase (Figure 3.23). All enzymes were reduced by titration with sodium dithionite, which had been previously calibrated with FMN, under anaerobic conditions. Reduced W102F and W102Y PETN reductases (40 μ M) were rapidly mixed with 10 times excess (400 μ M) TNT in the stopped-flow apparatus. Spectral changes associated with enzyme re-oxidation (Figures 3.24 and 3.25, respectively) were analysed by global analysis and numerical integration methods, using PROKIN software. Data for each enzyme were fitted best to a three state model: $A \rightarrow B \rightarrow C$, where A is dithionite reduced enzyme, B is a mixture of re-oxidised enzyme and the TNT hydride-Meisenheimer complex, and C is oxidized enzyme. Spectral changes for wild-type and mutant enzymes are comparable to one another. The formation of the TNT hydride-Meisenheimer complex is evident from the enhanced/increased absorbance at 460 nm and 580 nm, compared to the expected absorbance associated with 40 μ M oxidised enzyme. The increased absorbance at 460 nm and 580 nm correlate with peaks associated with the spectrum of purified hydride-Meisenheimer complex, characterized by Vorbeck *et al*, (Vorbeck *et al*, 1994; Figure 3.11). Further spectral analysis reveals the decay of the hydride-Meisenheimer complex, with the end spectrum corresponding to that for oxidised enzyme alone. Therefore, the Trp 102 mutant forms of PETN reductase retain the ability to catalyse the conversion of TNT to the corresponding hydride-Meisenheimer complex.

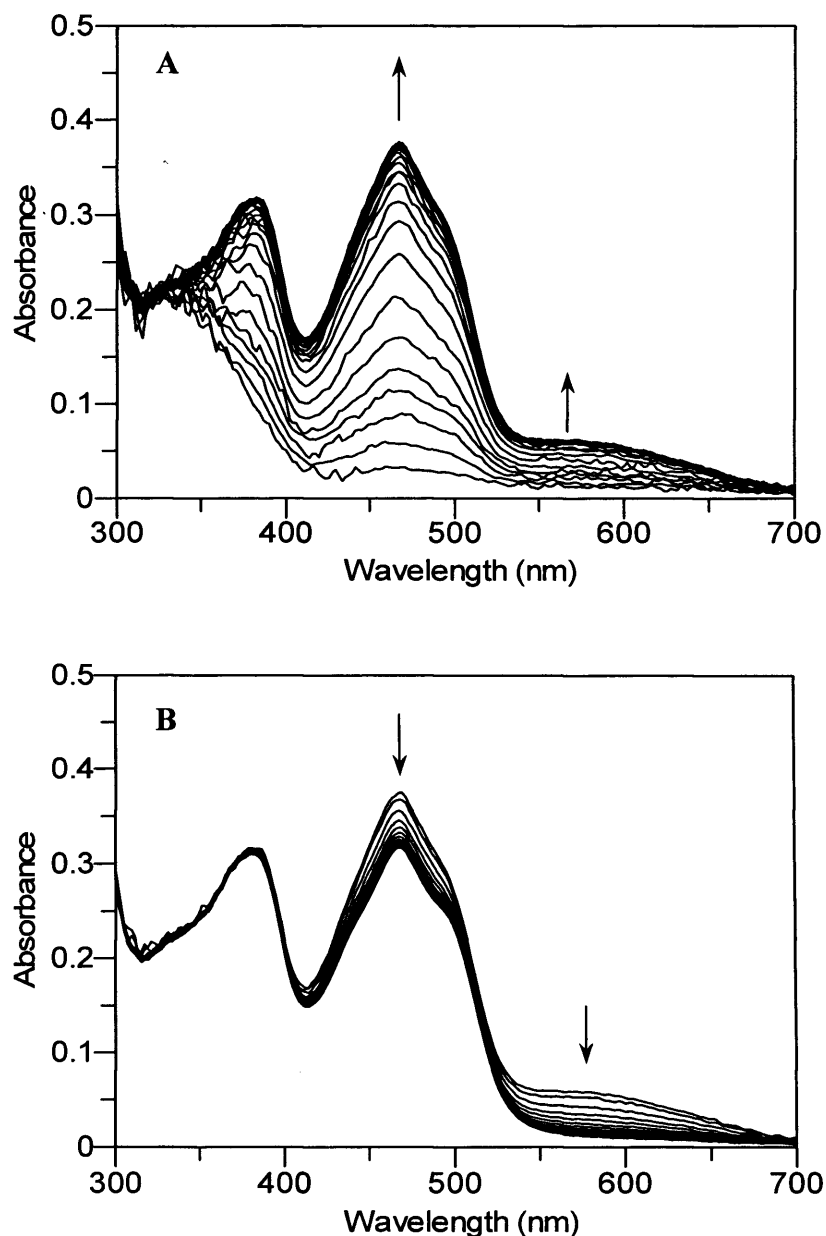


Figure 3.23. Time-dependent spectral changes associated with the reaction of dithionite-reduced wild-type PETN reductase with TNT, using stopped-flow spectroscopy. Dithionite-reduced wild-type PETN reductase ($\sim 35 \mu\text{M}$) was mixed with TNT ($400 \mu\text{M}$) at 25°C , in 1% acetone, potassium phosphate buffer, pH 7.0, under anaerobic conditions. Spectra were recorded on a log timescale for 500 s and 400 spectra collected. Panel A: spectral changes over 2 s from the mixing event, showing re-oxidation of the flavin and the formation of the hydride-Meisenheimer complex of TNT. Panel B: spectral changes for data acquisition in the 2-500 s time domain after mixing, showing the degradation of the hydride-Meisenheimer complex with the end spectrum corresponding to that of oxidized enzyme alone. Data kindly provided by Dr Richard Harris.

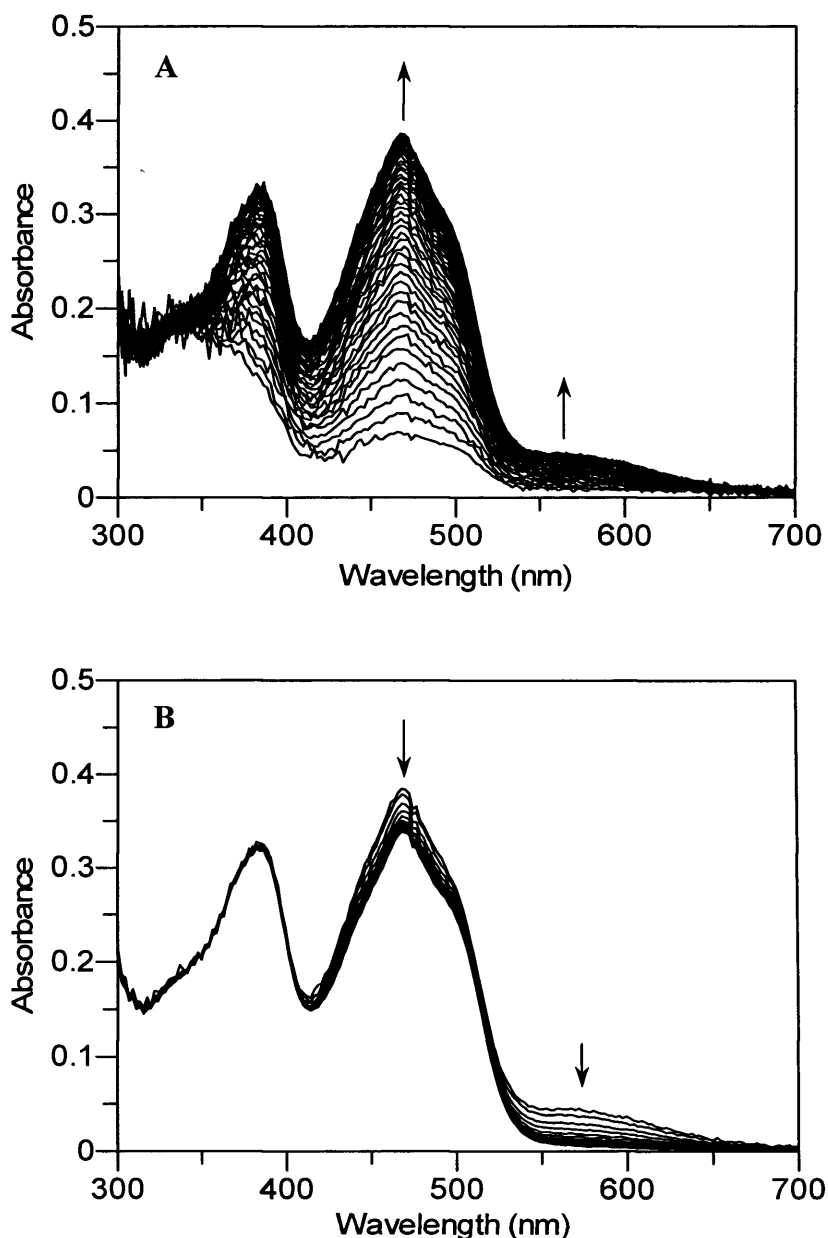


Figure 3.24. Time-dependent spectral changes associated with the reaction of dithionite-reduced W102F PETN reductase with TNT, using stopped-flow spectroscopy. Dithionite-reduced W102F PETN reductase ($\sim 35 \mu\text{M}$) was mixed with TNT ($400 \mu\text{M}$) at 25°C , in 1% acetone, potassium phosphate buffer, pH 7.0, under anaerobic conditions. Spectra were recorded on a log timescale for 500 s and 400 spectra collected. Panel A: spectral changes over 1 s from the mixing event, showing re-oxidation of the flavin and the formation of the hydride-Meisenheimer complex of TNT. Panel B: spectral changes for data acquisition in the 1-500 s time domain after mixing, showing the degradation of the hydride-Meisenheimer complex with the end spectrum corresponding to that of oxidized enzyme alone.

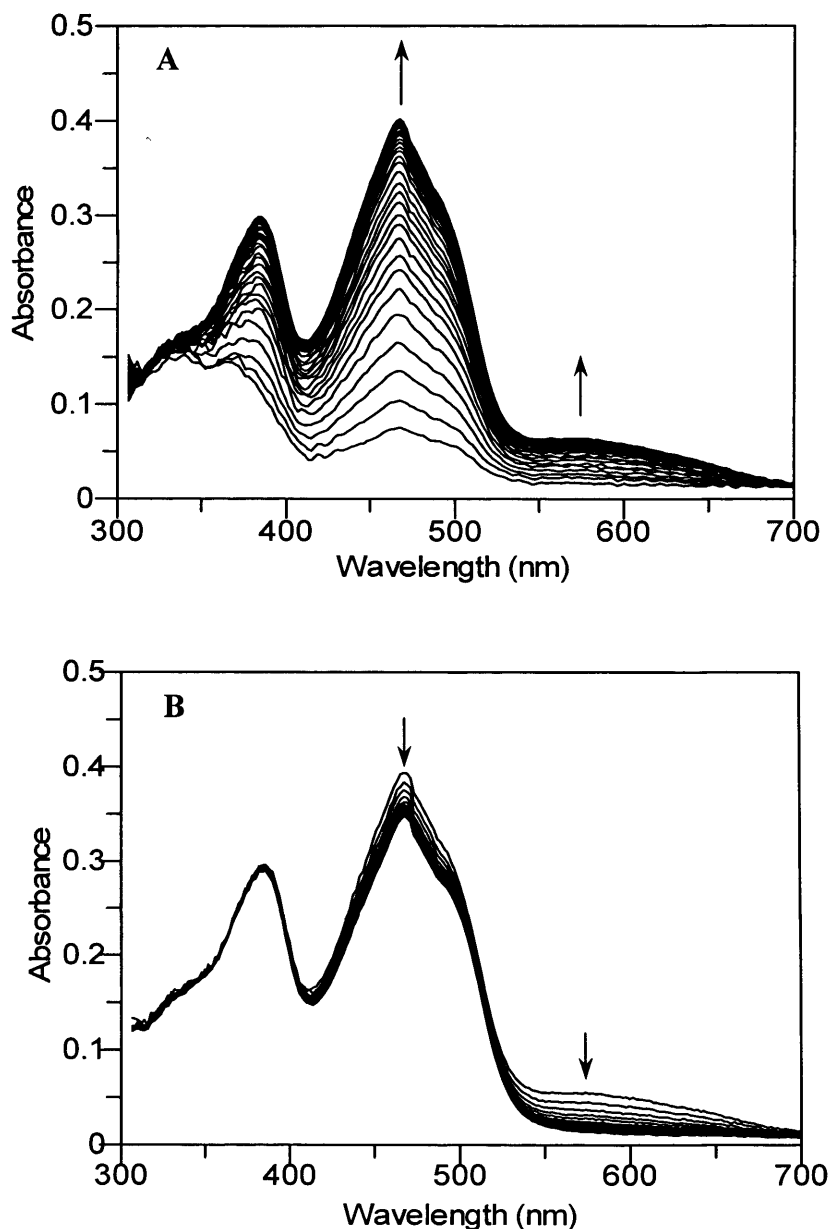


Figure 3.25. Time-dependent spectral changes associated with the reaction of dithionite-reduced W102Y PETN reductase with TNT using stopped-flow spectroscopy. Dithionite-reduced W102Y PETN reductase ($\sim 35 \mu\text{M}$) was mixed with TNT ($400 \mu\text{M}$) at 25°C , in 1% acetone, potassium phosphate buffer, pH 7.0, under anaerobic conditions. Spectra were recorded on a log timescale for 500 s and 400 spectra collected. Panel A: spectral changes over 2 s from the mixing event, showing re-oxidation of the flavin and the formation of the hydride-Meisenheimer complex of TNT. Panel B: spectral changes for data acquisition in the 2-500 s time domain after mixing, showing the degradation of the hydride-Meisenheimer complex with the end spectrum corresponding to that of oxidized enzyme alone.

3.2.10 Single wavelength stopped-flow studies of the oxidative half-reaction with TNT

Single wavelength stopped-flow spectroscopy was used to determine the kinetic parameters associated with the oxidative-half reactions of the W102F and W102Y PETN reductases with TNT. Studies were performed under anaerobic conditions using the method outlined in Section 2.9.1. A comparison of rate constants for TNT transformation by the wild-type and Trp 102 mutant enzymes should determine whether Trp 102 influences the kinetics of TNT degradation in PETN reductase.

Absorption changes associated with the mixing of dithionite-reduced enzyme (5 μM) with varying TNT concentrations at 25 $^{\circ}\text{C}$ were monitored at 464 nm, the flavin absorption maximum. Transients were best fitted to a single exponential process described by Equation 3.2, from which the observed rates were determined. Observed rates for TNT-mediated enzyme re-oxidation were subsequently plotted as a function of TNT concentration and fitted to a hyperbolic expression using GRAFIT 5.0 software (Figure 3.26). Fits of the data produced values for k_{lim} and K_{d} . A K_{d} value of $165 \pm 30 \mu\text{M}$ and a k_{lim} value of $6.08 \pm 0.38 \text{ s}^{-1}$ was determined for W102F PETN reductase, compared to a K_{d} of $235 \pm 25 \mu\text{M}$ and a k_{lim} of $12.92 \pm 0.53 \text{ s}^{-1}$ for W102Y enzyme (see also Table 3.3). In comparison, the wild-type enzyme (data kindly provided by Dr Richard Harris) has a K_{d} of $78 \pm 12 \mu\text{M}$ and a k_{lim} of $4.44 \text{ s}^{-1} \pm 0.14 \text{ s}^{-1}$ with TNT. These findings therefore indicate that TNT is bound less tightly and reduced at a slightly faster rate in the mutant enzymes than with wild-type PETN reductase.

To follow the formation of the hydride-Meisenheimer complex and its subsequent decay, spectral changes were monitored at 560 nm. Data were collected using 15 μM of dithionite-reduced enzyme and a range of TNT concentrations at 25 $^{\circ}\text{C}$. Transients showed a rapid increase in absorbance followed by a slower absorbance decrease; data were best fitted to an “up-down” equation described by Equation 3.3. Fits of the transients to an “up-down” expression were used to determine the observed rates for the formation of the hydride-Meisenheimer complex (increase in absorbance) and its subsequent decay (decrease in absorbance). The observed rates for the absorbance increase at 560 nm were equivalent to those calculated for the absorption changes at 464 nm at the same TNT concentration, indicating that the formation of the complex is directly related to flavin re-oxidation. Consequently, the rates for hydride-Meisenheimer formation were not analysed further as the larger absorption changes at 464 nm were best suited for the calculation of rate constants (see Table 3.3). The rates for hydride-Meisenheimer complex decay with each enzyme were independent of TNT concentration (data not shown). Observed rates of complex decay

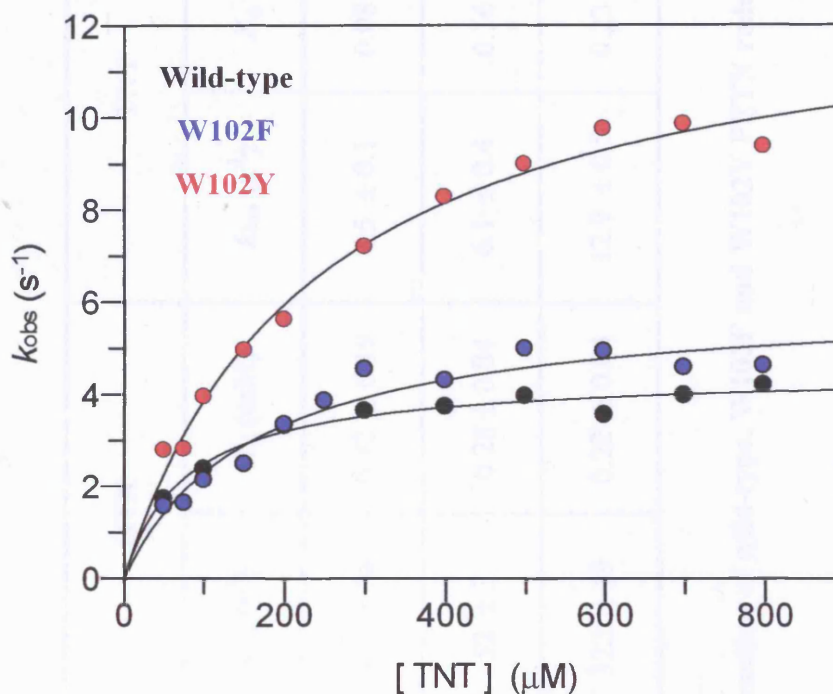


Figure 3.26. The concentration-dependence of the rate of hydride transfer from dithionite-reduced wild-type, W102F and W102Y PETN reductase to TNT. Anaerobic single wavelength spectroscopy at 464 nm was performed with 5 μM enzyme and a range of TNT concentrations (with a limit of 1 mM), in 50 mM potassium phosphate buffer, pH 7.0, 1% acetone, at 25 $^{\circ}C$. The transients were best fitted to a single exponential process and the observed rates were plotted as a function of TNT concentration. Data were fitted to a hyperbolic expression. Black circles represent the observed rates for wild-type enzyme; blue circles represent the observed rates for W102F PETN reductase and red circles represent the observed rates for W102Y PETN reductase.

	2-Cyclohexenone		GTN		TNT	
	k_{lim} (s ⁻¹)	K_d (mM)	k_{lim} (s ⁻¹)	K_d (mM)	k_{lim} (s ⁻¹)	K_d (mM)
Wild-type PETN reductase	35 ± 2	9.5 ± 1.6	313 ± 48	0.72 ± 0.19	4.5 ± 0.1	0.08 ± 0.01
W102F PETN reductase	68 ± 6	16 ± 4	52 ± 3	0.28 ± 0.04	6.1 ± 0.4	0.16 ± 0.03
W102Y PETN reductase	-	>100	322 ± 19	0.22 ± 0.04	12.9 ± 0.5	0.23 ± 0.02

Table 3.3. Rate constants for the oxidative half-reaction of wild-type, W102F and W102Y PETN reductases with TNT, GTN and 2-cyclohexenone.

differed between each enzyme. Typically, the rates for complex decay with 8 mM TNT for wild-type, W102F and W102Y PETN reductase (each 15 μM , at 25 $^{\circ}\text{C}$) are $5.3 \times 10^{-3} \text{ s}^{-1}$, $5.9 \times 10^{-2} \text{ s}^{-1}$ and $1.4 \times 10^{-1} \text{ s}^{-1}$, respectively. Thus, the complex decays approximately 10-fold and 30-fold faster with W102F and W102Y PETN reductases, respectively, when compared to the wild-type enzyme. Typical transients showing the rate of hydride-Meisenheimer formation and decay with each enzyme are displayed in Figure 3.27. This figure clearly demonstrates that the complex decays much faster with the mutant enzymes, but the rate of complex formation is similar in all enzymes. Hence, although the two mutant enzymes produce the TNT hydride-Meisenheimer complex at comparable rates to wild-type enzyme, the complex formed is less stable than when produced by wild-type PETN reductase.

3.2.11 Single wavelength stopped-flow studies of the oxidative half-reaction with 2-cyclohexenone and GTN

To determine whether Trp 102 influences the reduction of GTN and 2-cyclohexenone, rates of hydride transfer from reduced wild-type and mutant PETN reductases to these substrates were measured. Single wavelength stopped-flow spectroscopy under anaerobic conditions was used to monitor absorbance changes at 464 nm, which followed the re-oxidation of reduced flavin (Section 2.9.1). Previous studies with wild-type enzyme, using multiple wavelength spectroscopy, revealed that during GTN and 2-cyclohexenone reduction, no spectrally visible intermediates form (Craig, 2000).

A range of 2-cyclohexenone concentrations were mixed with 20 μM dithionite-reduced W102F and W102Y PETN reductase, at 25 $^{\circ}\text{C}$. Transients following flavin re-oxidation for both enzymes were best fitted to a triple exponential equation described in Equation 3.4:

$$A = C_1(1 - e^{-k_{\text{obs}1}}) + C_2(1 - e^{-k_{\text{obs}2}}) + C_3(1 - e^{-k_{\text{obs}3}}) + b$$

Equation 3.4

where A is the absorbance change, C is a constant related to the initial absorbance, b is an offset, and k_{obs} is the observed rate constant.

The largest absorbance change occurred in the second phase of the transient and fits to this phase were used to calculate k_{obs} . The remaining two phases had minor amplitude changes

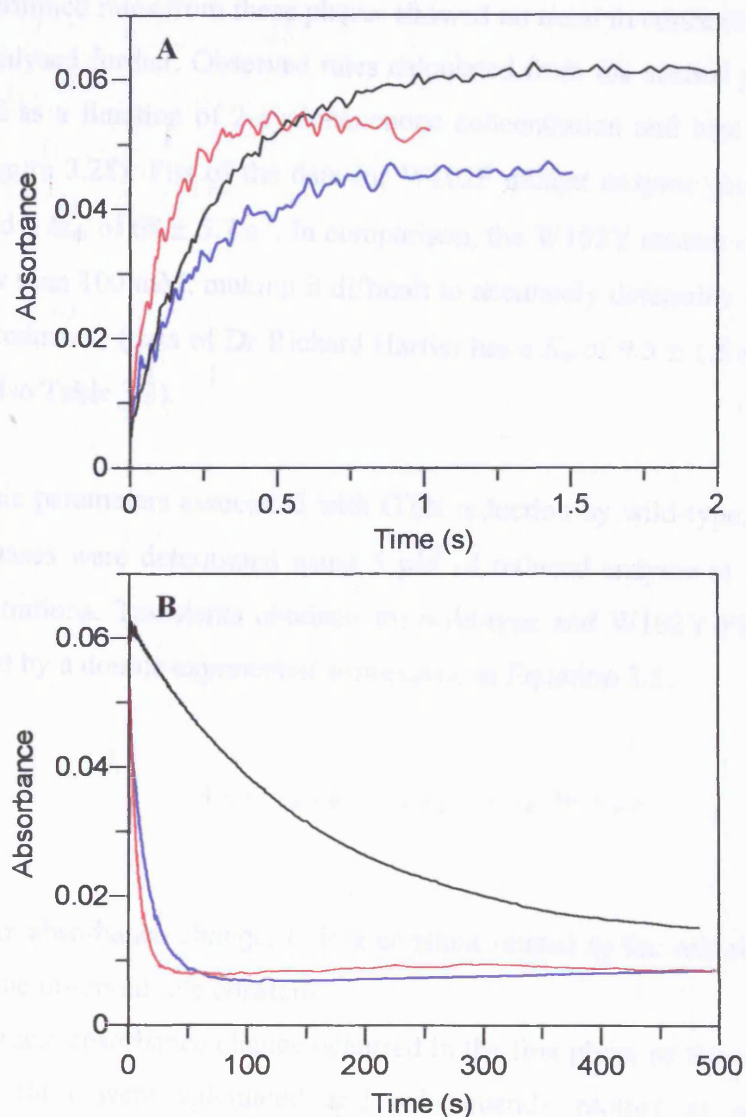


Figure 3.27. Transients following hydride-Meisenheimer complex formation and decay, at 560 nm. Transients were obtained using PDA data, where dithionite-reduced enzyme ($\sim 35 \mu\text{M}$) was mixed with TNT ($400 \mu\text{M}$) at 25°C , in 1% acetone, potassium phosphate buffer, pH 7.0, under anaerobic conditions. The reaction was monitored over a log scale of 500 s and the transients displayed follow the absorbance changes at 560 nm. Panel A, transients following hydride-Meisenheimer complex formation, over a period of 2 s. Rate constants from the fits to the transient shown are; 3.6 s^{-1} with wild-type (black line); 8.5 s^{-1} with W102Y (red line) and 4.0 s^{-1} with W102F (blue line) PETN reductase. Panel B, transients following complex decay. Rate constants from the fits to the transients shown are: $5.3 \times 10^{-3} \text{ s}^{-1}$ with wild-type (black line); $1.4 \times 10^{-1} \text{ s}^{-1}$ with W102Y (red line) and $5.9 \times 10^{-2} \text{ s}^{-1}$ with W102F (blue line) PETN reductase.

and the determined rates from these phases showed no trend in concentration dependence, and were not analysed further. Observed rates calculated from the second phase of the transients were plotted as a function of 2-cyclohexenone concentration and best fitted to a hyperbolic function (Figure 3.28). Fits of the data for W102F mutant enzyme produced a K_d of 16.4 ± 3.82 mM and a k_{lim} of 68 ± 5.7 s⁻¹. In comparison, the W102Y mutant enzyme produced a K_d value greater than 100 mM, making it difficult to accurately determine a value for k_{lim} . Wild-type PETN reductase (data of Dr Richard Harris) has a K_d of 9.5 ± 1.6 mM and a k_{lim} of 35 ± 2.2 s⁻¹ (see also Table 3.3).

Kinetic parameters associated with GTN reduction by wild-type, W102F and W102Y PETN reductases were determined using 5 μ M of reduced enzyme at 5 °C, and a range of GTN concentrations. Transients obtained for wild-type and W102Y PETN reductases were best described by a double exponential expression, in Equation 3.5:

$$A = C_1(1 - e^{-k_{obs1}}) + C_2(1 - e^{-k_{obs2}}) + b$$

Equation 3.5

where A is the absorbance change, C is a constant related to the initial absorbance, b is an offset, k_{obs} is the observed rate constant.

The largest absorbance change occurred in the first phase of the transients from which the observed rates were calculated and subsequently plotted as a function of GTN concentration (Figure 3.29). Fitting of data to a hyperbolic function produced a K_d of 718 ± 197 μ M and a k_{lim} of 313 ± 48 s⁻¹ for wild-type enzyme, while the W102Y mutant enzyme has K_d of 219 ± 38 μ M and a k_{lim} of 322 ± 19 s⁻¹ (see also Table 3.3). Transients obtained with W102F mutant enzyme were more complex and fitted best to a triphasic exponential expression (Equation 3.4). The rates obtained from the second phase of the transient (which had the largest absorbance change) showed a hyperbolic dependence on GTN concentration (Figure 3.29), from which a K_d of 280 ± 44 μ M and a k_{lim} of 52 ± 3 s⁻¹ was determined (see also Table 3.3). The rate constants for the oxidative half-reaction with TNT, GTN and 2-cyclohexenone with each enzyme form, are summarised in Table 3.3.

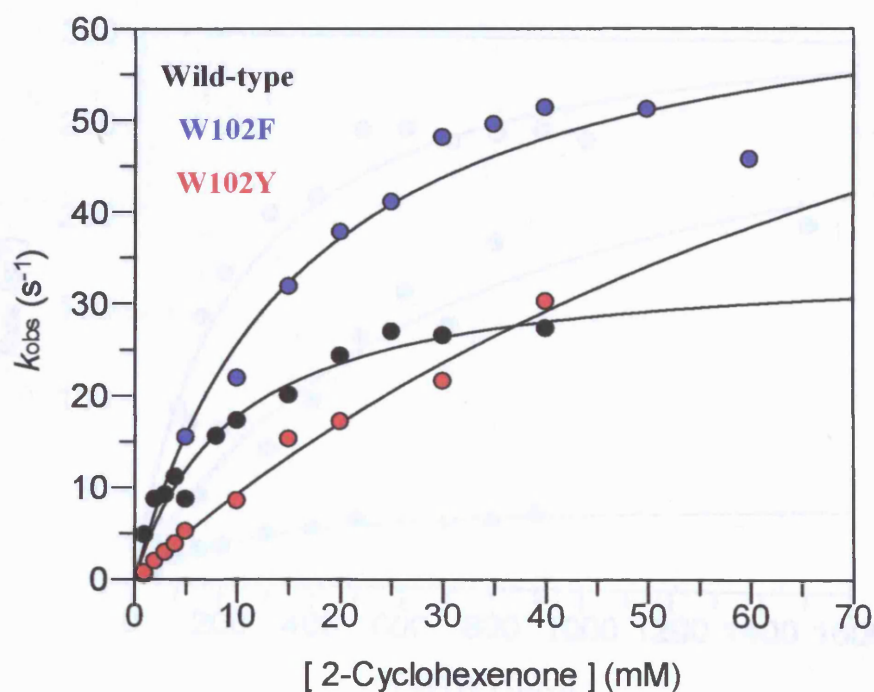


Figure 3.28. The concentration-dependence of the rate of hydride transfer from dithionite-reduced wild-type, W102F and W102Y PETN reductase to 2-cyclohexenone. Anaerobic single wavelength spectroscopy at 464 nm was performed with 20 μ M enzyme and a range of cyclohexenone concentrations, in 50 mM potassium phosphate buffer, pH 7.0 at 25 $^{\circ}$ C. Black circles represent the observed rates for wild-type enzyme; blue circles represent rates produced by W102F PETN reductase and red circles represent the data for W102Y PETN reductase.

3.2.13 Redox potential

Redox potentials for wild-type, W102Y and W102F PETN reductases were measured using the method published by Drapeau (Drapeau, 1978). Measuring the redox potential for each enzyme would determine whether the mutations had altered the thermodynamic propensity of the flavin and therefore help to explain any kinetic differences observed between the enzymes.

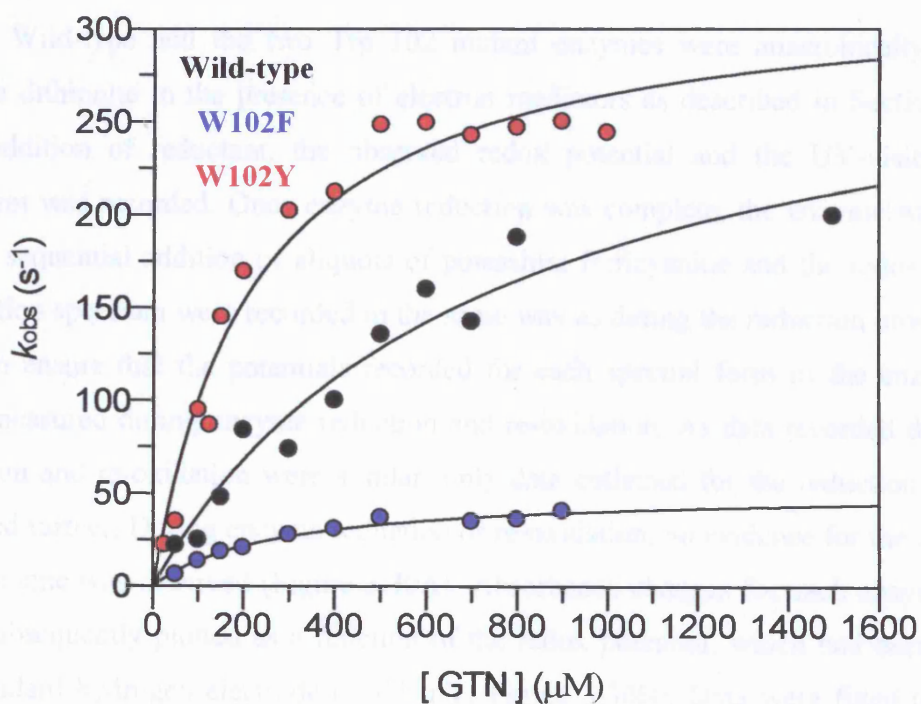


Figure 3.29. The concentration-dependence of the rate of hydride transfer from dithionite-reduced WT, W102F and W102Y PETN reductase to GTN. Anaerobic single wavelength spectroscopy at 464 nm was performed with 5 μM enzyme and a range of GTN concentrations, in 50 mM potassium phosphate buffer, pH 7.0, 1 % acetone at 5 $^{\circ}\text{C}$. Black circles represent the observed rates for wild-type enzyme; blue circles represent rates produced by W102F PETN reductase and red circles represent the data for W102Y PETN reductase.

3.2.12 Redox potentiometry

Redox potentials for wild-type, W102Y and W102F PETN reductases were measured using the method published by Dutton (Dutton, 1978). Measuring the redox potential for each enzyme would determine whether the mutations had affected the thermodynamic properties of the flavin and therefore help to explain any kinetic differences observed between the enzymes.

Wild-type and the two Trp 102 mutant enzymes were anaerobically titrated with sodium dithionite in the presence of electron mediators as described in Section 2.10. Upon each addition of reductant, the observed redox potential and the UV-visible absorption spectrum was recorded. Once enzyme reduction was complete, the enzyme was re-oxidised by the sequential addition of aliquots of potassium ferricyanide and the redox potential and absorption spectrum were recorded in the same way as during the reduction process. This was done to ensure that the potentials recorded for each spectral form of the enzyme matched those measured during enzyme reduction and re-oxidation. As data recorded during enzyme reduction and re-oxidation were similar, only data collected for the reduction process were analysed further. During enzyme reduction or re-oxidation, no evidence for the formation of a semiquinone was observed (Figure 3.30A). Absorbance changes for each enzyme at 468 nm were subsequently plotted as a function of the redox potential, which had been corrected to the standard hydrogen electrode (+244 mV; Figure 3.30B). Data were fitted to a concerted two-electron redox process, described by Equation 3.5 (Daff *et al.*, 1997))

$$A_{468} = \frac{(a + b10^{(E'-E)/29.5})}{1 + 10^{(E'-E)/29.5}}$$

Equation 3.5

where A_{468} is the absorbance value at 468 nm at the electrode potential E , and a and b are the absorbance values of the fully oxidised and reduced enzyme, respectively, at 468 nm. Good fits of the data were obtained with each enzyme (Figure 3.30B). The midpoint potential (E') determined from the fits for wild-type, W102F and W102Y PETN reductase were -267 ± 4 mV, -236 ± 5 mV and -241 ± 4 mV, respectively. The data reveal that the two mutant forms of PETN reductase have a slightly more positive midpoint potential than wild-type enzyme.

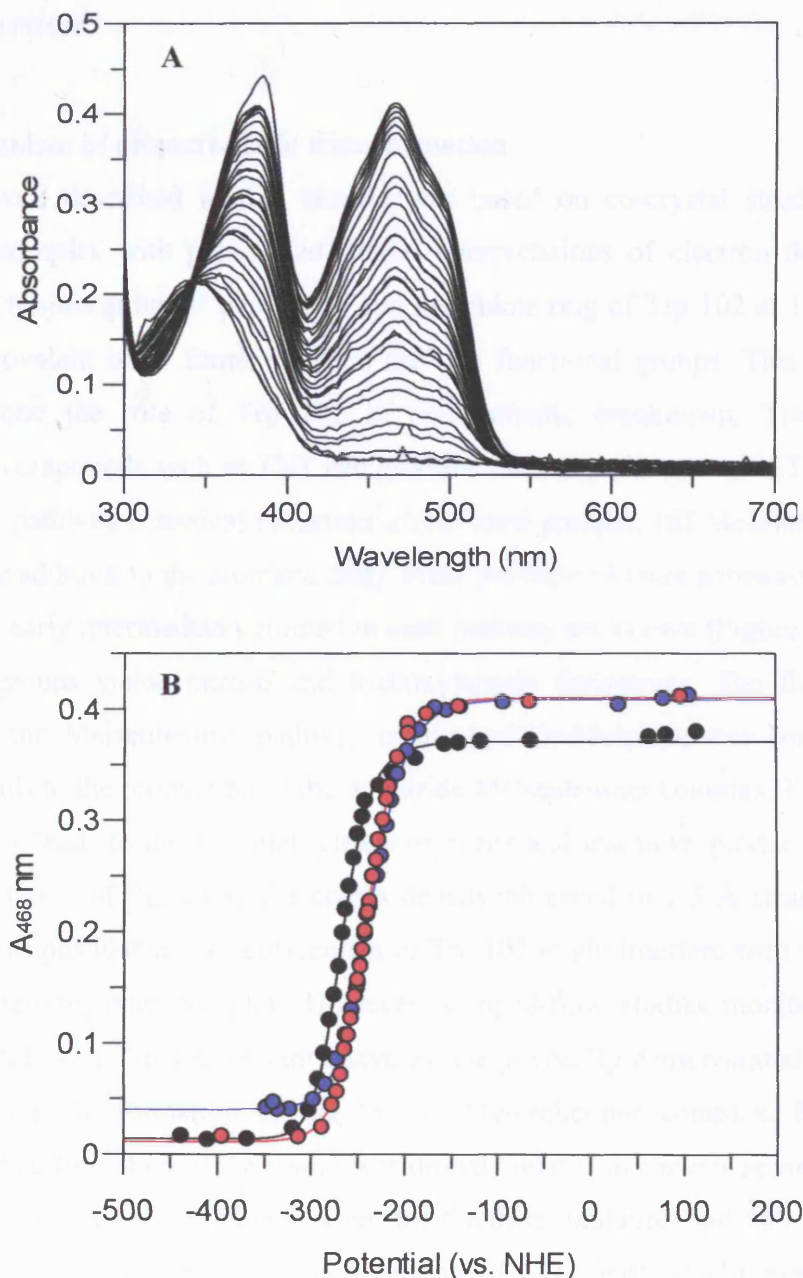


Figure 3.30. Spectral changes (Panel A) and plot of absorbance versus potential (Panel B) measured during the reductive titration of wild-type and Trp 102 mutant forms of PETN reductase. Panel A displays the spectral changes monitored during the titration for W102Y PETN reductase ($\sim 35 \mu\text{M}$). Similar spectral changes were observed with wild-type and W102Y PETN reductase. Panel B displays the absorbance profile at 468 nm for wild-type (black circles), W102F (blue circles) and W102Y (red circles) PETN reductases, plotted against the measured potential (corrected to the standard hydrogen electrode, +244 mV). Data were fitted to a concerted two-electron redox process (Equation 3.5), from which the midpoint potential was calculated.

3.3 Discussion

3.3.1 Mechanism of nitroaromatic transformation

The work described in this chapter was based on co-crystal structures of PETN reductase in complex with picric acid. Initial interpretations of electron density observed between the C6 nitro group of picric acid and the indole ring of Trp 102 at 1.5 Å resolution, suggested a covalent bond forms between the two functional groups. This led to solution studies to probe the role of Trp 102 in nitroaromatic breakdown. Transformation of nitroaromatic compounds such as TNT can proceed via two pathways in PETN reductase; (i) nitroreductase pathway (classical reduction of the nitro groups), (ii) Meisenheimer pathway (direct hydride addition to the aromatic ring). Final products of these pathways have yet to be identified, but early intermediates formed in each pathway are known (Figure 3.1). Reduction of the nitro groups yields nitroso and hydroxylamino derivatives. The first intermediate produced via the Meisenheimer pathway is the hydride-Meisenheimer complex of TNT, which then leads to the production of the dihydride-Meisenheimer complex. Further reduction of this complex leads to the eventual release of nitrite and unknown products. Based on the initial interpretation of the unusual electron density observed in 1.5 Å structures of PETN reductase, it was postulated that replacement of Trp 102 might interfere with the formation of the hydride-Meisenheimer complex. However, stopped-flow studies monitoring the single turnover of TNT with Trp 102 mutant enzymes unequivocally demonstrated that Trp 102 is not essential for the formation of the hydride-Meisenheimer complex. Further analysis demonstrated that formation of the complex is directly related to enzyme re-oxidation, evident from the identical rates observed at 464 nm for flavin re-oxidation and 560 nm for hydride-Meisenheimer formation, upon the rapid mixing of TNT with stoichiometrically reduced enzyme (Section 3.2.10). The unusual electron density observed in enzyme-picric acid complex structures at 1.5 Å, is therefore unlikely to reflect the formation of a covalent bond. Further stopped-flow studies with wild-type, W102F and W102Y PETN reductases revealed that the rate of hydride-Meisenheimer formation remained largely unaffected by the mutation of Trp 102, but the kinetics of complex decay differed substantially amongst the enzymes. Decay of the complex proceeded significantly faster in the mutant enzymes than with wild-type enzyme, indicating that hydride-Meisenheimer complex decay is an enzyme-catalysed process. Although mutation of Trp 102 does not affect the ability of PETN reductase to accumulate the hydride-Meisenheimer complex, the greater instability of the complex in the

mutant enzymes is likely to influence the eventual fate of TNT transformation products. This was demonstrated by TNT multiple turnover studies. Reactions for each enzyme were monitored using absorbance spectroscopy and assumed to be completed when a final stable absorbance spectrum was observed. Spectral properties of the reaction products for wild-type enzyme were observed to clearly differ from those of the two mutant enzymes, indicating that the nature of TNT metabolism differs between the wild-type and Trp 102 mutant enzymes. This was further exemplified by NMR analysis of multiple turnover reactions, where the W102Y enzyme produced a less complex final NMR spectrum compared to that for wild-type enzyme. However, some NMR signals were common to both enzyme-catalysed reactions, although the intensity of these signals differed. Collectively, these multiple turnover studies suggest that either (i) multiple reaction products accumulate in both wild-type and Trp 102 mutant enzymes but in different concentration distributions or, (ii) different reaction products accumulate in wild-type and Trp 102 mutant enzymes. The ability of PETN reductase to transform TNT via multiple pathways (nitroreductase and Meisenheimer) is consistent with either of these possibilities. In each enzyme reaction, accumulation of the hydride-Meisenheimer complex was not observed, consistent with its rapid decay as identified by stopped-flow studies. Identification of the nature of products produced was made difficult due to the presence of multiple compounds and the complexity of spectra. However, this may be the subject for future work, using a combination of NMR spectroscopy, HPLC and mass spectrometry. The time-dependent development of NMR signals which form during the course of the reaction for both enzymes, demonstrate that as TNT is consumed other signals/compounds develop and then decay, which in turn leads to the formation of other compounds/signals (Figure 3.17). Future studies would need to focus on the chemical identity of these intermediates and the kinetics of formation and decay of these intermediates.

Studies investigating the transformation of picric acid proved to be less informative than corresponding studies with TNT. Studies following the single turnover of picric acid gave some indication that the wild-type enzyme produces the picric acid hydride-Meisenheimer complex. However, the mutant enzymes reduced picric acid to form a product that differed spectroscopically to that observed with wild-type enzyme. Given that the product produced from W102F and W102Y enzyme-catalysed reactions showed little/no resemblance to the spectrum for the hydride-Meisenheimer complex, it is probable that the mutant enzymes do not produce the complex or that it is very short lived. The multiple turnover of picric acid proceeded at an extremely slow rate, in which time NADPH decomposed.

Collectively, although these studies have not provided useful information about the nature of picric acid degradation, they have clearly shown that Trp 102 does influence the single turnover of this substrate. Stopped-flow analysis of picric acid catalysis was not attempted owing to the explosive nature of this compound. Future work might involve NMR analysis (with HPLC and mass spectroscopy) of picric acid turnover, to identify the products of the reaction and the influence of Trp 102.

3.3.2 Role of Trp 102 in nitroaromatic binding

During the course of this study, the structure of PETN reductase in complex with picric acid was solved at 0.9 Å, and an alternative explanation for the unusual electron density observed in the 1.5 Å structure was proposed. At this resolution, it became clear that the side chain of Trp 102 adopts at least two conformations with partial occupancy, thus avoiding steric clash with the picric acid nitro group. In turn, this suggested that Trp 102 interferes with the binding of ligands (Harris *et al*, 2002). Support for this hypothesis comes from ligand binding studies where picric acid was observed to bind more tightly to oxidised W102Y and W102F PETN reductases in comparison to wild-type enzyme. These results are consistent with the removal of the steric clash observed between the nitro group of picric acid and the indole ring of Trp 102 in wild-type enzyme. The structures of the Trp 102 mutant enzymes in complex with picric acid have been solved and show no evidence of multiple conformations of the mutated residue at position 102 (Figure 3.31). Furthermore, the picric acid appears to fully occupy the active site indicating that the nitro group of this substrate is accommodated without steric clash, which as observed favours picric acid binding. The binding of 2,4-DNP remains largely unaffected in the Trp 102 mutant enzymes, suggesting that 2,4-DNP binds to the mutant enzymes in a similar manner to that observed in the crystal complex of wild-type PETN reductase and 2,4-DNP (Khan *et al*, 2002; Figure 3.2). In the 2,4-DNP-wild-type enzyme complex, no steric clash is observed between Trp 102 and a nitro group of 2,4-DNP (the nitro group that is observed to clash with Trp 102 is not present in 2,4-DNP). Progesterone also binds with similar affinity to all three enzymes indicating that Trp 102 has no role in the binding of steroids. This is consistent with recent crystallographic studies of PETN reductase in complex with steroid ligands (Barna *et al*, 2001; see also Chapter Four). Ligand binding studies with TNT elicited no spectral perturbations in the flavin spectrum, indicating very weak binding of this ligand to oxidised enzyme. This can be attributed to the poor interaction of the TNT methyl group with His 181 and 184, which form strong

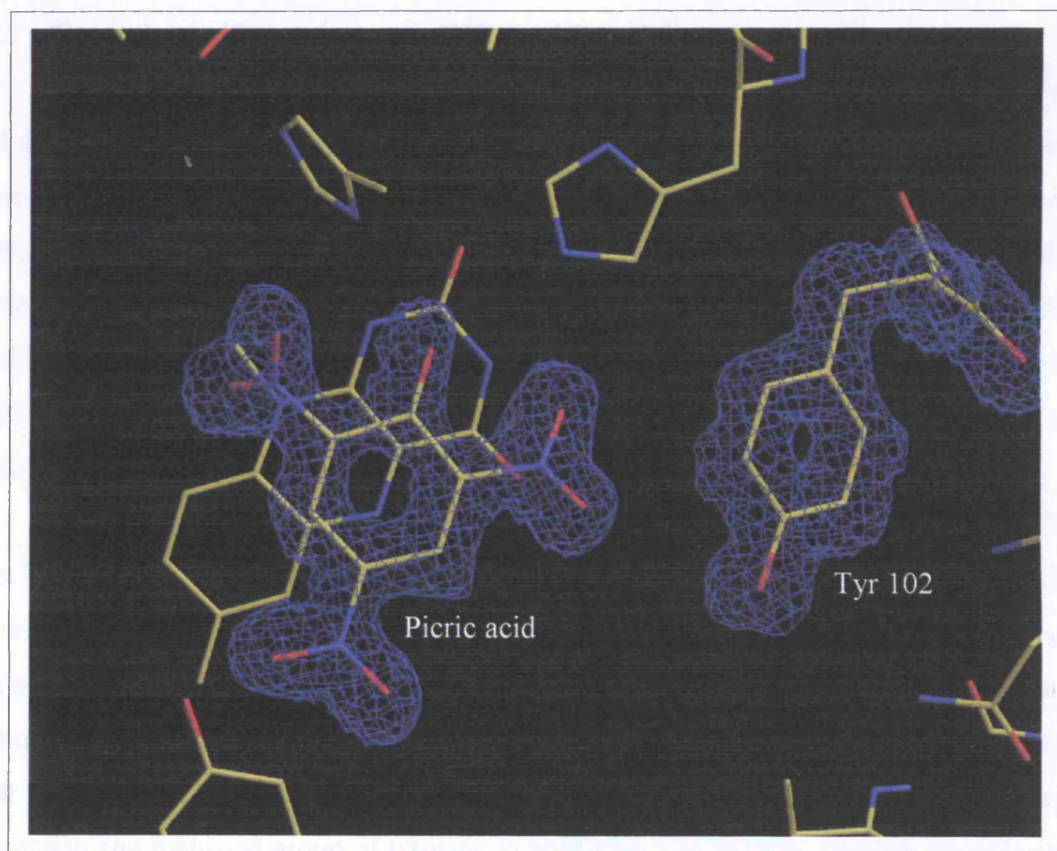


Figure 3.31. Crystal structure of the active site of W102Y PETN reductase in complex with picric acid. The observed multiple conformations of Trp 102 in wild-type PETN reductase-picric acid complexes indicated that the side chain of Trp 102 sterically clashes with the C6 nitro group of picric acid. Therefore, Trp 102 was mutated to Tyr 102 and as observed here the mutant enzyme can fully accommodate the C6 nitro group of picric acid without steric clash. (Khan *et al*, 2004)

interactions with the analogous hydroxyl group of picric acid. Given the structural similarity of TNT and picric acid, it is therefore assumed that TNT binds in a manner similar to picric acid.

3.3.3 Oxidative half-reaction with GTN and 2-cyclohexenone

The role of Trp 102 was further investigated in the catalysis of GTN and 2-cyclohexenone. Rates following enzyme re-oxidation showed hyperbolic dependence on substrate concentration from which the k_{lim} and dissociation constant was determined. Comparisons of dissociation constants (K_d) for GTN binding to reduced enzyme, revealed that the two Trp 102 mutant enzymes bind GTN with similar affinities, and this binding affinity is 3-fold tighter than wild-type enzyme. Unfortunately, there is no information on the mode of GTN binding to PETN reductase, as structures of the enzyme with bound GTN are not available.

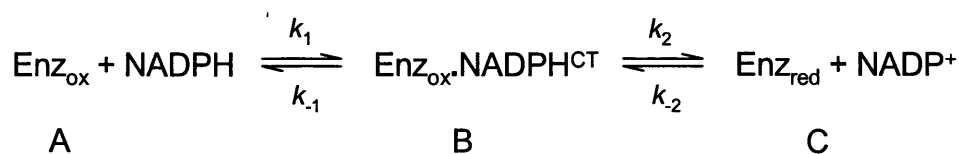
Analysis of the pre-steady rate constants for flavin re-oxidation by GTN with wild-type, W102F and W102Y PETN reductases revealed some notable differences. While the k_{lim} for wild-type and W102Y were similar (313 s^{-1} and 322 s^{-1} at $5\text{ }^\circ\text{C}$, respectively), a six-fold decrease in the rate constant was evident with W102F PETN reductase (k_{lim} of 52 s^{-1}). These findings suggest that an amino acid with the potential to form a hydrogen bond and/or have a polar group may be important in the reduction of nitrate esters. The indole nitrogen of tryptophan and hydroxyl group of tyrosine in wild-type and W102Y enzyme are polarised and therefore have the potential to form a hydrogen bond with a nitro group of GTN. In turn, the formation of such a bond might lead to the optimal alignment of GTN over the flavin for efficient electron transfer to GTN.

The pre-steady state rate constant for 2-cyclohexenone mediated flavin re-oxidation was nearly 2-fold higher (68 s^{-1}) with W102F PETN reductase compared to wild-type enzyme (35 s^{-1}). The k_{lim} value for W102Y PETN reductase could not be determined as the K_d was greater than 100 mM . W102F PETN reductase also showed a 2-fold increase in its K_d value compared to wild-type enzyme. The replacement of Trp 102 in W102F PETN reductase might provide more space in the active site for 2-cyclohexenone to align more optimally over the flavin ready for efficient hydride transfer. Structures of PETN reductase solved in the presence of 2-cyclohexenone do not suggest Trp 102 to be a primary determinant in the binding of this substrate. Instead, His 181 and His 184 are observed to be the main determinants in ligand binding (Khan *et al*, 2002; see Chapter 5). However, these are oxidised

enzyme-2-cyclohexenone structures, and the reduced enzyme complex might have a different geometry of binding.

3.3.4 Kinetics of the reductive half-reaction

The kinetics associated with the reductive half-reaction of each enzyme are consistent with similar studies of the reductive half-reaction of wild-type PETN reductase. In PETN reductase it is presumed that NADPH binds over the *si* face of the flavin and hydride transfer takes place from the A-side of the nicotinamide ring of NADPH, analogous to the known stereospecificity for OYE (Massey and Schopfer, 1986). Studies by Craig (Craig, 2000) have demonstrated that in the reductive half-reaction of PETN reductase a charge-transfer intermediate forms before hydride-transfer takes place. This charge-transfer complex consists of oxidised enzyme bound to NADPH, such that the mode of NADPH binding is optimal for hydride transfer to proceed. Consequently, this complex gives rise to increased absorbance in the longer wavelength region as a result of the π - π stacking of NADPH over the flavin ring. Collectively, studies investigating the reductive half-reaction of PETN reductase led to the model shown in Scheme 3.2.



Scheme 3.2

The studies reported in this chapter aimed to characterise the rate constants in Scheme 3.2 for the wild-type and Trp 102 mutant PETN reductases. This was achieved by analysing the dependence of the rates of charge-transfer formation and hydride transfer on NADPH concentration. Studies monitoring the formation and subsequent decay of the charge-transfer complex revealed that the rates for complex decay were identical to the observed rates for hydride-transfer. This indicates that the decay of the charge-transfer species is a direct consequence of flavin reduction, consistent with previous multiple wavelength stopped-flow studies (Craig, 2000). Minor deviations to the fitting of the early phase of transients following the formation of the charge-transfer species (560 nm data) might imply that a pre-charge-transfer intermediate accumulates in the early time domain. The formation of a pre-charge transfer complex has been proposed in studies performed with OYE (Massey and Schopfer, 1986) and estrogen-binding protein (Buckman and Miller, 2000b). However, as there is no

direct evidence for the formation of such an intermediate at this stage, the pre-charge transfer species is not incorporated into Scheme 3.2.

The rates for charge-transfer formation showed linear dependence on NADPH concentration, whereas the rates for flavin reduction were independent of NADPH concentration (this might be attributed to the rates being measured at NADPH concentrations of 100 μ M and above). Differences in the rate constants for the reductive half-reaction with wild-type, W102F and W102Y PETN reductase are small. These results are consistent with the measured redox potential values for each enzyme, where differences in the measured potentials were also quite small. Spectral changes accompanying the reductive (and oxidative) titration of wild-type and Trp 102 mutant enzymes showed no evidence for the formation of a semiquinone species. These findings contrast with those seen in the photoreduction of OYE where the anionic red semiquinone is populated (Massey and Hemmerich, 1978), but are similar to titrations performed with morphinone reductase (Craig *et al.*, 2001). Collectively, the results of the reductive half-reaction are consistent with Scheme 3.2, which is comparable to the scheme proposed for the reductive half-reaction of OYE (Massey and Schopfer, 1986), morphinone reductase (Craig *et al.*, 1998) and estrogen-binding protein (Buckman and Miller, 1998). In addition, studies conducted in this chapter have established that mutation of Trp 102 in PETN reductase causes only relatively small changes (25-30 mV) to the thermodynamic properties of the flavin, and has no significant effect on the binding and catalysis of NADPH

3.3.5 Summary

The multiple conformational states of Trp 102, observed in the high resolution structure of PETN reductase-picric acid complexes, indicates that the side chain of this residue sterically clashes with the C6 nitro group of picric acid. The results presented in this chapter are consistent with this analysis and mutation of Trp 102 appears to relieve the steric constraints placed on picric acid binding. This is as reflected from structural studies of W102F and W102Y PETN reductases in complex with picric acid and from the tighter binding of picric acid to these enzymes. Furthermore, it is demonstrated that mutation of Trp 102 in PETN reductase, influences the turnover of TNT by accelerating the decay of the hydride-Meisenheimer complex. These findings establish that hydride-Meisenheimer decay is an enzyme-catalysed process. Collectively, the results presented here reveal that small changes in the active site structure of PETN reductase can have profound effects on the

kinetics and chemistry of TNT transformation. This opens the exciting possibility of engineering new activities (such as the ability to reduce the aromatic ring) into structurally similar enzymes, such as OYE, which display almost exclusively nitroreductase activity towards TNT.

Chapter Four

*Role of Tyr 186 in the oxidative half-
reaction of PETN reductase: a
potential proton donor*

CHAPTER FOUR

Role of Tyr 186 in the oxidative half-reaction of PETN reductase: a potential proton donor

4.1 Introduction

The work covered in this chapter explores the possible role of Tyr 186 in the mechanism of reduction of α,β -unsaturated compounds and tests the hypothesis that Tyr 186 acts as an active site acid. The work is based on previous studies of OYE, which revealed that the equivalent residue, Tyr 196, acts as a proton donor in the reduction of similar substrates (Kohli and Massey, 1998). The chapter begins by reviewing the mode of steroid binding and a possible mechanism of steroid reduction in PETN reductase, based on NMR and structural analysis (Barna *et al*, 2001). The isolation and characterisation of a mutant form of PETN reductase in which Tyr 186 is replaced by Phe 186 is described. Detailed stopped-flow kinetic studies are reported that indicate Tyr 186 in PETN reductase is not a key proton donor in the oxidative half-reaction of the enzyme. The studies have major implications for our understanding of the mechanism of reduction of α,β -unsaturated compounds in the OYE family and these are discussed.

4.1.1 Mode of steroid binding

PETN reductase catalyses the reduction of a diverse range of compounds. In addition to high explosive substrates (Chapter 3) the enzyme reduces a variety of α,β -unsaturated carbonyl compounds, which range from simple structures (e.g. 2-cyclohexenone) to more complex compounds (e.g. steroids). These compounds are also good substrates for OYE (Stott *et al*, 1993). α,β -unsaturated compounds bind tightly to PETN reductase and can act as both substrates and inhibitors. Whether a steroid acts as a substrate or ligand is governed by the positioning of the unsaturated C-C bond with respect to the flavin N5 atom (Barna *et al*, 2001). NMR and mass spectrometry of products formed during the steady-state turnover of some steroids have established that PETN reductase selectively reduces an unsaturated bond positioned between the C1 and C2 carbon atoms of steroid substrates (Barna *et al*, 2001).

Therefore, 3-keto steroids such as prednisone and 1,4-androstadiene-3,17-dione, which contain an unsaturated bond between the C1 and C2 carbon atoms (Figure 4.1) are substrates for PETN reductase. Conversely, steroids containing an unsaturated bond between the C4 and C5 carbon atoms (but importantly not between the C1 and C2 atoms), such as progesterone and 4-androstene-3,17-dione (Figure 4.1) are potent inhibitors of PETN reductase.

Structures of oxidised PETN reductase in complex with a number of steroid compounds have been solved at high resolution (Figure 4.2; Barna *et al*, 2001). In all the solved structures, the steroids bind above the *si*-face of the flavin. The carbonyl oxygen of the steroid is hydrogen bonded with two active site histidine residues, His 181 and His 184. Analysis of co-crystal structures revealed only one mode of steroid binding in oxidised PETN reductase. Unexpectedly, the C4 and C5 carbon atoms of the steroid compounds are positioned above the flavin N5 atom, which is the site of hydride transfer. Although the C4,C5 double bonds of progesterone and 4-androstene-3,17-dione are optimally aligned for hydride transfer from the flavin N5 atom, these bonds are not reduced by the enzyme. Consequently, these steroids act as inhibitors of PETN reductase. The reducible C1,C2 double bond of prednisone and 1,4-androstadiene-3,17-dione on the other hand, are not positioned over the flavin N5 atom, in the oxidised enzyme-ligand complexes (Barna *et al*, 2001). This unfavourable positioning of the reducible C1,C2 bond led Barna *et al* (Barna *et al*, 2001) to suggest that the steroids must bind in an alternative conformation in the reduced form of the enzyme, so that the C1,C2 bond is located over the flavin N5 atom. For the reduced enzyme, the steroid must either move in a coplanar fashion over the flavin or “flip” 180° to realign the reducible bond so that it is in close proximity to the flavin N5 atom (Figure 4.2). Deuterium labelling studies and NMR analysis has indicated that in the reduced form of PETN reductase, steroid ligands bind in an orientation that is “flipped” by 180° compared to the orientation observed with oxidised enzyme. This mode of binding in reduced enzyme therefore positions the C1,C2 reducible bond of the steroid over the flavin N5 atom, thus facilitating hydride transfer (Barna *et al*, 2001). Similar alternative binding modes for steroids, influenced by the electronic state of the enzyme, have been observed with estrogen binding protein (EBP) from *Candida albicans* (Buckman and Miller, 1998). Estrogen binding protein catalyses the dismutation reaction of 19-nortestosterone, where the C1,C2 saturated bond of this compound is oxidised by the enzyme to form estradiol and reduced EBP. The reduced form of EBP subsequently reduces the C4,C5 double bond of estradiol. Further kinetic studies identified that 19-nortestosterone aligns in different orientations when the enzyme is in its oxidised and reduced forms (Buckman and Miller, 1998).

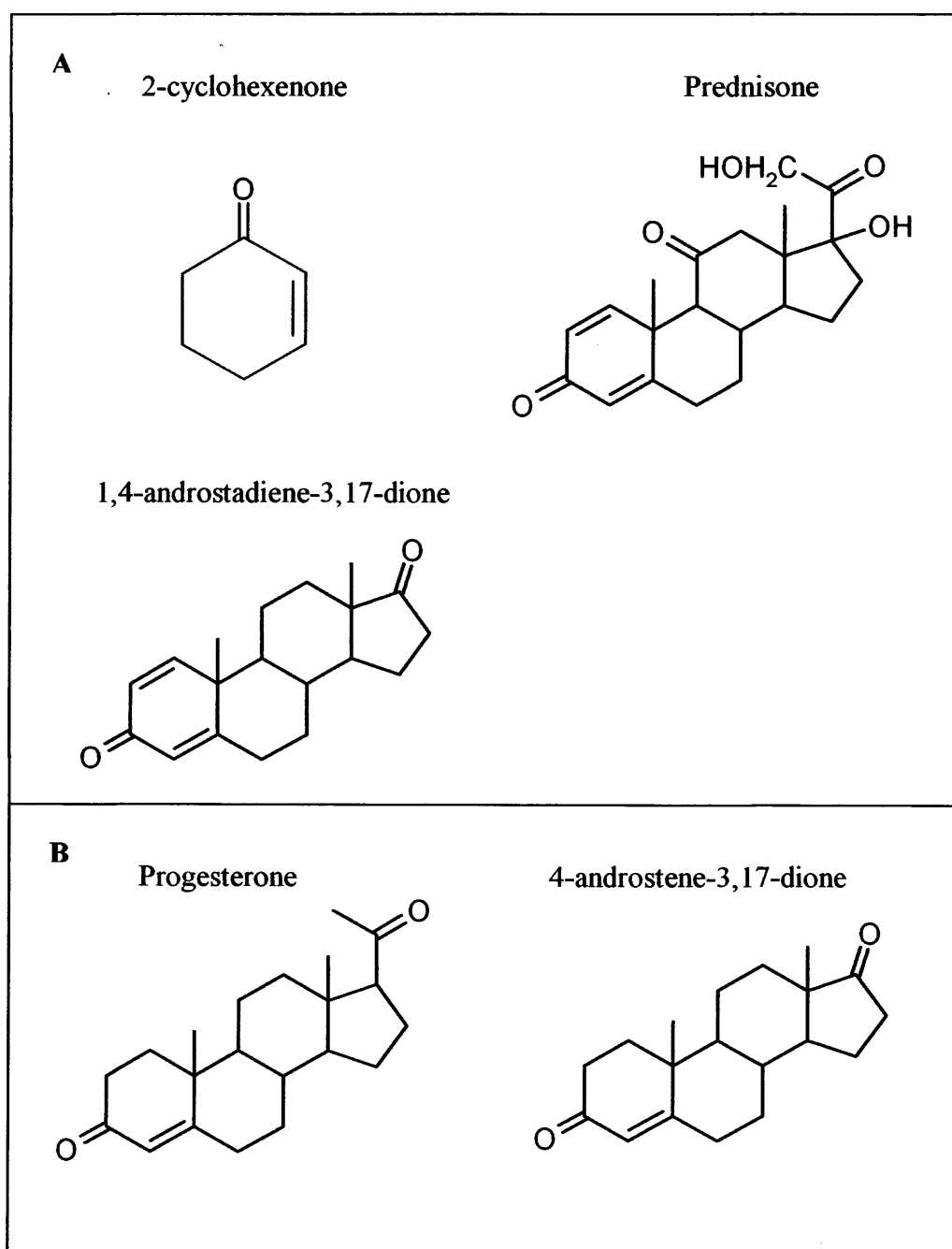


Figure 4.1. Structures of some of the α,β -unsaturated compounds that have been studied with PETN reductase. Panel A, structures of known substrates of PETN reductase. Panel B, structures of α,β -unsaturated steroids that are inhibitors of PETN reductase.

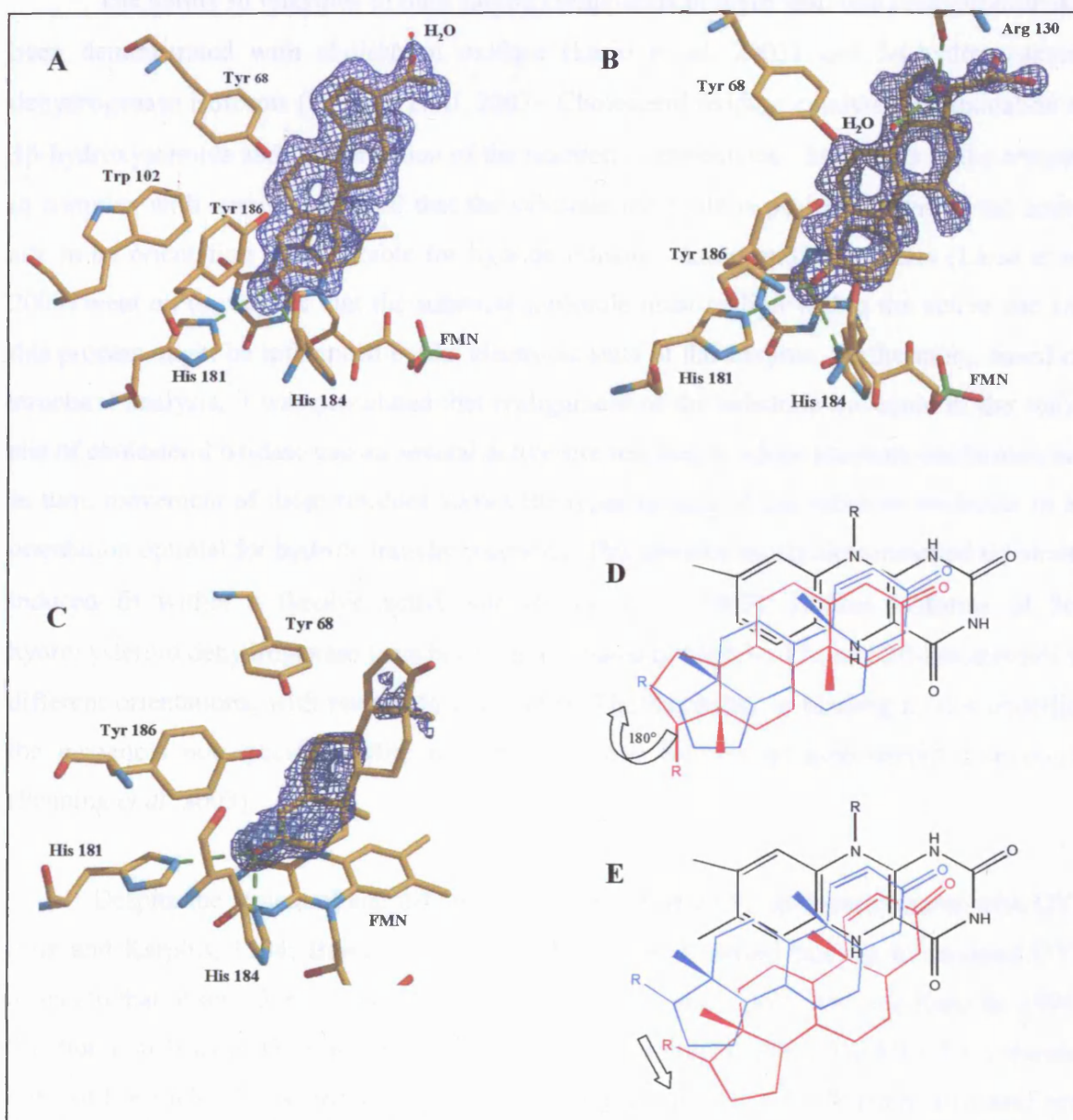


Figure 4.2. Difference electron density for steroid ligands in complex with oxidised PETN reductase and the geometry of the steroid substrate-flavin interaction in the different redox states of the enzyme Panel A, PETN reductase in complex with progesterone (inhibitor); Panel B, PETN reductase in complex with prednisone; Panel C, PETN reductase in complex with 1,4-androstadiene-3,17-dione; Panel D, the geometry of steroid binding in oxidised PETN reductase (steroid shown in light blue) and the “flipped” geometry proposed for the reduced enzyme complex (shown in red); Panel E, same as panel D except that a lateral movement of the steroid would lead to substrate realignment. (Figure abstracted from Barna *et al*, 2001).

The ability of enzymes to bind steroid compounds in more than one configuration has been demonstrated with cholesterol oxidase (Lario *et al*, 2003) and 3 α -hydroxysteroid dehydrogenase isoforms (Penning *et al*, 2003). Cholesterol oxidase catalyses the oxidation of 3 β -hydroxysteroids and isomerisation of the reaction intermediates. Structures of the enzyme in complex with steroids revealed that the substrate molecule is positioned within the active site in an orientation unfavourable for hydride transfer. Lario and co-workers (Lario *et al*, 2003) went on to propose that the substrate molecule must realign within the active site and this process might be influenced by the electronic state of the enzyme. Furthermore, based on structural analysis, it was postulated that realignment of the substrate molecule in the active site of cholesterol oxidase causes several active site residues to adopt alternate conformations. In turn, movement of these residues allows the repositioning of the substrate molecule in an orientation optimal for hydride transfer reactions. This enzyme nicely demonstrated substrate-induced fit within a flexible active site (Lario *et al*, 2003). Human isoforms of 3 α -hydroxysteroid dehydrogenase have been demonstrated to bind 3-, 17-, and 20-ketosteroids in different orientations, with respect to each other. The flexibility in binding modes underlies the enzyme's non-specific ability to reduce various isomers of keto-steroid compounds (Penning *et al*, 2003).

Despite the structural and catalytic similarities that PETN reductase shares with OYE (Fox and Karplus, 1994; Barna *et al*, 2001), the mode of steroid binding to oxidised OYE differs to that observed in oxidised PETN reductase (Vaz *et al*, 1995; Fox and Karplus, 1994). Structural analysis of OYE in complex with β -estradiol indicated that the C1,C2 unsaturated bond of β -estradiol is located above the flavin N5 atom and the C4, C5 atom is located near the N10 flavin atom (Vaz *et al*, 1995). Therefore, the steroids bound to oxidised PETN reductase are rotated by 180 $^{\circ}$, such that the opposite face of the steroid stacks above the *si* face of the flavin ring compared to the orientation of steroid binding in OYE (Figure 4.3).

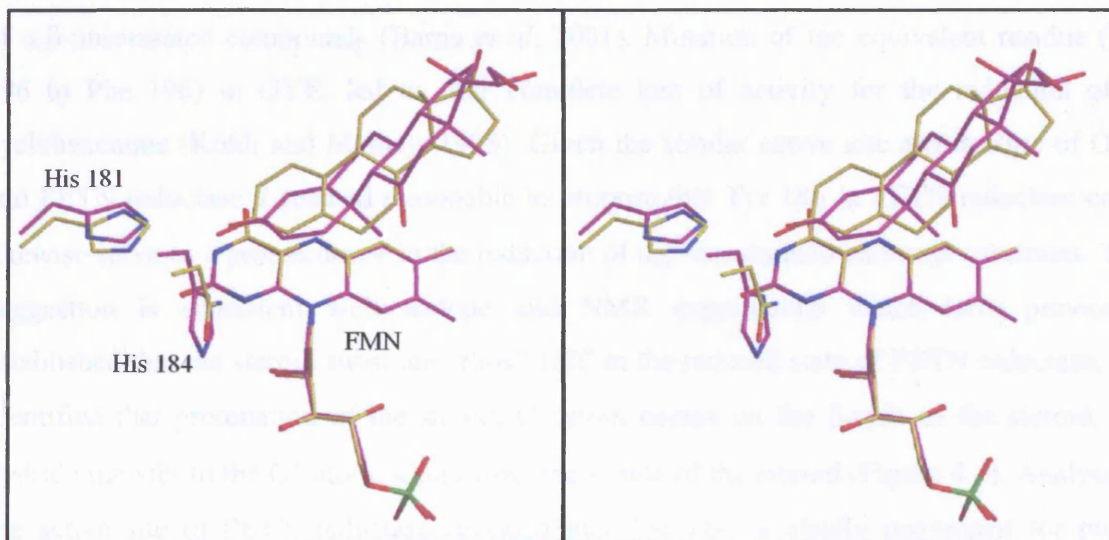


Figure 4.3. Stereo-view comparing the different modes of steroid binding in PETN reductase and OYE. The mode of steroid binding in PETN reductase is shown with the carbon atoms in magenta. The mode of β -estradiol binding to OYE is shown in yellow. The side chains of His 181 and His 184 from PETN reductase are shown along with His 191 and Asn 194 of OYE. (Figure taken from Barna *et al*, 2001).

4.1.2 Mechanism of reduction of α,β -unsaturated compounds: a search for the active site acid

Reduction of α,β -unsaturated compounds (e.g. 2-cyclohexenone and prednisone), proceeds by hydride transfer from the reduced flavin N5 atom to the partially positive C1 atom. Complete reduction of the double bond is achieved by the transfer of a proton to the C2 atom. Based on recent mutagenesis studies with OYE (Kohli and Massey, 1998), it was hypothesised that Tyr 186 of PETN reductase functions as the proton donor in the reduction of α,β -unsaturated compounds (Barna *et al*, 2001). Mutation of the equivalent residue (Tyr 196 to Phe 196) in OYE, led to near complete loss of activity for the reduction of 2-cyclohexenone (Kohli and Massey, 1998). Given the similar active site architecture of OYE and PETN reductase it seemed reasonable to propose that Tyr 186 in PETN reductase could likewise serve as a proton donor in the reduction of α,β -unsaturated carbonyl substrates. This suggestion is consistent with isotope and NMR experiments which have previously established that the steroid substrate “flips” 180° in the reduced state of PETN reductase, and identified that protonation of the steroid C2 atom occurs on the β -side of the steroid, and hydride transfer to the C1 atom occurs from the α -side of the steroid (Figure 4.4). Analysis of the active site of PETN reductase revealed that Tyr 186 is ideally positioned for proton donation to the β -side of the steroid C2 position, following substrate realignment and hydride transfer (Figure 4.4).

2-cyclohexenone is a α,β -unsaturated carbonyl compound and a substrate for PETN reductase and other members of the OYE family. This compound is often used as a generic substrate in studies with the OYE family of enzymes (Williams *et al*, 1999). Reduction of 2-cyclohexenone to cyclohexanone (see Chapter One for a detailed account on OYE mediated cyclohexenone reduction) has been used to identify members belonging to the NAD(P)H-dependent flavin oxidoreductase family of enzymes (Rohde *et al*, 1999). Close relatives to PETN reductase and OYE which also show reactivity with 2-cyclohexenone include: morphinone reductase (MR; French and Bruce, 1994a), estrogen binding protein (EBP; Buckman *et al*, 1996), multiple 12-oxophytodienoate (OPDA) reductase isozymes from *Arabidopsis thaliana* (Schaller and Weiler, 1997a and 1997b; Costa *et al*, 2000; Breithaupt *et al*, 2001) and tomato (Strabner *et al*, 1999) and NAD(P)H-dependent 2-cyclohexenone reductase from *Pseudomonas syringae* pv *glycinea* (Rhode *et al*, 1999).

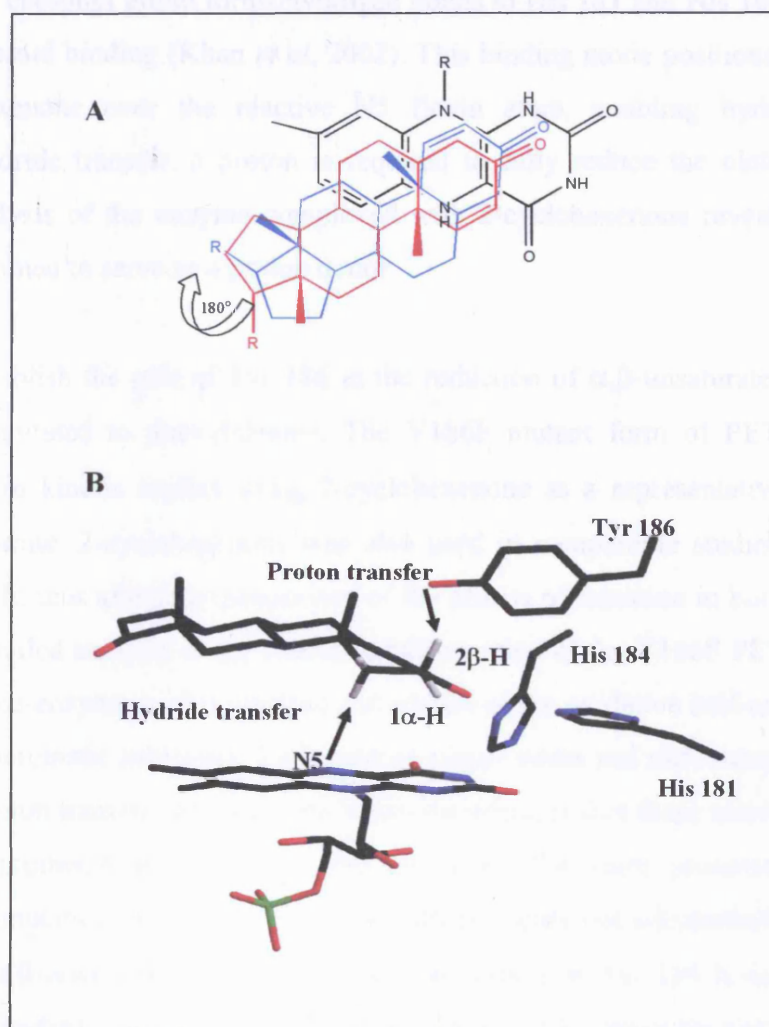


Figure 4.4. Scheme illustrating the orientation and location of the steroid over the flavin isoalloxazine ring and the direction of hydride ion transfer (from flavin N5) and proton transfer (from Tyr 186). Panel A, the geometry of the steroid substrate-flavin interaction in oxidised PETN reductase (steroid shown in light blue) and the “flipped” geometry proposed for the reduced enzyme complex (shown in red). Panel B, scheme illustrating the location of the steroid product 4-androstene-3,17-dione over the flavin. The steroid is shown in the flipped orientation to that seen in the oxidised enzyme-steroid substrate complex. The transfer of the hydride ion from flavin N5 is to the 1 α position of the steroid and proton transfer is to the steroid's 2 β position, with Tyr 186 ideally positioned for this role. (Figure taken from Barna *et al*, 2001).

The structure of PETN reductase in complex with 2-cyclohexenone has been determined (Figure 4.5; Khan *et al*, 2002). 2-cyclohexenone binds above the *si* face of the flavin and the carbonyl group forms hydrogen bonds to His 181 and His 184 in the active site as seen for steroid binding (Khan *et al*, 2002). This binding mode positions the olefinic bond of 2-cyclohexenone over the reactive N5 flavin atom, enabling hydride ion transfer. Following hydride transfer, a proton is required to fully reduce the olefinic bond. Again, structural analysis of the enzyme complexed with 2-cyclohexenone reveals that Tyr 186 is suitably positioned to serve as a proton donor.

To establish the role of Tyr 186 in the reduction of α,β -unsaturated compounds, the residue was mutated to phenylalanine. The Y186F mutant form of PETN reductase was characterised in kinetic studies using 2-cyclohexenone as a representative α,β -unsaturated carbonyl substrate. 2-cyclohexenone was also used in comparable studies with the Y196F mutant of OYE, thus allowing comparison of the effects of mutation in both OYE and PETN reductase. Detailed analysis of the reductive half-reaction of the Y186F PETN reductase with nicotinamide co-enzyme is also reported and studies of the oxidative half-reaction with nitrate ester and nitroaromatic substrates. Reduction of nitrate esters and nitroaromatic substrate does not require proton transfer, and the expectation therefore, is that these activities should not be severely compromised as a result of the mutation. The work presented in this chapter indicates that mutation of Tyr 186 in PETN reductase does not substantially compromise the reduction of α,β -unsaturated substrates, thus indicating that Tyr 186 is not a critical proton donor in the oxidative half-reaction. The implication of this result for the mechanism of the oxidative half-reaction in PETN reductase and OYE are discussed.

4.2 Construction and purification of the Y186F mutant of PETN reductase

4.2.1 Mutation of Tyr 186 to Phe 186 in PETN reductase

Mutation of Tyr 186 to Phe 186 in PETN reductase was performed using the QuikChange site-directed mutagenesis kit from Stratagene as described in Section 2.2.3. The pONR1 plasmid carrying the mutated *onr* gene was transformed into *E. coli* strain JM109 cells. To ensure (i) the successful incorporation of the Tyr 186 to Phe 186 mutation and (ii)

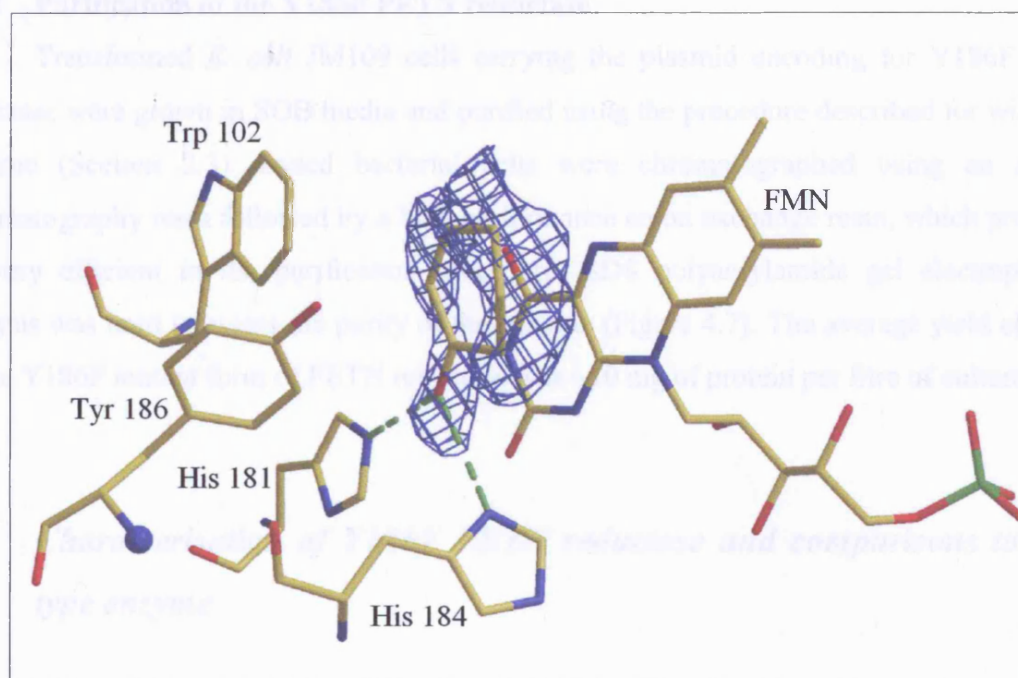


Figure 4.5. Difference electron density for PETN reductase in complex with 2-cyclohexenone. 2-cyclohexenone is observed to bind in the active site of PETN reductase by hydrogen bonding through its carbonyl oxygen to His 181 and His 184. The C1 atom of the substrate is ideally positioned above the N5 flavin atom so as to receive a hydride ion, and Tyr 186 is ideally located near the substrate C2 atom so as to donate a proton, leading to complete reduction of the substrates olefinic bond. (Figure abstracted from Khan *et al*, 2002).

that further mutations in the gene were not introduced, the entire mutated *onr* gene was sequenced (Figure 4.6).

4.2.2 Purification of the Y186F PETN reductase

Transformed *E. coli* JM109 cells carrying the plasmid encoding for Y186F PETN reductase were grown in SOB media and purified using the procedure described for wild-type enzyme (Section 2.3). Lysed bacterial cells were chromatographed using an affinity chromatography resin followed by a high performance anion exchange resin, which proved to be very efficient in the purification procedure. SDS polyacrylamide gel electrophoretic analysis was used to assess the purity of the enzyme (Figure 4.7). The average yield obtained of the Y186F mutant form of PETN reductase was ~10 mg of protein per litre of culture.

4.3 Characterisation of Y186F PETN reductase and comparisons to wild-type enzyme

4.3.1 Ligand binding studies

Equilibrium binding measurements were performed, as described in Section 2.5, so that the dissociation constants (K_d) for various oxidised enzyme-ligand complexes could be determined. These studies would ensure that the active site of the Y186F PETN reductase had not been grossly perturbed as a consequence of the mutation made. Titrations were performed with picric acid, 2,4-DNP and progesterone. Titrations with TNT were not investigated, as previous studies with wild-type enzyme (and Trp 102 mutant enzymes; Chapter 3) have shown that titrations with this ligand do not produce any spectral changes. Spectral changes accompanying the titrations and the associated isosbestic points (Figure 4.8) reveal that ligand binding to Y186F PETN reductase is a simple equilibrium process. However, upon the addition of high ligand concentrations, the isosbestic points become less defined. Therefore, spectra taken following the disruption of the isosbestic points were not analysed further. Absorption changes at 518 nm for each titration were plotted as a function of ligand concentration and data were fitted to a quadratic function (Equation 3.1; Figure 4.9) using ORIGIN 4.0 software. From the fits of the data the K_d for picric acid, 2,4-DNP and progesterone binding were determined as 10.8 μM , 1.87 μM and 0.05 μM , respectively. The

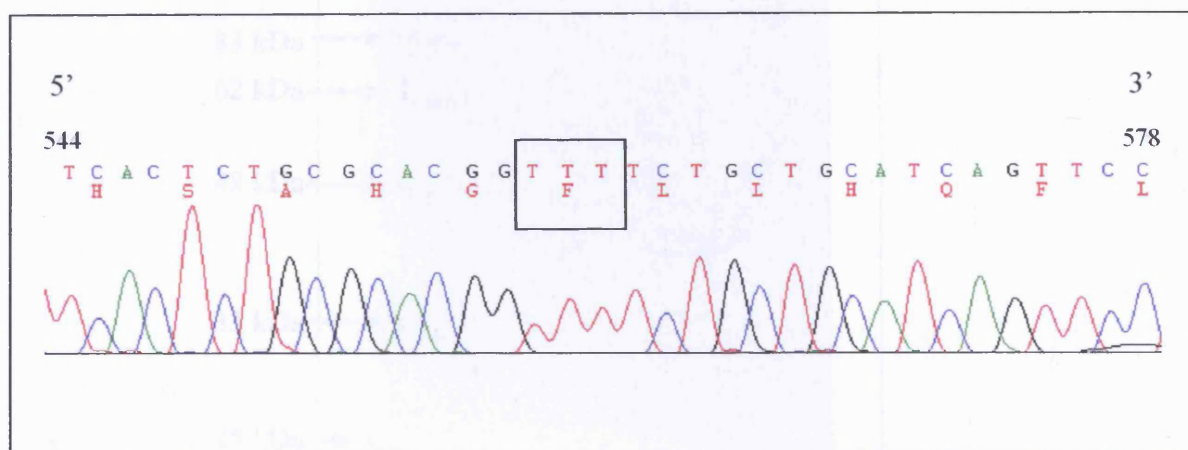


Figure 4.6. Gene sequence for the area encoding the mutation of Tyr 186 to Phe 186 in the Y186F mutant form of PETN reductase. The bases within the boxed area show the bases that were mutated to encode for phenylalanine at amino acid position 186. The corresponding base sequence in wild-type enzyme at amino acid position 186 is TAC.

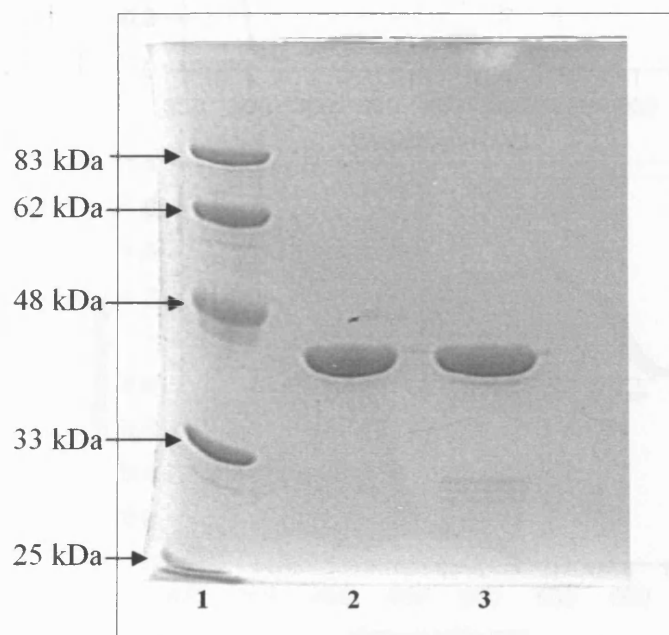


Figure 4.7. SDS PAGE analysis of the Y186F mutant form of PETN reductase. Lane 1, molecular weight marker; Lane 2, purified wild-type PETN reductase; Lane 3, purified Y186F PETN reductase.

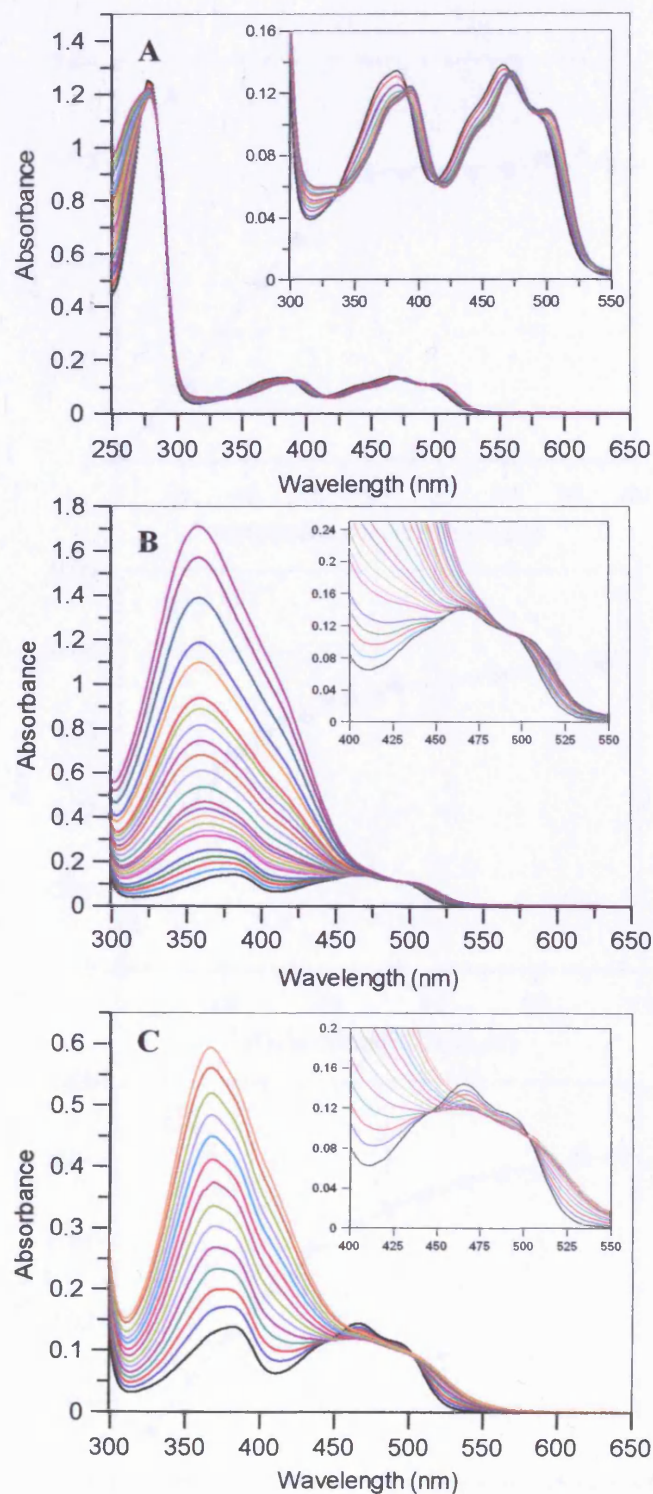


Figure 4.8. Spectra obtained during ligand-binding studies of Y186F PETN reductase. Spectral changes produced during the titration of oxidised Y186F PETN reductase ($\sim 10 \mu\text{M}$) with a known stock concentration of progesterone (panel A), picric acid (panel B) and 2,4-DNP (panel C). The starting spectrum (free enzyme) is shown in black in each titration. Insets to the panels show the isosbestic points at 336 nm, 390 nm, 415 nm and 470 nm in panel A; 494 nm in panel B; and 504 nm in panel C.

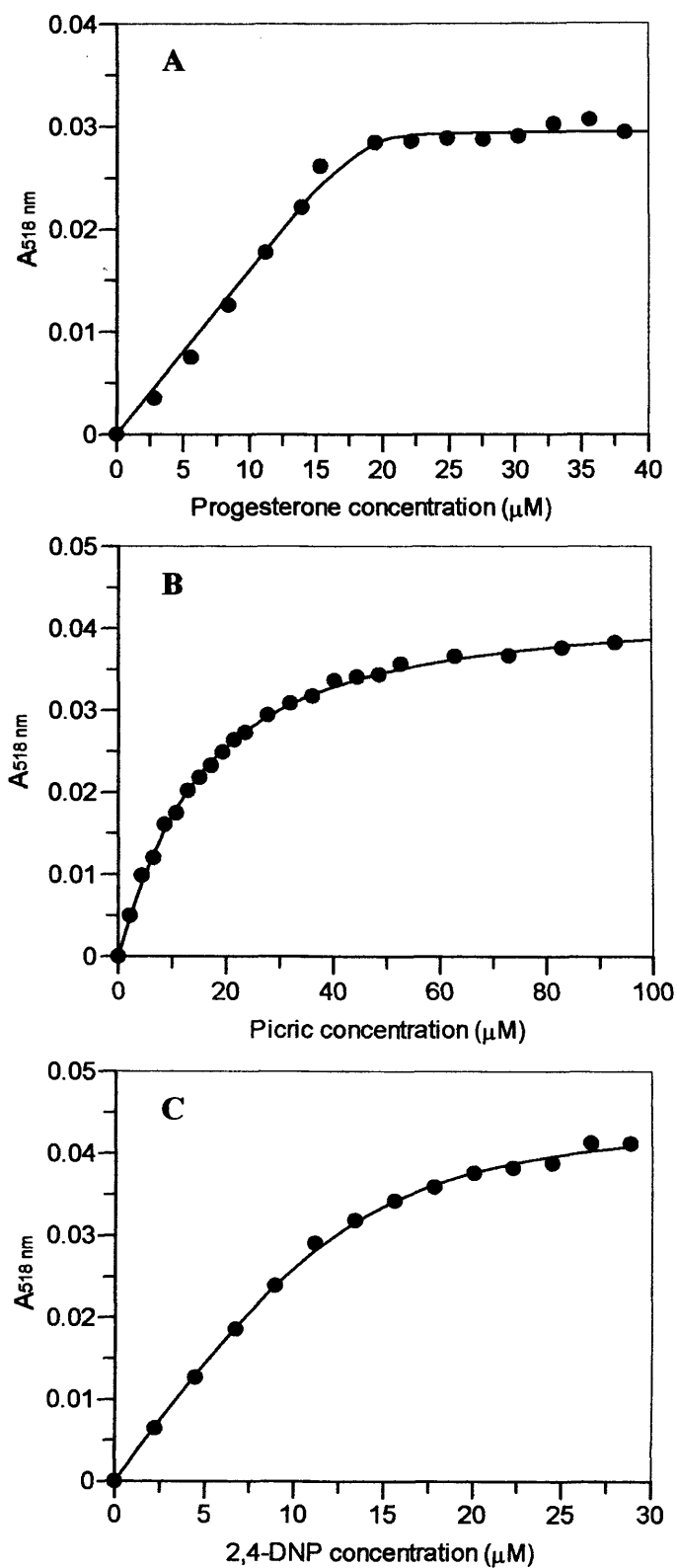


Figure 4.9. Ligand binding titration curves. Each panel shows the binding curve for progesterone (Panel A), picric acid (Panel B) and 2,4-DNP (Panel C), with the oxidised Y186F mutant form of PETN reductase ($\sim 10 \mu\text{M}$). The solid line shows the fit of the data to Equation 3.1.

calculated dissociation constants for Y186F and wild-type enzyme with each ligand are summarised in Table 4.1. Analysis of the dissociation constants reveals a two-fold increase in the K_d value for Y186F PETN reductase with picric acid and 2,4-DNP compared to wild-type enzyme, indicating that the mutant enzyme binds these ligand less tightly than the wild-type. The value obtained for the progesterone-enzyme complex, remains largely unaffected by the mutation of Tyr 186 in PETN reductase. These results indicate that Tyr 186 might have a minor influence on the binding of nitroaromatic compounds, but not on steroid binding.

4.3.2 Single wavelength stopped-flow studies of the reductive half-reaction

Stopped-flow studies on the reductive half-reaction of Y186F PETN reductase were performed (using conditions described in Section 2.6) to assess whether Tyr 186 has any influence in the kinetics and binding of NADPH. Absorption changes monitored at 560 nm were used to measure the rate of formation of the charge-transfer intermediate that forms prior to hydride transfer (see Section 3.3). To measure the rate of hydride transfer, absorption changes were monitored at 464 nm. Measurements were made by mixing oxidised enzyme (20 μM for absorption changes measured at 464 nm and 40 μM for measurements made at 560 nm), with a range of NADPH concentrations, at 5 °C. Averages of three to four reproducible transients were acquired to calculate rates (k_{obs}).

The mixing of Y186F PETN reductase with NADPH brought a decrease in flavin absorbance at 464 nm, similar to wild-type enzyme (Chapter 3; Figure 4.10A). These transients were best fitted to a single exponential expression (Equation 2.2), from which observed rates were determined. The observed rates were subsequently analysed for NADPH concentration dependence using Grafit 5.0 software (Figure 4.11B). The rates of hydride transfer are revealed to be independent of NADPH concentration. However, it is possible that at lower NADPH concentrations the rates exhibit hyperbolic dependency on NADPH concentration and therefore the rates measured here are in the k_{lim} region. Fitting of the observed rates to a linear function determined the value for k_2 (rate of hydride transfer) as $3.90 \text{ s}^{-1} \pm 0.04 \text{ s}^{-1}$, compared to a value of 12 s^{-1} for wild-type enzyme (Section 3.2.3). The rate of Y186F PETN reductase reduction by NADPH is therefore 3-fold slower than the wild-type enzyme.

Absorption changes measured at 560 nm produced a rapid increase in absorbance followed by a slower absorbance decrease, corresponding to the formation and decay of the

	Dissociation constant (K_d , μM)	
	Y186F PETN reductase	Wild-type PETN reductase
Picric acid	10.8 ± 1.0	5.4 ± 1.1
2,4-DNP	1.87 ± 0.47	0.95 ± 0.13
Progesterone	0.05 ± 0.09	0.07 ± 0.03

Table 4.1. Calculated dissociation constants for ligand complexes of wild type and Y186F PETN reductase. Enzymes (each 10 μM) were each titrated with picric acid, progesterone and 2,4-DNP in 50 mM potassium phosphate buffer, pH 7.0, in a 1 ml quartz cuvette. Spectra were recorded after the addition of ligand to the enzyme. From the resultant spectra (see Figure 4.8) the absorption changes at 518 nm were plotted as a function of ligand concentration and fitted to a quadratic function (see Figure 4.9), from which the dissociation constants were determined. Data for wild-type enzyme are taken from Section 3.2.2.

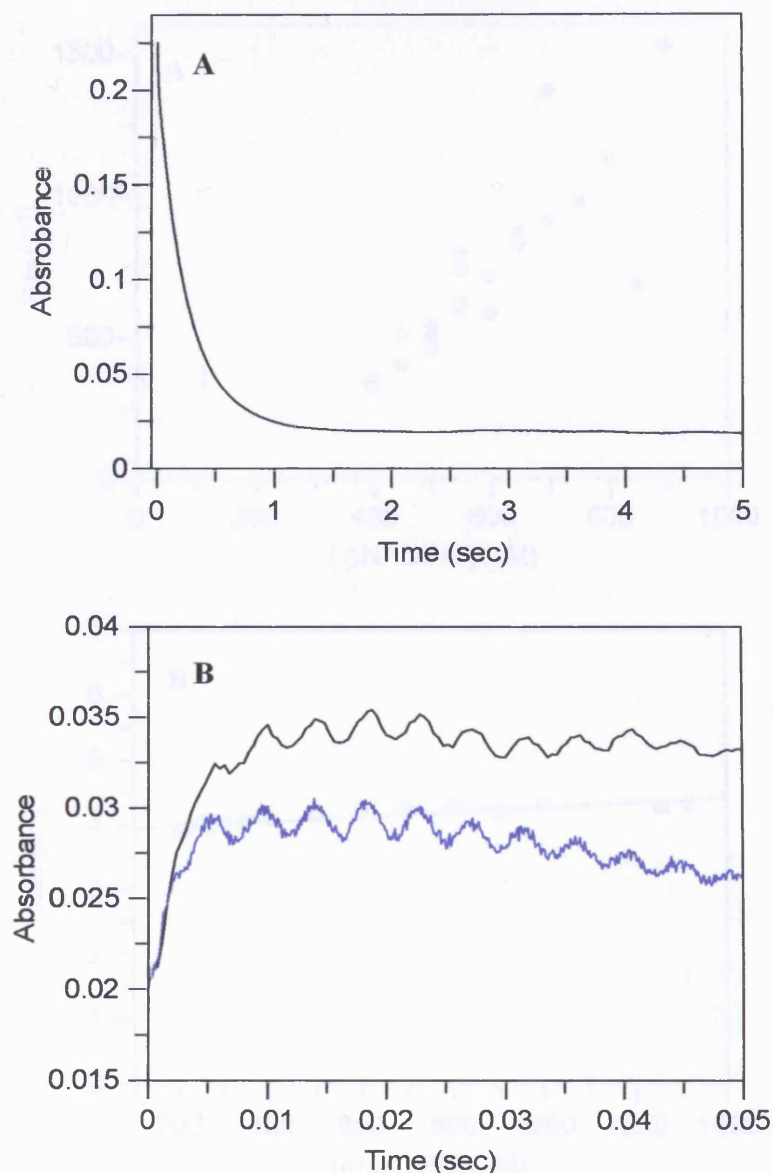


Figure 4.10. Typical stopped-flow transients obtained for the reductive half-reaction of **Y186F PETN reductase**. Panel A, transient obtained when measuring absorption changes associated with flavin reduction, at 464 nm. Measurements were made by mixing NADPH (200 μM) with Y186F PETN reductase (20 μM) in potassium phosphate buffer, pH 7.0, at 5 $^{\circ}\text{C}$. Panel B, transient obtained when measuring absorption changes at 560 nm. The figure shows the small absorbance changes for formation of the charge-transfer complex (followed by its decay - full time scale not shown). Measurements were made by mixing NADPH (400 μM , black line; 800 μM , blue line) with Y186F PETN reductase (40 μM) in potassium phosphate buffer, pH 7.0, at 5 $^{\circ}\text{C}$.

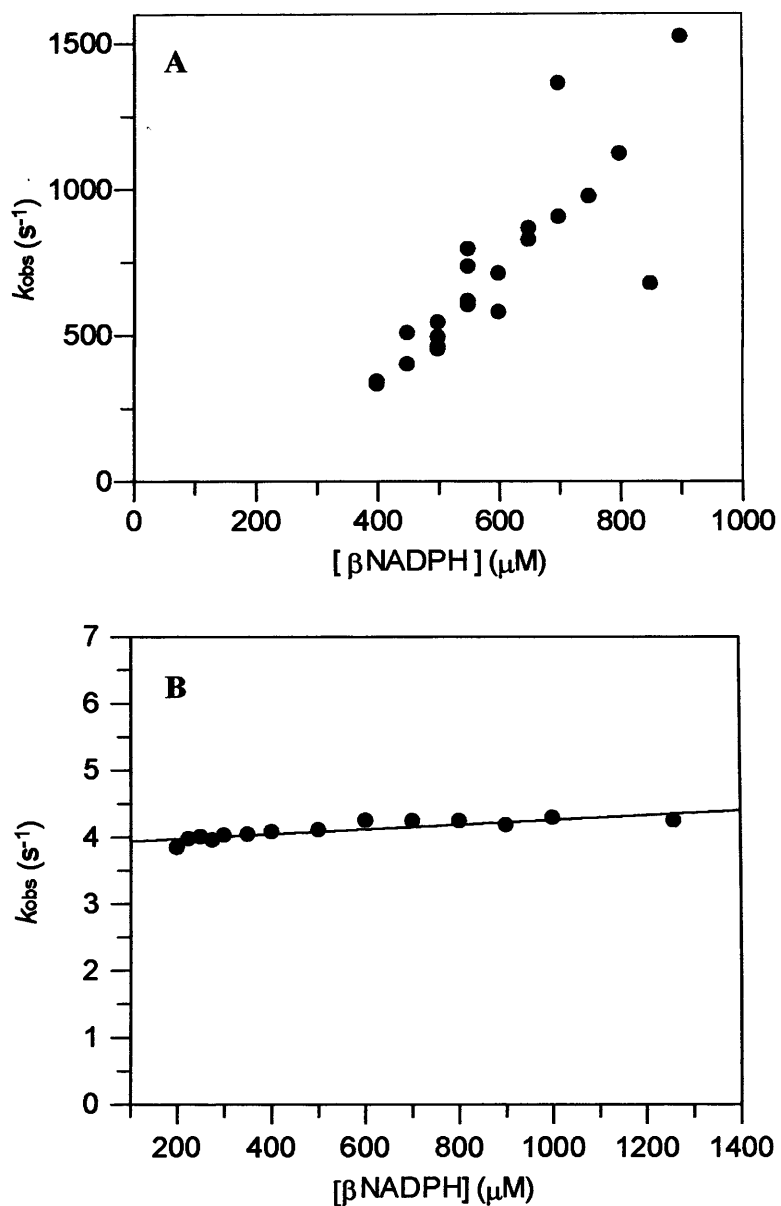


Figure 4.11. Concentration-dependence plots for the rate of charge-transfer formation and hydride transfer, in the reductive half-reaction of Y186F PETN reductase. Panel A, rate of formation of the charge-transfer intermediate (560 nm data); Panel B, rate of hydride transfer from NADPH to the flavin (464 nm data). Measurements were made using $\sim 20 \mu$ M of enzyme for the 464 nm data and $\sim 40 \mu$ M enzyme for the 560 nm data, in potassium phosphate buffer pH 7.0 at 5 °C.

charge-transfer complex, respectively (Figure 4.10B). Measurements at 560 nm were performed using an optimised 2 μl flow cell, with a dead time of 500 μs , fitted within the stopped-flow apparatus, allowing for faster rates to be measured. However, despite this, the rate of absorbance increase corresponding to charge-transfer formation was still too fast to be measured accurately. Consequently, transients measured at each NADPH concentration showed low reproducibility of the up-phase, hence, the observed rates were unreliable. The low validity of the data collected (once the transients were fit to Equation 2.3) can be seen in Figure 4.11A, where it is perceived that fitting of the data to a linear function would predict a negative value for k_{-1} (determined by the intercept), which is incorrect. Thus, the kinetic rate constants associated with the formation of the charge-transfer intermediate could not be determined.

Fits to the down phase of the 560 nm transients (to Equation 2.3) produced rates which were equal to the rates measured at 464 nm, indicating that the decay of the charge-transfer complex is a directly related to hydride transfer.

4.3.3 Multiple wavelength stopped-flow studies of the oxidative half-reaction with TNT

To ensure that Tyr 186 has no significant influence on the transformation of TNT, the single turnover of this substrate was followed using anaerobic stopped-flow photodiode array (PDA) spectroscopy, as described in Section 2.9.2. Measurements were made using 40 μM of sodium dithionite-reduced Y186F PETN reductase mixed with 10 times excess TNT. Spectral changes associated with enzyme re-oxidation were analysed by global analysis and numerical integration methods, using PROKIN software. As with wild-type enzyme, data fitted best to a three state-model: $A \rightarrow B \rightarrow C$, where A is dithionite-reduced enzyme, B is a mixture of re-oxidised enzyme and the TNT hydride-Meisenheimer complex and C is oxidised enzyme. Spectral changes associated with the reaction (Figure 4.12) indicate that TNT is reduced to the respective hydride-Meisenheimer complex. This is evident from the enhanced absorbance observed at 464 nm and 580 nm which corresponds to that for the hydride-Meisenheimer complex (see Figure 3.10 for the published spectrum of the complex), in addition to that associated with oxidised enzyme. Further analysis reveals that the complex decays in time, leaving the end spectrum corresponding to that for oxidised enzyme alone (Figure 4.12B). From the PDA data, the rate of hydride-Meisenheimer formation and decay was determined as 3.84 s^{-1} ($\pm 0.07 \text{ s}^{-1}$) and $3.6 (\pm 0.1) \times 10^{-3} \text{ s}^{-1}$, respectively. The rate of complex

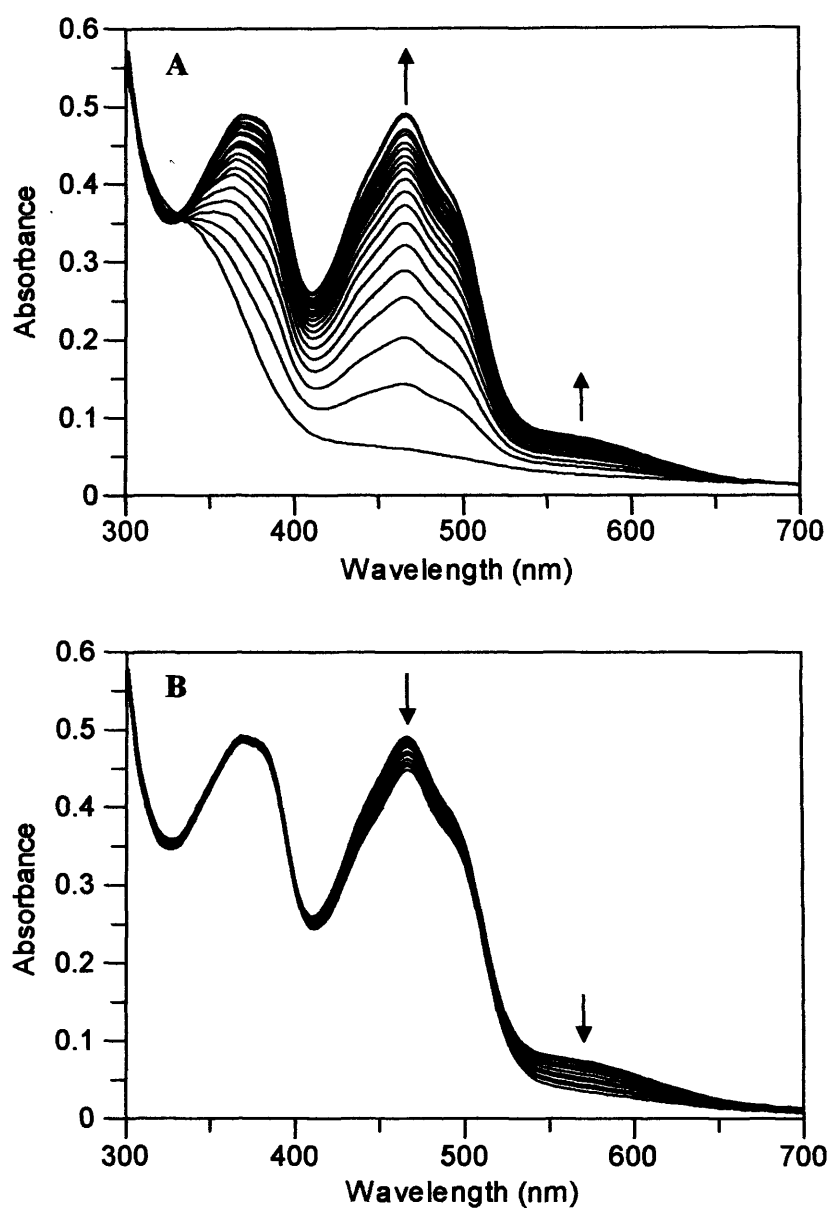


Figure 4.12. Time-dependent spectral changes associated with the reaction between dithionite-reduced Y186F PETN reductase and TNT, using stopped-flow spectroscopy. Dithionite-reduced Y186F PETN reductase (40 μM) was mixed with (400 μM) TNT at 25 $^{\circ}\text{C}$, in 1% acetone, potassium phosphate buffer, pH 7.0, under anaerobic conditions. Spectra were recorded on a log timescale for 500 s. Panel A: spectral changes over 2 s from the mixing event, showing re-oxidation of the flavin and the formation of the hydride-Meisenheimer complex of TNT. Panel B: spectral changes for data acquisition in the 2-500 s time domain after mixing, showing the degradation of the hydride-Meisenheimer complex with the end spectrum corresponding to that of oxidized enzyme alone.

formation is equivalent to the rate of flavin re-oxidation when measured at the same TNT concentration (see Section 4.3.5), indicating both processes are directly related. The rate of hydride-Meisenheimer decay (and formation) in Y186F PETN reductase is similar to the rate measured with wild-type enzyme ($5.3 \times 10^{-3} \text{ s}^{-1}$; Section 3.2.10). Hence Tyr 186 has no significant influence on hydride-Meisenheimer formation or on the complex's stability.

4.3.4 Single wavelength stopped-flow studies of the oxidative half-reaction with 2-cyclohexenone

Tyr 186 is hypothesised to act as the active site acid in the reduction of α/β -unsaturated compounds. Mutation of the equivalent residue in OYE, Tyr 196, produced an enzyme which showed almost complete loss of activity with 2-cyclohexenone (Kohli and Massey, 1998). Hence, to ascertain whether Tyr 186 functions as the proton donor in PETN reductase, the rate of 2-cyclohexenone reduction by Y186F PETN reductase was measured and compared to wild-type enzyme. Studies were performed by mixing 20 μM of dithionite-reduced Y186F PETN reductase with a range of 2-cyclohexenone concentrations, using anaerobic single wavelength stopped-flow spectroscopy (as described in Section 2.9.1). Absorption changes associated with 2-cyclohexenone mediated flavin re-oxidation were measured at 464 nm. Transients (averaged from three to four reproducible transients) were best fitted to a double exponential process (Equation 3.5) and the phase with the largest absorbance change was used to determine k_{obs} . Observed rates were plotted as a function of 2-cyclohexenone concentration and data were fitted to a hyperbolic expression using GRAFIT 5.0 software (Figure 4.13). Fitting of the data produced a k_{lim} value of $13.9 \pm 0.4 \text{ s}^{-1}$ and the K_{d} was determined as $2.07 \text{ mM} \pm 0.24 \text{ mM}$ (Table 4.2). When compared to the k_{lim} determined for wild-type enzyme (33.3 s^{-1} ; Section 3.2.11), it is revealed that Y186F PETN reductase catalyses the reduction of 2-cyclohexenone approximately 2-fold slower than wild-type PETN reductase. A 4-fold decrease in the K_{d} value for Y186F PETN reductase is revealed in comparison to that for wild-type enzyme (Table 4.2), indicating that the mutant enzyme binds the substrate tighter. These findings indicate that Tyr 186 is not the active site acid of PETN reductase, as the Y186F mutant enzyme is still able to reduce 2-cyclohexenone at an appreciable rate.

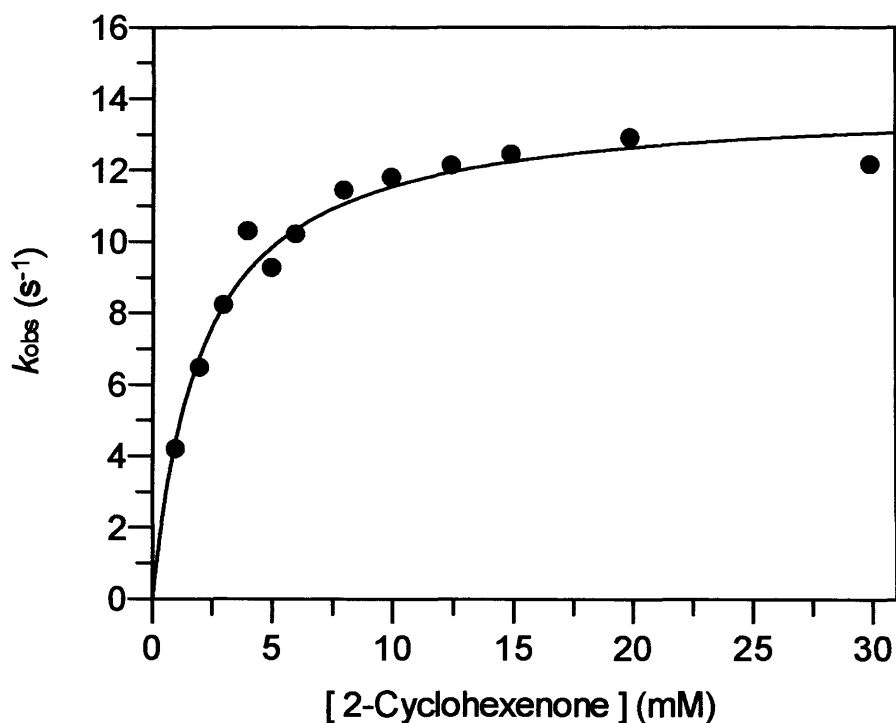


Figure 4.13. The concentration-dependence of the rate of hydride transfer from dithionite-reduced Y186F PETN reductase to 2-cyclohexenone. Anaerobic single wavelength spectroscopy at 464 nm was performed with 20 μ M enzyme and a range of 2-cyclohexenone concentrations, in 50 mM potassium phosphate buffer, pH 7.0 at 25 °C. The solid line shows the fit of the data to a hyperbolic function.

	2-Cyclohexenone		TNT		GTN	
	$k_{lim} (s^{-1})$	$K_d (mM)$	$k_{lim} (s^{-1})$	$K_d (mM)$	$k_{lim} (s^{-1})$	$K_d (mM)$
Wild-type PETN reductase	34.7 ± 2.2	9.6 ± 1.6	4.5 ± 0.1	0.08 ± 0.01	313 ± 48	0.72 ± 0.19
Y186F PETN reductase	13.9 ± 0.4	2.1 ± 0.2	6.9 ± 0.3	0.16 ± 0.02	72.3 ± 3.4	0.30 ± 0.04

Table 4.2. Rate constants determined for the oxidative half-reaction of wild-type and Y186F PETN reductase with a range of substrates. (Data for wild-type PETN reductase are taken from Table 3.3)

4.3.5 Single wavelength stopped-flow studies of the oxidative half-reaction with TNT and GTN

Previous multiple wavelength studies (Section 4.3.3) have shown that the Y186F PETN reductase still possesses the ability to transform TNT to the hydride-Meisenheimer complex. To determine whether the kinetics of TNT reduction are affected by the mutation of Tyr 186, the pre-steady state rate constant for the single turnover of TNT was determined. Experiments were performed using single wavelength stopped-flow spectroscopy under anaerobic conditions, at 25 °C (Section 2.9.1). Absorption changes associated with the mixing of dithionite-reduced Y186F PETN reductase (5 μM) with a range of TNT concentrations were measured at 464 nm. Transients following enzyme re-oxidation fitted best to a single exponential process (Equation 2.2), allowing calculation of k_{obs} . Observed rates exhibited hyperbolic dependency on TNT concentration and data were fitted to a hyperbolic function using GRAFIT 5.0 software (Figure 4.14). From the fits to the data a value of $6.89 \text{ s}^{-1} \pm 0.29 \text{ s}^{-1}$ was determined for k_{lim} and the K_{d} was calculated as $164 \mu\text{M} \pm 24 \mu\text{M}$ with Y186F PETN reductase. The kinetic constants for TNT reduction by Y186F and wild-type PETN reductase are summarised in Table 4.2. Comparison of the data (Table 4.2) reveals that the wild-type PETN reductase binds TNT tighter (2-fold) than the mutant enzyme, indicating that Tyr 186 has a small influence on nitroaromatic binding. In addition, Y186F PETN reductase is observed to catalyse the rate of TNT reduction at a slightly higher rate than the wild-type enzyme.

The pre-steady-state rate constants for GTN reduction were also determined for Y186F PETN reductase, to assess whether Tyr 186 has any influence on this reaction. Experiments were performed by mixing 5 μM of dithionite-reduced enzyme with a range of GTN concentrations, using anaerobic single wavelength stopped-flow spectroscopy at 5 °C (see Section 2.9.1 for details). Absorption changes at 464 nm followed enzyme re-oxidation. Transients fitted best to a double exponential expression (Equation 3.5) and observed rates were plotted as function of GTN concentration (Figure 4.15). Data were then fitted to a hyperbolic expression using GRAFIT 5.0 software, from which a K_{d} of $300 \mu\text{M} \pm 37 \mu\text{M}$ and a k_{lim} of $72.3 \text{ s}^{-1} \pm 3.4 \text{ s}^{-1}$ was determined (Table 4.2). Data comparison to the wild-type enzyme (Table 4.2) reveals that Y186F PETN reductase binds GTN approximately 2-fold tighter and reduces the substrate four-times slower than wild-type PETN reductase.

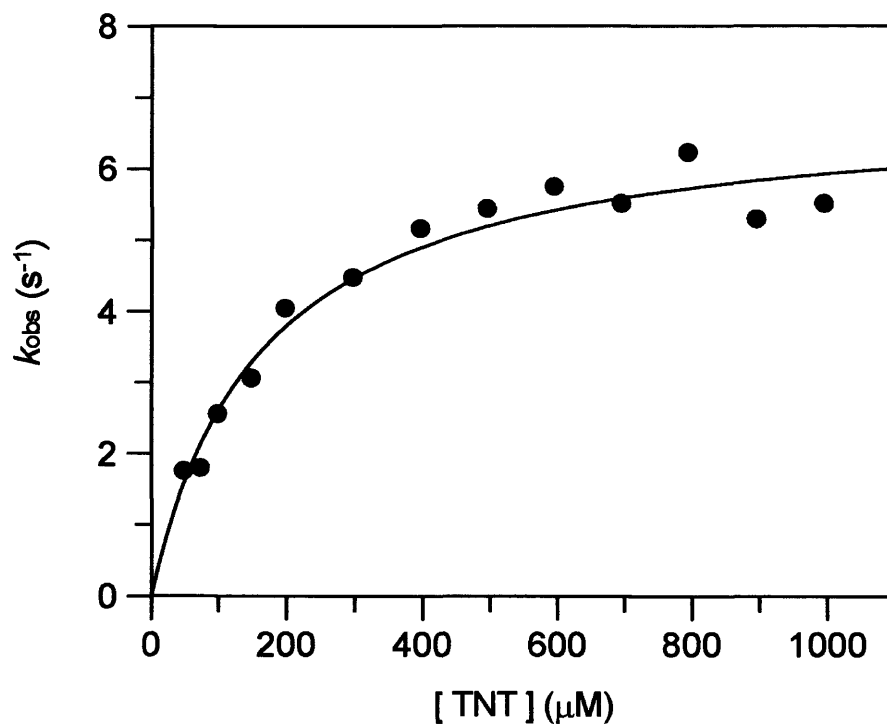


Figure 4.14. The concentration-dependence of the rate of hydride transfer from dithionite-reduced Y186F PETN reductase to TNT. Anaerobic single wavelength spectroscopy at 464 nm was performed with 5 μM enzyme and a range of TNT concentrations (with a limit of 1 mM), in 50 mM potassium phosphate buffer, pH 7.0, 1% acetone, at 25 $^{\circ}\text{C}$. The solid line shows the fit of the data to a hyperbolic function.

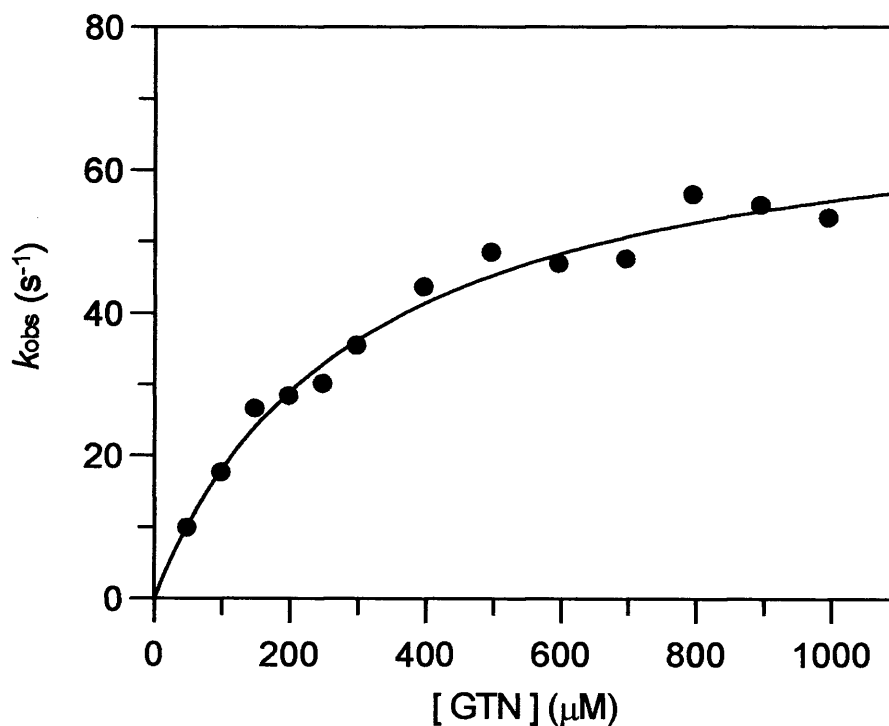


Figure 4.15. The concentration-dependence of the rate of hydride transfer from dithionite-reduced Y186F PETN reductase to GTN. Anaerobic single wavelength spectroscopy at 464 nm was performed with 5 μM enzyme and a range of GTN concentrations (with a limit of 1 mM), in 50 mM potassium phosphate buffer, pH 7.0 at 5 °C, 1 % acetone. The solid line shows the fit of the data to a hyperbolic function.

4.3.6 Anaerobic redox potentiometry

To ensure that the flavin environment and hence, the thermodynamic properties of the flavin had not been perturbed by the mutation made in Y186F PETN reductase, the midpoint potential for the mutant enzyme was determined and compared to the measured potential for wild-type enzyme.

Potentiometric studies were conducted by measuring the potential and absorption spectrum of ~40 μ M enzyme upon the titrative addition of sodium dithionite, in the presence of electron mediators (see Section 2.10 for details). This was done until the enzyme had undergone complete reduction. The absorbance and potential of the enzyme solution was also measured during the oxidative titration with potassium ferricyanide, to ensure that the potential measured during enzyme re-oxidation matched that measured during the reduction process (only the potential and absorbance values measured during enzyme reduction were analysed further). During enzyme reduction or re-oxidation no evidence for the formation of a semiquinone was observed (Figure 4.16A). The absorption values at 468 nm were plotted as a function of the measured potential, which had been corrected to the standard hydrogen electrode (i.e. a value of +244 mV was added to the measured potential). Data were subsequently fitted to a concerted two-electron redox process (Equation 2.4; Figure 4.16B), from which the midpoint potential was calculated. Good fits of the data were obtained and the midpoint potential for Y186F PETN reductase was determined as $-265 \text{ mV} \pm 5 \text{ mV}$, which is similar to the value obtained with wild-type enzyme (-267 mV ; Section 3.2.12).

4.3.7 X-ray crystallography

Crystallisation of Y186F PETN reductase was performed using the conditions published for wild-type enzyme (Barna *et al*, 2000). However, crystals obtained using the published conditions were not of a high quality due to their hollow nature. Accordingly, following a number of screens the published conditions were refined for the production of larger and better quality crystals (see Section 2.11 for details). Crystallisation of the Y186F enzyme with picric acid bound in the active site was also attempted.

Good quality crystals of the enzyme (4 μ l of 8-9 mg/ml protein, mixed with 4 μ l of the mother liquor solution) formed in most of the screens tested (see Section 2.11). However, for analytical purposes, crystals grown in a mother liquor solution of 10 % isopropanol, 0.5 M cacodylic acid and between 30-20 % PEG 3000 with either 0.1 M sodium acetate or sodium

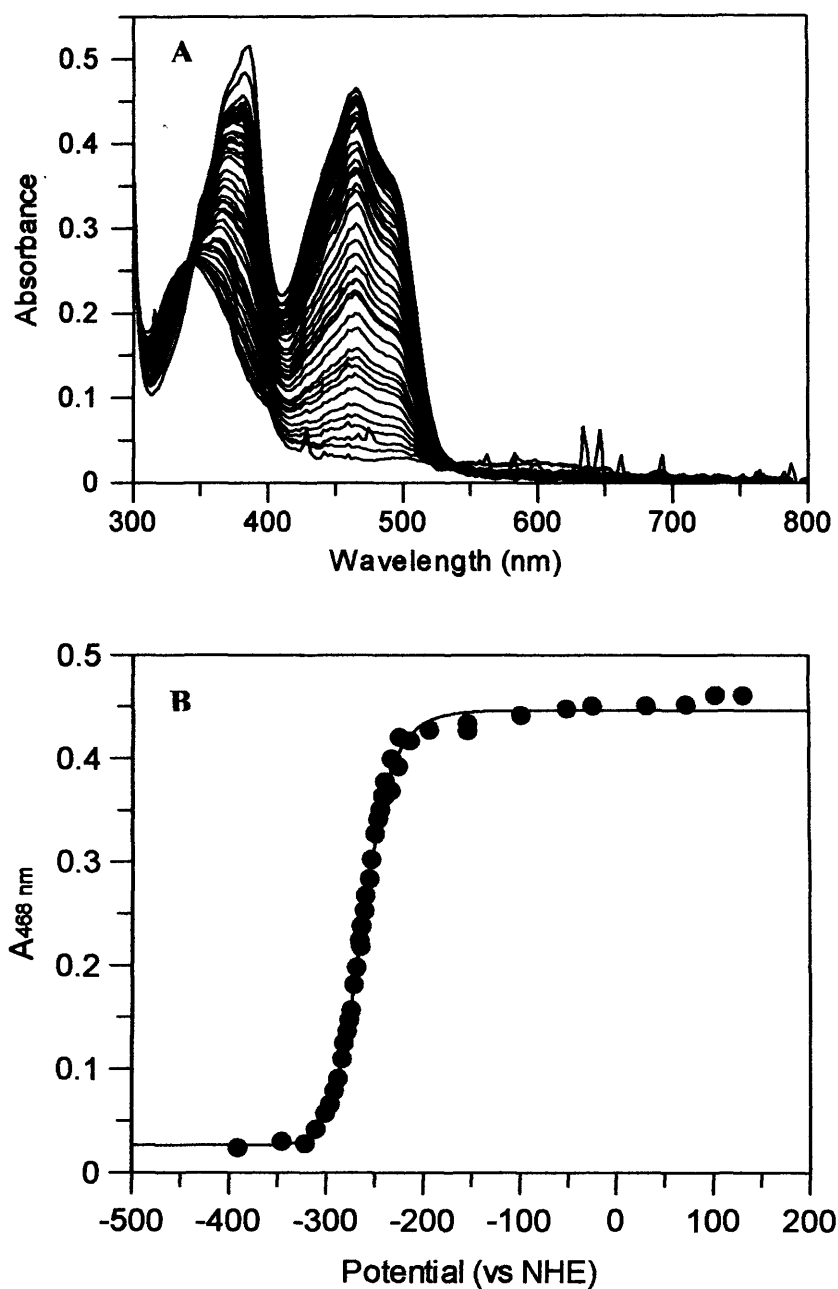


Figure 4.16. Spectral changes (Panel A) and plot of absorbance versus potential (Panel B) measured during the reductive titration of Y186F PETN reductase. Panel A, spectral changes monitored during the titration for Y186F PETN reductase ($\sim 35 \mu\text{M}$). Panel B, absorbance profile at 468 nm for Y186F PETN reductase, plotted against the potential. Data were fitted to a concerted two-electron redox process (Equation 3.5), from which the midpoint potential was calculated.

thiocyanate, at pH 6.2, were best suited. Crystals grown under these conditions were of a better quality (Figure 4.17).

X-ray analysis of the crystals and molecular replacement of the image was done by Dr David Leys, from the University of Leicester, who kindly provided images and the data for the solved structure (Figure 4.17). Data extending to 1.00 Å was collected on a single crystal at ESRF, Grenoble beamline 1D14.2. The HKL programmes, DENZO and SCALEPACK (Otwinowski and Minor, 1997) were used for data reduction and scaling and the structure was refined using REFMAC5 (Read, 1986). Refinement statistics and final model parameters are presented in Table 4.3.

Analysis of the Y186F mutant enzyme structure revealed that the mutation of Tyr 186 to Phe 186 was successful (Figure 4.17), consistent with the gene sequencing results (section 4.2.1). The overall structure of Y186F PETN reductase is comparable to the wild-type enzyme (Figure 4.18), confirming that no undesired perturbations had been made to the mutant enzyme's framework. Crystals of Y186F PETN reductase grown in the presence of picric acid were also analysed, however, picric acid is not observed to be bound in the active site.

4.4 Discussion

PETN reductase stereospecifically reduces α,β -unsaturated compounds which have their olefinic bonds positioned between the C1 and C2 atoms. Reduction proceeds by hydride ion transfer from reduced flavin N5 atom to the steroid C1 atom. This is followed by proton donation to the steroid C2 atom to fully saturate the double bond. Tyr 186 in PETN reductase was hypothesised to act as the potential active site acid in the reduction of α,β -unsaturated compounds. This was prompted by recent studies which established that the equivalent residue in OYE (Tyr 196) acted as the proton donor in the reduction of similar compounds (Kohli and Massey, 1998). Structural analysis of PETN reductase in complex with steroid substrates (Barna *et al*, 2001) highlighted that Tyr 186 was ideally positioned for the proton transfer role. Hence, the work described in this chapter aimed to elucidate the role of this residue which is conserved among family members of PETN reductase, such as isozymes of OYE (Kohli and Massey, 1998; Stott *et al*, 1993; Saito *et al*, 1991), estrogen binding protein (Madani *et al*, 1994), glycerol trinitrate reductase (Snape *et al*, 1997) and *N*-ethylmaleimide reductase (Miura *et al*, 1997). Another close member, morphinone reductase, has a cysteine

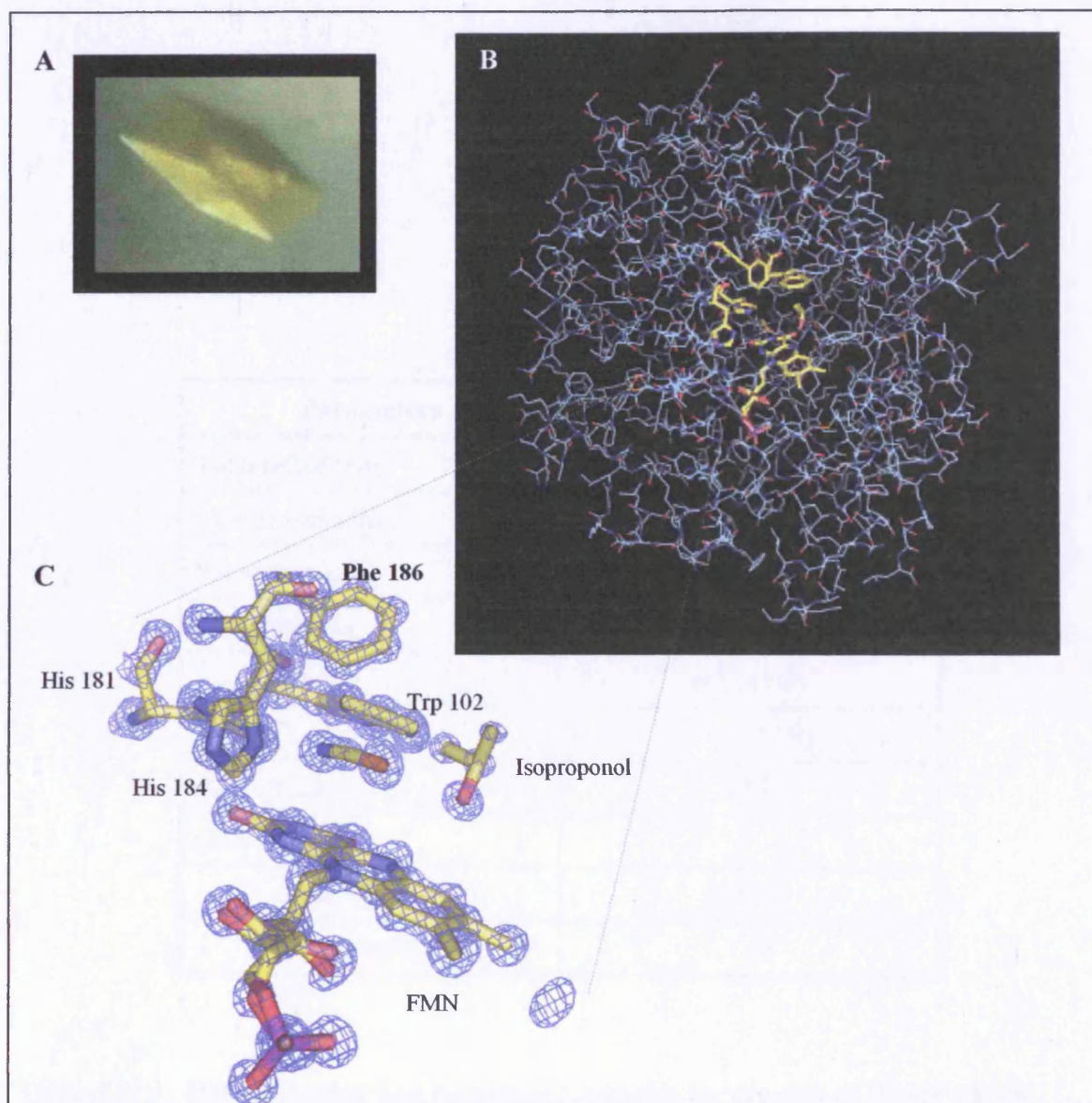


Figure 4.17. Crystallisation and structure of Y186F PETN reductase. Panel A, crystallisation of Y186F PETN reductase was performed by refining the conditions described for wild-type enzyme (Barna *et al*, 2000), resulting in the production of better quality crystals. Panel B, solved structure of Y186F PETN reductase; Panel C, magnification of the active site. Analysis of the structure revealed no gross perturbations had been made to the enzyme's framework and that the mutation of Tyr 186 to Phe 186 was successful (panel C). Thiocyanate and isoproponol is observed bound in the active site of the enzyme (panels B and C), reflective of the crystallisation buffer and the property of the enzyme to bind small negatively charged anions, consistent with the wild-type enzyme. The residues shown in panel B are the same as those shown in panel C. (Overall structure prepared using PYMOL. The magnified electron density image of the active site was kindly provided by Dr David Leys.)

Parameters	Statistics
Total reflections	1912182
Unique reflections	169624
Resolution (Å)	1.5 - 1.00
Completeness	95.8 (77.9)
R_{merge} (%)	6.1 (41.1)
$I / \text{sig}(I)$	17.5 (17.9)
R_{work} (R_{free})	13.8
r.m.s deviations	
Bond lengths (Å)	0.009
Bond angles (deg.)	1.51

Table 4.3. Data collection and refinement statistics for crystals of Y186F PETN reductase. (X-ray analysis and structure solution was kindly performed by Dr David Leys of the University of Leicester.)

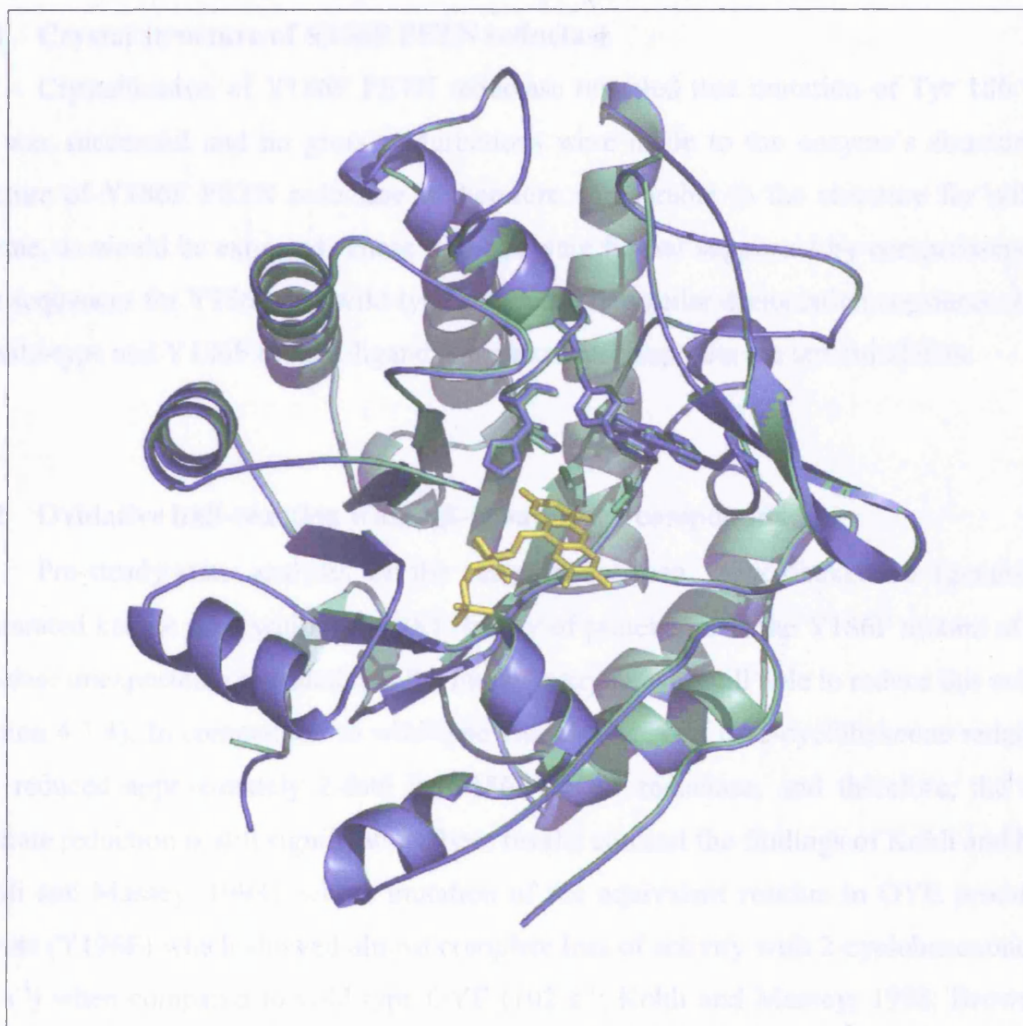


Figure 4.18. Superposition of the structures for Y186F PETN reductase and wild-type PETN reductase. The structure of Y186F PETN reductase (shown in green) is similar to the wild-type enzyme (shown in blue), confirming that the mutation of Tyr 186 to Phe 186 did not grossly perturb the overall framework of the enzyme. The active sites of the enzymes are shown in stick format. (Image kindly provided by Dr David Leys).

residue (Cys 191) substituted at the equivalent position to Tyr 186 in PETN reductase (French and Bruce 1994a).

4.4.1 Crystal structure of Y186F PETN reductase

Crystallisation of Y186F PETN reductase revealed that mutation of Tyr 186 to Phe 186 was successful and no gross perturbations were made to the enzyme's structure. The structure of Y186F PETN reductase is therefore comparable to the structure for wild-type enzyme, as would be expected. These findings were further supported by comparisons of the gene sequences for Y186F and wild-type enzyme. The similar dissociation constants obtained for wild-type and Y186F mutant-ligand complexes also supports the structural data.

4.4.2 Oxidative half-reaction with α,β -unsaturated compounds

Pre-steady-state analysis of the reaction between 2-cyclohexenone (generic α,β -unsaturated ketone used within the OYE family of proteins) and the Y186F mutant of PETN reductase unexpectedly revealed that the mutant enzyme was still able to reduce this substrate. (Section 4.3.4). In comparison to wild-type enzyme, the rate of 2-cyclohexenone reduction is only reduced approximately 2-fold in Y186F PETN reductase, and therefore, the rate of substrate reduction is still significant. These results contrast the findings of Kohli and Massey (Kohli and Massey, 1998), where mutation of the equivalent residue in OYE produced an enzyme (Y196F) which showed almost complete loss of activity with 2-cyclohexenone ($2.4 \times 10^{-4} \text{ s}^{-1}$) when compared to wild-type OYE (102 s^{-1} ; Kohli and Massey; 1998; Brown *et al.*, 1998). Their findings therefore established that Tyr 196 of OYE is essential for 2-cyclohexenone reduction. Estrogen binding protein (EBP), another close relative of PETN reductase, also has a tyrosine residue (Tyr 206) at the equivalent position to Tyr 186 in PETN reductase. Tyr 206 of EBP has been concluded to act as the active site acid in the reduction of α,β -unsaturated compounds (Buckman and Miller, 2000b). Although mutation of Tyr 206 to Phe 206 in EBP did not completely abolish the enzymes activity towards *trans*-2-hexenal (a 35-fold decrease in Y206F EBP activity was observed, compared to wild-type EBP), the stabilisation of a novel enzyme-substrate intermediate in the mutant protein was observed (similar species is also observed with Y196F OYE mutant protein; Kohli and Massey, 1998). The rapid mixing of Y206F EBP with *trans*-2-hexenal in stopped-flow produced a sudden

increase in absorbance in the long wavelength region of the enzyme's spectrum, followed by a much slower appearance of the oxidised flavin spectrum. Buckman and Miller (Buckman and Miller, 2000b) attributed the rapid increase in long wavelength absorbance to the formation a charge-transfer complex, which forms before enzyme re-oxidation proceeds and consists of reduced flavin bound to oxidised substrate. The formation of this intermediate had not been observed in similar reactions with the wild-type enzyme, hence, re-oxidation of wild-type EBP proceeded in a single phase, compared to the biphasic nature of re-oxidation observed with Y206F EBP (Buckman and Miller, 2000a and 2000b). Given the stabilisation of the novel intermediate, together with the 35-fold decrease in activity, the authors concluded that Tyr 206 of EBP is the active site acid. Although, PDA studies were not performed here, the studies presented in this chapter reveal only a 2-fold decrease in Y186F PETN reductases activity with 2-cyclohexenone which strongly indicates that Tyr 186 is not essential for the reduction of this compound. The decrease in activity in the mutant enzyme might be attributed to the altered mode of 2-cyclohexenone binding which compromises hydride transfer, as a 4-fold decrease in the K_d for the enzyme-2-cyclohexenone complex is revealed. Considering the similarity in physical and structural properties of PETN reductase and OYE, the results presented here are somewhat unexpected. However, these findings are not unusual when considering similar studies conducted with morphinone reductase. This enzyme has a cysteine residue in the equivalent position to Tyr 186 in PETN reductase. Given that morphinone reductase is also closely related to OYE, Barna and co-workers (Barna *et al*, 2002) postulated that Cys 191 would act as the active site acid in the reduction of 2-cyclohexenone. However, their studies too elucidated that this residue was not responsible for the protonation of α,β -unsaturated compounds. Collectively, these results infer that the physical properties of PETN and morphinone reductase are more similar to each other than they are with OYE.

4.4.3 Oxidative half-reaction with nitro compounds

Consistent with our initial hypothesis, the results of the oxidative half-reaction with TNT have shown that mutation of Tyr 186 in PETN reductase does not alter the kinetics of TNT reduction (or hydride-Meisenheimer stability). Although the rate of reduction remains unaffected, the dissociation constant (K_d) for the TNT-reduced enzyme complex is twice the value of that determined for wild-type enzyme (Section 4.3.5), suggesting that the mutant

enzyme binds TNT less tightly. Dissociation constants for picric acid and 2,4-DNP binding to oxidised Y186F enzyme (determined from the ligand binding experiments), also indicate that Y186F PETN reductase binds these ligands less tightly (two-fold) than wild-type PETN reductase. Hence, collectively these results indicate that Tyr 186 might have a minor influence on the binding of nitroaromatic compounds. The weaker binding of nitroaromatics is further evident from crystallisation studies of Y186F PETN reductase. Analysis of enzyme crystals grown in the presence of picric acid revealed that no picric acid was bound in the active site. However, co-crystal structures of wild-type enzyme in complex with nitroaromatics (Section 3.1.2; Khan *et al*, 2001) do not infer Tyr 186 to be involved in binding these compounds. It might be likely that the polar functional group of Tyr 186 has a slight electrostatic interaction with the nitro groups of these ligands or with other nearby residues which are more involved in the binding of nitroaromatics. Considering there was only a 2-fold increase in the K_d , it can be concluded that Tyr 186 is not a major determinant for nitroaromatic binding and is not also essential to the enzyme's catalytic efficiency towards TNT reduction.

The rate of GTN catalysis by Y186F PETN reductase is reduced approximately four-fold when compared to wild-type enzyme. In addition, the dissociation constant for GTN binding is lower, indicating that the mutant enzyme binds the nitrate ester tighter. These differences indicate that mutation of Tyr 186 leads to an altered mode of GTN binding which compromises substrate reduction. Alternatively, Tyr 186 might have a more catalytic role in GTN reduction, whereby it forms interactions with one of the nitro groups facilitating substrate reduction. Conclusively, it is shown that Tyr 186 plays a key role in nitrate ester reduction, but further studies are needed to ascertain its underlying role in this reaction

4.4.4 Kinetics of the reductive half-reaction

Characterisation of the reductive half-reaction revealed that the rate of hydride transfer from NADPH to the flavin of Y186F PETN reductase is slowed 3-fold in comparison to wild-type enzyme. In addition, the rate of charge-transfer formation between NADPH and Y186F PETN reductase proceeds too quickly, such that it cannot be measured accurately even with an optimised flow cell fitted in the stopped-flow apparatus. However, the rate of complex decay was measurable and is equivalent to the hydride transfer rates, indicating that the decay of the complex is a direct consequence of hydride transfer. These results suggest that Tyr 186 might function to precisely orientate NADPH in a position favourable for hydride transfer, by

stabilising/controlling the formation of the charge-transfer complex. Mutation of Tyr 186 allows NADPH to rapidly bind in any configuration (explaining the increased rates of charge-transfer formation) where there is π - π overlap between the flavin and NADPH, but this geometry is less favourable for hydride transfer (explaining slower rate of Y186F reduction compared to wild-type enzyme). It is unlikely that the decrease in the rate of hydride transfer is due to Tyr 186 having a catalytic function in this reaction, as the re-oxidation of NADPH is not believed to involve the use of a proton donor. If Tyr 186 did play such a role, the rate of NADPH catalysis would be negligible in the Y186F protein, and this is not observed. The kinetic differences observed between the reductive half-reaction of wild-type and Y186F PETN reductase is not due to changes in the thermodynamic properties of the flavin, as the redox potentials measured for both enzymes are similar. Hence, the results presented herein indicate that Tyr 186 in PETN reductase might directly or indirectly (via its polar functional group, or via contacts through other residues) be involved in the binding or the optimal positioning of NADPH over the flavin ring, for hydride transfer.

4.4.5 Implications into the mechanism of α,β -unsaturated compound reduction by the OYE family of enzymes

The results outlined in this chapter have identified that the conserved Tyr 186 residue is not the active site acid in the reduction of α,β -unsaturated compounds. This highlights an important difference in the mechanism of 2-cyclohexenone reduction between the OYE family of enzymes, despite the high structural similarity of their active sites. Consistent with the findings on PETN reductase are those on morphinone reductase where it is shown that Cys 191 (equivalent to Tyr 186 of PETN reductase) is not the active site acid (Barna *et al*, 2002). Given that mutation of seven other active site residues of morphinone reductase did not reveal the identity of the active site acid (Messiha, 2004), it is most likely that water is the true proton donor in the reduction of 2-cyclohexenone by morphinone reductase and therefore possibly PETN reductase. It is also plausible, as Buckman and Miller (Buckman and Miller, 200b) accounted for, that water is the proton donor in EBP and not Tyr 206. Although mutation of Tyr 206 in EBP decreases the rate of 2-cyclohexenone reduction, the activity is still appreciable. The assumption that Tyr 206 acts as the active site acid in EBP was based on the stabilisation of a novel intermediate (complex between reduced EBP and oxidised substrate) by the mutant protein. It is possible that this intermediate forms in the wild-type

enzyme too, but only becomes observable in the mutant protein due to the slower rate of substrate reduction. Although the authors highlighted that the residual activity in Y206F EBP might be due to water leaking in to the active site and therefore substituting the role of the proton donor, it is possible that water is the true proton donor. The water molecule might be bound to Tyr 206 in wild-type EBP and therefore mutation of this residue will compromise the efficacy of the rate of proton donation by the water molecule. A similar situation might occur in OYE. However, the Y196F mutant of OYE showed almost complete loss of activity with 2-cyclohexene which strongly supports the role of Tyr 196 being the active site acid. Furthermore, the mutant OYE was unable to fully reduce nitrocyclohexene (which requires hydride and proton transfer) and was only able to form the nitronate intermediate (produced by hydride transfer; see Chapter 5), indicating that proton transfer was strongly compromised in Y196F OYE. These findings might reflect the true role of OYE in sterol metabolism, such that it has evolved to employ an active site acid in the reduction of such compounds. However, in PETN reductase and morphinone reductase, the enzymes are not engineered to catalyse such a reaction and therefore water can fulfil the role of the proton donor. It is clear, however, that the mechanism of α,β -unsaturated compound reduction occurs via different mechanisms in the OYE family of enzymes and the findings suggest a closer physical relationship between PETN reductase and morphinone reductase, than to OYE.

The different mechanisms for α,β -unsaturated compound reduction undertaken by the OYE family is further exemplified by the more complicated mode of steroid binding and reduction in PETN reductase. Recently, the crystal structure of the reduced PETN reductase-progesterone complex has been solved by Dr David Leys at the University of Leicester (Figure 4.19). Studies were performed by crystallising dithionite-reduced enzyme in the presence of progesterone in an anaerobic environment. Structural comparisons revealed no major difference between the oxidised and reduced states of the enzyme (Figure 4.19). However, unexpectedly it is observed that progesterone is bound to the reduced enzyme in the same orientation to that observed in the oxidised structure (Figure 4.19; Dr David Leys, verbal communication; Barna *et al*, 2001), and not in the flipped orientation as proposed by Barna and co-workers (Barna *et al*, 2001). Previous structural and NMR analysis revealed that in oxidised enzyme, the steroid substrates are aligned such that their unreactive C4-C5 double bond is positioned close to the flavin N5 atom, whereas the reducible C1-C2 double bond is aligned far from the flavin N5 atom such that it is unfavourable for hydride transfer.

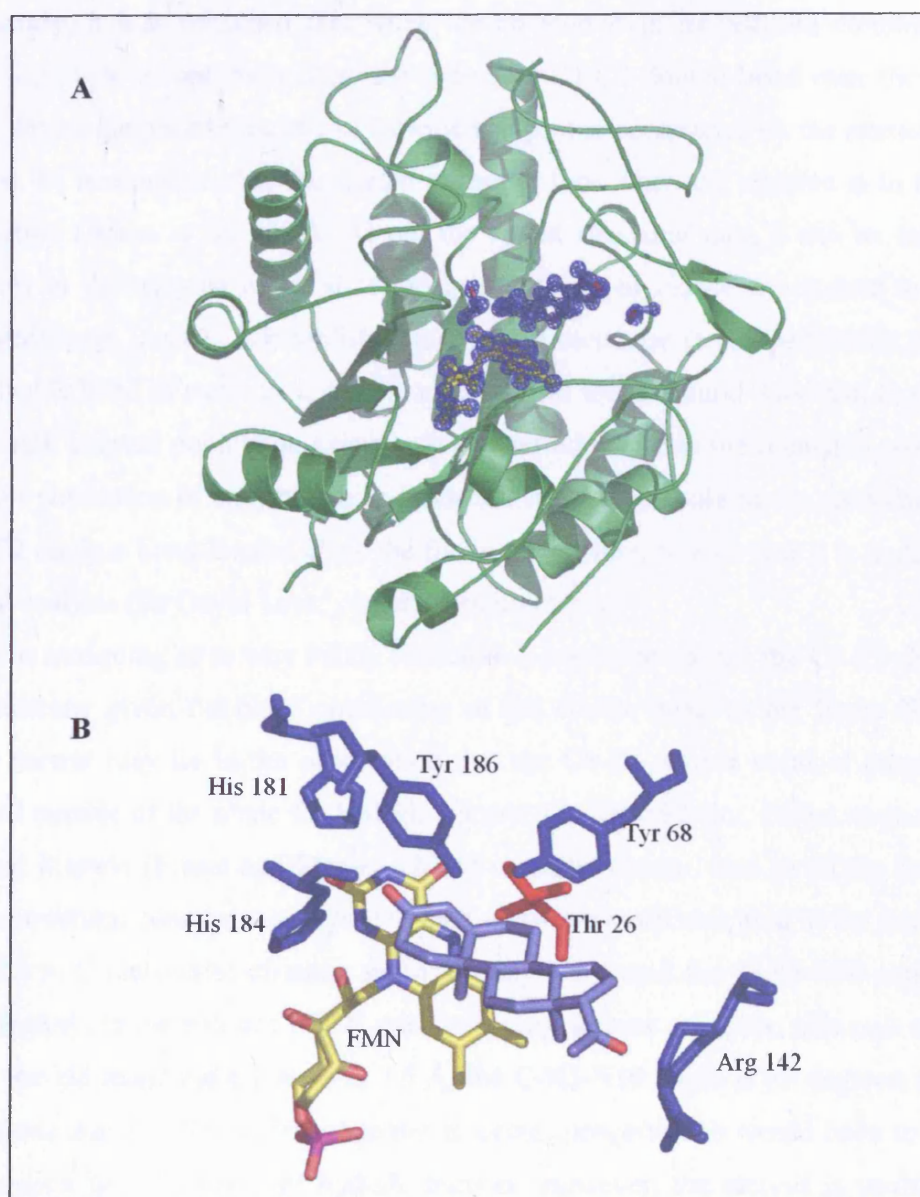


Figure 4.19. Structure of the reduced PETN reductase-progesterone complex. Crystals of the reduced protein-progesterone complex were grown under anaerobic conditions. Panel A, Overall structure of the reduced protein, with the electron density of the active site shown. Panel B, active site of the reduced protein-progesterone complex. Unexpectedly, progesterone (inhibitor; shown in light blue) is observed to bind to reduced enzyme in the same conformation as that for oxidised enzyme, i.e. with the irreducible C4-C5 double of the steroid positioned close to the flavin N5. Consequently, for the reduction of steroid substrates to occur a small population of enzyme must exist with the C1-C2 bond of steroids positioned close to the FMN N5 atom and that reduction of the enzyme alone does not cause the steroid molecule to flip 180°. (Images kindly provided by Dr David Leys).

Consequently, it was proposed that when the enzyme is in its reduced conformation the steroids flip so as to optimally align the reducible C1-C2 double bond over the flavin N5 position. Investigation into the site of hydride and proton acceptance on the steroid molecule supported the assumption that the steroid molecule flips when the enzyme is in its reduced conformation (Barna *et al*, 2001). Given the recent structural data it can be inferred that differences in the enzyme redox state alone is unlikely to induce the steroid to bind in a flipped geometry. Since it is established that PETN reductase stereospecifically reduces the C1-C2 double bond of steroids, it can be inferred from the structural data that, in the reduced state, a small enzyme population exists with the steroid bound in the reducible conformation. The minor population of enzyme which binds the steroid molecule in the conformation where the C1-C2 olefinic bond located close the flavin N5 position is such that it is undetectable in structural analysis (Dr David Leys; verbal communication).

It is intriguing as to why PETN reductase is unable to reduce the C4-C5 double bond of progesterone given the close positioning of the double bond to the flavin N5 atom. A possible answer may lie in the observation that the C4-C5 double bond of progesterone is positioned outside of the plane for hydride transfer (Dr David Leys; verbal communication). Fraaje and Mattevi (Fraaje and Mattevi, 2000) recently reported that in all the flavoprotein-substrate structural complexes analysed to date, substrate molecules bind to the flavin with the N5 (FMN) to C (substrate) distance approximately 3.5 Å and the C-N5-N10 angle between 98-117 degrees. In the reduced PETN reductase-progesterone complex, although the distance between the N5 atom and C1 atom is 3.5 Å, the C-N5-N10 angle is 88 degrees, which may limit hydride transfer. For hydride transfer to occur, progesterone would have to move in a planar fashion into the plane of hydride transfer. However, the steroid is unable to move sideways due to steric clashes between its substituent groups and active site residues, namely Thr 26 (Figure 4.19; Dr David Leys, verbal communication). In addition, if progesterone binds in the flipped orientation, although its C1-C2 bond would be located close to the FMN N5 atom, this bond of progesterone is already saturated and therefore irreducible. Consequently, it is probable that the out of plane positioning of the C4-C5 olefinic bond of progesterone over the flavin molecule explains why this steroid (and other steroids which have only a C4-C5 double bond) acts as an inhibitor of PETN reductase. However, further studies are needed to confirm this theory.

Although it is suggested that water is likely to function as the proton donor in the reduction of α,β -unsaturated compounds by PETN reductase, it is also plausible that other

active site residues of PETN reductase could function in this way. Therefore, the following chapter aims to investigate this hypothesis by exploring the roles of His 181 and His 184 in the reduction of 2-cyclohexenone.

Chapter Five

*Establishing the roles of His 181 and
His 184 in PETN reductase*

CHAPTER FIVE

Establishing the roles of His 181 and His 184 in PETN reductase

5.1 Introduction

This chapter reports on the characterisation of two mutant forms of PETN reductase, in which two active site histidine residues (His 184 and His 181) are replaced by alanine. A number of structures of PETN reductase complexed with several compounds have suggested that His 181 and His 184 play a key role in ligand binding. The studies in this chapter aim to provide solution evidence to confirm the importance of His 181 and His 184 in ligand binding. Accordingly, the chapter begins by describing structural studies of PETN reductase, highlighting the importance of His 181 and His 184 in the active site.

The studies described in Chapter 4 established that Tyr 186 of PETN reductase does not act as an active site acid in the reduction of 2-cyclohexenone. Subsequent to this finding, it was postulated that either His 181 or His 184 might fulfil this role. To probe the role of His 181 and His 184 as an active site acid, the reductive and oxidative half-reactions of H181A and H184A PETN reductases were also investigated and comparisons are made with the wild-type enzyme.

5.1.1 Active site structure of PETN reductase

The structure of PETN reductase alone and in complex with a range of compounds has been solved at high resolution (Barna *et al*, 2001; Khan *et al*, 2002). Within the active site, the FMN co-factor is positioned in the centre of the barrel axis and bound towards the C-terminal end of the α,β -barrel domain. The *re* face of the flavin is completely buried within the hydrophobic active site, while the *si* face of the flavin is exposed to a solvent filled access channel, which forms between the active site centre and the surface of the enzyme. The main and side chain interactions to the flavin of PETN reductase are also conserved in OYE (Barna *et al*, 2001; Fox and Karplus, 1994).

Structural analysis of oxidised PETN reductase indicates the presence of anions bound within the active site. This is represented by additional electron density observed on the *si* face of the flavin. These anions have been identified as acetate, thiocyanate or chloride, which

reflect the composition of buffers used in the crystallisation process (Figure 5.1). Kinetic measurements have shown that small negatively charged ions act as competitive inhibitors of PETN reductase. The structure of the two-electron reduced form of PETN reductase has also been solved and shown to lack an anion in the active site. In the structure of reduced enzyme, a water molecule replaces the anions that are observed in the structure of the oxidised enzyme (Barna *et al*, 2001). The anions bound in oxidised PETN reductase form close contacts with the side chains of two active site histidine residues, His 181 and His 184 (Figure 5.1). These residues have also been observed to form close contacts with steroid ligands and nitroaromatic compounds (Barna *et al*, 2001; Khan *et al*, 2002).

Structures of oxidised PETN reductase complexed with steroids such as prednisone, progesterone and 1,4-androstadiene, and with 2-cyclohexenone have been solved at high resolution (Barna *et al*, 2001). In all cases, the steroids bind above the *si* face of the isoalloxazine ring and are held in position by hydrogen bonding through their carbonyl oxygen group to His 181 and His 184 in the active site (Figure 5.2; Barna *et al*, 2001). The His 181 and His 184 pair are also observed to co-ordinate the hydroxy groups of picric acid and 2,4-DNP (Figure 5.2; Khan *et al*, 2002). Formation of these hydrogen bonds to the two histidine residues positions the ligand molecules over the flavin ring in an alignment optimal for hydride transfer. These co-crystallisation studies therefore imply that His 181 and His 184 are key determinants in ligand/substrate binding in the active site.

Sequence alignments of PETN reductase with related family members reveal that His 181 and His 184 are conserved across the large group of proteins (Figure 5.3). All of the homologues have a histidine residue at a position corresponding to His 181 in PETN reductase and either a histidine or asparagine residue at position His 184 (PETN reductase). The conservation of these residues across the family highlights their importance in protein function. Crystallographic and kinetic studies have confirmed that the equivalent residues in OYE (His 191 and Asn 194) function as the main determinants for ligand binding (Brown *et al*, 1998). In co-crystal structures of OYE, His 191 and Asn 194 were observed to co-ordinate the carbonyl oxygen of 2-cyclohexenone and the phenolate oxygen of phenol ligands, thus positioning these ligands in a similar geometry to that observed in co-crystal structures of PETN reductase (Fox and Karplus, 1994; Karplus *et al*, 1995; Barna *et al*, 2001; Khan *et al*, 2002).

The present chapter aims to characterise two mutant forms of PETN reductase in which either His 181 and His 184 is replaced by an alanine residue. The intention was to provide solution evidence for the importance of these residues in ligand binding. It was

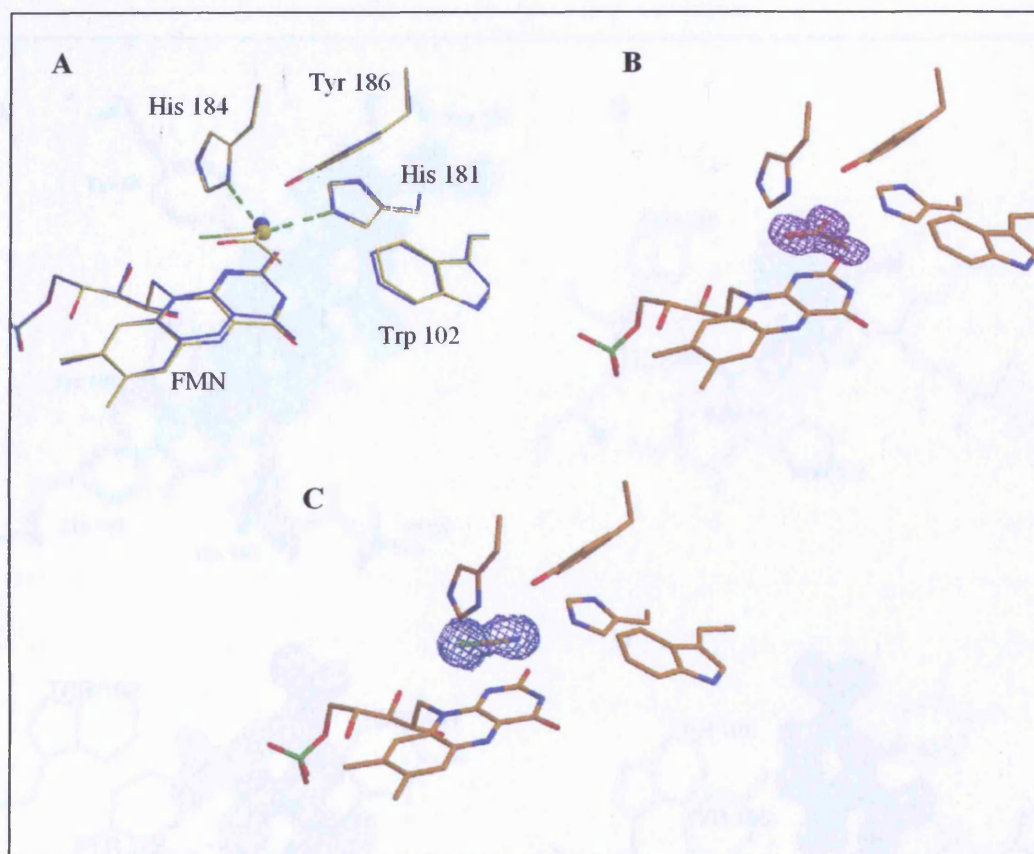


Figure 5.1. Active site structures of PETN reductase. Panel A, active site structure of PETN reductase illustrating the flavin environment and location of small ligands bound close to the flavin isoalloxazine ring in the oxidised and reduced forms. The oxidised forms of the enzyme have acetate, chloride or thiocyanate bound, depending on the composition of the mother liquor. The reduced form (shown in blue) has water bound. Hydrogen bonds to His 181 and His 184 are shown as broken lines. The electron density for the acetate ion is shown in panel B and the density for thiocyanate in panel C. (Figure taken from Barna *et al*, 2001)

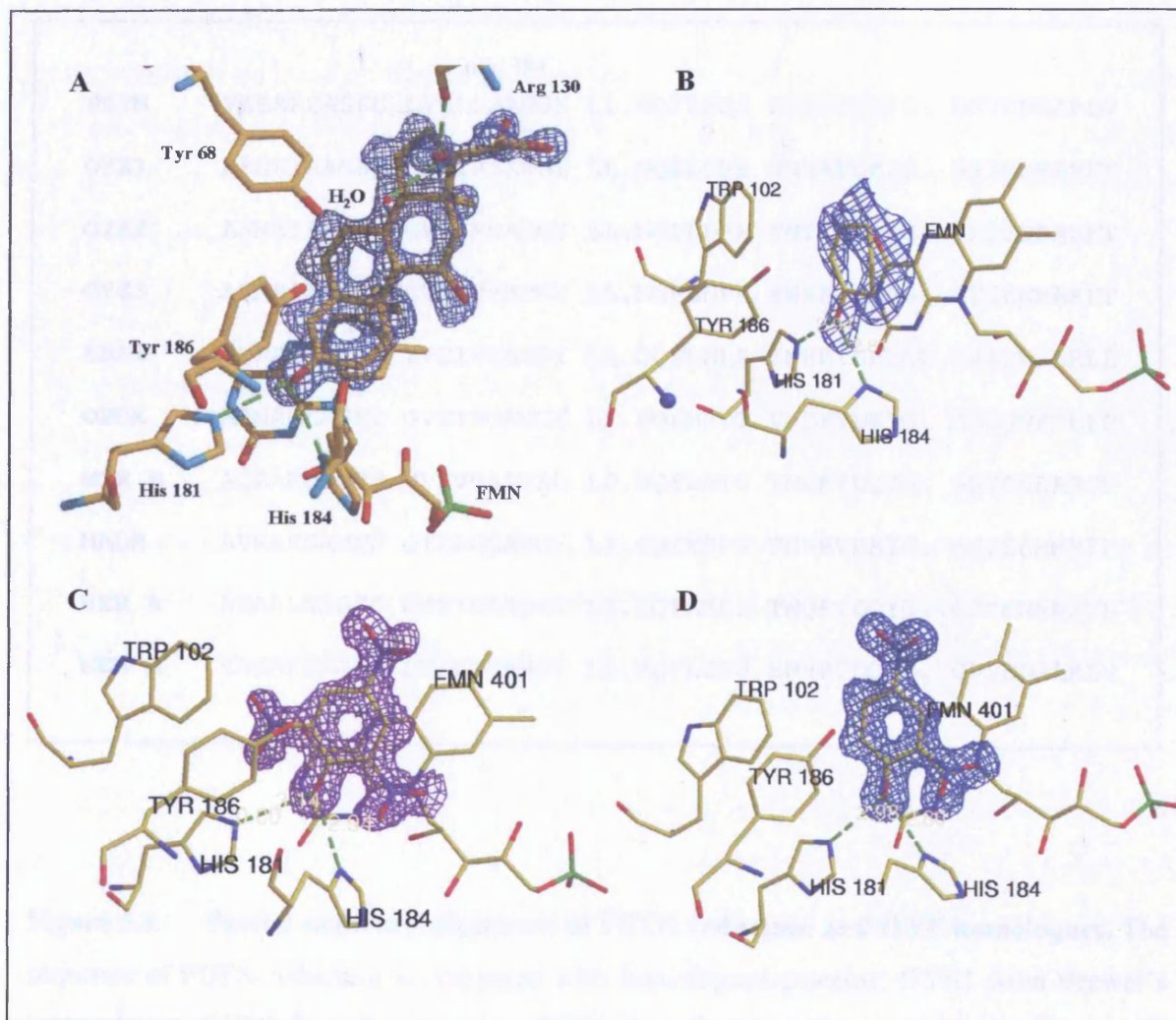


Figure 5.2. Difference electron density for oxidised PETN reductase in complex with various ligands. Active site structure of PETN reductase in complex with (A) prednisone; (B) 2-cyclohexenone; (C) TNT; and (D) 2,4-DNP. Each structure indicates the importance of His 181 and His 184 in ligand binding. These residues are observed to form hydrogen bonds (dashed lines) to the functional group of ligands. [Figures taken from Barna *et al*, 2001 (Panel A) and Khan *et al*, 2002 (Panel B, C and D)]

	181	184	
PETN	VABAREAGFD	LVELHSAHGY	LL.HQFLSPS SNQRTDQYG. GSVENRARLV
OYE1	AKNSIAAGAD	GVEIHSANGY	LL.NQFLDPH SNNRTDEYG. GSIENRARFT
OYE2	AKNSIAAGAD	GVEIHSANGY	LL.NGFLDPH SNTRTDEYG. GSIENRARFT
OYE3	AKNSIAAGAD	GVEIHSANGY	LL.NGFLDPH SNKRTDEYG. GTIENRARFT
EBP1	AKHALEAGFD	YVEIHGAHGY	LL.DQFLNLA SNKRTDKYGC GSIENRARLL
OPDA	ARNAMEAGFD	GVEIHGANGY	LI.DQFMKDT VNDRTDEYG. GSLQNRCKFP
MOR B	AQRAKRAGFD	MVEVHAANAC	LP.NQFLATG TNRRTDQYG. GSIENRARFP
NADH	AVRAKGAMFD	GIELHGAHGY	LI.GQFMSPR TNRRVDKYG. GSFERRMRFP
NER A	ARAALWAGFD	GVEIHAANGY	LI.EQFLKSS TNQRTDDYG. GSIENRARFL
NEM A	IANAREAGFD	LVELHSAHGY	LL.HQFLSPS SNHRTDQYG. GSVENRARLV

Figure 5.3. Partial sequence alignment of PETN reductase and OYE homologues. The sequence of PETN reductase is compared with homologous proteins; OYE1 from Brewer's bottom yeast, OYE2 from *S. cerevisiae*, OYE3 from *S. cerevisiae*, estrogen binding protein (EBP1) from *Candida albicans*, 12-oxophytodienoate reductase (OPDA) from *A. thaliana*, morphinone reductase (MOR B) from *P. putida*, NADH oxidase from *Thermobacillus brockii*, glycerol trinitrate reductase (NER A) from *Argobacterium radiobacter*, and *N*-ethylmaleimide reductase (NEM A) from *E. coli*. Letters denoted in red highlight the conserved residues His 181 and His 184 of PETN reductase. (Figure is adapted from Brown *et al*, 1998.)

anticipated that the kinetics of the oxidative half-reaction of each mutant form of PETN reductase would be altered owing to the weaker binding of substrates. Although a structure for PETN reductase in complex with NADPH is not available, it is hypothesised that His 181 and His 184 might also be involved in binding this coenzyme, with concomitant effects on the reductive half-reaction in the mutant enzymes. Dissociation constants determined from studies on each half-reaction and ligand binding experiments were expected to demonstrate that the binding of ligands is significantly weaker in the two mutant enzymes in comparison to the wild-type enzyme. The results of detailed kinetic and binding studies are presented.

5.1.2 Search for the active site acid of PETN reductase

PETN reductase reduces the double bond of α,β -unsaturated compounds, by hydride ion transfer from reduced flavin to the C1 atom and proton transfer to the C2 atom of the substrate (see Chapter 4 for a detailed discussion). Based on crystallographic evidence and studies with OYE, it was proposed that Tyr 186 of PETN reductase would act as the proton donor in the reduction of steroids. However, the results described in Chapter 4 have indicated that Tyr 186 does not fulfil this role. It is proposed therefore, that either His 181 or His 184 might serve as the proton donor. The present chapter aims to elucidate whether either of the histidine residues is the active site acid in the reduction of 2-cyclohexenone. This substrate is a generic α,β -unsaturated ketone used in studies with related enzymes. Accordingly, the reduction of 2-cyclohexenone was investigated by stopped-flow methods. The turnover of nitrocyclohexene was also explored. Nitrocyclohexene can be reduced by hydride transfer from FMNH₂ in OYE, in the absence of a concerted proton transfer from the enzyme (Figure 5.4; Meah and Massey 2000). In morphinone reductase, reduction of 2-cyclohexenone has been shown to be concerted with proton transfer using double isotope studies (Basran *et al*, 2003). Unlike with 2-cyclohexenone, the reduction of nitrocyclohexene proceeds via the formation of a spectrally visible intermediate, which is produced by the transfer of a hydride ion from the enzyme to the substrate. This transfer occurs in the absence of proton transfer. The nitronate species can then be converted subsequently to nitrocyclohexane by proton transfer (Figure 5.4). Given that each species formed during nitrocyclohexene reduction is spectrally distinguishable, the reduction of this compound and identification of the hydride and proton transfer steps can be monitored easily. Thus, the reduction of nitrocyclohexene by

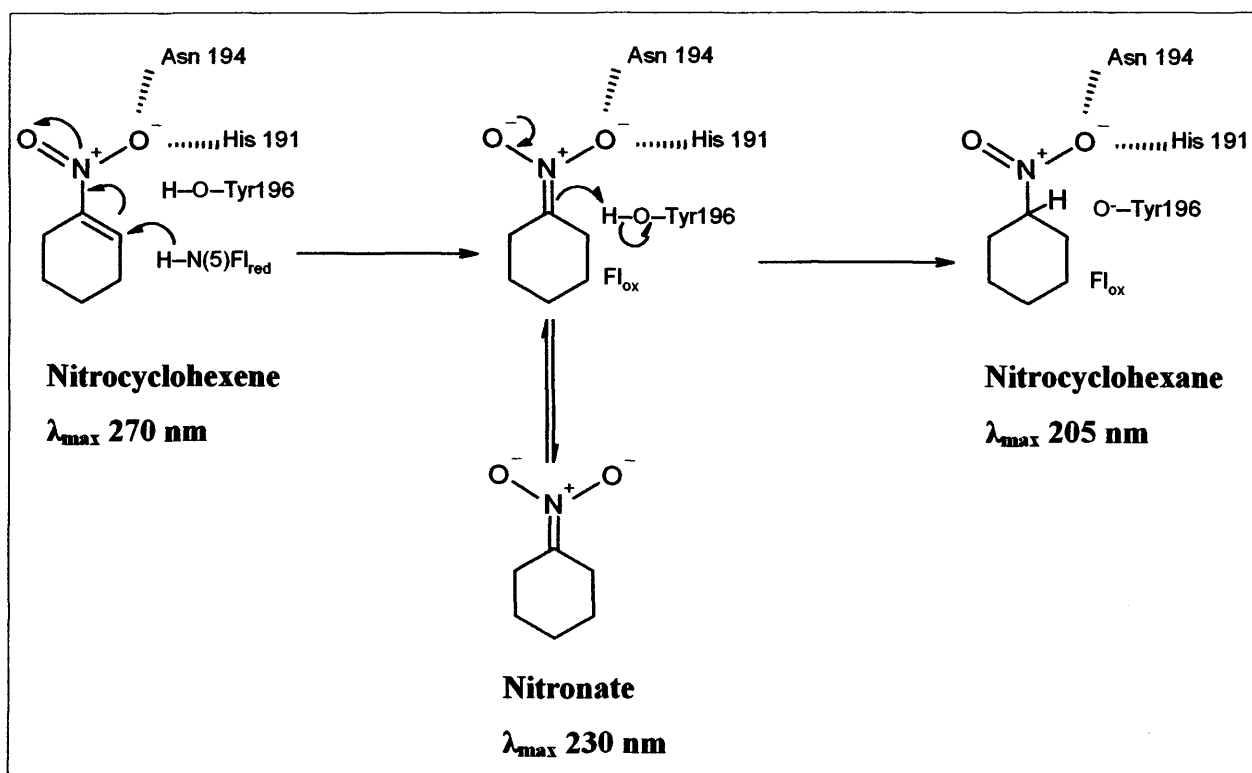


Figure 5.4. Mechanism of nitrocyclohexene reduction by OYE. OYE catalyses the reduction of nitrocyclohexene via the formation of a transient intermediate. Hydride transfer from reduced flavin to the aromatic olefinic bond of nitrocyclohexene leads to the formation of the intermediate species, nitronate. Proton transfer to the nitronate intermediate, mediated by Tyr 196 of OYE, leads to the formation of nitrocyclohexane. The formation of each species is observable spectrally at the wavelengths indicated. (Figure adapted from Meah and Massey, 2000).

wild-type PETN reductase was characterised and the studies were then extended to the two mutant forms of PETN reductase altered at residue His 181 and His 184.

5.2 Purification of the H181A and H184A mutant forms of PETN reductase

Glycerol stocks of *E. coli* cells carrying the pONR1 plasmid encoding for H181A and H184A mutant PETN reductases were kindly provided by Dr Terez Barna. Cells were grown and harvested using the procedure described for wild-type enzyme (Section 2.3). The purification procedure for the two mutant enzymes had to be modified in comparison to that described for wild-type enzyme, as the mutant forms of PETN reductase did not bind to the Biomimetic orange chromatography column. Various ionic strengths of potassium phosphate buffer were used in an attempt to enhance the binding capability of the enzymes to the resin, but this proved to be ineffective. This result is not unexpected as the Biomimetic orange resin is an affinity chromatography resin and if His 181 and His 184 are responsible for the binding of ligands, then it is most likely that it is these residues that interact with the affinity chromatography matrix. Therefore, replacement of the two histidine residues in each of the single mutant forms of PETN reductase is expected to reduce the enzymes ability to bind to the resin. In turn, this provided an early indication that the histidine residues are key in the binding of ligand molecules. Consequently, the Biomimetic orange resin was used to bind unwanted proteins, collecting the enzyme of interest as an eluent when washing the column. However, the mutant enzymes passed through the column in a large volume. In concentrating the sample under high pressure, the enzymes were observed to precipitate from solution over the extended time required to reduce the sample volume. Owing to this instability the Biomimetic orange resin was excluded during future protein preparations. Various other resins, such as DE 52 and Phenyl Sepharose were also employed to remove unwanted proteins from the initial crude extract (i.e. after the cells were French pressed). However, owing to the weak interaction of the enzymes with these resins, these resins were not used in the final procedure. The purification procedure adopted involved two steps of Q-Sepharose chromatography, where one resin was kept for the initial crude enzyme extract and another Q-Sepharose resin column was used for the final step. This method produced relatively pure samples of the H181A and H184A PETN reductases (Figure 5.5). Although a few additional faint-staining bands were observed in SDS PAGE, the purity of the H181A and H184A PETN reductases were judged to be sufficient for detailed spectroscopic analysis. Owing to the

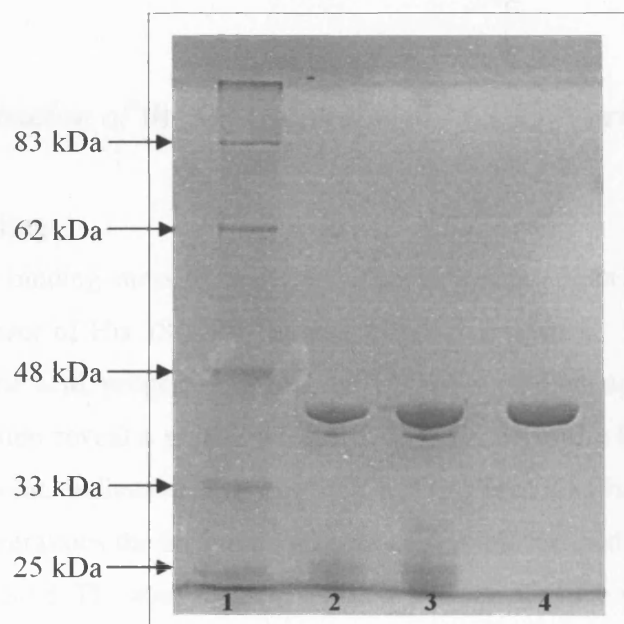


Figure 5.5. SDS PAGE analysis of purified H181A and H184A PETN reductases. Lane 1, molecular weight marker; Lane 2, purified H181A PETN reductase; Lane 3, purified H184A PETN reductase; Lane 4, purified wild-type PETN reductase (displayed for comparative purposes). The histidine mutant forms of PETN reductase were purified using the same procedure as described for wild-type enzyme (Section 2.3) except that the Biomimetic orange chromatography step was replaced by an additional Q-Sepharose step.

instability of the proteins, further handling of enzyme solutions had to be undertaken with care, especially during overnight dialysis steps (typically 16 h), to prevent the protein from precipitating. Consequently, overnight dialysis steps were conducted only once (compared to three, with wild-type enzyme) between purification steps, and two final dialysis steps were used when pure protein was obtained.

5.3 *Characterisation of the H181A and H184A PETN reductases*

5.3.1 **Ligand binding**

Equilibrium binding measurements were performed as described in Section 2.5, to assess the involvement of His 181 and His 181 in binding ligands. Binding titrations were performed with picric acid, progesterone and 2,4-DNP. Spectral changes accompanying each enzyme-ligand titration reveal a small increase in absorbance in the long wavelength region and an isosbestic point, indicative of a one step binding process (Figure 5.6). However, at higher ligand concentrations the isosbestic points became less defined owing to the increased absorbance of the ligand. The absorbance changes at 518 nm for each titration were plotted as a function of ligand concentration and fitted to a simple hyperbolic expression using Origin 4.0 software (Figure 5.7). The analysis indicated that ligands bind less tightly to the mutant enzymes compared with wild-type enzyme. Data for the mutant enzymes were therefore fitted to a hyperbolic function in contrast to the wild-type enzyme, where a quadratic fit was used (Section 3.2.2). Dissociation constants for oxidised enzyme-ligand complexes are summarised in Table 5.1. Comparison of the dissociation constants clearly indicates that the binding of ligands is weaker with H181A and H184A PETN reductases. The most pronounced difference in the measured dissociation constant is observed with progesterone (Table 5.1).

As with wild-type enzyme (Section 3.2.2), titrations of the mutant enzymes with TNT did not elicit any spectral changes in the enzyme spectrum, and thus dissociation constants for this ligand could not be determined.

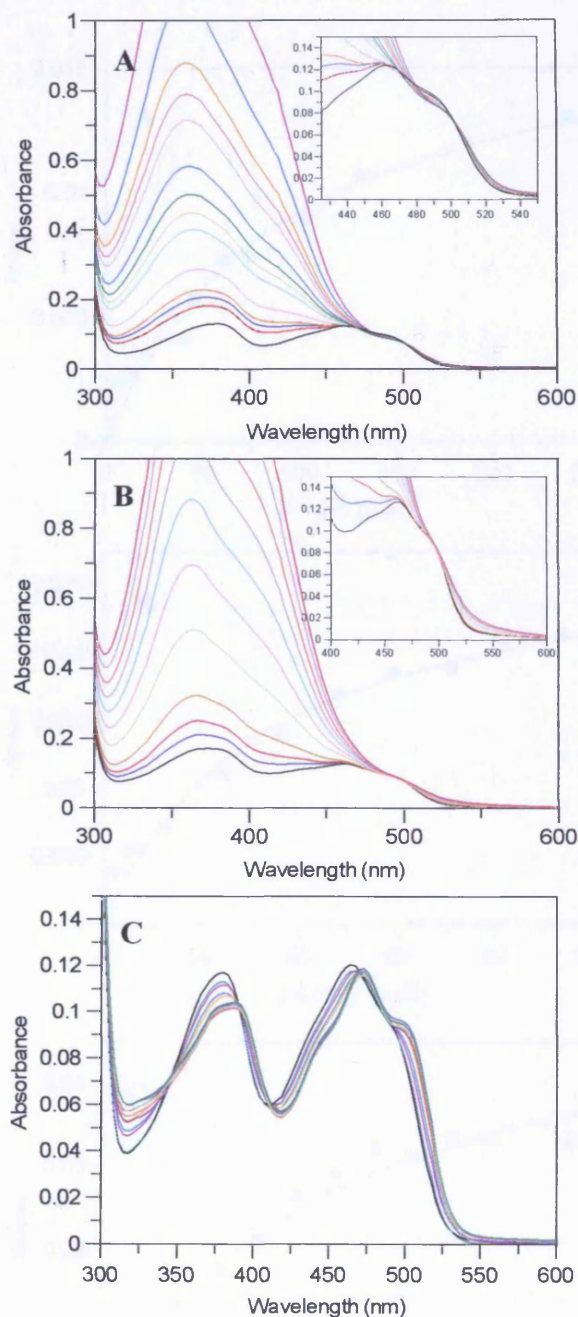


Figure 5.6. Spectra obtained during ligand binding studies of H181A and H184A PETN reductases. Spectral changes produced during the titration of oxidised H181A and H184A PETN reductase ($\sim 10 \mu\text{M}$ each) with a stock concentration of ligand. The starting spectrum (free enzyme) is shown in black in each titration. Panel A, titration of H184A PETN reductase with picric acid; Panel B, titration of H181A PETN reductase with 2,4-DNP; Panel C, titration of H184A PETN reductase with progesterone. Insets to the panels show the isobestic points at 500 nm in panel A; 495 nm in panel B; and 344 nm, 390 nm, 411 nm and 470 nm in panel C. Similar data sets were also observed for other enzyme-ligand combinations (spectra not shown).

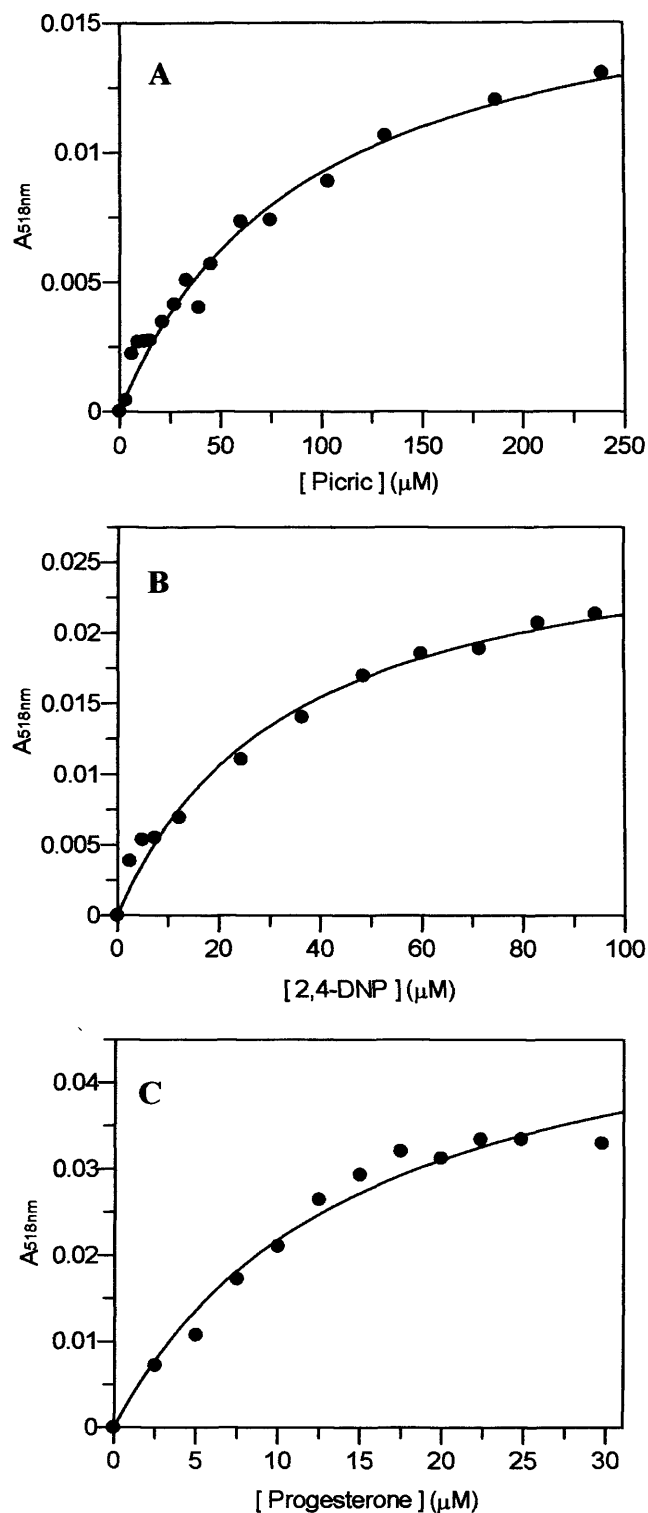


Figure 5.7. Examples of ligand binding titration curves. Each panel shows a representative binding curve for oxidised enzyme ($\sim 10 \mu\text{M}$ each) with ligand. Panel A, titration of H181A PETN reductase with picric acid; Panel B, titration of H184A PETN reductase with 2,4-DNP; Panel C, titration of H184A PETN reductase with progesterone. Similar data sets were collected for other enzyme-ligand combinations (data not shown).

	Dissociation constant (K_d , μM)		
	Wild-type PETN reductase	H181A PETN reductase	H184A PETN reductase
Picric acid	5.4 ± 1.1	91.9 ± 12.4	73.3 ± 16.1
2,4-DNP	0.95 ± 0.1	55.8 ± 7.3	34.0 ± 5.5
Progesterone	0.07 ± 0.03	16.3 ± 4.9	14.8 ± 3.0

Table 5.1. Calculated dissociation constants for ligand complexes of wild-type, H181A and H184A PETN reductases. Enzymes ($\sim 10 \mu\text{M}$ each) were titrated with picric acid, progesterone and 2,4-DNP in 50 mM potassium phosphate buffer, pH 7.0, in a 1 ml quartz cuvette. Spectra were recorded after the addition of ligand to the enzyme. From the resultant spectra (see Figure 5.6) the absorption changes at 518 nm were plotted as a function of ligand concentration and fitted to a hyperbolic expression (see Figure 5.7), from which the dissociation constants were determined. Data for wild-type enzyme are taken from Section 3.2.2.

5.3.2 Anaerobic single wavelength stopped-flow studies on the reductive half-reaction

The reductive half-reaction of each mutant enzyme was investigated to assess the role of His 181 and His 184, if any, in the binding and oxidation of NADPH. Although the structure of PETN reductase bound with NADPH has not been solved, it is likely that the histidine pair are responsible for binding this substrate. Indeed, a recent determination of the structure of morphinone reductase with tetrahydro-NADP⁺ bound indicates that the histidine and asparagine residues that correspond to His 181 and His 184 in PETN reductase form good interactions with the ligand (Dr Terez Barna, University of Leicester, unpublished work). It was expected, therefore, that the binding of NADPH would be weaker in the two mutant PETN reductases, which in turn might affect the formation of the observed charge-transfer complex and the rate of hydride transfer from NADPH to the flavin. These two processes were monitored using single wavelength stopped-flow spectroscopy, by mixing enzyme over a range of NADPH concentrations. Absorption changes were monitored at 560 nm to follow the rate of formation of the charge-transfer species, and also at 464 nm to monitor the rate of hydride transfer. These studies were conducted under anaerobic conditions as the rate of flavin reduction in the H181A and H184A PETN reductases was expected to be much slower than that for wild-type enzyme, and the oxidase rate of the mutant proteins might interfere with enzyme reduction in an aerobic experiment. In wild-type PETN reductase, the oxidase rate was much slower than that of enzyme reduction, allowing studies of the reductive half-reaction to be undertaken under aerobic conditions.

The mixing of the H181A and H184A mutant proteins with NADPH did not elicit any significant absorbance change at 560 nm, indicating that the charge-transfer intermediate does not arise in the mutant enzymes. To provide direct evidence for this suggestion, the reductive half-reaction was later monitored using multiple wavelength stopped-flow spectroscopy, so that any absorbance changes that may occur over the whole enzyme spectrum can be observed (see Section 5.3.3).

Absorbance changes at 464 nm were monitored using the same conditions described for wild-type enzyme (Section 3.2.3), where each enzyme (20 μ M) was rapidly mixed with a range of NADPH concentrations at 5 °C. A decrease in flavin absorbance was observed, indicative of hydride ion transfer from NADPH to the enzyme flavin. Analogous to the data for wild-type enzyme, transients were averaged and best fit to a single exponential equation (Equation 2.2), for which the observed rate constant (k_{obs}) was determined for each NADPH concentration used. The observed rates for the H181A and H184A PETN reductases were

plotted as a function of NADPH concentration and fitted to a hyperbolic equation in Grafit 5.0 software (Figure 5.8). In contrast to wild-type enzyme (Section 3.2.3), the rates of hydride transfer with the mutant enzymes were found to be dependent on NADPH concentration, and were therefore fitted to a hyperbolic function. From the fits to the data, dissociation constants (K_d) for NADPH-oxidised enzyme complexes and the limiting rate of hydride ion transfer (k_2) were determined, and are summarised in Table 5.2, in addition to the kinetic constants determined for wild-type enzyme. Data comparison for wild-type, H181A and H184A PETN reductase reveals that the binding of NADPH to the mutant proteins is significantly disrupted, in particular with the H184A PETN reductase. However, the rate of hydride transfer from NADPH to the flavin in each mutant protein was found to be faster than for wild-type enzyme.

5.3.3 Anaerobic multiple wavelength stopped-flow analysis of the reductive half-reaction

Previous single wavelength stopped-flow studies on the reductive half-reaction of H181A and H184A PETN reductases (Section 5.3.2) suggested that the charge-transfer intermediate does not form in these enzymes. Therefore, to confirm that no absorbance changes, other than a reduction in flavin absorbance, is produced during the mixing of NADPH with each mutant enzyme, anaerobic photodiode array (PDA) spectroscopy was used. For comparative purposes, the spectral changes exhibited during the reduction of wild-type PETN reductase (Craig, 2000) is displayed in Figure 5.9.

Spectral changes accompanying the rapid mixing of H184A PETN reductase (40 μM) with either stoichiometric or ten times excess of NADPH (400 μM), showed no indication of charge-transfer formation (Figure 5.10). Reactions were monitored over a range of timescales. The only spectral change observed was a decrease in flavin absorbance, indicative of hydride transfer. Data were therefore best fitted to a single step model ($A \rightarrow B$) in PROKIN software, where oxidised enzyme (A) proceeds to form reduced enzyme (B). Similar absorbance changes were observed with H181A PETN reductase, confirming that the charge-transfer species that accumulates with wild-type enzyme is absent in the reductive half-reaction of H181A and H184A PETN reductases.

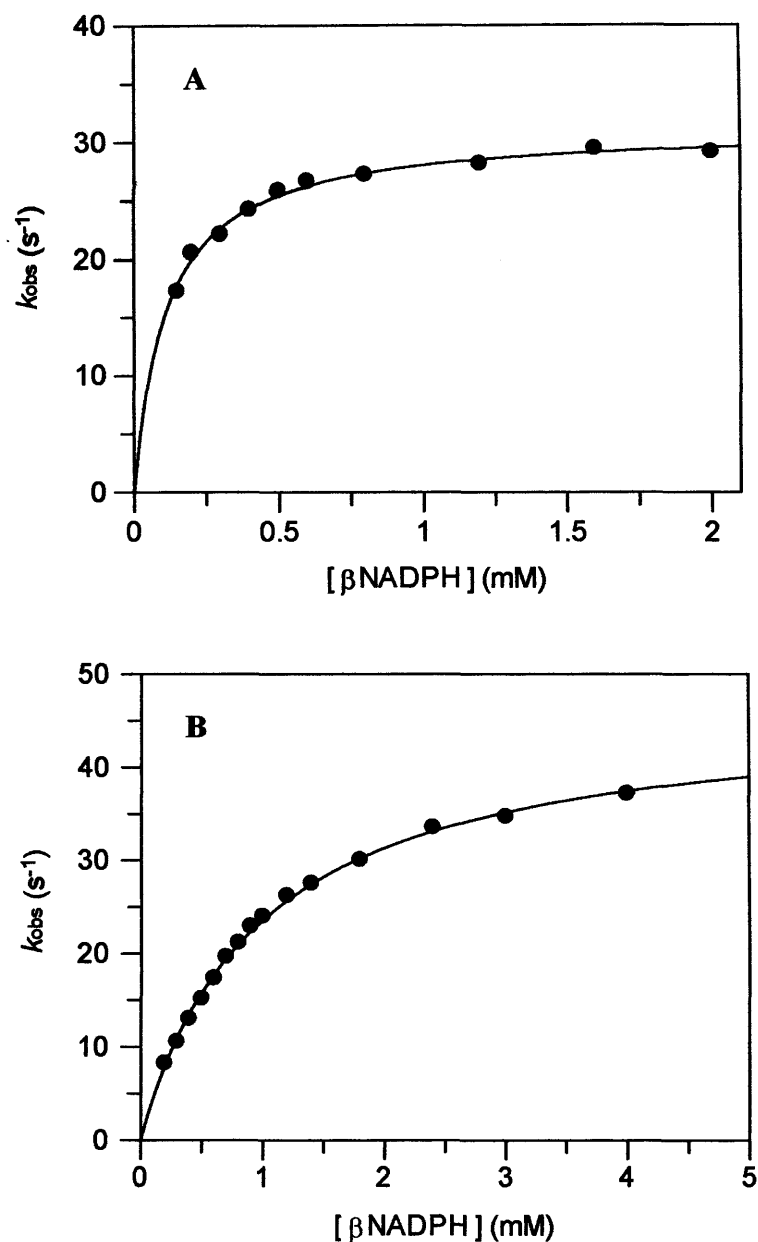


Figure 5.8. The concentration dependence for the observed rate of hydride transfer from NADPH to the flavin in the H181A and H184A PETN reductases. Panel A, H181A PETN reductase; Panel B, H184A PETN reductase. The solid line shows the fit of the data to a hyperbolic function. Measurements were made under anaerobic conditions, using $\sim 20 \mu\text{M}$ of each enzyme in potassium phosphate buffer, pH 7.0, at 5°C .

	k_2 (s ⁻¹)	K_d (μM)
Wild-type PETN reductase	11.6 ± 0.2	33.4 ± 8.5
H181A PETN reductase	31.2 ± 0.3	113 ± 6
H184A PETN reductase	46.6 ± 0.6	973 ± 28

Table 5.2. The pre-steady-state rate constants for the reductive half-reaction of wild-type, H181A and H184A PETN reductases. Rate constants were calculated using 20 μM of each enzyme and various concentrations of NADPH, in 50 mM potassium phosphate buffer, pH 7.0, at 5 °C. Stopped-flow absorbance spectroscopy was used to monitor the rate of flavin reduction at 464 nm. Observed rates were analysed for their dependence on NADPH concentration, and hyperbolic fits to the data (Figure 5.8) produced values for k_2 , the rate constant for flavin reduction, and K_d , the dissociation constant for the NADPH-oxidised enzyme complex. (Data for wild-type enzyme are taken from Chapter 3).

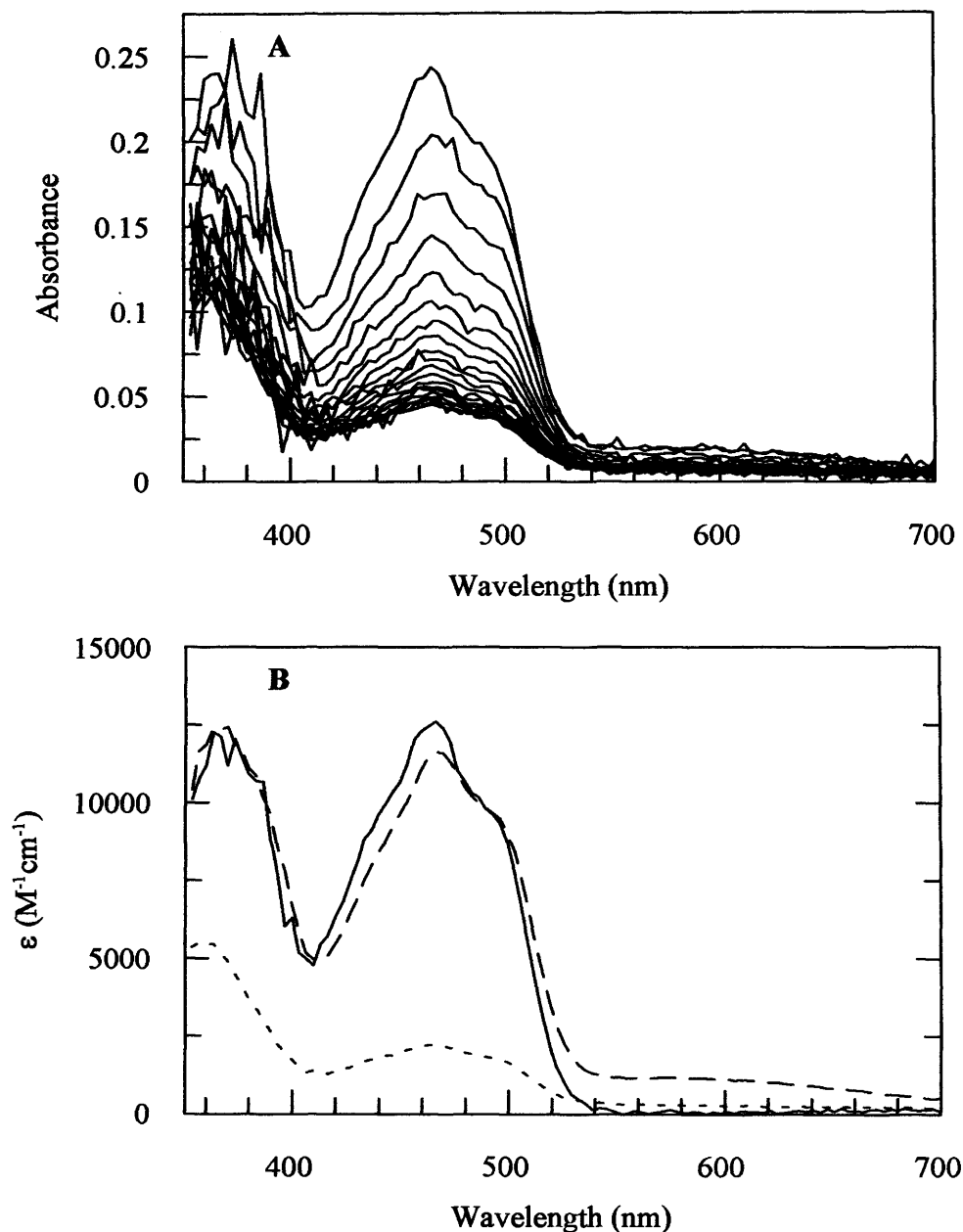


Figure 5.9. Time-dependent photodiode array spectra for the reduction of wild-type PETN reductase by β -NADPH. Panel A, PETN reductase (20 μ M) and β -NADPH (20 μ M) were mixed at 5 $^{\circ}$ C, pH 7.0, and four hundred spectra were recorded over a period of 1 s. One in every twenty of the spectra are displayed above. Panel B, the three spectral intermediates observed during the reduction of PETN reductase by β -NADPH. All 400 spectra from the reaction shown in Panel A were analysed by global analysis and numerical integration methods using PROKIN software. The solid line represents oxidised enzyme, the dashed line is a charge-transfer intermediate and the dotted line is two electron-reduced enzyme. (Figures taken from Craig, 2000).

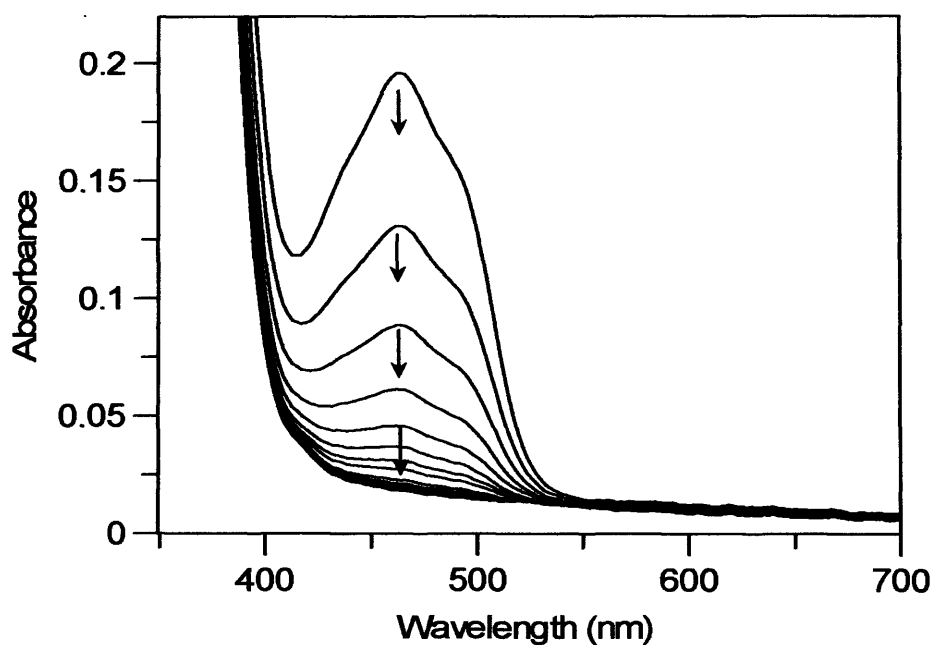


Figure 5.10. Time-dependent photodiode array spectra monitoring the reduction of H184A PETN reductase by β -NADPH. H184A PETN reductase (20 μ M) was mixed with 10 times excess β -NADPH (200 μ M) in potassium phosphate buffer, pH 7.0, at 5 $^{\circ}$ C. Four hundred spectra were recorded over a period of one second. One in every twenty-five of the spectra is displayed. Spectra following the reaction were analysed by global analysis and numerical integration methods using PROKIN software and shown to follow a single step reaction ($A \rightarrow B$). Similar absorption changes were recorded for H181A PETN reductase.

5.3.4 Single wavelength stopped-flow studies of the oxidative-half reaction with 2-cyclohexenone

The mechanism of reduction of α,β -unsaturated compounds by PETN reductase requires a proton donation either by an active site residue or water (see Chapter 4). It was initially proposed that Tyr 186 in PETN reductase might function as an active site acid, but the studies outlined in Chapter 4 revealed that this is not the case. Of the remaining residues in the active site, either His 181 or His 184 of PETN reductase might serve as proton donor. The reduction of 2-cyclohexenone, an α,β -unsaturated ketone, was investigated with the H181A and H184A PETN reductases. Studies were conducted using the procedure described in Section 2.9.1. Spectral changes following flavin re-oxidation at 462 nm were monitored using anaerobic single wavelength stopped-flow spectroscopy. H181A and H184A PETN reductases (20 μ M) were stoichiometrically reduced with sodium dithionite (which had been previously calibrated with FMN) and rapidly mixed with a range of 2-cyclohexenone concentrations, at 25 °C. Transients accompanying the reaction were averaged and best fitted to a double exponential expression (Equation 3.5), and the phase with the largest absorbance change (the faster of the two phases) was used to determine k_{obs} . The biphasic nature of the reaction transients contrasts those observed with wild-type enzyme, where 2-cyclohexenone mediated enzyme re-oxidation proceeded in a single exponential manner (Section 3.2.11). Observed rates for the H181A and H184A PETN reductases were plotted as a function of 2-cyclohexenone concentration and data were fitted to a hyperbolic expression using Grafit 5.0 software (Figure 5.11). Values for k_{lim} of $0.49 \pm 0.02 \text{ s}^{-1}$ and $0.34 \pm 0.01 \text{ s}^{-1}$ for the H184A and H181A PETN reductases, respectively, were calculated. These compare to a value of $34.7 \pm 2.2 \text{ s}^{-1}$ for wild-type PETN reductase (Section 3.2.11). The rate of 2-cyclohexenone reduction is therefore significantly reduced in both mutant enzymes. Values for K_d were determined as $44.0 \pm 3.7 \text{ mM}$ for H184A PETN reductase and $19.2 \pm 1.5 \text{ mM}$ for H181A PETN reductase. The wild-type enzyme has a K_d of $9.5 \pm 1.6 \text{ mM}$ (see Table 5.3 for a summary of all the kinetic constants). The binding of 2-cyclohexenone to H181A and H184A PETN reductases is therefore weaker than in the wild-type enzyme. The weak binding might lead to a poor geometry for hydride transfer from the FMN, thus accounting for the poor hydride transfer rates observed in the mutant enzymes. Alternatively, the decreased rate of 2-cyclohexenone reduction in the mutant enzymes might be attributed to the replacement of the potential active site acid. In an attempt to distinguish between these two possibilities, multiple turnover

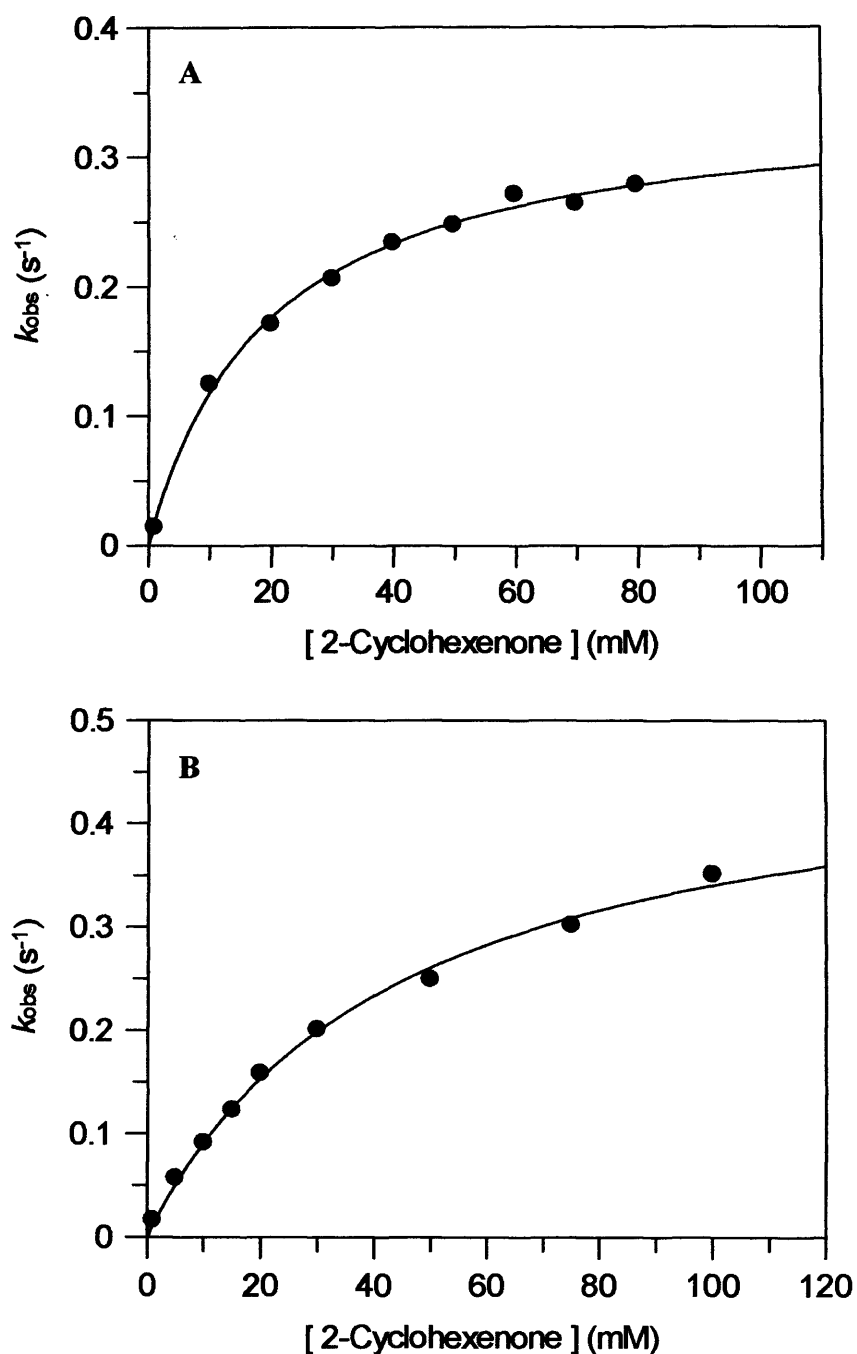


Figure 5.11. The concentration dependence for the rate of hydride transfer from dithionite-reduced H181A and H184A PETN reductase to 2-cyclohexenone. Panel A, rates measured with H181A PETN reductase; Panel B, rates measured with H184A PETN reductase. Anaerobic single wavelength spectroscopy at 464 nm was performed with 20 μ M enzyme and a range of cyclohexenone concentrations, in 50 mM potassium phosphate buffer, pH 7.0, at 25 $^{\circ}$ C. The solid line shows the fit of the data to a hyperbolic function.

	2-Cyclohexenone		TNT	
	$k_{\text{lim}} (\text{s}^{-1})$	$K_d (\text{mM})$	$k_{\text{lim}} (\text{s}^{-1})$	$K_d (\mu\text{M})$
Wild-type PETN reductase	34.7 ± 2.2	9.5 ± 1.6	4.44 ± 0.14	78.4 ± 11.7
H181A PETN reductase	0.34 ± 0.01	19.2 ± 1.5	9.35 ± 0.37	194 ± 27
H184A PETN reductase	0.49 ± 0.02	44 ± 4	15.8 ± 0.3	134 ± 11

Table 5.3. Rate constants for the oxidative half-reaction of wild-type, H181A and H184A PETN reductases with 2-cyclohexenone and TNT. (Data for wild-type enzyme are taken from Chapter 3)

studies were performed with nitrocyclohexene in which hydride transfer is uncoupled from proton transfer (Section 5.3.5).

5.3.5 Anaerobic studies following the multiple turnover of nitrocyclohexene

Reduction of nitrocyclohexene has been characterised with OYE and is demonstrated to proceed via two steps (Figure 5.12; Meah and Massey, 2000). The first step leads to the formation of a nitronate intermediate, which is formed by hydride ion transfer from flavin to the compounds unsaturated bond. The formation of this intermediate is observable spectrally (with an absorbance maxima at 230 nm). The next step involves the transfer of a proton to the olefinic bond, leading to the formation of nitrocyclohexane (Figure 5.12). This product has different spectral characteristics (λ_{max} at 205 nm) compared with the preceding intermediate. The mechanism of nitrocyclohexene reduction is therefore comparable to the mechanism of 2-cyclohexenone reduction. However, in morphinone reductase it has been established that hydride ion and proton transfer to 2-cyclohexenone occurs in a concerted manner (Figure 5.12; Basran *et al*, 2003). This differs to the mechanism of nitrocyclohexene reduction by OYE, where each transfer step occurs in a stepwise fashion, with the individual steps being spectrally characterisable (Figure 5.4). Therefore, to determine if the reduced activity of both mutant proteins with 2-cyclohexenone (Section 5.3.4) is due to disruption of the protonation step, the multiple turnover of nitrocyclohexene was analysed. If one of the histidine residues in PETN reductase functions as an active site acid, then either mutant protein will transform nitrocyclohexene to the nitronate intermediate, but the formation of the fully reduced product should not be observed.

The multiple turnover of nitrocyclohexene was first characterised with wild-type PETN reductase and then extended to the H181A and H184A mutant enzymes, using the conditions reported for OYE (Meah and Massey, 2000) and described in Section 2.8.4. The multiple turnover of nitrocyclohexene was achieved using an NADPH regeneration system, with NADPH (8 μM) and enzyme (0.1 μM), which after equilibration at 25 °C, was set as the spectrophotometric blank for the reaction. The reaction was initiated by the addition of 80 μM of nitrocyclohexene and followed spectrophotometrically at 2 min intervals. The progress of the reaction was monitored until no further significant absorption changes could be observed (i.e. typically for 24 h).

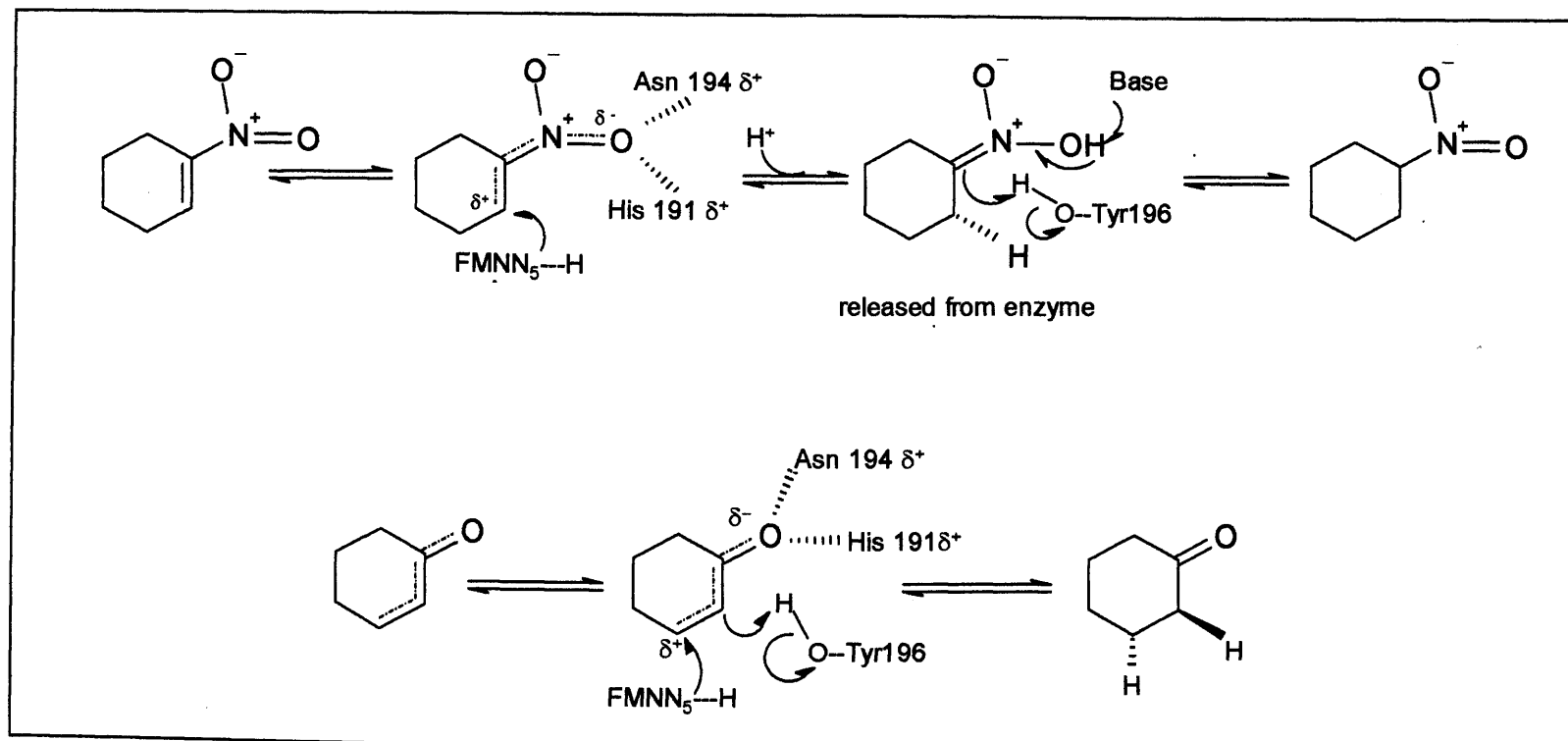


Figure 5.12. Proposed pathways for the mechanism of nitrocyclohexene and 2-cyclohexenone reduction by OYE. Upper pathway; reduction of nitrocyclohexene proceeds by the formation of an aci-nitro intermediate. Formation of this intermediate occurs by hydride transfer from flavin N5 to the C^β atom of the substrate. This is followed by proton transfer from Tyr 196 of OYE to the intermediate, to fully reduce the substrate, forming nitrocyclohexane. Lower pathway; reduction of 2-cyclohexenone proceeds by a concerted reaction where transfer of the hydride is made possible by the presence of Tyr 196 of OYE, primed to protonate the C^α atom. (Figure adapted from Kohli and Massey, 1998)

Spectral changes accompanying the reaction with wild-type enzyme (Figure 5.13A) reveal a decrease in nitrocyclohexene absorbance (λ_{max} at 270 nm) with a concurrent increase in absorbance at 230 nm, indicative of nitronate formation. Following its formation, the decay of the nitronate intermediate is observed (Figure 5.13B), represented by a decrease in 230 nm absorbance. As the absorbance at 230 nm decreases, absorbance at 210 nm and 278 nm increases. These absorbance changes might correspond to the formation of the fully reduced product, nitrocyclohexane (λ_{max} 205 nm), in addition to the re-conversion of nitronate to nitrocyclohexene (λ_{max} 270 nm). However, this is not a definitive conclusion as the absorbance maxima observed here at 210 nm and 278 nm, differs slightly to that reported for the reduced product at 205 nm and nitrocyclohexene at 270 nm, by Meah and Massey (Meah and Massey, 2000) with OYE. A decrease in 340 nm absorbance is also observed, which is likely due to the natural decomposition of NADPH, owing to the long time course of the reaction (~20 hrs). Consequently, the change in NADPH absorbance is likely to have an effect on the absorbance profile of any compounds produced during the reaction, as NADPH was part of the spectrophotometric blank. Therefore, the observed shift in the absorbance maxima of nitrocyclohexene and nitrocyclohexane, if formed, might be attributed to the absorbance effects arising from NADPH decomposition.

Spectral changes associated with the reduction of nitrocyclohexene by the H181A and H184A PETN reductases were similar (Figure 5.14), but differed to that observed with wild-type enzyme (Figure 5.13). First, the time course of the reaction to reach near completion was longer with the mutant enzymes. Spectral changes for both mutant proteins reveal a decrease in 340 and 278 nm absorbance. The decrease at 340 nm is most likely to result from the natural decomposition of NADPH, while the decrease at 278 nm might be due to the decay of nitrocyclohexene (λ_{max} 270 nm). However, the conversion of nitrocyclohexene to nitronate is not observed. Consequently, it is possible that the decrease and shift from 270 to 278 nm in nitrocyclohexene absorbance might also be due to NADPH decay. The change in absorbance brought about by NADPH decay is likely to elicit a negative effect on the absorbance profile for nitrocyclohexene, as NADPH was part of the spectrophotometric blank. Collectively, these studies suggest that wild-type PETN reductase is able to reduce nitrocyclohexene to nitrocyclohexane via the formation of the nitronate intermediate, similar to OYE (Meah and Massey, 2000), but on a longer timescale. The mutant enzymes, however, are unable to reduce nitrocyclohexene, indicating that His 181 and His 184 might have a catalytic and/or binding function in the reduction of nitrocyclohexene.

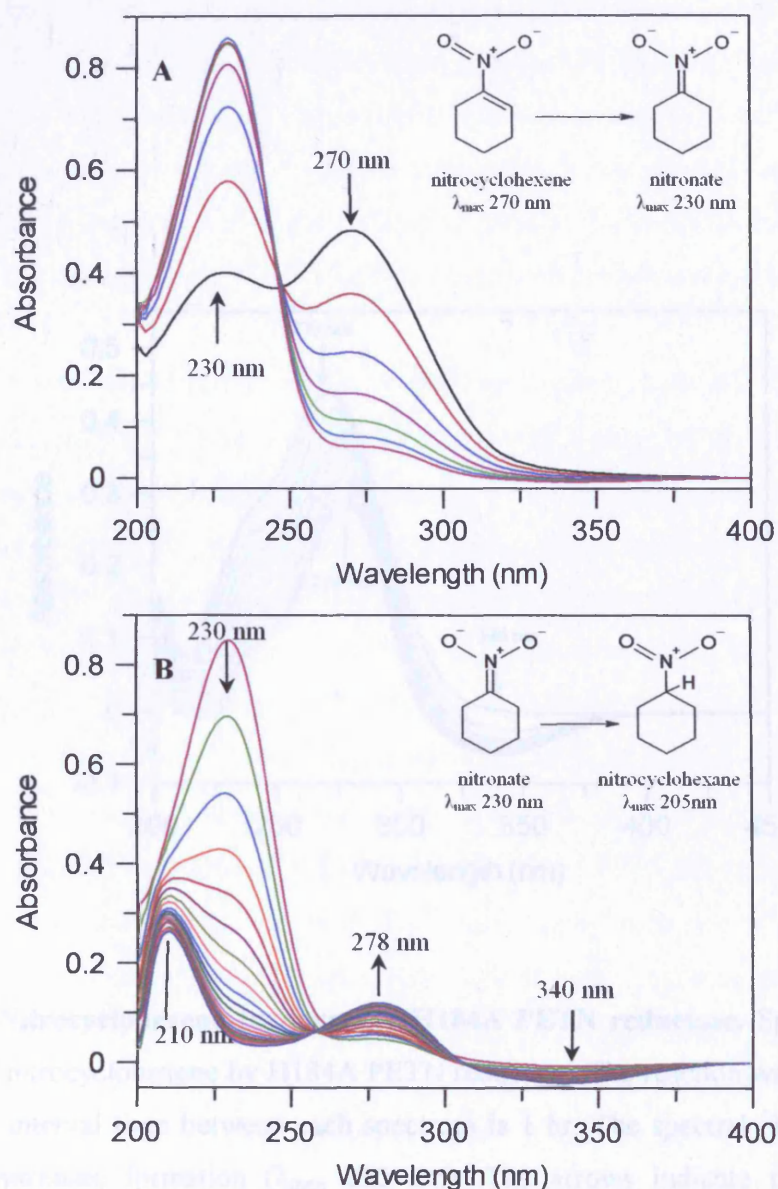


Figure 5.13. Nitrocyclohexene turnover by wild-type PETN reductase. Panel A, spectral changes observed during the first 60 minutes of nitrocyclohexene turnover. Spectra displayed follow the reaction at 10 min intervals. Panel B, Spectral changes observed subsequent to the reaction being left for 60 mins (i.e. spectral changes observed following the changes recorded in panel A). Spectra displayed were recorded at 1 hr intervals. The reaction was recorded for a total of 20 hrs. The arrows indicate the direction of absorbance change in time, at the λ_{\max} specified. Measurements were made using an NADPH regeneration system, with NADPH (8 μM) and enzyme (0.1 μM), which after equilibration at 25 $^{\circ}\text{C}$, was set as the spectrophotometric blank for the reaction. The reaction was initiated with the addition of 80 μM of nitrocyclohexene.

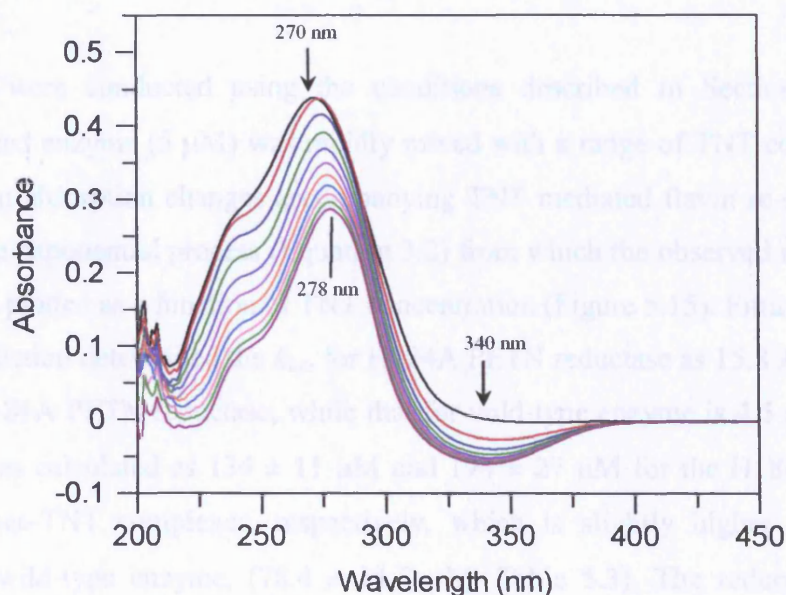


Figure 5.14. Nitrocyclohexene turnover by H184A PETN reductase. Spectra following the turnover of nitrocyclohexene by H184A PETN reductase. The reaction was monitored for 20 hrs and the interval time between each spectrum is 1 hr. The spectral changes show no indication of nitronate formation (λ_{\max} 230 nm). The arrows indicate the direction of absorbance change in time, at the λ_{\max} specified. Measurements were made using an NADPH regeneration system, with NADPH (8 μM) and enzyme (0.1 μM), which after equilibration at 25 $^{\circ}\text{C}$, was set as the spectrophotometric blank for the reaction. The reaction was initiated with the addition of 80 μM of nitrocyclohexene. Similar absorption changes were observed with H181A PETN reductase.

5.3.6 Single wavelength stopped-flow studies of the oxidative-half reaction with TNT

The kinetics of TNT transformation were investigated with the H181A and H184A PETN reductases, using anaerobic stopped-flow spectroscopy at 464 nm. Given that the reduction of TNT proceeds without the involvement of an active site acid, it is expected that the kinetics of this reaction should not be altered greatly. The kinetics may, however, be influenced by the perturbation of TNT binding, where both histidine residues are anticipated to be involved.

Studies were conducted using the conditions described in Section 2.9.1, where dithionite-reduced enzyme (5 μM) was rapidly mixed with a range of TNT concentrations at 25 °C. Transient absorption changes accompanying TNT mediated flavin re-oxidation, were fitted to a single exponential process (Equation 3.2) from which the observed rates (k_{obs}) were determined and plotted as a function of TNT concentration (Figure 5.15). Fitting of the data to a hyperbolic function determined the k_{lim} for H184A PETN reductase as $15.8 \pm 0.3 \text{ s}^{-1}$ and $9.3 \pm 0.4 \text{ s}^{-1}$ for H181A PETN reductase, while that for wild-type enzyme is $4.5 \pm 0.1 \text{ s}^{-1}$ (Table 5.3). The K_d was calculated as $134 \pm 11 \text{ }\mu\text{M}$ and $194 \pm 27 \text{ }\mu\text{M}$ for the H184A and H181A PETN reductases-TNT complexes, respectively, which is slightly higher than the value obtained with wild-type enzyme, ($78.4 \pm 11.7 \text{ }\mu\text{M}$; Table 5.3). The reduced H181A and H184A PETN reductases therefore bind TNT less tightly than the wild-type enzyme, reflecting perhaps a different binding geometry. This in turn may account for the slightly elevated rate of TNT reduction by H181A and H184A PETN reductases.

Single wavelength analysis of TNT transformation was also monitored at 560 nm, to follow the rate of hydride-Meisenheimer complex formation and decay. Studies were conducted using 15 μM of dithionite-reduced enzyme and a range of TNT concentrations at 25 °C. However, no significant increase in absorbance was observed at this wavelength with the mutant proteins. Although the formation of the hydride-Meisenheimer was not observed, a very small decrease in absorbance was identifiable at high TNT concentrations. The decrease in absorbance, suggestive of hydride-Meisenheimer complex decay, was not analysed owing to the absorbance changes being very small (< 0.01 absorbance units) and therefore unreliable. To ascertain whether the minor absorbance changes observed at 560 nm were indicative of hydride-Meisenheimer complex formation/decay, multiple wavelength analysis of TNT reduction was undertaken (Section 5.3.7).

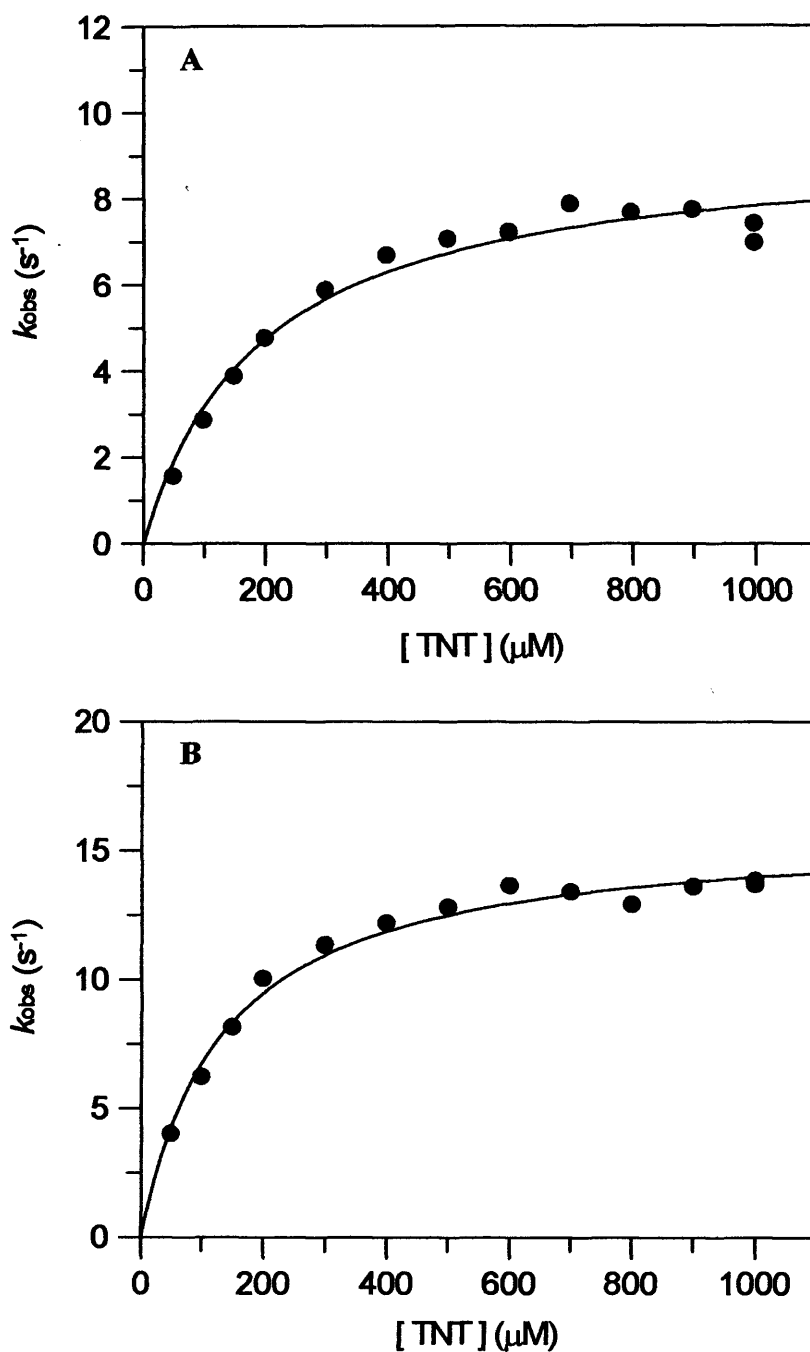


Figure 5.15. The concentration dependence for the rate of electron transfer from dithionite-reduced H181A (Panel A) and H184A (Panel B) PETN reductases to TNT. Anaerobic single wavelength spectroscopy at 464 nm was performed with 5 μM enzyme and a range of TNT concentrations (with a limit of 1 mM), in 50 mM potassium phosphate buffer, pH 7.0, 1% acetone, at 25 °C. Transients were best fit to a single exponential process and the observed rates were plotted as a function of TNT concentration. Data were fitted to a hyperbolic expression.

5.3.7 Anaerobic multiple wavelength stopped-flow studies with TNT

To assess whether the H181A and H184A PETN reductases are able to reduce TNT to the hydride-Meisenheimer complex, anaerobic PDA stopped-flow spectroscopy was used. Studies were conducted using the procedure outlined in Section 2.9.2, where H181A or H184A PETN reductase (40 μM) were stoichiometrically reduced with sodium dithionite (previously calibrated with FMN) and subsequently mixed with either stoichiometric or ten times excess (400 μM) TNT. Reactions were monitored over a range of timescales. Absorption changes accompanying the reaction for both histidine mutant proteins (Figure 5.16) displayed only an increase in flavin absorbance. Data were best fitted to a two-state model ($A \rightarrow B$) using PROKIN software, where reduced enzyme (A) proceeds to form re-oxidised enzyme (B). Given that an increase in absorbance at 560 nm was not evident, it is clear that the two mutant enzymes do not reduce TNT to the respective hydride-Meisenheimer complex.

5.3.8 Anaerobic redox potentiometry

The redox potential for H181A and H184A PETN reductases were measured to ensure that the mutations did not affect the thermodynamic properties of the flavin. The redox potential for both mutant forms of PETN reductase were measured using the method published by Dutton (Dutton, 1978; and is described under Section 2.10), where the reductive titration of each enzyme with sodium dithionite was performed under anaerobic conditions. Each titration was performed in the presence of electron mediators and upon each aliquot of reductant the absorption spectrum was measured and the observed redox potential for that spectrum was noted. Upon complete enzyme reduction, re-oxidation of the enzyme was performed by the titrative addition of potassium ferricyanide. This was done to ensure that the enzyme was able to revert back to its fully re-oxidised state. The redox potential and absorption spectrum was again measured during enzyme re-oxidation to ascertain that the observed potential measured during enzyme reduction matched those measured during the re-oxidation process. During each process, no evidence suggesting the formation of a semiquinone was observed (Figure 5.17A). Taking the absorbance value at 468 nm during enzyme reduction and oxidation and plotting A_{468} as a function of the relevant redox potential (corrected to the standard hydrogen electrode; +244 mV) revealed that the apparent absorption at identical potentials for enzyme reduction and enzyme oxidation were the same.

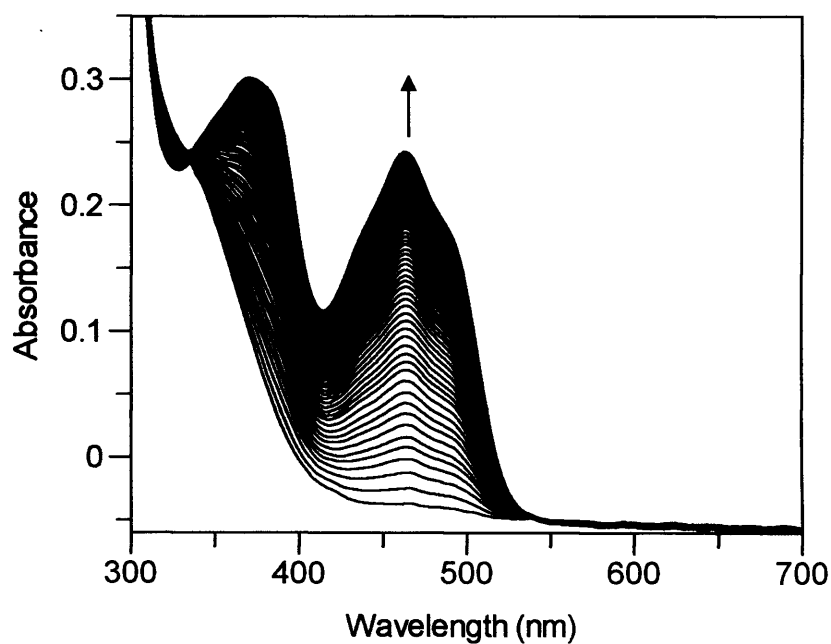


Figure 5.16. Time-dependent spectral changes associated with the reaction of dithionite-reduced H184A PETN reductase and TNT using stopped-flow spectroscopy. Dithionite-reduced H184A PETN reductase (40 μM) was mixed with (400 μM) TNT at 25 $^{\circ}\text{C}$, in 1% acetone, potassium phosphate buffer, pH 7.0, under anaerobic conditions. Spectra were recorded for 4 sec. The arrow indicates the direction of absorbance change in time. A similar data set was observed with H181A PETN reductase

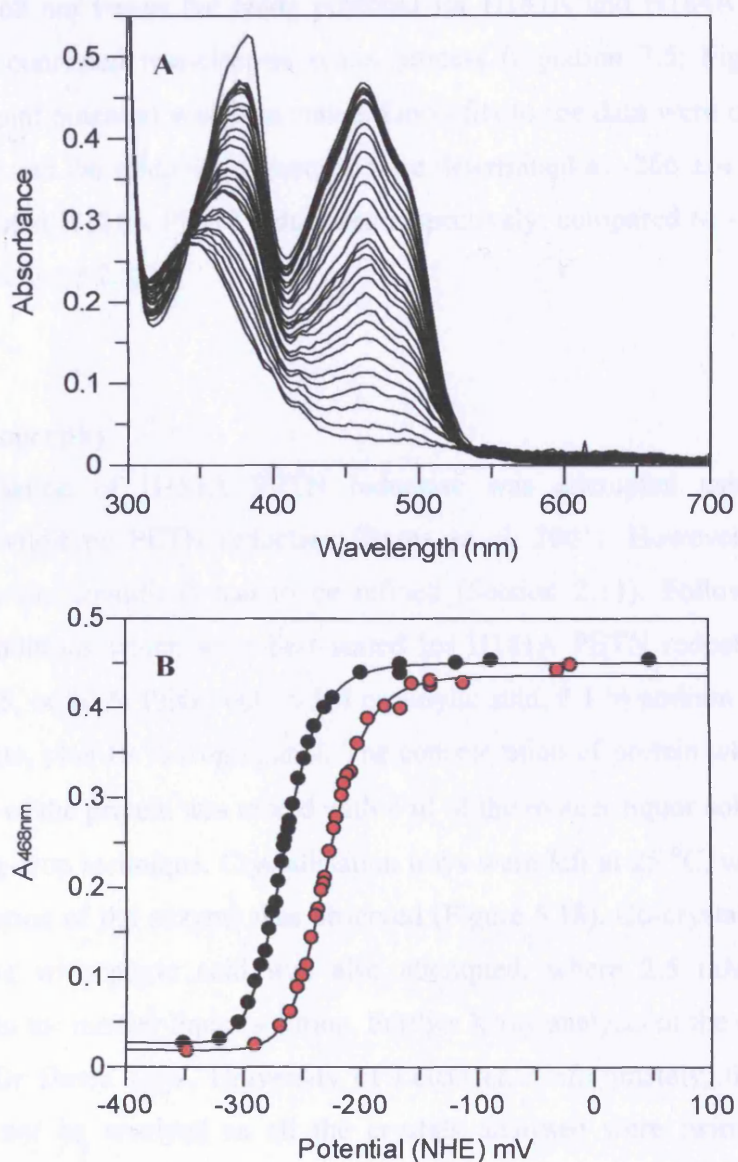


Figure 5.17. Spectral changes (Panel A) and plot of absorbance versus potential (Panel B) measured during the reductive titration of H181A and H184A mutant forms of PETN reductase. Panel A, spectral changes monitored during the titration of H184A PETN reductase with sodium dithionite ($\sim 38 \mu\text{M}$). Similar spectral changes were observed with H181A PETN reductase ($\sim 38 \mu\text{M}$). Panel B, 468 nm absorbance profile of H184A (black circles) and H181A (red circles) PETN reductases, plotted against the measured potential (corrected to the standard hydrogen electrode, +244 mV). Data were fitted to a concerted two-electron redox process (Equation 3.5), from which the midpoint potential was calculated. (NHE is the abbreviation for normal hydrogen electrode).

Consequently, only the data recorded during enzyme reduction were analysed further. Plots of absorbance at 468 nm versus the redox potential for H181A and H184A PETN reductase, fitted best to a concerted two-electron redox process (Equation 3.5; Figure 5.17B), from which the midpoint potential was determined. Good fits to the data were obtained with both mutant enzymes and the midpoint potentials were determined as -266 ± 4 mV and -229 ± 5 mV for H184A and H181A PETN reductases respectively, compared to -267 mV for wild-type enzyme (Section 3.2.12).

5.3.9 Crystallography

Crystallisation of H181A PETN reductase was attempted using the published conditions for wild-type PETN reductase (Barna *et al*, 2001). However, to obtain better quality crystals, the conditions had to be refined (Section 2.11). Following a number of screens, the conditions which were best suited for H181A PETN reductase crystallisation were with 30, 25, or 20 % PEG 3000, 0.5M cacodylic acid, 0.1 M sodium thiocyanate or 0.1 M sodium acetate, plus 10 % isopropanol. The concentration of protein was approximately 9 mg/ml and 4 μ l of the protein was mixed with 4 μ l of the mother liquor solution in each well, using the sitting-drop technique. Crystallisation trays were left at 25 °C, where after nearly a week crystallisation of the enzyme was observed (Figure 5.18). Co-crystallisation of H181A PETN reductase with picric acid was also attempted, where 2.5 mM picric acid was incorporated into the mother liquor solution. Further X-ray analysis of the crystals was kindly performed by Dr David Leys, University of Leicester. Unfortunately, the structure of the enzyme could not be resolved as all the crystals analysed were twinned, and therefore diffraction patterns for a single crystal could not be obtained.

5.4 Discussion

The structure of PETN reductase in complex with a variety of ligands has been reported (Barna *et al*, 2001; Khan *et al*, 2002 and Figure 5.2). In all co-crystal structures it is clear that the ligands are held within the active site by hydrogen bonding to two active site histidine residues, His 181 and His 184, suggesting these residues are key for ligand binding. The work undertaken in this chapter aimed to provide solution evidence for this role. Further

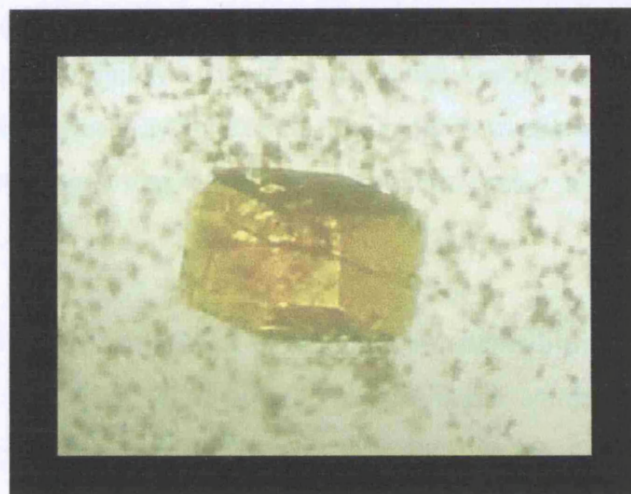


Figure 5.18. Crystallisation of H181A PETN reductase. Good quality crystals were obtained when crystals were grown in a mother liquor solution of 10 % isopropanol, 0.5 M cacodylic acid and between 30-20 % PEG 3000, 0.5M cacodylic acid, and either 0.1 M sodium acetate or sodium thiocyanate, at pH 6.2. The concentration of protein was approximately 9 mg/ml and 4 μ l of the protein was mixed with 4 μ l of the mother liquor solution in each well, using the sitting-drop technique. Crystallisation trays were left at 25 °C, where, after nearly a week, crystal formation of the enzyme was observed. Further analysis of the crystals was kindly performed by Dr David Leys, but unfortunately diffraction patterns could not be solved as all the crystals analysed were twinned.

support for the involvement of these residues in ligand binding comes from the high degree of conservation of His 181 and His 184 among orthologues of PETN reductase, such as OYE, morphinone reductase, and EBP (Figure 5.3). Additionally, the equivalent residues in OYE, His 191 and Asn 194, have been established as being the primary determinants in ligand binding. These findings further prompted an investigation into the role of His 181 and His 184 in PETN reductase. As a result, the histidine pair in PETN reductase were replaced with alanine residues to produce H181A and H184A PETN reductase. The chapter also extends the analysis to assess the possibility of whether either histidine residue could serve as an active site acid in the reduction of 2-cyclohexenone, in addition to characterising the mechanism of nitrocyclohexene reduction by wild-type and mutant enzymes.

5.4.1 Function of His 181 and His 184 in ligand/substrate binding

Dissociation constants for oxidised enzyme-ligand complexes (Table 5.1) revealed that in comparison to wild-type PETN reductase, the binding of picric acid, 2,4-DNP and progesterone is significantly weaker in H181A and H184A PETN reductases. Although the absorption changes were small on ligand binding, reproducible changes were observed and clear isosbestic points were obtained. Also, the dissociation constants determined from studies of the reductive and oxidative half-reaction of both mutant enzymes support the findings obtained from ligand binding studies. In comparison to wild-type enzyme, the dissociation constant for 2-cyclohexenone binding is higher with reduced H181A and H184A PETN reductase, indicating that these mutant enzymes bind 2-cyclohexenone less tightly than wild-type PETN reductase. This is consistent with the structure of wild-type enzyme in complex with 2-cyclohexenone, which reveals that this ligand is held within the active site by forming close contacts through its carbonyl oxygen group to the active site histidine pair (Figure 5.2). Replacement of one of the histidine residues is therefore expected to affect the binding of this substrate. In each of the mutant enzymes only one of the histidine residues is replaced, and one of the binding interactions should remain intact in each enzyme. This might explain why the dissociation constant for 2-cyclohexenone binding is not greatly elevated in the mutant enzymes when compared to wild-type PETN reductase.

5.4.2 Implications of His 181 and His 184 in TNT binding and transformation

The binding of TNT to reduced enzyme, established from studies of the oxidative half-reaction, is weaker in the two histidine mutant enzymes. This is somewhat surprising as the structure of PETN reductase in complex with TNT shows no evidence for the formation of hydrogen bonds between TNT and the histidine residues. However, it is assumed that weak interactions exist between the methyl group of TNT and His 181 and His 184. This is plausible since TNT is observed to bind in a geometry similar to picric acid, where the equivalent hydroxyl group of picric acid is observed to form close contacts with the histidine pair (Khan *et al.*, 2002). The dissociation constants determined from the oxidative half-reaction therefore lends further support to the presumption that TNT is held within the active site by forming weak interactions with His 181 and His 184.

Although it is observed that TNT binds more weakly to the reduced mutant enzymes, this mode of binding leads to a slight increase in the activity of the H181A and H184A PETN reductases towards TNT. Determination of the k_{lim} from stopped-flow studies reveals almost a 2-fold and 4-fold increase in the rate of TNT reduction with H181A and H184A PETN reductase, respectively, in comparison to wild-type enzyme. In the mutant proteins, removal of one of the weak interactions between each histidine residue and TNT might allow the substrate molecule to move more freely within the active site. In turn, this greater degree of flexibility might allow the molecule to orientate above the flavin N5 atom in a position more favourable for hydride transfer. However, and perhaps surprisingly, the mutant enzymes are unable to transform TNT to the respective hydride-Meisenheimer complex. Studies following the single turnover of TNT using single and multiple wavelength stopped-flow spectroscopy, showed no spectral indication for hydride-Meisenheimer complex formation in both mutant enzymes (Section 5.3.6 and 5.3.7). Owing to the mutant enzymes' inability to reduce TNT to the hydride-Meisenheimer complex, it can be inferred that reduction of this substrate therefore occurs via the enzymes nitroreductase activity. These findings contrast with those observed for wild-type PETN reductase, which is believed to transform TNT predominantly via the Meisenheimer pathway (see Chapter 3 and Williams *et al.*, 2004). However, similar findings have been reported recently by Williams and co-workers (Williams *et al.*, 2004) studying the transformation of nitroaromatic compounds by H184N PETN reductase and a number of proteins from the OYE family. These authors demonstrated that the ability to reduce TNT to the respective hydride-Meisenheimer complex is practically abolished in the H184N mutant of PETN reductase, unlike wild-type PETN reductase (Williams *et al.*, 2004). The differences observed here, in the route of TNT degradation between wild-type and the mutant PETN

reductases, might also account for the slight increase in the rate of TNT reduction by H181A and H184A PETN reductase. The change in the preferred route of TNT degradation in each mutant protein might result from TNT binding in an alternative mode to that found in wild-type enzyme. As mentioned earlier, replacement of one of the histidine residues in the mutant PETN reductases would allow TNT to move more freely within the active site due to the removal of one of the binding interactions, which would otherwise hold the molecule in a given orientation above the flavin ring. This allowed freedom might therefore lead to the TNT molecule binding in an orientation where one of the nitro groups is more closely positioned to the flavin N5 atom favouring nitro group reduction. In wild-type enzyme, both histidine residues would form weak interactions with the methyl group of TNT, which might restrict alternative modes of TNT binding. In turn, this restricted mode of binding places the C3 atom of TNT close to the flavin N5 atom (as observed from co-crystal structures) ready for hydride transfer to occur from the flavin to the aromatic ring of TNT, yielding the hydride-Meisenheimer complex. Given that the H181A and H184A PETN reductases are unable to transform TNT via hydride addition to the aromatic ring, it is clear that the histidine residues have a key role in determining the initial route of TNT transformation. This suggestion has also been made recently by Williams and co-workers (Williams *et al*, 2004), based on their finding that the mechanism of TNT transformation by H184N PETN reductase was very similar to OYE. In their study, they observed that OYE and morphinone reductase are able to use TNT as a substrate, but unlike PETN reductase they are unable to reduce the aromatic ring of this compound. These enzymes were therefore only observed to transform TNT to hydroxylaminodinitrotoluene (HADNT) and aminodinitrotoluene (ADNT), via reduction of the nitro groups of TNT, similar to their findings with H184N PETN reductase. Although OYE, morphinone reductase and H184N PETN reductase were unable to produce the hydride-Meisenheimer complex, they were still able to use the purified complex as a starting substrate, reducing it to the dihydride-Meisenheimer complex of TNT. Hence, the initial step in the reduction of TNT plays an important part in governing the eventual route of transformation. Williams and co-workers went on to speculate that the different routes of TNT transformation between OYE, morphinone reductase and PETN reductase (and the H184N mutant enzyme) might reflect the fact that His 184 of PETN reductase is replaced by an asparagine residue in OYE and morphinone reductase (and in H184N). Hence, the histidine residue at position 184 might be important in determining the initial outcome of TNT reduction and so the eventual partitioning between the two routes available for nitroaromatic degradation. However, studies performed in this chapter have also revealed that

replacement of His 181 in PETN reductase produces an enzyme which is unable to form the hydride-Meisenheimer complex. It is, therefore, unlikely that only one residue (i.e. the residue at position 184) of PETN reductase and the equivalent in related enzymes, governs the route of TNT transformation. Although His 184 is replaced by an asparagine in OYE and morphinone reductase, His 181 is highly conserved throughout the family (Figure 5.1). These findings indicate that related enzymes with only one histidine residue at position 181 or 184 (or equivalent position), such as OYE, morphinone reductase, H181A H184A and H184N PETN reductase, are unable to transform TNT to the hydride-Meisenheimer complex. Wild-type PETN reductase, however, has both histidine residues present and preferentially transforms most of the TNT to the hydride-Meisenheimer complex. Generally, the findings presented here and by Williams and co-workers (Williams *et al*, 2004), have interesting implications for our understanding of the different routes of TNT degradation by the OYE family of proteins.

5.4.3 Mechanism of 2-cyclohexenone and nitrocyclohexene reduction

The results outlined in Chapter 4 revealed that Tyr 186 of PETN reductase does not function as the active site acid in the reduction of 2-cyclohexenone. Consequently, it was proposed that either His 181 or His 184 might act as the active site acid. The roles of these residues in the mechanism of α,β -unsaturated compound reduction were therefore investigated. In comparison to wild-type enzyme, the activity of the two mutant proteins towards 2-cyclohexenone was significantly lower. The k_{lim} for 2-cyclohexenone reduction was approximately 77-fold and 111-fold slower than the wild-type enzyme with the H184A and H181A PETN reductases, respectively. Although these findings indicate that the histidine residues play an important role in the reduction of 2-cyclohexenone, it is unlikely that they serve to function as the active site acid. This is evident from the similar rates and degree of decrease in activity with both mutant enzymes. Additionally, studies establishing the role of Tyr 196 as the proton donor in OYE, revealed that the Y196F mutant form of OYE showed almost complete loss of activity towards 2-cyclohexenone ($2.4 \times 10^{-4} \text{ s}^{-1}$) when compared to wild-type OYE (102 s^{-1} ; Kohli and Massey; 1998; Brown *et al*, 1998). In contrast, H181A and H184A PETN reductase are still able to reduce 2-cyclohexenone, albeit at a rate that is significantly slower than wild-type PETN reductase. The decrease in the rate of 2-cyclohexenone reduction by H181A and H184A PETN reductases is therefore likely to be

attributed to other factors, such as alternative modes of 2-cyclohexenone binding in the mutant enzymes. Each histidine residue is known to co-ordinate with the carbonyl oxygen of 2-cyclohexenone, which orientates the substrate molecule over the central flavin ring in a position favourable for hydride transfer. Replacement of one of the residues is therefore likely to affect the binding of 2-cyclohexenone in the mutant proteins, as demonstrated from the increased dissociation constant (Table 5.3). It is plausible that removal of one of the binding interactions allows the molecule to bind in an alternative conformation to that observed with wild-type enzyme, which in turn might be less favourable for hydride transfer. This non-optimal geometry of substrate binding would decrease the mutant proteins' activity towards 2-cyclohexenone, as observed experimentally. Additionally, the formation of hydrogen bonds between His 181 and His 184 and the carbonyl oxygen group of 2-cyclohexenone in wild-type enzyme, activates the β -carbon atom of the substrate rendering the molecule more susceptible to hydride attack from the flavin (see Figure 5.12). Consequently, removal of one of these hydrogen bonds in the H181A and H184A PETN reductases would deactivate the β -carbon atom. This might help to explain why the rate of 2-cyclohexenone reduction is slower for the H181A and H184A PETN reductases. The mutant proteins however, are still able to reduce the substrate and one hydrogen bond is clearly sufficient to partially activate the substrate. To ensure that the decrease in activity towards 2-cyclohexenone with the H181A and H184A PETN reductases is not due to the replacement of a active site acid, further studies with nitrocyclohexene were conducted.

Nitrocyclohexene belongs to the class of unsaturated nitro compounds. These compounds are similar to α,β -unsaturated carbonyls, e.g. 2-cyclohexenone. The nitro group, like a carbonyl group, exerts a strong electron attracting influence within the molecule, which in turn, makes the carbon α atom to the substituent group susceptible to hydride attack (Meah and Massey, 2000). The mechanism of nitrocyclohexene reduction has been characterised by Meah and Massey with OYE (Meah and Massey, 2000) and proceeds in a manner similar to the reduction of 2-cyclohexenone, whereby hydride and proton transfer reduces the olefinic bond in these substrates. However, important mechanistic differences between the reduction of 2-cyclohexenone and nitrocyclohexene exist. Meah and Massey (Meah and Massey, 2000) established that during nitrocyclohexene reduction by OYE, the hydride and proton transfer steps occur in a step-wise fashion, leading to the formation of a spectrally visible intermediate (Figure 5.12). Alternatively, 2-cyclohexenone reduction by PETN reductase proceeds without the formation of an intermediate, with hydride and proton transfer occurring in a concerted

manner. Given that each species present in the reduction of nitrocyclohexene is visible at different wavelengths, the hydride and proton transfer steps can be followed easily. Therefore, to establish whether the lower activity of H181A and H184A PETN reductase with 2-cyclohexenone results from the replacement of the proton donating residue, the reduction of nitrocyclohexene by wild-type and mutant enzymes was characterised. Reactions with wild-type PETN reductase indicated the formation of the nitronate intermediate, which proceeded more slowly than that reported for OYE [OYE complete in ~10 min (Meah and Massey, 2000); PETN reductase complete in ~60 min]. Although the decay of the nitronate was evident, it is difficult to ascertain whether the fully reduced product, nitrocyclohexane, is formed. Nitrocyclohexene has a λ_{\max} at 205 nm, while in the studies reported in this thesis, following nitronate decay the formation of a peak at 210 nm is observed. In addition, increased absorbance at 278 nm is observed at the same time, which might correspond to nitrocyclohexene, which has λ_{\max} at 270 nm. Given the slow rate of the reaction (~20 hrs), these results suggest that following nitronate formation, some of the intermediate is reduced further to form nitrocyclohexane, while some reconverts to nitrocyclohexene. Hence, the combined absorbance of nitrocyclohexene and nitrocyclohexane might cause the observed shift in the λ_{\max} for each compound. Also, negative absorbance changes at 340 nm were observed during nitronate turnover, which is likely to result from NADPH decomposition. Decomposition of NADPH, which was part of the spectrophotometric blank, is also likely to influence the spectral profile of products formed during the reaction. Overall, these findings suggest that wild-type PETN reductase is able to transform nitrocyclohexene to the nitronate intermediate and possibly the fully reduced product, nitrocyclohexane. Spectral profiles following the reaction with the H181A and H184A PETN reductases, although comparable to each other, were clearly different to that described for wild-type enzyme. Each of the histidine mutant proteins is unable to reduce nitrocyclohexene to the nitronate intermediate. Although a decrease in nitrocyclohexene absorbance was observed, it is probably not due to substrate reduction. A significant decrease in absorbance at 340 nm was evident, resulting from NADPH decomposition. The degree of 340 nm absorbance decrease coincides with the negative absorbance change found in other regions of the spectrum indicating that both processes are related. Given that NADPH was part of the spectrophotometric blank, it is likely that the decrease in nitrocyclohexene absorbance reflects the decomposition of NADPH and not substrate turnover. These findings indicate that the two histidine mutant enzymes are unable to reduce nitrocyclohexene, which strongly indicates that the initial hydride transfer step is disrupted. It is therefore, most likely that the decreased rate for 2-cyclohexenone

reduction in the H181A and H184A PETN reductases results from the inability of the enzymes to transfer a hydride ion (rather than a proton) as efficiently as the wild-type enzyme. Disruption of the hydride ion transfer process during 2-cyclohexenone and nitrocyclohexene turnover is likely to result from the failure of the mutant enzymes to bind the substrates as effectively as the wild-type enzyme. His 181 and His 184 are also assumed to form hydrogen bonds with the nitro group of nitrocyclohexene, in a mode comparable to the binding of 2-cyclohexenone. Additionally, like 2-cyclohexenone, hydrogen bonding to the nitro group of nitrocyclohexene further activates the carbon atom attached to the functional group, making it more susceptible to hydride attack. Removal of one of the bonds would therefore leave the molecule less susceptible to hydride attack, as is observed. More pronounced effects on the degree of substrate “inactivation” following mutagenesis are observed with nitrocyclohexene than with 2-cyclohexenone, as the mutant proteins’ activity towards nitrocyclohexene seems to be abolished. This might be attributed to the initial slower rate of nitrocyclohexene turnover by wild-type enzyme.

Overall, the studies reported in this chapter indicate that neither His 181 or His 184 is a proton donor in the oxidative half-reaction of PETN reductase.

5.4.4 Function of His 181 and His 184 in the reductive half-reaction of PETN reductase

Studies characterising the reductive half-reaction of H181A and H184A PETN reductase with NADPH revealed significant differences between these enzymes and wild-type protein. A significant change was found in the dissociation constant for NADPH binding, where the mutant proteins were shown to bind NADPH less tightly than wild-type PETN reductase. The binding of NADPH was mostly perturbed with H184A PETN reductase, which showed almost a 30-fold increase in K_d , while H181A PETN reductase showed approximately a 4-fold increase compared to the wild-type enzyme (Table 5.2). Weaker binding affinity was primarily evident from the change in the dependence of flavin reduction rates on NADPH concentration. While the rates of hydride transfer for wild-type enzyme are shown to be independent of NADPH concentration (Section 3.2.3), both mutant proteins produced rates that exhibited hyperbolic dependence on NADPH concentration. Hence, both His 181 and His 184 are involved in the binding of NADPH, with histidine 184 having a more significant interaction. Replacement of each of the histidine residues also increases the limiting rate of flavin reduction, with the most significant increase being for the H184A PETN reductase. In comparison to wild-type enzyme, the rate of flavin reduction is increased approximately 30-

fold with H184A PETN reductase and 3-fold with H181A PETN reductase. His 184 is inferred to have a more important role in orientating the NADPH molecule parallel to the flavin ring, owing to the faster rate of flavin reduction in H184A PETN reductase. Collectively, these results indicate that in wild-type enzyme, the mode of NADPH binding (which is dependent to some extent on the interactions made between the co-enzyme and each histidine residue) is one that is not completely optimal for hydride transfer, but this might need to be balanced against optimising the active site structure for the oxidative half-reaction. In support of this view is the finding that, on mutation, the limiting flavin reduction rate is increased in the reductive half-reaction, but the oxidative half-reaction with 2-cyclohexenone is compromised.

Studies investigating the reductive half-reaction also revealed that the mutant enzymes do not produce the charge-transfer species which forms prior to flavin reduction in wild-type PETN reductase. Formation of the charge-transfer proceeds quickly in the wild-type enzyme, with part of the transient following its formation in single wavelength stopped-flow studies being lost in the dead-time of the stopped-flow. A possibility is that the charge-transfer signature is lost in the dead-time of the stopped-flow apparatus with the mutant enzymes, but this will require further and more detailed investigation. For the efficient transfer of a hydride ion, NADPH must orientate over the flavin in a position where π - π interactions between NADPH and the flavin ring occur and therefore lead to the formation of a charge-transfer species. Overall, these findings indicate that the histidine residues have an orientating function, whereby they position NADPH in a geometry that favours hydride transfer.

In conclusion, the findings presented in this chapter strongly support a role for His 181 and His 184 as key determinants in the binding of ligands. In addition, findings from studies investigating 2-cyclohexenone and nitrocyclohexene turnover suggest that His 181 and His 184 are unlikely to serve as the active site proton donors in PETN reductase. Interestingly, the histidine pair have also been demonstrated to influence the degradation of TNT in PETN reductase.

Chapter Six

Discussion

CHAPTER SIX

Discussion

Each of the results chapters concludes with a brief discussion; the purpose of this chapter is to provide an overall critical summary of the results obtained and outline their implications for PETN reductase mediated catalysis. In addition, the findings are compared to equivalent studies performed with close homologues of PETN reductase, namely OYE and morphinone reductase. The chapter ends by suggesting future areas of research.

5.1 General properties of PETN reductase and residues involved in ligand binding

PETN reductase was purified to homogeneity using a two-step chromatography procedure (affinity and ion-exchange chromatography) as reported previously by French *et al.*, (French *et al.*, 1996). Mutant forms of PETN reductase, i.e. the W102F, W102Y, and Y186F, enzymes, were all purified using the same procedure described for wild-type enzyme (Section 2.3). The H181A and H184A PETN reductases, which showed low levels of binding to the affinity chromatography matrix (Biomimetic orange resin), were purified using a two-step anion-exchange column (Q-Sepharose). The inability of the H181A and H184A PETN reductases to bind well to the affinity chromatography column provided the first indication of compromised ligand binding in these enzymes. Further detailed studies, involving ligand binding and stopped-flow experiments, supported the presumption that His 181 and His 184 are crucial residues in the binding of picric acid, 2,4-DNP, 2-cyclohexenone, progesterone and nitrocyclohexene, consistent with the structural analysis of wild-type enzyme-ligand complexes (Barna *et al.*, 2001; Khan *et al.*, 2002). These structural studies indicated that His 181 and His 184 form hydrogen bonds with the functional groups of ligands, facilitating their binding in the active site of PETN reductase. Further investigation of the reductive half-reaction of H181A and H184A PETN reductases indicated that His 181 and His 184 are also likely to be involved in binding NADPH (Section 5.3.2). Although the structure of the enzyme bound to NADPH has not been solved, it is anticipated that His 181 and His 184 hydrogen bond to the carbonyl group of NADPH, in a similar fashion to that observed with

other substrates. Compromised binding of NADPH in the mutant enzymes was initially evident from the hyperbolic dependence of hydride transfer rates on NADPH concentration, while those for wild-type enzyme were independent of NADPH concentration. Mutation of His 181 and His 184 therefore led to increased dissociation constants for the enzyme-NADPH complex (113 μM and 973 μM , respectively, compared to 33 μM for wild-type). It has also been hypothesised that TNT binds in the active site of PETN reductase in a geometry similar to that observed for the picric acid-enzyme complex (Khan *et al*, 2002). This assumption is supported by the elevated dissociation constants determined from studies of the oxidative half-reaction with TNT, indicating that the two active site histidines form weak interactions with the methyl group of TNT.

The dissociation constants determined from ligand binding and kinetic studies are not greatly elevated upon mutation of each histidine residue. Presumably, the second histidine residue still interacts with the ligand, preventing gross perturbation of the geometry of ligand binding. In addition, it is plausible that other residues also become actively involved in binding the ligands. Consequently, to ascertain the binding roles of His 181 and His 184, a double mutant should be made and characterised. The roles of the equivalent residues in OYE (His 191 and Asn 194) and morphinone reductase (His 186 and Asn 189) have also been established as the main determinants in ligand binding (Brown *et al*, 1998; Dr Hanan Messiha, University of Leicester, unpublished data), consistent with the high degree of conservation of these residues.

Mutation of Trp 102 in the active site of PETN reductase to Phe 102 and Tyr 102, produces enzymes which are able to bind nitroaromatic explosives more tightly than the wild-type enzyme (Chapter 3). This suggests that Trp 102 interferes with the binding of nitroaromatic compounds, consistent with the observation of multiple conformation states of this residue in crystal structures of enzyme-picric acid complexes (Figure 3.4; Khan *et al*, 2004). Upon picric acid binding, the conformational mobility of Trp 102 relieves the steric clash observed between the C6 nitro group of picric acid and the indole ring of Trp 102. These findings are further supported by structural studies of Trp 102 mutant enzymes in complex with picric acid, which show that the enzymes accommodate the C6 nitro group of picric acid without steric clash. Trp 102, however, does not interfere with the binding of 2,4-DNP (this molecule is structurally similar to picric acid, except for the absence of the C6 nitro group) and progesterone, as anticipated.

In all of the mutations studied (i.e. W102F, W102Y, Y186F, H181A and H184A), none of the residues make direct contact with the FMN moiety. This is consistent with the absence of major perturbations in the redox properties of the mutant enzymes.

5.2 Reductive half-reaction

Despite the high structural similarity between OYE, PETN reductase and morphinone reductase, key differences are discernible in the reductive half-reaction of these enzymes. First, OYE and PETN reductase show preference for NADPH, while morphinone reductase preferentially uses NADH as its reducing co-enzyme. Second, OYE stabilises the red semiquinone of FMN, but the reductive titration of PETN reductase (and morphinone reductase) proceeds directly to the dihydroquinone without stabilising the semiquinone (Section 3.2.12). This therefore indicates that key differences exist in the active sites of these enzymes.

Findings from the kinetic studies on the reductive half-reaction of PETN reductase reported in this thesis are consistent with previous studies (Craig, 2000). The process of enzyme reduction occurs via two distinguishable kinetic steps. In the first step, NADPH binds rapidly to oxidised enzyme forming a charge-transfer complex, which exhibits a charge-transfer absorbance band in the long wavelength region of the enzyme spectrum. Decay of this complex is a direct consequence of hydride transfer from NADPH to the flavin N5 atom, the second step in enzyme reduction. Stopped-flow analysis of the reductive half-reaction indicates that an additional step may occur, prior to charge-transfer formation. This is inferred from the poor fits to the up-phase of the 560 nm data, following charge-transfer formation. This additional step might involve the initial rapid binding of NADPH to oxidised enzyme, but the orientation of NADPH over the flavin is one that is not optimal for hydride transfer. Typically, this step occurs in the dead-time of the stopped-flow. Although direct evidence for this additional binding step is not yet provided in PETN reductase, it has been shown for morphinone reductase (Barna *et al*, 2002) and is suggested to occur in OYE (Massey and Schopfer, 1986; Porter and Bright, 1980). Overall, the reductive half-reaction of PETN reductase has close mechanistic similarities to OYE and morphinone reductase.

Studies with H181A and H184A mutant PETN reductases reveal that these histidine residues play a role in binding NADPH; the K_d for the oxidised enzyme-NADPH complex is increased 30-fold in H184A and 4-fold in H181A PETN reductases, indicating that His 184

has a more significant role in this process than His 181. In addition, both of the mutant enzymes are unable to stabilise the charge-transfer complex that forms prior to flavin reduction, such that it forms and decays at a rate too fast to be captured in PDA or single wavelength stopped-flow studies. The rate of hydride transfer in the mutant proteins is also faster than wild-type enzyme (30-fold in H184A and 4-fold in H181A PETN reductases), which might explain why formation of the charge-transfer complex was unobservable. Alternatively, it is possible that the charge-transfer complex does not form in the mutant enzymes due to perturbation of NADPH binding. The higher rates of hydride transfer in H181A and H184A enzymes can be attributed to the more favourable alignment of the C4 atom of NADPH over the flavin N5 atom for hydride transfer. The increased rates of flavin reduction indicate that the wild-type enzyme is not optimised for this process. This is not surprising given that the enzyme has only one active site that carries out two redox reactions. Therefore, the enzyme cannot optimise one half-reaction without compromising its activity in the other half-reaction, hence the enzyme has effectively evolved to balance the two processes. It is plausible, therefore, that the two histidine residues contribute to maintaining this balance whereby they function to orientate substrates in a position that allows hydride transfer to occur at an appreciable rate, but without compromising the enzyme's activity in the either half-reaction.

Studies with the Y186F mutant of PETN reductase reveal that the rates of charge-transfer formation are too fast to be measured accurately in the stopped-flow. However, the rate of hydride transfer in the mutant enzyme is decreased 3-fold in comparison to wild-type protein. It is probable that, in the mutant enzyme, NADPH binds rapidly in any given orientation over the flavin (explaining faster rates of complex formation) and this limits hydride transfer as the orientation of NADPH binding is non-optimal for this process. In wild-type enzyme Tyr 186 might function to more precisely orientate NADPH over the flavin in a position that favours hydride transfer, thus charge-transfer formation becomes more controlled and hydride transfer is more efficient.

Collectively, studies on the reductive half-reaction show that His 184, His 181 and possibly Tyr 186 have roles in binding and orientating NADPH over the flavin for efficient charge-transfer formation and hydride transfer. The differences in the kinetics are not attributed to changes in the flavin environment as the redox potentials for the mutant enzymes are comparable to those of wild-type enzyme.

5.3 Oxidative half-reaction

5.3.1 Oxidative half-reaction with TNT

PETN reductase reduces nitroaromatic compounds by (i) reduction of the nitro groups leading to the formation of nitroso and HADNT metabolites and (ii) reduction of the aromatic ring leading to the formation of hydride-Meisenheimer complexes. In the case of TNT, under multiple turnover conditions, the hydride-Meisenheimer complex breaks down to form a dihydride-Meisenheimer complex, which is further transformed to unknown products leading to the eventual release of nitrite. Final products of both pathways are unknown, although studies with xenobiotic reductase B suggest the possible abiotic condensation of the dihydride-Meisenheimer complex with HADNT (Pak *et al*, 2000). However, PETN reductase has been shown to transform the chemically synthesised hydride-Meisenheimer complex of TNT through to unidentified products, via formation of the dihydride-Meisenheimer complex and without the production of HADNT and ADNTs (Williams *et al*, 2004). Although PETN reductase is known to transform TNT via the two competing pathways mentioned above, reduction of TNT to the hydride-Meisenheimer complex is favoured, evident from single turnover studies (Chapter 3) demonstrating the transient accumulation of the Meisenheimer complex. Formation of this intermediate complex can be studied conveniently using single turnover stopped-flow studies which demonstrate that formation of the hydride-Meisenheimer is directly related to flavin re-oxidation and that the complex decays as a function of time. The crystal structure of TNT and picric acid bound enzyme complexes reveal that the C3 atom of the substrate is ideally located near the flavin N5 atom so as to receive a hydride from FMN, leading to the production of the hydride-Meisenheimer complex (Khan *et al*, 2002). Given this relatively simple reaction for the reductive attack of the nitroaromatic ring and the close similarity of the active site structure, it is intriguing why OYE and other family members aren't able to reduce TNT via hydride addition to the aromatic ring. The activity of a number of enzymes from the OYE family towards TNT has been investigated and each protein showed some activity in multiple turnover assays (Williams *et al*, 2004). HPLC analysis revealed that each enzyme possesses nitroreductase activity, but the ability to reduce the aromatic ring of TNT is limited to *E. cloacae* and *E. coli* enzymes. Therefore, OYE and morphinone reductase are only shown to reduce the nitro groups of TNT yielding HADNT and ADNT metabolites. However, and interestingly, although these enzymes were unable to produce the hydride-Meisenheimer complex, they were able to transform the chemically

synthesised hydride-Meisenheimer of TNT to the dihydride-Meisenheimer complex and further through to unidentified products, indicating the partial operation of the ring reduction pathway (Williams *et al*, 2004). These findings emphasise that despite the high structural and active site similarity between PETN reductase and OYE, key differences exist that confer the differential reactivity of the enzymes towards the same oxidising substrates. Williams and co-workers suggested that the basis of the ability to reduce the aromatic ring of TNT might be attributed to His 184 in the active site of PETN reductase. In their study, Williams *et al* (Williams *et al*, 2004) demonstrated that the activity of the H184A mutant of PETN reductase was very similar to that of OYE and morphinone reductase, in that the mutant enzyme was unable to transform TNT to the respective hydride-Meisenheimer complex, but was able to transform the chemically synthesised hydride-Meisenheimer complex to the dihydride-Meisenheimer and further reduced products. These results indicated that His 184 of PETN reductase plays a role in the initial reductive reaction of TNT and not further reactions. Studies presented in Chapter 5 are consistent with these results, where re-oxidation of H184A PETN reductase by TNT proceeded without the observable formation of the TNT hydride-Meisenheimer complex, in single wavelength and PDA stopped-flow studies. This differs to the wild-type enzyme which is shown to accumulate the hydride-Meisenheimer complex under single turnover conditions. However, studies presented in Chapter 5 demonstrated that the ability to accumulate the hydride-Meisenheimer complex is also abolished in the H181A mutant of PETN reductase. Both H181A and H184A PETN reductases showed a small increase in their limiting rate constant for TNT reduction when compared to wild-type enzyme. It is plausible that these mutant enzymes transform TNT via nitroreductase activity only given their inability to produce the hydride-Meisenheimer complex, and this might account for their increased activity towards TNT. The above findings suggest that His 184 does not solely confer the ability of PETN reductase to transfer a hydride to the TNT ring, as Williams *et al* (Williams *et al*, 2004) implicated, although it may contribute towards this activity. It is more plausible that both His 181 and His 184 are critical residues for TNT ring reduction activity. In morphinone reductase and OYE the histidine at position 181 of PETN reductase is conserved, but His 184 of PETN reductase is replaced with an asparagine in both these enzymes (Figure 5.3). Therefore, OYE, morphinone reductase, H181A and H184A PETN reductases contain only one active site histidine residue and have been shown to be unable to transfer a hydride ion to the TNT ring. On the other hand, PETN reductase has two active site histidine residues and clearly is able to produce the hydride-Meisenheimer complex of TNT. The inference that the two active site histidine residues at positions 181 and 184 (or

equivalent) of PETN reductase confer ring reduction activity is further supported by the observation of *N*-ethylmaleimide (NEM A) from *E. coli* being able to transform TNT to the hydride-Meisenheimer complex (Williams *et al*, 2004). This enzyme too has two histidine residues at the equivalent position to His 181 and His 184 of PETN reductase (Figure 5.3). These findings suggest an underlying basis for the ability of OYE family of enzymes to reduce the aromatic ring of TNT. The question now remains as to how the two histidine residues influence this process. The histidine pair are key residues in ligand binding (Section 5.1). Stopped-flow studies of the oxidative half-reaction with TNT have shown that mutation of His 181 and His 184 slightly compromises the binding of TNT, as evident from the small increase (approximately 2-fold) in the dissociation constant for the reduced enzyme-TNT complex. Although the structure of the TNT-enzyme complex does not directly indicate that His 181 and His 184 provide direct contacts with TNT, it is possible these residues influence the geometry of TNT binding. This might facilitate TNT in binding to allow the C3 atom of TNT to be positioned close to the FMN N5 atom, favouring hydride attack on the aromatic ring. In the histidine mutant enzymes, loss of one of these weak interactions might lead to the altered alignment of TNT above FMN, such that nitro group reduction is favoured. Alternatively, the histidine residues might have more of a catalytic function whereby they hydrogen bond to one of the nitro groups causing the further depolarisation of the N-O bond, which enhances the electrophilicity of the TNT C3 atom, facilitating hydride attack.

In addition to His 181 and His 184, Trp 102 in the active site of PETN reductase also influences the transformation of TNT (Chapter 3). Although mutation of Trp 102 does not affect the ability of PETN reductase to accumulate the hydride-Meisenheimer complex in single turnover stopped-flow studies, it does seem to influence further reactions. The hydride-Meisenheimer complex accumulated in reactions with W102Y and W102F PETN reductases is shown to be significantly less stable than that for wild-type enzyme, demonstrating that decay of the complex is an enzyme-catalysed process. This kinetic imbalance between wild-type and Trp 102 mutant enzymes is sufficient to generate a different and less complex distribution of reaction products under multiple turnover conditions with W102F and W102Y PETN reductases. This is exemplified by spectroscopic and NMR analysis of multiple turnover reactions, where initially it was observed that the spectroscopic profile of the end products differed between wild-type and Trp 102 mutant enzymes. NMR analysis demonstrated that the mutant enzymes produce a less complex final NMR spectrum than wild-type enzyme. Although some NMR peaks were common in the spectrum for wild-type and the W102Y enzyme, they differed in their relative intensity. These findings indicate that

either (i) different reaction products accumulate in wild-type and Trp 102 mutant PETN reductases or (ii) multiple reaction products accumulate in wild-type and mutant enzymes, but in different concentration distributions. The ability of PETN reductase to transform TNT via two pathways is consistent with both of these possibilities. Unfortunately, the chemical identification of the TNT transformation products catalysed by each enzyme form was made difficult owing to the presence of multiple compounds and hence the complexity of the NMR spectra. However, the less complex distribution of reaction products with Trp 102 mutant enzymes might suggest the more favoured partitioning along the ring reduction pathway in these enzymes. Differences in the mechanism of picric acid transformation were also identifiable between wild-type and Trp 102 mutant enzymes, although detailed analysis of this reaction was made difficult owing to the slow rate of substrate turnover and the volatile nature of picric acid. Trp 102 is conserved throughout the OYE family of proteins, and the ability of these enzymes to transform the chemically synthesised hydride-Meisenheimer complex, but not produce this complex from TNT, suggests interesting implications into the role of this residue in reactions following hydride-Meisenheimer formation.

The striking effect of the mutation of His 181, His 184 and Trp 102 on TNT transformation suggests that His 181 and His 184 play an important role in governing the initial reduction mechanism of TNT (i.e. nitro group or ring reduction), while Trp 102 influences further reductive reactions following hydride-Meisenheimer formation.

5.3.2 Oxidative half-reaction with 2-cyclohexenone

The high degree of conservation in the active site of OYE, MR and PETN reductase reflects the ability of this family of enzymes to reduce "generic" substrates such as 2-cyclohexenone. The crystal structure of PETN reductase-2-cyclohexenone complexes indicate a mechanism whereby hydride transfer to the C1 atom and protonation of C2 atom of the substrate leads to the reduction of the olefinic bond. A similar mechanism operates in the reduction of more complex α,β -unsaturated compounds such as the steroids prednisone and 1,4-androstadiene-3,17-dione, where the stereospecific reduction of the C1-C2 olefinic bond occurs. However, structure determination of steroid-enzyme complexes indicates that reduction of these compounds is somewhat more complicated. In oxidised enzyme-steroid structures the unreactive C4-C5 double bond of steroids is positioned close to the FMN N5 atom, although this bond is not reduced by PETN reductase. NMR studies indicated that in

the reduced state of the enzyme, the steroid substrate flips 180°, so that the substrates C1-C2 double bond is optimally aligned to receive a hydride ion from the flavin N5 atom (Barna *et al.*, 2001). However, recently the crystal structure of the reduced PETN reductase-progesterone complex has been solved and it is observed that progesterone binds to the reduced enzyme in the same orientation to that observed in the oxidised structure (Dr David Leys, verbal communication; Barna *et al.*, 2001), and not in the flipped orientation as proposed by Barna and co-workers (Barna *et al.*, 2001). Since it is established that PETN reductase stereospecifically reduces the C1-C2 double bond of steroids, it can be inferred from the structural data that, in the reduced state, a small enzyme population exists with the steroid bound in the reducible conformation and that differences in the enzyme's redox state alone, is unlikely to induce the steroid to bind in a flipped geometry (Dr David Leys; unpublished data). In contrast to steroid reduction, the mechanism of 2-cyclohexenone reduction is presumed simpler. In morphinone reductase, transfer of a hydride ion and proton to 2-cyclohexenone is shown to be concerted (Basran *et al.*, 2003), consistent with the observation of no spectral intermediates (Craig, 2000). It is therefore most likely that, a concerted transfer operates in OYE and PETN reductase mediated 2-cyclohexenone reduction. Studies with OYE established that the proton donation step is conferred by Tyr 196 in the active site (Kohli and Massey, 1998). This residue is conserved in PETN reductase as Tyr 186, but is substituted by Cys 191 in morphinone reductase. By analogy, it was presumed that Tyr 186 in PETN reductase would be the potential active site acid in the reduction of 2-cyclohexenone. This was further emphasised by structural and NMR studies which indicated that Tyr 186 was ideally located in a position close to the unsaturated bond of the substrate so as to donate a proton (Barna *et al.*, 2001; Khan *et al.*, 2002). However, kinetic studies presented in Chapter 4 have demonstrated that Tyr 186 is unlikely to be the active site acid of PETN reductase. Although replacement of Tyr 186 decreased the limiting rate constant for 2-cyclohexenone reduction in comparison to wild-type enzyme (k_{lim} for Y186F enzyme is 14 s⁻¹, while that for wild-type is 35 s⁻¹), the mutant enzyme still reduced the substrate at a respectable rate, unlike the Y196F mutant of OYE which showed almost complete loss of activity with 2-cyclohexenone (2.4 x 10⁻⁴ s⁻¹ compared to the wild-type OYE rate of 102 s⁻¹; Kohli and Massey, 1998). The decrease in the rate of 2-cyclohexenone reduction by Y186F PETN reductase might be attributed to the altered binding of substrate in the active site, inferred from the change in the dissociation constant determined from stopped-flow studies (Section 4.3.4). 2-cyclohexenone binds more tightly to the mutant enzyme than to wild-type enzyme, but the mode of binding might be one that is non-optimal for hydride-transfer, such

that the C2 atom is positioned far from the flavin N5 atom. The finding that Tyr 186 of PETN reductase is not the active site acid is further supported by the fact that the equivalent residue in morphinone reductase, Cys 191, is not the active site acid (Barna *et al*, 2003). These results highlight further key differences in the mechanism of substrate reduction between OYE, PETN reductase and morphinone reductase.

Studies in Chapter 5 explored further the potential role of His 181 and His 184 as the active site acid in PETN reductase. Stopped-flow kinetic studies revealed a significant reduction in H181A and H184A PETN reductases activity towards 2-cyclohexenone (0.34 s^{-1} and 0.49 s^{-1} , respectively) compared to that of wild-type (35 s^{-1}), accompanied with a considerable increase in the dissociation constant for the reduced enzyme-2-cyclohexenone complex (111-fold and 77-fold, respectively). Although these results indicate that His 181 and His 184 could potentially serve as the proton donor, it is unlikely that both residues fulfil this role. The elevated dissociation constants indicate that the weaker binding of 2-cyclohexenone might compromise substrate reduction. The histidine pair have been shown to form key interactions with the carbonyl oxygen of 2-cyclohexenone, which is presumed to orientate the molecule over the flavin for hydride transfer. In the mutant proteins, removal of one of the hydrogen bonds leads to a presumed different geometry of substrate binding, such that it compromises hydride transfer. To ascertain if the slower rate of 2-cyclohexenone reduction with H181A and H184A PETN reductases is due to compromised hydride transfer and not due to the absence of the proton donor, the turnover of nitrocyclohexene was explored. The advantage of studying this compound is that, unlike in 2-cyclohexenone, the hydride and proton transfer step in OYE is demonstrated to occur stepwise, with the formation of a spectral nitronate intermediate (Meah and Massey, 2000). Studies with the Y196F mutant of OYE and nitrocyclohexene demonstrated that the enzyme could form the nitronate but not the protonated product, consistent with the role of Tyr 196 as the active site acid of OYE (Meah and Massey, 2000). Initially, the turnover of nitrocyclohexene was characterised with wild-type PETN reductase, which was shown to convert the substrate to the nitronate intermediate and possibly nitrocyclohexane, the protonated product. Reactions with H181A and H184A PETN reductases demonstrated that these enzymes were unable to react with nitrocyclohexene. This indicates that hydride transfer is compromised in the mutant proteins which might result from the enzyme's inability to bind the substrate. Removal of one of the hydrogen bonds might compromise the enzyme's ability to bind 2-cyclohexenone and nitrocyclohexene and therefore hinder the optimal alignment of the substrate over FMN. In addition, hydrogen bonding to the carbonyl group in 2-cyclohexenone is suggested to

facilitate reduction of the olefinic bond by activating the carbon atom adjacent to the functional group, rendering the molecule more susceptible to hydride attack from FMN. It is logical to assume similar electrochemical effects on nitrocyclohexene binding. Removal of a hydrogen bond in the mutant enzymes is consistent with the molecule being less susceptible to hydride attack leading to a decrease in the enzymes' activity towards substrate.

The finding that Tyr 186, His 181 and His 184 are unlikely to function as key active site acid residues in PETN reductase raises questions about the identity of the proton donor. However, one should look critically at the results obtained here as the studies described were with artificial substrates, and the active site of the enzyme is not optimised for their reduction. 2-cyclohexenone is a relatively small molecule and it is plausible that a water molecule can leak into the active site and substitute the role of the proton donor in either Y186F, H181A or H184A PETN reductases. This could explain the considerable decrease in activity and the enzymes' residual activity towards the substrate i.e. decreased activity results from mutation of the potential active site acid, but residual activity remains as the substrate can abstract a proton from the solvent. In addition, a water molecule might be hydrogen bonded to either histidine residue or Tyr 186 and therefore in the mutant enzymes the water molecule can protonate the substrate. These suggestions are also consistent with the idea that water is the true proton donor in PETN reductase and decreased activity in the mutant enzymes results from compromised binding as explained above. The inability of the histidine mutant enzymes to react with nitrocyclohexene provides strong support for compromised binding which results in limiting the hydride transfer step and not the protonation step. These suggestions can be extended further to OYE, such that Tyr 196 might not be the true active site acid and a water molecule might play this role. However, the Y196F mutant of OYE was shown to transfer a hydride to nitrocyclohexene, but was unable to transfer a proton, consistent with its role as the active site acid. Further studies are needed to ascertain the identity of the active site acid in PETN reductase and studies with steroids might be more revealing as these bulky molecules would be more effective in excluding solvent from the active site.

5.3.3 Oxidative half-reaction with GTN

PETN reductase was originally isolated on the basis of its ability to degrade nitrate esters, and this activity has now been shown to be a common feature for the OYE family of enzymes. Reduction of nitrate esters has been demonstrated for the xenobiotic reductases of *Pseudomonas fluorescens* I-C and *Pseudomonas putida* II-B (Blehert *et al.*, 1997), *E. coli* N-

ethylmaleimide reductase (Williams *et al*, 1999) and OYE (Meah *et al*, 2001). Recent detailed stopped-flow studies demonstrated that OYE catalyses the NADPH-dependent reduction of the primary nitrate of GTN and PETN, leading to nitrate liberation (Meah *et al*, 2001). Studies presented here reveal that PETN reductase is considerably more active with GTN (313 s^{-1} at $5 \text{ }^{\circ}\text{C}$) than OYE (40 s^{-1} at $25 \text{ }^{\circ}\text{C}$). In fact, GTN is the best substrate known so far for PETN reductase.

Although the mechanism of GTN reduction has not been researched thoroughly in PETN reductase, the effects of a few mutations on this reaction have been investigated, allowing some inferences to be made. Most notably, the presence of an active site residue with the potential to hydrogen bond at position 102 and 186 in PETN reductase plays a significant role in GTN catalysis. This is supported by the finding that GTN reduction is considerably impaired when Trp 102 or Tyr 186 is mutated to phenylalanine (residue with non-polar functional group). In fact, W102F and Y186F PETN reductases reduce GTN with comparable rate constants (52 s^{-1} and 72 s^{-1} , respectively). When Trp 102 is mutated to tyrosine, however, the mutant enzyme retains the ability to reduce GTN with the same limiting rate constant as wild-type enzyme. From these findings it is clear that replacement of a hydrogen bond donating residue with one that is unable to hydrogen bond compromises the ability of the enzyme to reduce GTN.

5.4 Conclusion

The research described in this thesis involved the characterisation of PETN reductase and allowed comparisons with the OYE family. This in turn highlighted key differences in the reactivity of OYE and PETN reductase towards oxidising substrates, although the reductive half-reactions are comparable. This study has indicated the importance of two active site histidine residues in governing the initial route of TNT transformation in PETN reductase, with Trp 102 determining the fate of further reaction products. In addition, a key difference in the mechanism of 2-cyclohexenone reduction between OYE and PETN reductase is that the active site acid of OYE is not conserved in PETN reductase. Furthermore preliminary investigations into GTN catalysis suggest the importance of Tyr 186 and Trp 102 in this reaction. Collectively, the results have demonstrated that small changes in the active site of PETN reductase (and therefore of related enzymes), opens up the possibility of selectively engineering enzymes to catalyse reactions of interest. For phytoremediation purposes, the

possibility of engineering enzymes to reduce the aromatic ring of nitroaromatic explosives promises to be an efficient and exciting strategy. However, further detailed studies are needed to ascertain the mechanism and identity of products formed from PETN reductase mediated catalysis.

5.5 Future areas of research

An important area of research based on the findings presented herein, is to provide further evidence for the identity of the active site acid in PETN reductase. It is suggested that water might act as the proton donor in the reduction of 2-cyclohexenone, but this needs to be ascertained. This would be of particular interest as the active site structure of PETN reductase and OYE are considerably similar, yet the conserved Tyr residue that functions as the active site acid in OYE does not act in the same way in PETN reductase. Such findings highlight important differences between the two enzymes and also question the true role of Tyr 196 in OYE.

A second and important area of research is to fully characterise the mechanism of nitrocyclohexene transformation by PETN reductase, as only preliminary investigations were made in this study. PETN reductase is shown to transform this substrate to the nitronate intermediate and it is suggested that the protonated product forms, but this cannot be confirmed due to slight differences in the reported spectral properties of the product and that found here. Detailed analysis of nitrocyclohexene reduction might provide further insight into the roles of active site residues in PETN reductase, in particular the identity of the proton donating residue.

The mechanism of GTN reduction should also be explored in PETN reductase, as the findings presented here have suggested important roles for Trp 102 and Tyr 186 in this reaction. The roles of these residues in GTN reduction should be investigated further, and complemented by structural studies. Investigations of this type would be particularly useful given the high activity of PETN reductase with this substrate and its potential use in remediating GTN contaminated soil and water. Therefore, an investigation into the products formed and their associated toxicity would be of particular interest.

Solving the structure of the mutant enzymes studied in this thesis with substrates bound would be informative, as many of the differences found between wild-type and mutant enzymes have been attributed to altered modes of substrate binding. This would be extremely useful if the structure of the reduced enzyme-substrate complexes could be solved, as the enzyme is catalytically active when in its reduced form. Furthermore, solving the structure of PETN reductase with an NADPH analogue would help to identify key active site residues that confer NADPH over NADH specificity. Mutagenic studies would ascertain the roles of any residues inferred to be involved in this process. Sequence and structural alignment studies of OYE, PETN reductase and morphinone reductase will identify further potential residues that confer NADPH/NADH specificity, as each enzyme shows considerable structural and sequence similarity.

An area of particular interest is the ability of PETN reductase to transform persistent explosives such as TNT. Characterisation of the mechanism of TNT catalysis by PETN reductase would therefore make a considerable contribution to the enzyme's potential application in phytoremediation. In particular, the identity of transformation products from the nitroreductase and ring reduction pathways should be identified. Characterisation of products through their spectral properties, NMR profiles and mass spectrometry, would be extremely useful in identifying transformation products produced by mutant enzymes or other enzymes able to degrade explosives. In particular, the roles of Trp 102, His 181 and His 184 in TNT transformation should be investigated further as these residues play a key role in TNT catalysis and will therefore aid in our understanding of the mechanism of TNT reduction and help to explain why related enzymes that possess nitroreductase activity are unable to reduce the aromatic ring of TNT. In turn, these studies would open the exciting possibility of engineering such enzymes to transform TNT, via ring reduction, to products which are less toxic than TNT and biodegradable.

A final area of research would be to find the physiological substrate of PETN reductase, so that its natural function can be identified.

References

REFERENCES

- Abramovitz, A.S., and Massey, V. (1976a) Purification of intact old yellow enzyme using an affinity chromatography matrix for the sole chromatographic step. *Journal of Biological Chemistry* **251**, 5321-5326.
- Abramovitz, A.S., and Massey V. (1976b) Interaction of phenols with old yellow enzyme. Physical evidence for charge-transfer complexes. *Journal of Biological Chemistry* **251**, 5327-5336.
- Accashian, J.V., Vinopal, R.T., Kim, B.J. and Smets, B.F. (1998) Aerobic growth on nitroglycerin as the sole carbon, nitrogen, and energy source by a mixed bacterial culture. *Applied and Environmental Microbiology* **64**, No. 9, 3300-3304.
- Anderson, T.A., Guthrie, E.A. and Walton, B.T., (1993) Bioremediation in the rhizosphere. *Environmental Science Technology* **27**, 2630-2636.
- Anusevicius, Z., Sarlauskas, J., Nivinskas, H., Segura-Aguilar, J. and Cenas, N. (1998) DT-diaphorase catalyses the N-denitration and redox cycling of tetryl. *FEBS letters* **436**, 144-148.
- Anusevicius, Z., Soffers, A.E.M.F., Cenas, N., Sarlauskas, J., Martinez-Julvez, M. and Rietjens, I.M.C.M. (1999) Quantitative structure-activity relationships for electron transfer reactions of *Anabaena PCC 7119* ferredoxin-NADP⁺ oxidoreductase with nitrobenzene and nitrobenzimidazolene derivatives: mechanistic implications. *FEBS letters* **450**, 44-48.
- Banerjee, H.N., Verma, M., Hou, L.H, Ashraf, M. and Dutta, S.K. (1999) Cytotoxicity of TNT and its metabolites. *Yale Journal of Biological Medicine* **72**, 1-4.
- Barna, T., Khan, H., Bruce, N.C., Baruskov, I., Scrutton, N.S. and Moody, P.C.E. (2001) Crystal structure of pentaerythritol tetranitrate reductase: "flipped" binding geometries for steroid substrates in different redox states of the enzyme. *Journal of Molecular Biology* **310**, 433-447.

- Barna, T., Messiha, H.L., Petosa, C., Bruce, N.C., Scrutton, N.S. and Moody, P.C.E. (2002) Crystal structure of bacterial morphinone reductase and properties of the C191A mutant enzyme. *Journal of Biological Chemistry* **277**, 30976-30983.
- Basran, J., Harris, R.J., Sutcliffe, M.J. and Scrutton, N.S. (2003) Hydrogen-tunnelling in the multiple hydrogen-transfers of the catalytic cycle of morphinone reductase and in the reductive half-reaction of the homologous pentaerythritol tetranitrate reductase. *Journal of Biological Chemistry* **278**, 43973-43982.
- Behrend, C. and Heesche-Wagner, K. (1999) Formation of hydride-Meisenheimer complexes of picric acid (2,4,6-trinitrophenol) and 2,4-dinitrophenol during mineralisation of picric acid by *Norcardioides* sp. strain CB 22-2. *Applied and Environmental Microbiology* **65**, 6912-6920.
- Best, E.P.H, Zappi, M.E., Fredrickson, H.L., Sprecher, S.L., Larson, S.L. and Ochn, M. (1997) Screening of aquatic and wetland plant species for phytoremediation of explosive-contaminated groundwater for the Iowa Army Ammunition Plant. *Annual New York Academy of Science* **829**, 179-194.
- Bhadra, R., Wayment, D.G., Williams, R.K., Barman, S.N, Stone, M.B Hughes, J.B. and Shanks, J.V (2001) Studies on plant-mediated fate of the explosives RDX and HMX. *Chemosphere* **44**, 1259-1264.
- Bhushban, B., Trott, S., Spain, J.C., Halasz, A., Paquet, L. and Hawari, J. (2003) Biotransformation of hexahydro-1,3,5-trinitro-1,3,5-triazine (RDX) biodegradation by *Rhodococcus* sp. strain DN 22. *Applied and Environmental Microbiology* **69**, 1347-1351.
- Binks, P.R., C.E. French, Nicklin, S. and Bruce, N.C. (1996) Degradation of pentaerythritol tetranitrate by *Enterobacter cloacae* PB2. *Applied and Environmental Microbiology* **62**, 1214-1219.
- Blehert, D.S., Fox, B.G. and Chambliss, G.H. (1999) Cloning and sequence analysis of two *Pseudomonas* flavoprotein xenobiotic reductases. *Journal of Bacteriology* **181**, 6254-6263.

Blehert, D.S., K.L. Knoke, Fox, B.G. and Chambliss G.H. (1997) Regioselectivity of nitroglycerin denitration by flavoprotein nitroester reductases purified from two *Pseudomonas* species. *Journal of Bacteriology* **179**, 6912-6920.

Boopathy, R. (2002) Effect of food-grade surfactant on bioremediation of explosive contaminated soil. *Journal of Hazardous Material* **92**, 103-114.

Boyd, E. and Bruce, N.C. (2002) Defusing the environment. *Microbiology Today* **29**, 72-74.

Boyd, G., Mathews, F.S., Packman, L.C. and Scrutton, N.S (1992) Trimethylamine dehydrogenase of bacterium W₃A₁: molecular cloning, sequence determination and over expression of the gene. *FEBS Letters* **308**, 271-276.

Breinlinger, E.C., Keeman, C.J. and Rotello, V.M. (1998) Modulation of flavin recognition properties through donor atom - π interactions. *Journal of the American Chemical Society* **120**, 8606-8609.

Breithaupt, C., Strassner, J., Breitingner, U., Huber, R., Macheroux, P., Schaller, A. and Clausen, T. (2001) X-ray structure of 12-oxophytodienoate reductase provides structural insight into substrate specificity within the family of OYE. *Structure* **9**, 419-429.

Brown, B.J., Dheng, Z., Karplus, P.A and Massey, V. (1998) On the active site of old yellow enzyme. Role of Histidine 191 and Asparagine 194. *Journal of Biological Chemistry* **273**, 32753-32762.

Bruce, N.C., Wilmot, C.J., Jordan, K.N., Gray Stephens, L.D and Lowe, C.R (1991) Microbial degradation of the morphine alkaloids. Purification and characterisation of morphine dehydrogenase from *Pseudomonas putida* M10. *Biochemical Journal* **274**, 875-880.

Bruce, N.C., Wimot, C.J., Jordan, K.N., Trebilcock, A.E., Gray Stephens, L.D. and Lowe C.R. (1990) Microbial-degradation of the morphine alkaloids - identification of morphinone as an intermediate in the metabolism of morphine by *Pseudomonas putida* M10. *Archives of Microbiology* **154**, 465-470.

- Buckman, J. and Miller, S.M. (1998) Binding and reactivity of *Candida albicans* estrogen binding protein with steroids and other substrates. *Biochemistry* **37**, 14326-14336.
- Buckman, J. and Miller, S.M. (2000a) Transient kinetics and intermediates formed during the electron transfer reaction catalysed by *Candida albicans* estrogen binding protein. *Biochemistry* **39**, 10521-10531.
- Buckman, J. and Miller, S.M. (2000b) Stabilisation of a novel enzyme-substrate intermediate in the Y206F mutant of *Candida albicans* EBP1: Evidence for acid catalysis. *Biochemistry* **39**, 10532-10541.
- Buckman, J., Miller, S.M., Malloy, P. and Feldman, D. (1996) in *Flavins and flavoproteins 1996: Twelfth international symposium*, (Eds, Stevenson K.J., Massey V. and Williams C.H), 81, University of Calgary Press, Calgary, Alberta Canada.
- Burken, J.G and Schnoor, J.L. (1997) Uptake and metabolism of atrazine by poplar trees. *Environmental Science Technology* **31**, 1399-1402.
- Byrant, C. and De Luca, M. (1991) Purification and characterisation of an oxygen-insensitive NAD(P)H nitroreductase from *Enterobacter cloacae*. *Journal of Biological Chemistry* **266**, 4119-4125.
- Cenas, N., Nemeikaite-Ceniene, A., Stergediene, E., Nivinskas, H., Anusevicius, Z. and Sarlauskas, J. (2001) Quantitative-structure-activity relationships in enzymatic single electron reduction of nitroaromatic explosives: implications for their cytotoxicity. *Biochimica et Biophysica Acta* **1528**, 31-38.
- Chen, Z., Zhang, J. and Strauler, J.S. (2002) Identification of the enzymatic mechanism of nitroglycerin bioactivation. *Proceedings of the National Academy of Science* **99**, 8306-8311.
- Cole, S.T. (1982) Nucleotide sequence for the flavoprotein subunit of fumurate reductase of *Escherichia coli*. *European Journal of Biochemistry* **122**, 479-4784.

- Coleman, N.V., Spain, J.C. and Duxbery, T. (2002) Evidence that RDX biodegradation by *Rhodococcus* strain DN 22 is plasmid-borne and involves a cytochrome P-450. *Journal of Applied Microbiology* **93**, 464-472.
- Costa, C.L., Arruda, P. and Benedetti, C.E. (2000) An *Arabidopsis* gene induced by wounding, is functionally homologous to flavoprotein oxidoreductases. *Plant Molecular Biology* **44**, 61-71.
- Craig D.H., Barna, T., Moody P.C.E., Bruce N.C., Chapman, S.K., Munro, A.W. and Scrutton, N.S. (2001) Effects of environment on flavin reactivity in morphinone reductase: analysis of an enzyme displaying differential charge near the N-1 atom and C-2 carbonyl region of the active site flavin. *Biochemical Journal* **359**, 315-323.
- Craig, D. (2000) Mechanistic and kinetic studies of morphinone reductase and PETN reductase. *Ph. D. Thesis*.
- Craig, D.H., Moody, P.C.E., Bruce N.C. and Scrutton, N.S. (1998) Reductive and oxidative half-reactions of morphinone reductase from *Pseudomonas putida* M10: A kinetic and thermodynamic analysis. *Biochemistry* **37**, 7598-7607.
- Daff, S.N., Chapman, S.K., Turner, K.L., Holt, R.A., Govindaraj, S., Poulos, T.L., and Munro, A.W. (1997) Redox control of the catalytic cycle of flavocytochrome P-450 BM3. *Biochemistry* **36**, 13816-13823.
- Decker, K. (1991) Covalent flavoproteins (Chapter 13). in *Chemistry and Biochemistry of Flavoenzymes* Vol II, (Ed, Muller, F.), CRC Press.
- Doel, J.L., Godber, B.L.J., Eisenthal, B. and Harrison, R. (2001) Reduction of organic nitrates catalysed by xanthine oxidoreductase under anaerobic conditions. *Biochimica et Biophysica Acta* **1527**, 81-87.
- Dreyer, J.L. (1984) Electron transfer in biological systems: an overview. *Experientia* **40**, 653-776.

- Duine, J.A. (2001) Co-factor diversity in biological oxidations: implications and applications. *Chemical Record* **1**, 74-83.
- Duque, E., Haidour, A., Godoy, F. and Ramos, J.L. (1993) Construction of a *Pseudomonas* hybrid strain that mineralises 2,4,6-trinitrotoluene. *Journal of Bacteriology* **175**, 2278-2283.
- Dutton, P. (1978) Redox Potentiometry: Determination of midpoint potentials of oxidation-reduction components of biological electron transfer systems. *Methods in Enzymology* **54**, 411-435.
- Ebert, S., Fischer, P. and Knackmuss, H-J. (2001) Converging catabolism of 2,4,6-trinitrophenol (picric acid) and 2,4-dinitrophenol by *Nocardioides simplex* FJ2-1A. *Biodegradation* **12**, 367-376.
- Ebert, S., Rieger, P.G. and Knackmuss, H-J. (1999) Function of co-enzyme F420 in aerobic catabolism of 2,4,6-trinitrophenol and 2,4-dinitrophenol, by *Nocardioides simplex* FJ2-1A. *Journal of Bacteriology* **181**, 2669-2674.
- Esteve-Nunez, A., Cabellero, A. and Ramos, J.L. (2001) Biological degradation of 2,4,6-trinitrotoluene. *Microbiology and Molecular Biology Reviews* **65**, 335-352.
- Esteve-Nunez, A., Lucchesi, G., Phillip, B., Schink, B. and Ramos, J.L. (2000) Respiration of 2,4,6-trinitrotoluene by *Pseudomonas* sp. strain JL RII. *Journal of Bacteriology* **182**, No. 5, 1352-1355.
- Fiorella, P.D. and Spain, J.C. (1997) Transformation of 2,4,6-trinitrotoluene by *Pseudomonas pseudoalcaligenes* JS 52. *Applied and Environmental Microbiology* **63**, 2007-2015.
- Fitzpatrick, P.F. (2001) Substrate dehydrogenation by flavoproteins. *Accounts of Chemical Research* **34**, 299-307.
- Fitzpatrick, T.B., Amrhein, N. and Macheroux, P. (2003) Characterisation of Yqj M, an old yellow enzyme homolog from *Bacillus subtilis* in oxidative stress response. *Journal of Biological Chemistry* **278**, 19891-19897.

Fournier, D., Halasz, A., Spain, J., Fiurasek, P. Hawari, J. (2002) Determination of key metabolites during biodegradation of hexahydro-1,3,5-trinitro-1,3,5-triazine with *Rhodococcus* sp. strain DN 22. *Applied and Environmental Microbiology* **68**, 166-172.

Fox, K.M. and Karplus, P.A. (1994) Old yellow enzyme at 2.Å resolution: overall structure, ligand binding and comparison with related flavoproteins. *Structure* **2**, 1089-1105.

Fox, K.M. and Karplus, P.A. (1999) The flavin environment in OYE. An evaluation of insights from spectroscopic and artificial flavin studies. *Journal of Biological Chemistry* **274**, 9357-9362.

Fraaije, M.W. and Mattevi, A. (2000) Flavoenzymes: diverse catalysts with recurrent features. *Trends in Biochemical Sciences* **25**, 126-132.

French, C.E. and Bruce, N.C. (1994) Purification and characterisation of morphinone reductase from *Pseudomonas putida* M10. *Biochemical Journal* **301**, 97-103.

French, C.E. and Bruce, N.C. (1995) Bacterial morphinone reductase is related to old yellow enzyme. *Biochemical Journal* **312**, 671-678.

French, C.E., Nicklin, S. and Bruce, N.C. (1996) Sequence and properties of pentaerythritol tetranitrate reductase from *Enterobacter cloacae* PB2. *Journal of Bacteriology* **178**, 6623-6627.

French, C.E., Nicklin, S. and Bruce, N.C. (1998) Aerobic degradation of 2,4,6-trinitrotoluene by *Enterobacter cloacae* PB2 and by pentaerythritol tetranitrate reductase. *Applied and Environmental Microbiology* **64**, 2864-2868.

French, C.E., Rosser, S.J., Davies, G.J., Nicklin, S. and Bruce, N.C. (1999) Biodegradation of explosives by transgenic plants expressing pentaerythritol tetranitrate reductase. *Nature Biotechnology* **17**, 491-494.

- George, S.E., Higgins-Clark, G. and Brooks, L.R. (2001) Use of a *Salmonella microsuspension* bioassay to detect the mutagenicity of munition compounds at low concentrations. *Mutational Research* **490**, 45-46.
- Gerlt, J.A. and Raushel, F.M. (2003) Evolution and function in (β/α)₈-barrel enzymes. *Current opinions in Chemical Biology* **7**, 252-264.
- Ghisla, S. and Massey, V. (1989) Mechanism of flavoprotein-catalysed reactions. *European Journal of Biochemistry* **181**, 1-17.
- Giri, A., Dhingra, V.F., Giri, C.C., Singh, A., Ward, O.P. and Narasu, M.L. (2001) Biotransformation using plant cells, organ cultures and enzyme systems: current trends and future prospects. *Biotechnological Advances* **19**, 175-199.
- Goel, A., Kumar, G., Payne, G. and Dube, S. (1997) Plant cell biodegradation of xenobiotic nitrate ester, nitroglycerine. *Nature Biotechnology* **15**, 174-177.
- Haidour, A. and Ramos, J.L. (1996) Identification of products resulting from the biological reduction of 2,4,6-trinitrotoluene, 2,4,-dinitrotoluene and 2,6-dinitrotoluene by *Pseudomonas* sp. *Environmental Science Technology* **30**, 2365-2370.
- Haigler, B.E., Johnson, G.R., Shen, W.C. and Spain, J.C. (1999) Biochemical and genetic evidence for meta-ring cleavage of 2,4,5-trihydroxytoluene in *Burkholderia* sp. strain DNT. *Journal of Bacteriology* **181**, 965-972.
- Hailes, A.M. and Bruce, N.C. (1993) Biological synthesis of the analgesic hydromorphone, and intermediate in the metabolism of morphine by *Pseudomonas putida* M10. *Applied and Environmental Microbiology* **59**, 2166-2170.
- Hannik, N., Rosser, S.J., French, C.E., Basran, A., Murray, J.A.H., Nicklin, S. and Bruce, N.C. (2001) Phytodetoxification of TNT by transgenic plants expressing a bacterial nitroreductase. *Nature Biotechnology* **9**, 1168-1172.

Harris, R.J., Khan, H., Barna, T., Moody, P.C.E. and Scrutton, N.S. (2002) Mechanistic studies of Trp 102 mutant forms of pentaerythritol tetranitrate reductase. In *Flavins and Flavoproteins 2002: Fourteenth International Symposium*, (Eds, Perham, R.N., Chapman, S.K. and Scrutton, N.S.), Rudolf Weber, Berlin, 247-252.

Harvey, S., Fellows, R.J., Cataldo, D.A. and Bean, R.M. (1991) The fate of explosive hexahydro-1,3,5-trinitro-1,3,5-triazine (RDX) in soil and bioaccumulation in bush bean hydroponic plants. *Environmental Toxicological Chemistry* **10**, 845-855.

Hawari, J., Halasz, L., Palquet, E., Zhou, B., Spencer, B., Ampleman, G. and Thiboutot, S. (1998) Characterisation of metabolites in the biotransformation of 2,4,6-trinitrotoluene with anaerobic sludge: A role of triaminotoluene. *Applied and Environmental Microbiology* **64**, 2200-2206.

Haynes, C.A., Koder, R.L., Miller, A-F. and Rodgers, D.W. (2002) Structure of nitroreductases in three states: Effects of inhibitor binding and reduction. *Journal of Biological Chemistry* **277**, 11513-1520.

Heiss, G. and Knackmuss, H-J. (2002) Bioelimination of trinitroaromatic compounds: immobilisation versus mineralisation. *Current Opinions in Microbiology* **5**, 282-287.

Heiss, G., Hofmann, K.W., Trachtmann, N., Walters, D.M., Ronviere, P. and Knackmuss, H-J. (2002) *npd* gene functions of *Rhodococcus (opacus) erythropolis* HL PM-1 in the initial steps of 2,4,6-trinitrophenol degradation. *Microbiology* **148**, 799-806.

Higson, F.K. (1992) Microbial degradation of nitroaromatic compounds. *Advances in Applied Microbiology* **37**, 1-19.

Hocker, B., Jurgens, C., Wilmanns, M. and Sterner, R. (2001) Stability, catalytic versatility and evolution of the (β/α)₈-barrel fold. *Current opinions in Biotechnology* **12**, 376-381.

Hocker, B., Schmidt, S. and Sterner, R. (2002) A common evolutionary origin of two elementary enzyme folds. *FEBS Letters*, 510, 133-135.

- Hofrichter, M., Scheibner, K., Schneegab, I. and Fritsche, W. (1998) Enzymatic combustion of aromatic and aliphatic compounds by manganese peroxidase from *Nematoloma frowardii*. *Applied and Environmental Microbiology* **64**, No. 2, 399-404.
- Honeycutt, M.E., Jarvis, A.S. and McFarland, V.A. (1996) Cytotoxicity and mutagenicity of 2,4,6-trinitrotoluene and its metabolites. *Ecotoxicological and Environmental Safety* **35**, 282-287.
- Hooker, B.S. and Skeen, R.S. (1997) Transgenic phytoremediation blasts onto the scene. *Nature Biotechnology* **17**, 428.
- Huang, M-J. and Leszczynski, J. (2002) The mechanism of the radical-anion reduction of 2,4,6-trinitrotoluene: a theoretical insight. *Journal of Molecular Structure: THEOCHEM* **592**, 105-113.
- Huang, S., Lindahl, P.A., Wang, C., Bennett, G.N., Rudolph, F.B. and Hughes, J.B. (2000) 2,4,6-trinitrotoluene reduction by carbon monoxide dehydrogenase from *Clostridium thermoaceticum*. *Applied and Environmental Microbiology* **66**, 1474-1478.
- Hughes, J.B., Wang, C., Yesland, K., Bhadra, R., Richardson, A., Bennet, G. and Rudolph, F. (1998) Reduction of 2,4,6-trinitrotoluene by *Clostridium acetobutylicum* through hydroxylamino intermediates. *Environmental Toxicological Chemistry* **17**, 343-348.
- Hughes, J.S., Shanks, J., Vanderford, M., Lauritzen, J. and Bhadra, R. (1997) Transformation of TNT by aquatic plants and plant tissue cultures. *Environmental Science Technology* **31**, 266-271.
- Kalafut, T., Wales, M.E., Rastogi, V.K., Naumova, R.P., Zaripova, S.K. and Wild, J.R. (1998) Biotransformation patterns of 2,4,6-trinitrotoluene by aerobic bacteria. *Current Microbiology* **36**, 45-54.
- Karplus, P.A., Fox, K.M and Massey, V. (1995) Structure-function relations for old yellow enzyme. *FASEB Journal* **9**, 1518-1526.

- Khan, H., Harris, R.J, Barna, T., Craig D.H., Bruce N.C., Munro, A.W., Moody, P.C.E. and Scrutton, N.S. (2002) Kinetic and structural basis of reactivity of pentaerythritol tetranitrate reductase with NADPH, 2-cyclohexenone, nitroester and nitroaromatic explosives. *Journal of Biological Chemistry* **277**, 21906-21912.
- Kobori, T., Sasaki, H., Lee, W.C., Zenno, S., Saigo, K., Murphy, M.E.P. and Tanokura, M. (2001) Structure and site-directed mutagenesis of a flavoprotein from *Escherichia coli* that reduces nitro-compounds: alteration of pyridine nucleotide binding by a single amino acid substitution. *Journal of Biological Chemistry* **276**, 2816-2823.
- Koder, R.L. and Miller A.F. (1998) Steady-state kinetic mechanism, stereospecificity, substrate and inhibitor specificity of *Enterobacter cloacae* nitroreductase. *Biochimica et Biophysica Acta* **1387**, 395-405.
- Koder, R.L., Haynes, C.A., Rodgers, M.E., Rodgers, D.W. and Miller, A-F. (2002) Flavin thermodynamics explain the oxygen sensitivity of enteric nitroreductases. *Biochemistry* **41**, 14197-14205.
- Kohli, R.M. and Massey, V. (1998) The oxidative half-reaction of old yellow enzyme: the role of Tyr-196. *Journal of Biological Chemistry* **73**, 32763-32770.
- Kraulis, P. J. (1991) MOLSCRIPT: a program to produce both detailed and schematic plots of protein structures. *Journal of Applied Crystallography* **24**, 946 – 949.
- Kumagai, Y., Wakayama, T., Li, S., Shinchara, A., Iwamatsu, A., Sun, G. and Shimojo, N. (2000) ζ -crystallin catalyses the reductive activation of 2,4,6-trinitrotoluene to generate reactive oxygen species: a proposed mechanism for the induction of cataract. *FEBS Letters* **478**, 295-298.
- Lenke, H. and Knackmuss, H-J. (1992) Initial hydrogenation during the catabolism of picric acid by *Rhodococcus erythropolis* HL 24-2. *Applied and Environmental Microbiology* **58**, 2922-2937.

- Lenke, H. and Knackmuss, H-J. (1996) Initial hydrogenation and extensive reduction of substituted 2,4-dinitrophenols. *Applied and Environmental Microbiology* **62**, 784-790.
- Lenke, H., Pieper, D.H., Bruhn, C and Knackmuss, H-J. (1992) Degradation of 2,4-dinitrophenol by two *Rhodococcus erythropolis* strain HL24-1 and HL24-2. *Applied and Environmental Microbiology* **58**, 2928-2932.
- Lesk, A.M., Branden, C-I. and Chothia, C. (1989) Structural principles of α/β -barrel proteins: the packing of the interior of the sheet. *PROTEINS: Structure, Function and Genetics* **5**, 139-148.
- Lewis, T.A., Goszczynski, S., Crawford, R.L., Korus, R.A. and Adamassu, W. (1996) Products of anaerobic 2,4,6-trinitrotoluene (TNT) transformation by *Clostridium bifermentans*. *Applied and Environmental Microbiology* **62**, 4669-4674.
- Louie, T.M., Webster, C.M. and Xun, L. (2002) Genetic and biochemical characterisation of a 2,4,6-trichlorophenol degradation pathway in *Ralstonia eutropha* JMP134. *Journal of Bacteriology* **184**, 3492-3500.
- Merritt, E.A. (1994) Raster 3D version 2.0. A program for photorealistic molecular graphics. *Acta Crystallographica Section D. Biological Crystallography* **50**, 869-873.
- Madani, N.D., Massey, P.J., Rodriguez-Pombo, P., Krishnan, A.V. and Feldman, D. (1994) *Candida albicans* estrogen-binding protein gene encodes an oxidoreductase that is inhibited by estradiol. *Proceedings of the National Academy of Sciences of the United States of America* **91**, 922-926.
- Manstein, D.J., Massey, V., Ghisla, S. and Pai, E.F. (1988) Stereochemistry and accessibility of prosthetic groups in flavoproteins. *Biochemistry* **27**, 2300-2305.
- Massey, V. (1995) Introduction: flavoprotein structure and mechanism. *FASEB Journal* **9**, 473-475.

- Massey, V. (2000) The chemical and biological versatility of riboflavin. *Biochemical Society Transactions* **28**, 283-296.
- Massey, V. and Hemmerich, P. (1978) Photoreduction of flavoproteins and other biological compounds catalysed by deazaflavins. *Biochemistry* **17**, 9-17.
- Massey, V. and Hemmerich, P. (1980) Active-site probes of flavoproteins. *Biochemical Society Transactions* **8**, 246-257.
- Massey, V. and Schopfer, L.M. (1986) Reactivity of old yellow enzyme with α -NADPH and other pyridine nucleotide derivatives. *Journal of Biological Chemistry* **261**, 1215-1222.
- Massey, V., Meah, Y., Xu, D. and Brown, B.J. (1999) New things about old yellow enzyme. In *Flavins and Flavoproteins 1999: Thirteenth International Symposium*, (Eds, Ghisla, S., Kroneck, P., Macheroux, P. and Sund, H.) Rudolf Weber, 645-653.
- Mathews, R. and Massey, V. (1971) Free and complexed forms of OYE. In *Flavins and Flavoproteins 1971: Third international symposium*, (Ed, Kamin, H.) University Park Press, Baltimore and Butterworth and Co. (Publishers), London, 329-348.
- Mathews, R.G. and Massey, V. (1969) Isolation of OYE in free and complexed forms. *Journal of Biological Chemistry* **244**, 1779-1789.
- Mathews, R.G., Massey, V. and Sweeley, C.C. (1975) Identification of p-hydroxybenzaldehyde as the ligand in the green form of old yellow enzyme. *Journal of Biological Chemistry* **250**, 9294-9298.
- McCormick, N.G., Feeherry, F.E. and Levinson, H.S (1976) Microbial transformation of 2,4,6,-trinitrotoluene and other nitroaromatic compounds. *Applied and Environmental Microbiology* **31**, 949-958.
- McRee, D.E. (1999) XtalView/Xfit- A versatile program for manipulating atomic coordinates and electron density. *Journal of Structural Biology* **125**, 156-165.

- Meah, Y. and Massey, V. (2000) Old yellow enzyme: stepwise reduction of nitro-olefins and catalysis of aci-nitro tautomerisation. *Proceedings of the National Academy of Sciences* **97**, 10733-10738.
- Meah, Y., Brown, B.J., Chakraborty, S. and Massey, V. (2001) Old yellow enzyme: reduction of nitrate esters, glycerin trinitrate and propylene-1,2,-dinitrate. *Proceedings of the National Academy of Sciences* **98**, 8560-8565.
- Medina, V.F. and McCutcheon, S.C. (1996) Phytoremediation: modelling removal of TNT and its breakdown products. *Remediation* **6**, 31-45.
- Meng, M., Sun, W-Q., Geelhar, L.A., Kumar, G., Patel, A.R., Payre, G-F., Speedie, M.K. and Stacy, J.R. (1995) Denitration of glycerol trinitrate by resting cells and cell extracts of *Bacillus thuringiensis/cereus* and *Enterobacter agglomerans*. *Applied and Environmental Microbiology* **61**, No. 7, 2548-2453.
- Mewies, M., McIntire, W.S. and Scrutton, N.S (1998) Covalent attachment of flavin adenine dinucleotide (FAD) and flavin mononucleotide (FMN) to enzymes: The current state of affairs. *Protein Science* **7**, 7-20.
- Michels, J. and Gottschalk, G. (1995) Pathway of 2,4,6-trinitrotoluene degradation by *Phanerochaete chrysosporium*. In *Biodegradation of nitroaromatic compounds* (Ed, Spain, J.C.), Plenum Press, 135-149
- Miura, K., Tomioka, Y., Suzuki, H., Yonezawa, M., Hishinuma, T. and Mizugaki, M. (1997) Molecular cloning of the *nem A* gene encoding N-ethylmaleimide reductase from *Escherichia coli*. *Biological Pharmacological Bulletin* **20**, 110-112.
- Miura, R. (2000) Versatility and specificity in flavoenzymes: control mechanisms of flavin reactivity. *The Chemical Record* **1**, 183-194.
- Miura, R., Yamano, T. and Miyake, Y. (1986) The heterogeneity of Brewers Yeast old yellow enzyme. *Journal of Biochemistry* **99**, 901-906.

- Muller, F. (1983) The flavin redox-system and its biological function. *Topics in Current Chemistry* **108**, 71-107.
- Muller, F. (1991) Free flavin: synthesis, chemical and physical properties. In *Chemistry and Biochemistry of Flavoenzymes* Vol I, (Ed, Muller, F.) CRC Press, Boca Raton.
- Nakamura, T., Yoshimura, J. and Ogura, Y. (1965) Action mechanism of the old yellow enzyme. *Journal of Biochemistry* **57**, 554-564.
- Niino, Y.S., Chakraborty, S., Brown, B.J. and Massey, V. (1995) A new old yellow enzyme of *Saccharomyces cerevisia*. *Journal of Biological Chemistry* **270**, 1983-1991.
- Nivinskas, H., Koder, R.L. Anusevicius, I., Sarlauskas, J., Muller, A-F. and Cenas, N. (2000) Two-electron reduction of nitroaromatic compounds by *Enterobacter cloacae* NAD(P)H nitroreductase: description of quantitative structure-activity relationships. *Acta Biochimica Polonica* **47**, 941-949.
- Nokhbeh, M.R., Boroumnadi, S., Pokorny, N., Koziarz, P., Paterson, E.S. and Lambert, I.B. (2002) Identification and characterisation of SnRA, an inducible oxygen-insensitive nitroreductase in *Salmonella enteric serovar Typhimurium* TA 1535. *Mutation Research* **508**, 59-70.
- Oh, B-T., Sarath, G., Shea, P.J., Drijber, R.A. and Comfort, S.D. (2000) Rapid spectrophotometric determination of 2,4,6-trinitrotoluene in a *Pseudomonas* enzyme assay. *Journal of Microbiological Methods* **42**, 149-158.
- Otwinowski, Z. and Minor, W. (1997) Processing of X-ray diffraction data collected in oscillation mode. *Methods in Enzymology* **276**, 307-326.
- Pai, E.F. (1992) Chapter 12: The stereochemistry of the prosthetic group of flavoproteins. In *Chemistry and Biochemistry of Flavoenzymes* vol III, (Ed, Muller, F.) 357-366.

- Pak, J.W., Knoke, K.L., Noguera, D.R., Fox, B.G. and Chambliss, G-H. (2000) Transformation of 2,4,6-trinitrotoluene by purified xenobiotic reductase B from *Pseudomonas fluorescens* I-C. *Applied and Environmental Microbiology* **66**, 4742-4750.
- Palfey, B.A. and Massey, V. (1998) Chapter 29: Flavin dependent enzymes. From *Comprehensive Biological catalysis, A mechanistic reference* Vol III, (Ed, Sinnott, M.) Academic Press.
- Parales, R.E., Bruce, N.C., Schmid, A. and Wackett, L.P. (2002) Biodegradation, Biotransformation and Biocatalysis (B3). *Applied and Environmental Microbiology* **68**, 4699-4709.
- Pasti-Grigsby, M.B., Lewis, T.A., Crawford, D.L. And Crawford, R.L. (1996) Transformation of 2,4,6-trinitrotoluene (TNT) by *Actinomycetes* isolated from TNT-contaminated and uncontaminated environments. *Applied and Environmental Microbiology* **62**, 1120-1123.
- Perec, C.M. and Agathos, S.N. (2000) Biodegradation of nitroaromatic compound pollutants: from pathways to remediation. *Biotechnology Annual Reviews* **6**, 197-220.
- Pflugmacher, S., Schroder, P. and Sandermann, Jr. H. (2000) Taxonomic distribution of plant glutathione-s-transferases acting on xenobiotics. *Phytochemistry* **54**, 267-273.
- Phillips, D.C., Sternberg, M.J.E., Thornton, J.M. and Wilson, I.A. (1978) Structure of triose phosphate isomerase and its comparison with lactate dehydrogenase. *Journal of Molecular Biology* **119**, 329-351.
- Porter, D.J.J. and Bright, H.J. (1980) Oxidation of dihydronicotinamides by flavins in enzymes and model reactions. Old yellow enzyme and lumniflavin. *Journal of Biological Chemistry* **255**, 7362-7370.
- Preub, A. and Rieger, P-G. (1995) Anaerobic transformation of 2,4,6-trinitrotoluene and other nitroaromatic compounds. In *Biodegradation of nitroaromatic compounds* (Ed, Spain, J.C.), Plenum Press, 69-85.

- Preuss, A., Fimpel, J. and Dickert, G. (1993) Anaerobic transformation of 2,4,6-trinitrotoluene (TNT). *Archives of Microbiology* **59**, 345-353.
- Rafii, F., Hehman, G. and Lunsford, P. (2001) Purification and characterisation of an enzyme from *Mycobacterium* sp. Pyr-1, with nitroreductase activity and an N-terminal sequence similar to lipoamide dehydrogenase. *Archives of Microbiology* **176**, 381-385.
- Rafii, F., Selby, A.L., Newton, R.K. and Cerniglia, C.E. (1994) Reduction and mutagenic activation of nitroaromatic compounds by a *Mycobacterium* sp. *Applied and Environmental Microbiology* **60**, 4263-4267.
- Raine, A.R.C., Scrutton, N.S. and Mathews, F.S. (1994) On the evolution of alternate core packing in eightfold β/α -barrels. *Protein Science* **3**, 1889-1892.
- Ramos, J.L., Haidour, A., Delgado, A., Duque, E., Fandila, M.D. and Pinar, G. (1995) Potential of a toluene-degrading system for construction of hybrid pathways for nitrotoluene metabolism. In *Biodegradation of nitroaromatic compounds* (Ed, Spain, J.C.), Plenum Press, 53-67.
- Read, R. (1986) Improved Fourier coefficients for maps using phases from partial structures with errors. *Acta crystallographia, section A* **42**, 140-149.
- Reardon, D. and Farber, G.K. (1995) The structure and evolution of α/β -barrel proteins. *FASEB Journal* **9**, 497-503.
- Riefler, R.G. and Smets, B.F. (2002) NAD(P)H: flavin mononucleotide oxidoreductase inactivation during 2,4,6-trinitrotoluene reduction. *Applied Environmental Microbiology* **68**, 1690-1696.
- Rieger, P.G. and Knackmuss, H-J. (1995) Basic knowledge and perspectives on biodegradation of 2,4,6-trinitrotoluene and related nitroaromatic compounds in contaminated soil. In *Biodegradation of nitroaromatic compounds* (Ed, Spain, J.C.), Plenum Press, 1-18.

- Rieger, P.G., Meier, H-M., Gerle, M., Vogt, U., Groth, T. and Knackmuss, H-J. (2002) Xenobiotics in the environment: present and future strategies to obviate the problem of biological persistence. *Journal of Biotechnology* **94**, 101-123.
- Rieger, P.G., Sinnwell, V., Preub, A., Francke, W. and Knackmuss, H-J. (1999) Hydride-Meisenheimer complex formation and protonation as key reactions of 2,4,6-trinitrophenol biodegradation by a *Rhodococcus erythropolis*. *Journal of Bacteriology* **181**, 1189-1195.
- Rohde, B.H., Schmid, R. and Ullrich, M.S. (1999) Thermoregulated expression and characterisation of an NAD(P)H-dependent 2-cyclohexen-1-one reductase in plant pathogenic bacterium *Pseudomonas syringae* pv. *glycinea*. *Journal of Bacteriology* **181**, 814-822.
- Saez, L.P., Garcia, P., Martinez-Luque, M. Klipp, W., Blasco, R. and Castillo, F. (2001) Role for *draTG* and *rnf* genes in reduction of 2,4,-dinitrophenol by *Rhodobacter capsulatus*. *Journal of Bacteriology* **83**, 1780-1783.
- Saito, K., Thiele, D.J., Davio, M., Lockridge, O. and Massey, V. (1991) The cloning and expression of a gene encoding old yellow enzyme from *Saccharomyces carlsbergensis*. *Journal of Biological Chemistry* **266**, 2072-20724.
- Sambrook, J., Fritsch, E.F. and Maniatis, T. (1989) Molecular cloning: a laboratory manual. 2nd Edition, Cold Spring Harbor Lab Press, Cold Spring Harbour, New York.
- Schaller, F. and Weiler E.W. (1997a) Molecular cloning and characterisation of 12-oxophytodienoate reductase, an enzyme of the octadecanoid signalling pathway from *Arabidopsis thaliana* - structural and functional relationships to yeast old yellow enzyme. *Journal of Biological Chemistry* **272**, 28066-28072.
- Schaller, F. and Weiler, E.W. (1997b) Enzyme of the octadecanoid biosynthesis in plants - 12-oxophytodienoate-10,11-reductase. *European Journal of Biochemistry* **245**, 294-299.
- Schenzle, A., Lenke, H., Spain, J.C and Knackmuss, H-J. (1999) Chemoselective nitro group reduction and reductive dechlorination initiate degradation of 2-chloro-5-nitrophenol by *Ralstonia eutropha* JMP134. *Applied and Environmental Microbiology* **65**, 2317-2323.

- Schnoor, J.L., Licht, L.A., McCutcheon, S.C., Wolfe, N.L. and Carriera, L.H. (1995) Phytoremediation of organic and nutrient contamination. *Environmental Science Technology* **29**, 318A-323A.
- Schopfer, L. M. and Massey, V. (1991) Chapter 10: Old Yellow Enzyme. In *A Study of Enzymes* (volume II) (ed. Kuby, S. A.), pp. 247 – 269, CRC Press, Cleveland, Ohio.
- Science News (1987) The electronic look of explosives (research on arrangement of electrons in molecules of explosives). **87**, 121.
- Schneiber, K., Hofrichter, M. and Fritsche, W. (1997) Mineralisation of 2-amino-4,6-dinitrotoluene by manganese peroxidase of the white rot fungus *Nematoloma frowardii*. *Biotechnology Letters* **19**, 835-839.
- Scrutton, N.S. (1994) Alpha/beta barrel evolution and the modular assembly of enzymes: emerging trends in the flavin oxidase/dehydrogenase family. *Bioessays* **16**, No. 2, 115-121.
- Shah, M.M. and Spain, J.C. (1996) Elimination of nitrite from the explosive 2,4,6-trinitrophenylmethylnitramine (tetryl) catalysed by ferredoxin NADP oxidoreductase from spinach. *Biochemical and Biophysical Research Communication* **220**, 563-568.
- Snape, J.R., Walkley, N.A., Morby, A.P., Nicklin, S. and White, G.F. (1997) Purification, properties and sequence of glycerol trinitrate reductase from *Agrobacterium radiobacter*. *Journal of Bacteriology* **179**, 7796-7802.
- Snellinx, Z., Neparim, A., Taghavi, S., Vangeronsneld, J., Vanek, F. and Lelie, D.V.D. (2002) Biological remediation of explosives and related nitroaromatic compounds. *Environmental Science Pollution Research* **9**, 48-61.
- Sommerville, C.C., Nishino, S.F. and Spain, J.C (1995) Purification and characterisation of nitrobenzene nitroreductase from *Pseudomonas pseudoalcaligenes* JS45. *Journal of Bacteriology* **177** 3837-3842.

- Spain, J.C. (1995a) Biodegradation of nitroaromatic compounds. *Annual Reviews in Microbiology* **49**, 523-535.
- Spain, J.C. (1995b) Bacterial degradation of nitroaromatic compounds under aerobic conditions. In *Biodegradation of nitroaromatic compounds* (Ed, Spain, J.C.), Plenum Press, 19-35.
- Stahl, J.D and Aust, S.D (1993) Metabolism and detoxification of TNT by *Phanerochaete chrysosporium*. *Biochemical and Biophysical Research Communication* **192**, 477-482.
- Stahl, J.D. and Aust, S.D (1995) Biodegradation of 2,4,6-trinitrotoluene by the white rot fungus *Phanerochaete chrysosporium*. In *Biodegradation of nitroaromatic compounds* (Ed, Spain, J.C.), Plenum Press, 117-134.
- Stewart, R.C. and Massey, V. (1985) Potentiometric studies of native and flavin substituted old yellow enzyme. *Journal of Biological Chemistry* **260**, 13639-13647.
- Stott, K., Saito, K., Thiele, D.J and Massey, V. (1993) Old yellow enzyme, the discovery of multiple isozymes and a family of related proteins. *Journal of Biological Chemistry* **268**, 6097-6106.
- Strabner, J., Furholz, A., Macheroux, P., Amrhein, N. and Schaller, A. (1999) A homolog of old yellow enzyme in tomato; spectral properties and substrate specificity of the recombinant protein. *Journal of Biological Chemistry* **274**, 35067-35073.
- Susarla, S., Medina, V.F. and McCutcheon, S.C. (2002) Phytoremediation: An ecological solution to organic chemical contamination. *Ecological Engineering* **18**, 647-658.
- Tamalge, S.S., Opresko, D.M., Maxwell, C.J., Welsh, C.J.E., Cretella, M., Reno, P.H. and Daniel, F.B. (1999) Nitroaromatic munition compounds: environmental effects and screening values. *Reviews in Environmental Contamination Toxicology* **161**, 1-156.
- Thompson, P.L., Ramer, L.A. and Schnoor, J.L. (1998) Uptake and transformation of TNT by hybrid poplar trees. *Environmental Science Technology* **32**, 975-980.

- Tocher, J.H. (1997) Reductive activation of nitroheterocyclic compounds. *General Pharmacology* **28**, 485-487.
- Trott, S., Nishino, S.F., Hawari, J. and Spain, J.C. (2003) Biodegradation of the nitramine explosive CL-20. *Applied and Environmental Microbiology* **69**, 1871-1874.
- Van Aken, B., Hofrichter, M., Scheibner, K., Hatakka, A.I., Naveau, H. and Agathos, S.N. (1999) Transformation and mineralization of 2,4,6-trinitrotoluene (TNT) by manganese peroxidase from the white rot basidiomycete *Phlebia radiata*. *Biodegradation* **110**, 83-91.
- Van Aken, B., Skubusz, K., Naveau, H. and Agathos, S.N. (1997) Biodegradation of 2,4,6-trinitrotoluene by the white-rot basidiomycete *Phlebia radiata*. *Biotechnology Letters* **19**, 813-817.
- Vanderford, M., Schanks, J.V. and Hughes, J.B. (1997) Phytotransformation of trinitrotoluene and distribution of metabolic products in *Myriophyllum aquaticum*. *Biotechnology Letters* **19**, 227-280.
- Vaz, A.D.N., Chakraborty, S. and Massey, V. (1995) Old yellow enzyme: aromatisation of cyclic enones and mechanism of a novel dismutation reaction. *Biochemistry* **34**, 4246-4256.
- Vorbeck, C., Lenke, H., Fischer, P. and Knackmuss, H-J. (1994) Identification of a hydride-Meisenheimer complex as a metabolite of 2,4,6-trinitrotoluene by a *Mycobacterium* strain. *Journal of Bacteriology* **176**, 932-934.
- Vorbeck, C., Lenke, H., Fischer, P., Spain, J.C. and Knackmuss, H-J. (1998) Initial reductive reactions in aerobic microbial metabolism of 2,4,6-trinitrotoluene. *Applied and Environmental Microbiology* **64**, 246-252.
- Walsh, C. (1979) Flavin-dependent dehydrogenases and oxidases (Chapter 11). In *Enzymatic Reaction Mechanisms* (Ed, Walsh, C.) 1st Edition, Freeman and Company, San Francisco.
- Walsh, C. (1980) Flavin co-enzymes: at the crossroads of biological redox chemistry. *Accounts of Chemical Research* **13**, 146-155.

- Wang, C.Y., Zheng, D. and Hughes, J.B. (2000) Stability of hydroxylamino and amino intermediates from reduction of 2,4,6-trinitrotoluene, 2,4-dinitrotoluene and 2,6-dinitrotoluene. *Biotechnology Letters* **22**, 15-19.
- Warburg, O. and Christian, W. (1932) Ein zweites saurstoff-übertragendes ferment und sein absorption-specktrum. *Naturwissenschaften* **20**, 688-697.
- Watanabe, M., Nishino, T., Takio, K., Sofuni, T. and Nohmi, T. (1998) Purification and characterisation of wild-type and mutant classical nitroreductases of *Salmonella Typhimurium*. *Journal of Biological Chemistry* **273**, 23922-23928.
- Watrous, M., Cark, S., Kutty, R., Huang, S., Rudolph, F.B., Hughes, J.B. and Bennett, G.N. (2003) 2,4,6-trinitrotoluene reduction by and Fe-only hydrogenase in *Clostridium acetobutylicum*. *Applied and Environmental Microbiology* **69**, 1542-1547.
- White, G.F. and Snape, J.R. (1993) Microbial cleavage of nitrate esters: defusing the environment. *Journal of General Microbiology* **36**, 693-699.
- White, G.F, Snape, J.R. and Nicklin, S. (1996) Biodegradation of GTN and pentaerythritol tetranitrate by *Agrobacterium radiobacter*. *Applied and Environmental Microbiology*, **62**, 637-642.
- Williams, R.E. and Bruce, N.C. (2002) "New uses for an old enzyme"- the old yellow enzyme family of flavoproteins. *Microbiology* **148**, 1607-1614.
- Williams, R.E., Rathbone, D., Bruce, N.C., Moody, P.C.E. and Nicklin, S. (1999) In *Flavins and Flavoproteins* (Eds, Ghisla, S., Kroneck, P., Macheroux, P. and Sund, H.) Rudolf Weber, Berlin, 663-666.
- Williams, R.E., Rathbone, D.A., Moody, P.C., Scrutton, N.S. and Bruce, N.C. (2001) Degradation of explosives by nitrate ester reductases. *Biochemical Society Symposium* **68**, 143-153.

- Williams, R.E., Rathbone, D.A., Scrutton, N.S. and Bruce, N.C. (2004) A comparison of the old yellow enzyme family of flavoproteins and their activity towards explosives. *Applied Environmental Microbiology* **70**, 3566-3574.
- Wong, P. S-Y. and Futuko, J.M. (1999) Reaction of organic nitrate esters and S-nitrosothiols with reduced flavin: a possible mechanism of bioactivation. *Drug Metabolism and Disposition* **27**, 502-509.
- Xu, D., Kohli, R.M. and Massey, V. (1999) The role of Thr 37 in flavin reactivity of the old-yellow enzyme. *Biochemistry* **96**, 3556-3561.
- Yano, Y. (2001) Artificial flavin receptors: effects of hydrogen bonding on redox properties of a flavin mimic. *Antioxidants and Redox Signalling* **3**, 899-909.
- Zaripoz, S.A., Naumov, A.V., Abdokhmanova, J.F., Garusov, A.V. and Naumova, R.P. (2002) Models of 2,4,6-trinitrotoluene (TNT) initial conversion by yeasts. *FEMS Microbiology Letters* **217**, 213-217.
- Zhao, J-S. and Ward, O.P. (2001) Substrate selectivity of a 3-nitrophenol induced metabolic system in *Pseudomonas putida* 2NP8 transforming nitroaromatic compounds into ammonia under anaerobic conditions. *Applied and Environmental Microbiology* **67**, 1388-1391.